Molecular changes in the aging osteoblast

by

Gustavo Duque, MD

Department of Medicine

Division of Experimental Medicine

McGill University

March 2003

A thesis submitted to the

Faculty of Graduate Studies and Research

in partial fulfillment of the requirements of the degree of

Doctor of Philosophy

© Copyright by Gustavo Duque, MD (2003)

ABSTRACT

Molecular changes in the aging osteoblast. Ph.D. Thesis Abstract. 2003. Gustavo Duque. Department of Medicine, Division of Experimental Medicine. McGill University.

Aging is the consequence of an array of phenotypic variations that appear to involve intrinsic or constitutional properties in all cells and systems, including qualitative and quantitative alterations in development, maturational structure and function. The aging process in bone involves a set of changes in bone cells differentiation, interaction and premature death. Osteoblasts are the cells most affected during the aging process in bone due to their complex mechanisms of differentiation, their interaction with hormones and growth factors and their progression to apoptosis.

In the process of differentiation of human mesenchymal stem cells (hMSC) into osteoblasts there is a significant change (up or down regulation) in 74 genes occurs between the phase of differentiation (week 1) and mineralization (week 3). Among these genes affected, a group called "Interferon-inducible genes" plays an important role during the first phase of differentiation. In addition, interferon γ (IFNγ) *per se* plays a pivotal role in this process *in vitro* and *in vivo*. *In vitro*, IFNγ induces early osteoblastic differentiation of hMSC and up-regulates Cbfa1, the most important transcription factor for osteoblast differentiation. *In vivo* IFNγ absence results in low bone turnover osteoporosis. Furthermore, in the SAM-P/6 mouse model (a previously described model of senile osteoporosis) age-related changes in osteoblasts are regulated by the administration of $1,25(OH)_2D_3$. Treated mice show a significant increase in bone mass as

a consequence of concomitant increase in osteoblastogenesis together with a decrease in both adipogenesis and osteoclastogenesis. The changes in gene expression induced by1,25$(OH)_2D_3$ in these mice indicate a predominant osteogenic effect and provide a better understanding of the aging process in the osteoblast. In addition to gene changes, during their aging process osteoblasts show a significant reduction in the number and bioresponse of vitamin D receptors (VDR) *in vivo*. These changes can be reversed by the administration of E_2 indicating a close interaction between E_2 and vitamin D in the aging process of bone. Finally, the pathways involved in osteoblast apoptosis were assessed. We found that osteoblast apoptosis *in vitro* is induced predominantly by the activation of the Fas pathway with further activation of the cascade of caspases. Additionally, a mitochondrial role for 1,25$(OH)_2D_3$ in osteoblast apoptosis was found through the increasing levels of pro-apoptotic Bax and decreasing levels of the anti-apoptotic Bcl-2. All these apoptotic pathways were found to be inhibited by 1,25$(OH)_2D_3$ which induced Fas resistance through the inactivation of caspase-8 and stimulation of Bcl-2 expression. In summary, these findings elucidate several molecular changes that occur during the aging process in the osteoblast. These changes also identify potential targets that may be regulated to provide better function and extend the life span of these cells which are essential to maintain bone integrity.

SOMMAIRE

Changements moléculaires dans les ostéoblastes vieillissants. Ph.D. Thèse sommaire. 2003. Gustavo Duque.Département de médecine, Division de médecine gériatrique. Université McGill.

Le vieillissement est la conséquence d'un éventail de variations phénotypiques impliquant des propriétés intrinsèques ou constitutives pour tous systèmes et cellules. Ce processus implique des altérations quantitatives et qualitatives dans le développement, la structure et la fonction des cellules. Dans l'os, le processus du vieillissement implique un ensemble d'évènements incluant des changements dans la différenciation des cellules osseuses, leur interaction et leur mort prématurée. Les ostéoblastes sont les cellules les plus affectées lors de ce processus de vieillissement osseux a cause de leur mécanisme complexe de différenciation, de leur interaction avec des hormones ou des facteurs de croissance ainsi que de leur progression vers l'apoptose. Au cours du processus de différenciation des cellules souches mésenchymateuses humaines (CSMh) en ostéoblastes, il y a un changement significatif (positive ou négatif) dans 74 gènes entre la phase de différenciation (semaine 1) et la phase de minéralisation (semaine 3).

Parmi ces gènes on retrouve le groupe de gènes inductibles par l'interférons qui jouent un rôle important durant la première phase de différenciation. De plus l'interféron γ (INFγ) joue un rôle pivot dans ce processus à la fois *in vitro* et *in vivo*. *In vitro*, l'INFγ accélère la différenciation ostéoblastique des CSMh et augmente l'expression du Cbfa1, le plus important facteur de transcription pour la différenciation des ostéoblastes. *In vivo* son absence entraîne une ostéoporose à turnover réduit.De plus, chez les souris SAM-P/6 (un modèle connu d'ostéoporose sénile) les changements associés au vieillissement dans les

ostéoblastes sont régulés par l'administration de $1,25(OH)_2D_3$. Ainsi les souris traitées à la $1,25(OH)_2D_3$ montrent une augmentation significative de leur masse osseuse résultant a la fois d'une osteóblastogénèse augmentée et d'une ostéoclastogénèse et d'une adipogénèse diminuées. Les changements des gènes induits par la $1,25(OH)_2D_3$ dans ce type de souris montrent un effet ostéogénique prédominant ce qui indiquerait un nouveau mécanisme du processus de vieillissement des ostéoblastes. De plus, durant le processus de vieillissement des ostéoblastes, on observe une réduction significative du nombre et de la réponse biologique des récepteurs de la vitamine D (RVD) *in vivo*. Ces changements sont réversibles par l'administration d'estrogènes démontrant ainsi un nouveau rôle des hormones stéroïdes comme régulateurs du processus du vieillissement osseux.

Finalement, les signaux impliqués lors de l'apoptose des ostéoblastes ont été évalués.Nous avons démontré que l'apoptose des osteóblastes *in vitro* est en grande partie induite par l'activation du signal Fas avec activation subséquente de la cascade des caspases. De plus, nous avons découvert que les mitochondries jouent un rôle dans la régulation par la $1,25(OH)_2D_3$ de l'apoptose des ostéoblastes en augmentant le niveau de facteur anti-apoptotique Bcl-2 et en diminuant le niveau du facteur anti-apoptotique Bax. Nous avons découvert que tout ces signaux apoptotique étaient inhibés par la $1,25(OH)_2D_3$ qui entraîne une résistance au Fas durant l'inactivation de la caspase-8 tout en augmentant le niveau de l'expression du Bcl-2. En bref, ces découvertes ont permit d'élucider des changements moléculaires qui se produisent durant le processus de vieillissement des ostéoblastes. Ceci suggère la possibilité de cibler la régulation de signaux intracellulaires dans le but d'améliorer leur fonction et de prolonger leur longévité afin que ces cellules puissent continuer d'assurer le maintien de l'intégrité osseuse.

FOREWORD

The following excerpt is taken from the Guidelines Concerning Thesis Preparation, Faculty of Graduate Studies and Research, McGill University, and applies to this thesis:

Candidates have the option of including, as part of the thesis, the text of a paper(s) submitted or to be submitted for publication, or the clearly-duplicated text of a published paper. These texts must be bound as an integral part of the thesis.

If this option is chosen, connecting text (s) that provide logical bridges between the different papers are mandatory. The thesis must be written in such a way that it is more than a mere collection of manuscripts; in other words, results of a series of papers must be integrated.

The thesis must still conform to all other requirements of the "Guidelines for Thesis Preparation". **The thesis must include**: A Table of Contents, an abstract in English and French, an introduction which clearly states the rationale and objectives of the study, a comprehensive review of the literature, a final conclusion and summary, and a thorough bibliography or reference list.

Additional material must be provided where appropriate (e.g. appendices) and in sufficient detail to allow a clear and precise judgment to be made of the importance and originality of the research reported in the thesis.

In the case of manuscripts co-authored by the candidate and others, **the candidate is required to make an explicit statement in the thesis as to who contributed to such work and to what extent.** Supervisors must attest to the accuracy of such statements at the doctoral oral defense. Since the task of the examiners is made more difficult in these cases, it is in the candidate's interest to make perfectly clear the responsibilities of all the

authors of the co-authored papers. **Under no circumstances can a co-author or any component of such a thesis serve as an examiner for that thesis.**

DEDICATION

To my lovely and devoted parents,

Maximo Duque & Rubiela Naranjo

To Professor Jaime Marquez Arango (RIP)

my role model,

a wonderful teacher, outstanding researcher, and excellent geriatrician

To my Country,

Colombia

Because making science is more valuable for the Humanity than making war

and

To GOD

The Great Architect of everything that is described in this Thesis

ACKNOWLEDGEMENTS

First, I want to express my gratitude to my supervisor Dr. Richard Kremer. From our first meeting when I was doing my Fellowship in Geriatric Medicine, until today when I submitted this thesis Dr. Kremer has been always extremely supportive. He understood the difficulty in a professional like me returning to school, and offered me his appreciation and support as my colleague and supervisor. I would also like to thank my friend and first "tutor" at the calcium lab, Dr. Khadija El-Abdaimi. Her generosity and willingness to explain to me the simplest techniques during my early days in a research lab marked my future role as a supervisor. I would like to thank my partners at the Calcium lab, Michael Macoritto, Mrs. Isabel Bolivar, Mrs. Miren Gratton and Dr. Dao Huang. They were always available when I needed them for advice, technical assistance or even to steal their tips and solutions. Thanks to my friend Dr. Janet Henderson, for the right comments at the right time, to Dr. George Kuchel who traveled from his new job in Connecticut to participate on my thesis committee, and Drs. Louis George Ste Marie and Natalie Dion from St. Luc's Hospital for their prompt and excellent job with the histology samples. My gratitude is also extended to my academic advisor Dr. Hendy for his exigency to me to produce a very good PhD, to Drs. Howard Chertkow and Mark Wainberg for their financial and academic support, to the members of the Division of Geriatric Medicine, especially to my friend and mentor Dr. Howard Bergman, who really knows what trust and support mean. Thanks to Dr. Susan Gold, always available to review my "spanglish" and to the "Geriatrics Angels": Myra, Amy and Elizabeth for their secretarial assistance. I also extend my most sincere thanks to the Fonds de la Recherche en Sante du Quebec, the McCall Hutchinson Foundation and the Royal Victoria Research

Institute for their financial support. And finally, I would like to thank my good friends Jean François, Walter, Mauricio, Ceci and Pilar who have been there when I needed them, and who forgave my absences while I was working on this life project.

TABLE OF CONTENTS

LIST OF FIGURES

LIST OF TABLES

LIST OF PUBLICATIONS

1- **Duque G.**, El Abdaimi K, Macoritto M, Miller MM, Kremer R. 2002. Estrogens (E_2) regulate expression and response of 1,25-Dihydroxyvitamin D_3 Receptors in bone cells: Changes with aging and hormone deprivation. *Biochemical and Biophysical Research Communications,* 299:446-454.

2- **Duque G.**, Macoritto M., Dion N., Ste. Marie L.G., Kremer R. 2003. Interferon γ regulates bone formation and its deficiency results in osteoporosis. Submitted to the *Journal of Experimental Medicine.*

3- **Duque G.**, Macoritto M., Dion N., Ste. Marie L.G., Kremer R. 2003. $1,25(OH)_2D_3$ acts as a bone forming agent in the hormone independent Senescence Accelerated Mouse (SAM-P/6) model of Osteoporosis. Submitted to the *Journal of Clinical Investigation.*

4- **Duque G**, El Abdaimi K, Henderson J, Lomri A, Kremer R. 2003. Vitamin D exerts its anti-apoptotic effect in osteoblasts through a Fas related mechanism. Submitted to *American Journal of Physiology: Endocrinology:*

CONTRIBUTIONS OF AUTHORS

In Chapter Two, I proposed the original concept of osteoblast differentiation and the experimental designs. I also performed most of the experiments, except the histomorphometric and histologic analysis which were performed by Drs. St. Marie and Dion. The semi-quantitative RT-PCR was performed by Mr. Macoritto. Micro chip cDNA analysis was performed by the Genome Centre at McGill University. Mr. Papavasiliou was in charge of the mice intervention and care. Micro CT analysis of bone was performed at the Centre for Bone and Periodontal Research, McGill University. I analyzed the data obtained from all the experiments. Dr. Kremer contributed to the initial experimental concept and supervised most of the experiments.

In Chapter Three, I proposed the complete concept and experimental design. Most of the experiments were performed by myself with the exception of the histomorphometrical and histological analysis which were performed by Drs. St. Marie and Dion. The semi-quantitative RT-PCR was performed by Mr. Macoritto. Mr. Papavasiliou was in charge of the mice intervention and care. Micro chip cDNA arrays analysis were performed at McMaster University. I analyzed the data from all experiments. Dr. Kremer supervised the entire project.

In Chapter Four, I proposed the complete concept and experimental design. All experiments were performed by myself with the considerable help of Dr. El-Abdaimi. Dr. Miller was in charge of the mice surgeries. Bones were embebbed in paraffin and

mounted on slides at the Department of Pathology, Jewish General Hospital. I analyzed and interpreted the results. Dr. Kremer supervised the entire project.

In Chapter Five, I proposed entirely the concept and experimental design. All experiments were performed by myself. Dr. Lomri developed the cell lines at the INSERM # 3, Paris, France. Dr. Henderson co-supervised the project and helped me with the TUNEL assay. Dr. Kremer supervised the entire project.

LIST OF ABBREVIATIONS

$1,25(OH)_2D_3$:	1,25-Dihydroxyvitamin D3:
25-OHD:	25-Hydroxyvitamin D
AD:	Adipogenesis
AIM:	Adipogenesis induction media
Aj.Ar:	Adjusted apposition rate
ANOVA:	Analysis of variance
aP:	Fatty acid binding protein
ALP:	Alkaline phosphatase
Apaf:	Apoptosis protease-activating factor
ATP:	Adenosyn tri-phosphate
ATPase:	Adenosyn tri-phosphatase
B.Pm:	Bone perimeter
BFR/BS:	Bone formation rate (per bone surface)
BFR/BV:	Bone formation rate (per bone volume)
BFR/TV:	Bone formation rate (per tissue area)
BMD:	Bone mineral density
BMP:	Bone morphogenic protein
BMU:	Basic multicellular unit
BV/TV:	Bone volume
CEB/P:	CCAAT/enhancer-binding protein
CK:	Casein kinase
Coll:	Collagen

CSF:	Colony-stimulating factors
Ct.Wi:	Cortical width
Cyto-c:	Cytochrome-c
DEXA:	Dual-energy-x-ray absorptiometry
dLS/BS:	Double labelled surface per bone surface
dLS/LS:	Double labelled surface per labelled surface
DMEM:	Dubelcco's modified Eagle's Medium
DNA:	Deoxyribonucleic acid
DRIP:	vitamin D receptor-interacting protein
E_2:	Estrogens (Estradiol)
ECF:	Extracellular fluid
EDTA:	Ethylene diamino tetra acetic acid
ELISA:	Enzyme linked immunosorbent assay
ES/BS:	Eroded surface
EST:	Expressed sequences tags
FADD:	Fas-associated death domain
FCS:	Fetal calf serum
FGF:	Fibroblast growth factor
GAPDH:	Glyceraldehyde-3-Phosphate Dehydrogenase
GF:	Growth factors
GSTM1:	Glutathione S-transferase M1
H+E:	Hematoxylin-eosin
hMSC:	Human mesenchymal stem cells
IBMX:	Isobutylmethylxanthine

IFGR:	Interferon gamma receptor
Ihh:	Indian hedgehog
IL:	Interleukin
IFN:	Interferon
IFNIG:	Interferon inducible genes
IrLTh:	Interlable thickness
ISRE:	IFN stimulated response elements
LIF:	Lymphocyte inhibiting factor
LPL:	Lipoprotein lipase
M.Oc/T.Ar.:	Osteoclast number (per tissue area)
MAPK:	Mitogen activated protein kinase
MAR:	Mineral apposition rate
MS/BS:	Mineralizing surface
MS/OS:	Mineralized surface
MSC:	Mesenchymal stem cells
MSCGM:	Mesenchymal stem cell growth media
N.Oc/B.Pm:	Osteoclast number (per bone perimeter)
N.Oc/E.Pm:	Osteoclast number (per eroded centimeter)
NCP:	Non-collagen proteins
NO:	Nitric oxide
O.Th:	Osteoid thickness
Ob.S/BS:	Osteoblast surface
OB:	Osteoblastogenesis
Oc.S/BS:	Osteoclast surface

OC:	Osteoclastogenesis
OD:	Optical density
OIM:	Osteoblastogenesis induction media
OPG:	Osteoprotegerin
OPN;	Osteopontin
OS/BS:	Osteoid surface
OSE:	Osteoblast specific cis-acting element
Osf:	Osteoblast specific factor
OSN:	Osteocalcin
Osx:	Osterix
OV/BV:	Osteoid volume
OVX:	Oophorectomy
PARP:	Poly (ADP-ribose) polymerase
PBS:	Phosphate buffered saline
PCNA:	Proliferating cell nuclear antigen
PDGF:	Platelet derived growth factor
PE:	Polyethylene
PEPCK:	Phosphoenolpyruvate carboxykinase
PG:	Prostaglandin
PI:	Propidium iodine
p-NA:	p-nitroaniline
PPARγ:	Peroxisome proliferator-activator receptor gamma
PTH:	Parathyroid Hormone

PTHrP:	Parathyroid hormone related peptide
RANK:	Receptor activator of nuclear factorκB
RANK-L:	Receptor activator of nuclear factorκB ligand
RIA:	Radio immunoassay
RNA:	Ribonucleic acid
RT-PCR:	Reverse transcription-polymerase chain reaction
Runx:	Runt domain transcription factors
SAM:	Senescence accelerated mouse
SD:	Serum deprivation
SEM:	Standard error of median
sLS/BS:	Single labelled surface per bone surface
sLS/LS:	Single labelled surface per labelled surface
SRC:	Steroid receptor co-activators
T.Ar:	Tissue area
Tb.N:	Trabecular number
Tb.Sp:	Trabecular separation
Tb.Th:	Trabecular thickness
TGF:	Transforming growth factor
TNF:	Tumor necrosis factor
TRAD:	Tumor necrosis factor death receptor associated domain
TRAIL:	TNF-related apoptosis-inducing ligand
TRACP:	Tartrate-resistant acid phosphatase

TUNEL:	terminal deoxynucleotidyl transferase-mediated dUTP biotin nick end labeling
TZD:	Thiazolidinediones
VDR:	Vitamin D receptor
VDRE:	Vitamin D response element
VEGF:	Vascular endothelial growth factor

ERUDITION

"One of the great undiscovered joys of life comes from doing everything one attempts to the best of one's ability. There is a special sense of satisfaction, a pride in surveying such a work, a work which is rounded, full, exact, complete in its parts, which the superficial person who leaves his or her work in a slovenly, slipshod, half-finished condition, can never know. It is this conscientious completeness which turns any work into art. The smallest task, well done, becomes a miracle of achievement."

Og Mandino

CHAPTER 1

Introduction

1.1 The bone micro-environment

Bone is a mineralized tissue that performs multiple mechanical and metabolic functions for the body. Bone acts as a support and protection for the different organs, hosts the bone marrow and represents an important source of calcium when it is required in its ionized form (1). In order to accomplish these functions, bones undergo a complex process of turnover that replaces old and low quality bone with a new and stronger bone. This process of turnover involves two very well known mechanisms: resorption and formation. The cells responsible for bone resorption and formation are the osteoclasts and the osteoblasts respectively. These cells act in a well synchronized manner that starts with bone resorption by osteoclasts and ends with the formation of new bone by osteoblasts (1-3).

In addition to these two specialized cells, the bone micro-environment has other components that enhance the cells' activity and interaction. The bone matrix is a mixture of collagen fibers, glycoproteins and proteoglycans as well as non-collagenous proteins that are mostly secreted by bone cells (2-4). Furthermore, there is a complex communication system between the bone micro-environment and the rest of the body through the interaction with hormones, cytokines and growth factors (GF) that regulate the process of bone turnover (4) this will be described later in this chapter.

1.1.1 The osteoblast

Osteoblasts are cells of mesenchymal origin that in cell culture take a fibroblastic phenotype (1,5,6). They play an important role in both embryonic development and bone

turnover. During embryonic development the two types of ossification known as endochondral ossification and intramembranous ossification require the presence of active osteoblasts (1,5,6). During development, the entire future skeleton — with the exception of the clavicles, the mandibles and certain bones of the skulls— have a cartilage template surrounded by a bone collar. The chondrocytes of this cartilaginous tissue die through apoptosis and are replaced by osteoblasts which start the building of a bone matrix which is then mineralized; this process is known as endochondral ossification (1,6). By contrast, in clavicles, mandibles and certain bones of the skull, multipotential mesenchymal stem cells (MSC) differentiate directly into osteoblasts without the presence of cartilaginous templates (1,6).

Osteoblasts have the typical morphology of a cell engaged in the secretion of connective tissue matrix, with a large nucleus, enlarged Golgi and extensive endoplasmic reticulum (1,2,5,6). Osteoblasts are found in clusters of cuboidal cells along the bone surface (~100 to 400 cells per bone-forming site) (Fig. 1). They are always found lining the layer of bone matrix that they are producing before it is calcified (osteoid) (Fig. 2). At the ultra-structural levels, the osteoblast is characterized by (a) the presence of an extremely well-developed rough endoplasmic reticulum with dilated cisternae and a dense granular content, and (b) the presence of a large circular Golgi complex comprising multiple Golgi stacks (6). The secreting side has some cytoplasmic processes that extend deep into the osteoid matrix and are in contact with the osteocytes (1). The plasma membrane of the osteoblasts is rich in alkaline phosphatase (ALP), which is also secreted into the circulation by the osteoblasts and can be used as a marker of their function. The role of ALP in bone turnover and bone cells interactions remains unknown (5,6).

Osteocalcin (OSN), one of the bone matrix non-collagen proteins (NCPs), is also secreted by osteoblasts and is used as a marker of their function as well. Although its function is somewhat unclear, it may function in the inhibition of mineral apposition (1).

Active osteoblasts secretes type-I collagen and specialized bone-matrix proteins as osteoid toward the mineralizing front of the tissue. The osteoid acts also as a substrate for the interaction between osteoblasts and two important factors for osteoblast differentiation, integrins and cadherins. In addition osteoid is the substrate for the mineral apposition in a rate of 0,55 μm/day in adults (1).

Osteoblasts have been shown to express receptors for the main calcium-regulating hormones (parathyroid hormone (PTH) and vitamin D_3) (1,2,7,8), with the exception of calcitonin (1,2,7). They also express receptors for sex steroid hormones (Androgens and E_2) in their nuclei (8-11), as well as several adhesion molecules (integrins) and receptors for cytokines (1,6).

After completing their function of secreting the osteoid, osteoblasts have three different fates: they can become flat lining-cells, differentiate into osteocytes or finally die by apoptosis (Fig. 2) (11). These three different fates are the consequence of changes in the bone microenvironment that will be reviewed later in this chapter.

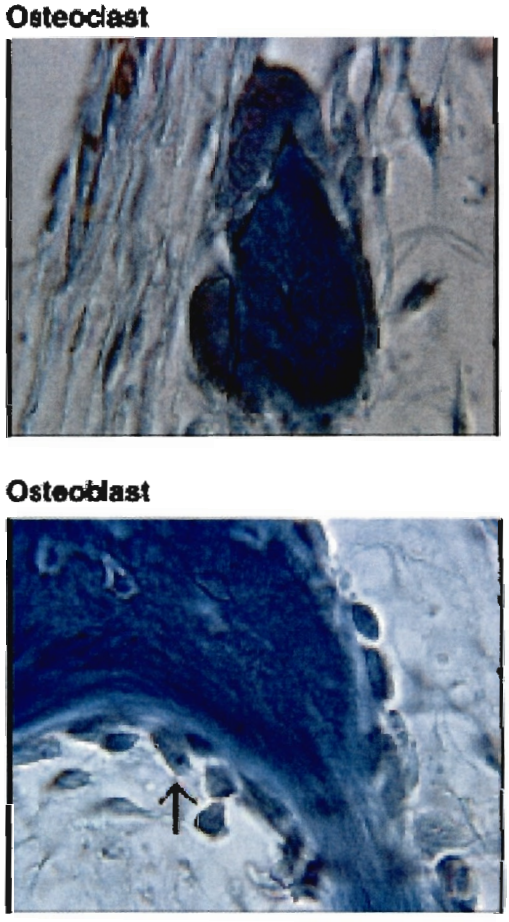

Figure 1. The two cells of the bone microenvironment. Osteoclasts (upper panel, 100X) belong to the macrophage –like family. Their main feature, the ruffled border, enhances their enzymatic activity and serves as attachment mechanism. By contrast, osteoblasts (lower panel, 40X) have a fibroblastic phenotype with a large nucleus and enlarged Golgi. Usually, osteoblasts are located along the bone-forming surface.

1.1.2 The osteocyte

As mentioned above, becoming osteocytes is one of the final fates of osteoblasts after the secretion period. When mature osteoblasts are submerged inside the osteoid they change their phenotype and developing numerous extensions of the plasma membrane that lie in the canaliculi (Fig. 2).

Osteocytes are known to secrete high amounts of OSN; they are also in close communication with the lining surface osteoblasts through their cellular processes (1,2). Osteoblasts and osteoclasts are metabolically and electrically coupled through different gap-junction proteins called connexins (1). This evidence supports the theory that there is a close connection between osteoblasts and osteocytes in response to multiple physiological stimuli including mechanical stress (1) or apoptotic stimuli (11).

As in the case of osteoblasts, it has been demonstrated that osteocytes may undergo apoptosis (8,12).

1.1.3 The osteoclast

Osteoclasts play a very important role in the process of bone turnover. These cells are the first to arrive in the basic multicellular unit (BMU) to initiate the resorption of old bone. They are giant multinucleated cells (Fig. 1) differentiated from bone marrow precursors as macrophage-like cells (Fig. 2) (1,12-15).

Osteoclasts are usually found in contact with a calcified bone surface and within a lacuna (Howship's lacunae) that is the result of its own resorptive activity. Usually there are one or two osteoclasts per resorptive site. Their ultrastructural characteristics include abundant Golgi complexes disposed around each nucleus, the mitochondria, and the transport vesicles loaded with lysosomal enzymes (1,15).

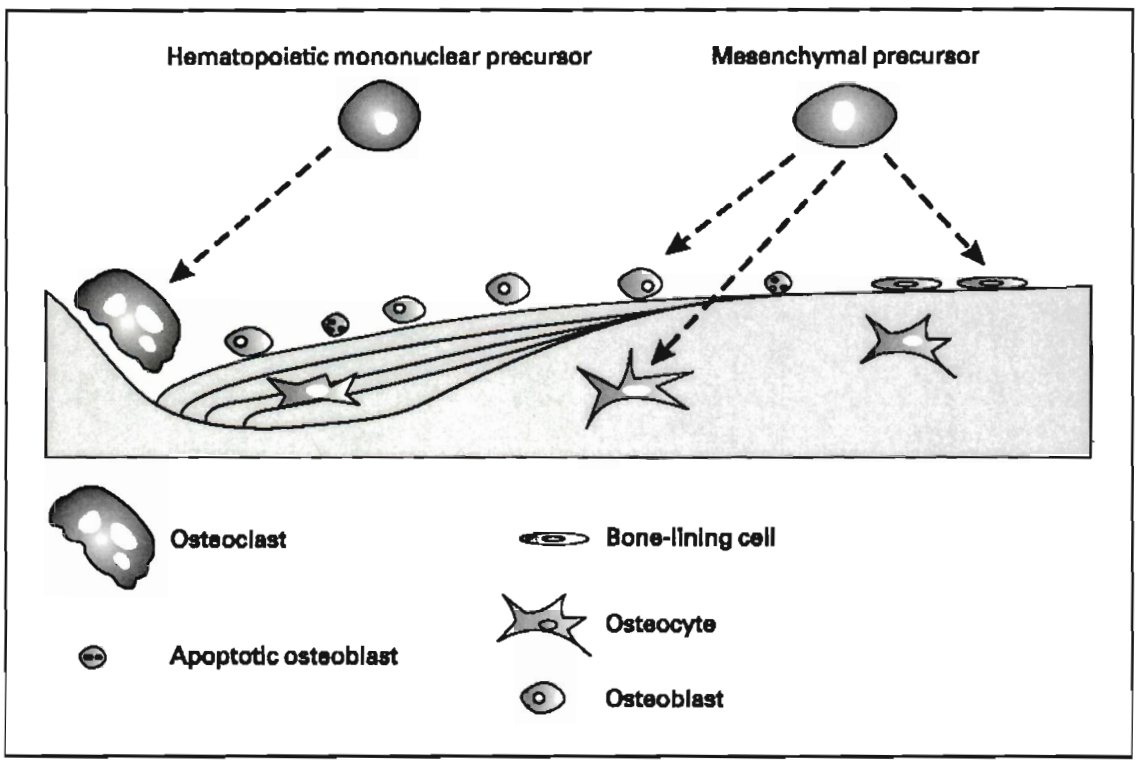

Figure 2. Coupled bone resorption. Osteoblasts and osteoclasts form the BMU responsible for bone remodeling. Once bone is resorbed by osteoclasts, osteoblasts migrate to the area of excavated bone and begin to deposit osteoid. Osteoblasts can become embedded in the osteoid, thus becoming osteocytes. The osteoid is later mineralized, and this end product represents the newly formed bone. Osteoblasts remaining on the surface of the newly formed bone are referred to as bone-lining cells. From: Chan, G.K. and G. Duque. 2002. *Gerontology*. **48**: 62-71.

A very particular feature, the ruffled border, is the consequence of deep foldings of the plasma membrane in the area facing the bone matrix. This border is surrounded by a ring of contractile proteins (sealing zone) that serves as an attachment mechanism to improve the surface of bone resorption (1,2,13). There is a close attachment between the osteoclast and the bone matrix by integrin receptors that bind to specific sequences in the matrix proteins (1). The ruffled border area has not only lysosomic enzymes but also a specific electrogenic proton adenosine triphosphatase (ATPase), involved in acidification (1,2,14). The plasma membrane in the basolateral surface of the osteoclast is highly and specifically enriched in (Na^+, K^+) ATPase (sodium potassium pumps), HCO_3^-/Cl^- exchangers, and Na^+/H^+ exchangers(14).

Once osteoclasts are activated, some changes happen in their structure that includes polarization and formation of the ruffled border (1,14). This change in their cytoskeleton is followed by activation of the enzymatic activity and consequently by bone resorption. The process of bone resorption by the osteoclasts is initiated by lysosomal enzymes secreted through the ruffled border (1,14). Furthermore, metalloproteinases are also secreted to the bone resorbing compartment. In addition, a complex electrolyte interaction also happens in the compartment due to changes in the local pH (acidification), secondary active transport of calcium in association with a $Na+/Ca^{++}$ exchanger and/or Na^+/H^+ antiport. The subsequent phases of bone resorption will include: first, dissolving of the crystals by the low pH; second, the enzymatic degradation of the matrix and third, the release of the residues at the basolateral domain (1,14). Once the resorbing phase of the bone turnover process is completed, osteoclasts undergo apoptosis to be replaced by the new bone forming osteoblasts (2).

1.1.4 Trabecular and cortical bone

There are two different type of bone in the adult skeleton: cortical and trabecular (or cancellous) bone. Trabecular bone is present in vertebral column, the wrist and elsewhere, and represents >60% of the total bone while cortical bone is located in higher proportion in the femur. There are very significant differences in the structural characteristics of each type. Cancellous bone is composed of multiple trabeculae in intimate contact with the bone marrow cavity (Fig. 3,A) while cortical bone is on the surface of the bone and is mostly composed of lamellar disposition of collagen with a "haversian" and canalicular system (Fig. 3,B)(2).

Although there are contradictory findings, it seems that the rate of bone turnover in cortical bone is lower than the trabecular one (1,16-18). This is probably due to the fact that trabecular bone is in closer contact with the bone marrow environment and as a result it is under the permanent influence of cytokines and GF (12). The higher levels of exposure to cytokines by trabecular bone will induce an increased number of active bone cells (9-12) with higher levels of bone turnover.

1.1.5 Overview of osteoblast-osteoclast interaction

The coupling of bone formation to previous bone resorption is a well described system of coordination between osteoblasts and osteoclasts (1-3,8,13). This process is the consequence of the multiple intracellular and extracellular signals in the bone microenvironment.

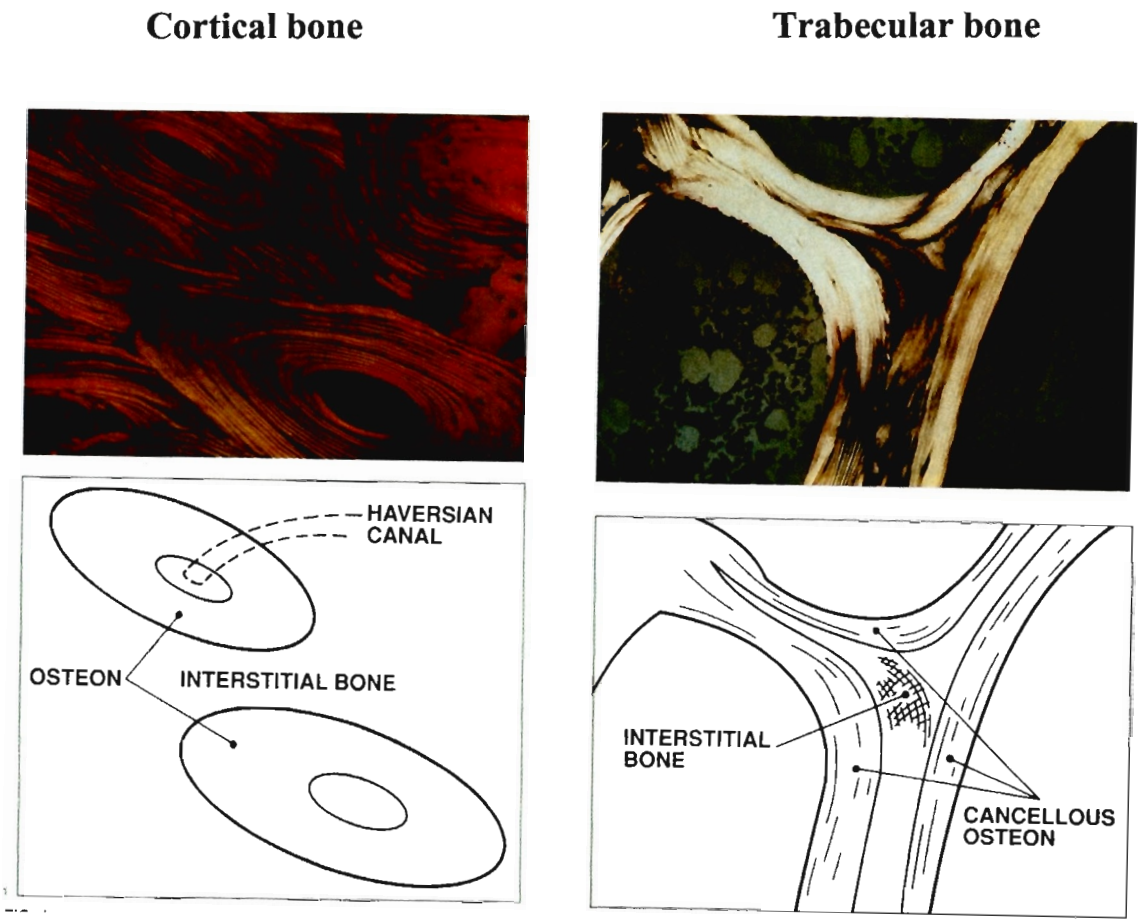

Figure 3. Cortical and trabecular bone. The figure shows the particular features of the two types of bone. Cortical bone has a haversian distribution while trabecular or cancellous bone is formed of multiple trabeculae, which harbor the bone marrow. From: *Bone Histomorphometry*, ASBMR, 1998.

Osteoblasts and osteoclasts are closely connected by a very specialized mechanism of communication. Osteoclast precursors and mature osteoclasts have a membrane receptor known as receptor activator of nuclear factorκB (RANK) which belongs to the family of Tumor Necrosis Factor (TNF) receptors required for osteoclast differentiation, maturation, and survival (1,2,14). RANK activation depends on the presence of its ligand (RANK-L) produced by osteoblasts after exposure to different stimuli such as hormones and cytokines. Osteoblast precursors express RANK-L in their membranes or release it into the bone matrix to stimulate osteoclastogenesis (OC) and differentiation (14). RANK-L is mostly produced in the osteoblast precursor (pre-osteoblasts). Interestingly, the fact that only osteoblasts precursors are able to produce RANK-L explains why, during the first phase of the coupling process, there is an active osteoclastic differentiation and activation. Furthermore, as a regulation process, mature osteoblasts produce a decoy receptor for RANK called osteoprotegerin (OPG) (11-14). OPG binds to RANK by a competitive manner and prevents the interaction between RANK and RANK-L, thus decreasing OC and osteoclast differentiation and increasing osteoclast apoptosis (Fig. 4) (12).

There are multiple regulators of either RANK-L or OPG expression by the osteoblasts. While vitamin D and PTH are known to induce RANK-L expression by osteoblast precursors (2), sex steroids (androgens and E_2) have been shown to suppress RANK-L by blocking some of the key transcription factors (19-23). They also induce OPG expression by mature osteoblasts thus reducing the number of active osteoclasts and inducing osteoclast apoptosis (19).

In addition, cytokines and GF play an important role as regulators of the osteoblast-osteoclast interaction. The most important factors that induce RANK-L expression by osteoblastic stromal cells include prostaglandins (PG) of the E series(24,25), TGF-beta (26) and cytokines such as interleukin (IL)-6, IL-11, lymphocyte-inhibiting factor (LIF) and oncostatin M (26).

In summary, osteoblasts are important regulators of the osteoclast differentiation and activity through the release of RANK-L and OPG whose secretion is regulated by external factors like such as hormones and cytokines. The fact that RANK-L is only secreted by osteoblast precursors while OPG is secreted by mature osteoblasts explains why there is a well coordinated mechanism of bone resorption followed by bone formation.

1.1.6 The bone matrix

The main component of bone matrix is type-I collagen (constituting 90% of the total protein). The rest is composed of non-collagenous proteins, mostly serum-derived proteins such as albumin and α2-HS glycoprotein with a high affinity for hydroxyapatite. Crystals of hydroxyapatite are found on the collagen fibers in a closely binding -bonded complex (1,12,25) .

Osteocytes are the only cellular component of the bone matrix since they are embedded inside the matrix in the osteocytic lacunae (25.000 mm^2 of bone). Osteocytes are surrounded by the periosteocytic space which is filled with extracellular fluid (ECF). This space is a constant source of calcium exchange between the newly mineralized matrix and

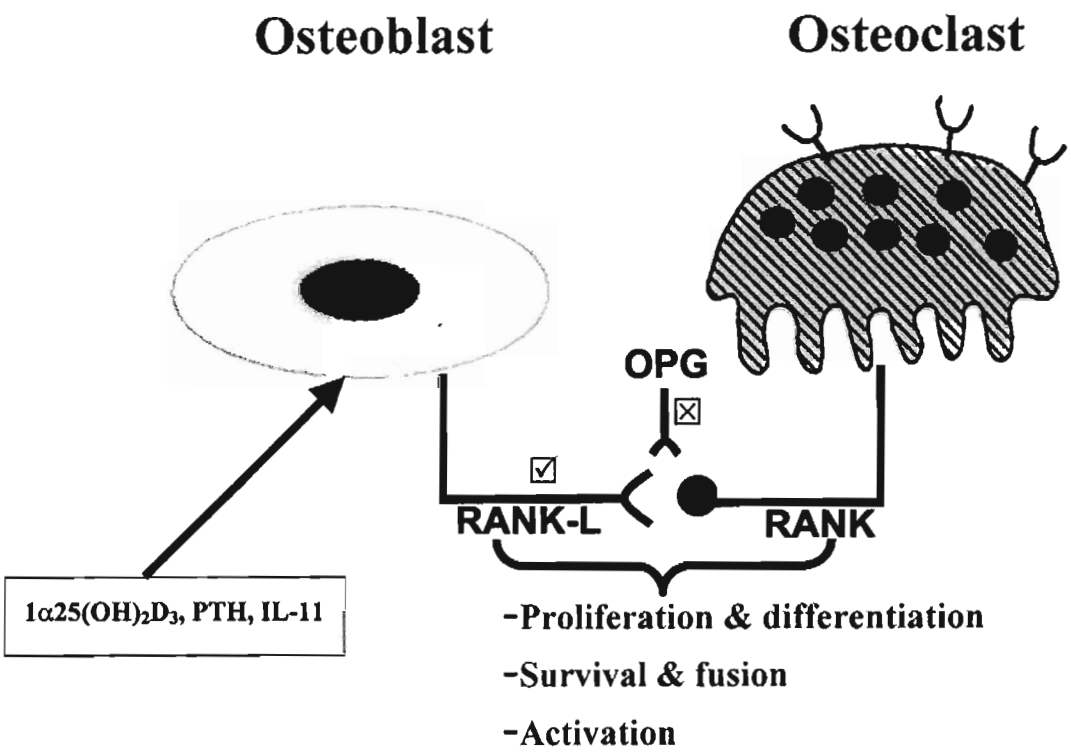

Figure 4. A schematic representation of osteoclast differentiation and function supported by osteoblasts stromal cells. Osteoblasts respond to PTH, $1,25(OH)_2D_3$ and IL-11 by expressing the ligand for RANK (RANK-L), thus stimulating osteoclast differentiation, proliferation and activation. OPG acts as a decoy receptor for RANK-L, thus regulating this mechanism.

the ECF (1,12). Finally, other components of the bone matrix include GF, cytokines, PGs and enzymes, which diffuse from the circulation (1,26).

1.1.7 The role of systemic hormones and local factors in regulating bone turnover

The synchronization between the two cells involved in bone remodeling is due to the specific effect that both systemic hormones and local factors have on either osteoblasts or osteoclasts. These effects include: (a) replication and differentiation of undifferentiated cells, (b) the recruitment of cells, and (c) the differentiated function of cells (2). Local factors include GF, cytokines and PGs that are secreted by skeletal cells(19,26), while systemic hormones include vitamin D, PTH, calcitonin and sex steroids (E_2 and androgens).

GF are polypeptides that regulate the replication and differentiated function of cells. The main GF in the bone micro-environment are the insulin-like GF (IGFs), transforming growth factor-β (TGF-β) family, fibroblast GF (FGFs) and platelet platelet-derived growth factor (PDGF). Additionally, cytokines such as IL-1,-4,-6 and -11, colony-stimulating factors (CSFs), and TNFs play an important role in the regulation of bone bone-cells function (26-28).

Systemic hormones also have also divergent effects on bone cells. PTH induces osteoclastic activity and differentiation (2,29) and induces osteoclast apoptosis (11) additionally preventing osteoblast apoptosis (29). Furthermore, vitamin D_3 has been shown to induce osteoclastic activity *in vitro* while inhibiting it *in vivo* and also stimulates the expression of RANK-L by osteoblasts (2,11,12). Calcitonin, produced by the thyroid gland, is a potent inhibitor of osteoclastic bone resorption and (1,11,12) has been shown

to be able to inhibit osteoblast apoptosis (30). Finally, E_2 induces osteoclast apoptosis and enhances osteoblastogenesis (OB) (12,18) while androgens have been shown to have an anti-apoptotic effect on osteoblasts (11) and also induce OB (11,12).

In summary, the interaction between these factors is responsible for the coordinated process of bone remodeling and suggests an attractive potential for therapeutic agents. However, some divergent results have been obtained between the effects of these factors *in vitro* vs. *in vivo* and these results require further investigation.

1.2 Mechanisms of OB

1.2.1 Osteogenic differentiation of MSC

The process by which MSC differentiate into adipogenic or osteogenic cells is defined by lineage-specific gene expression and enzyme activity (31,32). Thus MSC have the potential to become either osteoblasts or adipocytes depending on the genes that they express in response to external or internal factors. It is also known that mature osteoblasts and adipocytes have the potential to trans-differentiate, which is known as "plasticity". This is an important field for research since adipocytes in bone marrow could become osteoblasts after exposure to the appropriate factors (33-38).

There are two osteoblast-specific transcripts: Runx2/Cbfa1, a transcription factor, and the other encoding OSN, a secreted molecule that inhibits osteoblast function (39-44). More recently, a novel zinc finger-containing transcription factor, osterix (Osx), was found to be required for osteoblast differentiation and bone formation (Fig. 5) (45).

In general, when MSC are exposed to stimuli, two osteoblast-specific cis-acting elements (OSEs) — the promoters of the OSN gene (bgp) — are activated: OSE1 and OSE2 (39,40). Runx2/Cbfa1 binds to OSE2 and acts as a transcription factor inducing MSC

differentiation into the osteoblast lineage (39,40). Mice deficient in Runx2/Cbfa1 develop to term with a normally patterned skeleton that is made exclusively of cartilage with a total absence of osteoblast differentiation (41,42).

In summary, Runx2/Cbfa1 is the earliest and most specific marker of osteogenesis (12,39-40). However, the transcription factors that act upstream of Runx2/ Cbfa1 to control its expression remain to be identified (45).

Osx is specifically expressed in all developing bones (45). As in Runx2/Cbfa1, no bone formation occurs in Osx-null mice (45). In addition, Osx is not expressed in Runx2/Cbfa1-null mice, indicating that Osx acts downstream of Runx2/Cbfa1 (45).

The osteogenic differentiation of MSC involves not only the activation of specific transcription factors, but also the repression of potent inducers of adipogenic differentiation such as peroxisome proliferator activated receptors (PPAR) $\gamma 2$, a member of the PPAR super-family, and CCAAT/enhancer binding protein alpha 2(CEB/Pα2) (12,46-50). The predominance of the adipogenic or osteogenic effect of internal and external factors will determine the differentiation of MSC into the osteoblastic or adipocytic lineage (51)(Fig. 6).

Once MSC are committed to become osteoblasts their process of differentiation happens in three developmental stages that have been well described *in vitro* (Fig. 7). When MSC are exposed to osteoblastogenesis induction media (OIM), it takes on average 21 days to become mature osteoblasts. This 21-day- period has been divided to three phases of around 7 days in length: proliferation, matrix maturation and mineralization (Fig. 7) (32).

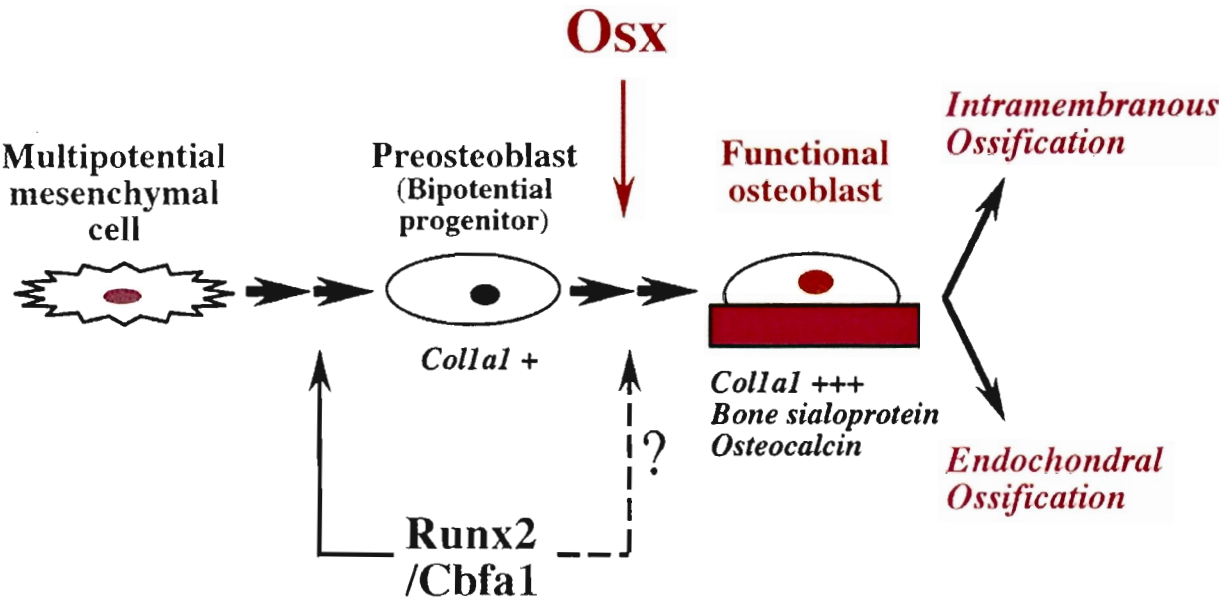

Figure 5. The pathway of osteoblastic differentiation. MSC are committed to differentiate into pre-osteoblasts after expressing Runx2/Cbfa1. Once they differentiate into pre-osteoblasts, another factor, Osx, is required to inhibit their possible differentiation into chondrocytes. The pre-osteoblasts will then differentiate into functional osteoblasts able to produce collagen, bone sialoprotein and OSN. From: Nakashima, K. et al. 2002. *Cell*. **108**:17-29. (Adapted with authors' permission).

During proliferation, (H4) histone, growth factors (TGF-β1), adhesion proteins (fibronectin), collagen, and low levels of osteopontin (OPN) are expressed. During the matrix-maturation period there is a characteristic and marked increase in ALP levels. Finally, during the mineralization period, there is an increase in mRNA transcripts of OSN, OPN, and bone sialoprotein which reflects Ca^{+} deposition (32).

Although the genes involved in this process have been extensively described in human and murine tissues, however, the role of several of the new genes found in this process remains to be elucidated.

1.2.2 The signaling of OB

Members of all major families of GF have been implicated in the control of osteoblast differentiation during embryonic development and mature life (52-54).

Indian hedgehog (Ihh) is the growth factor that has the greatest impact on osteoblast differentiation *in vivo* (55,56). Its main role is the regulation of chondrocyte apoptosis followed by the recruitment of osteoblast precursors during embryonic development mainly during endochondral ossification (56).

The first step is the differentiation into pre-osteoblasts of MSC present in the mesenchymal condensations of both endochondral and membranous skeletal elements. Although both Runx2/Cbfa1 and Ihh play an important role in this process, their direct interaction remains unclear (40,44,45). Dlx5 and Dlx6 are homeobox proteins that affect also osteoblast differentiation *in vivo* (40). These proteins act downstream of Runx2/Cbfa1and may interact with OSE1 to continue the process of differentiation (44).

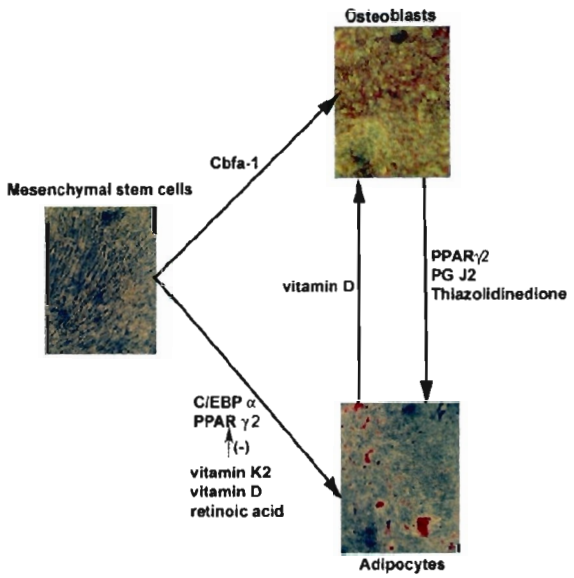

Figure 6. MSC differentiation.

Multi-potent MSC can differentiate down several lineages depending on the activation of specific transcription factors and the presence of specific hormones or GF in the bone marrow microenvironment. Expression of Runx2/Cbfa1 and Osx are required for osteogenic differentiation, whereas C/EBP α and PPARγ 2 are required for adipogenic differentiation. Vitamin K2, $1,25(OH)_2D_3$ and retinoic acid have all been shown to inhibit PPARγ 2 and thus AD.

Under the influence of PG J2 and thiazolidinedione, cell plasticity allows for the trans-differentiation of osteoblasts to adipocytes. In a similar manner, $1,25(OH)_2D_3$ has been shown to induce osteogenic trans-differentiation of adipocytes.

Pre-osteoblasts have the potential to differentiate into both osteoblasts and chondrocytes (38). In this step, the presence of Osx is required to inhibit the expression of pro-chondrogenic factors (Sox9 and Sox5) (45). Once these factors are inhibited, the pre-osteoblast becomes a functional osteoblast with the capacity to express ALP and produce bone matrix.

1.3 AD inside the bone marrow

1.3.1 The PPAR family

Multipotential stem cells have the potential to differentiate into osteoblasts, chondrocytes and adipocytes in the bone marrow microenvironment depending on the activated pathway. It is important to understand the factors that activate or inhibit this differentiation process since a predominance of the osteogenic differentiation must be maintained to keep an appropriate bone mass.

Adipogenic differentiation of MSC is stimulated by endogenous hormones including insulin, growth hormone and glucocorticoids, as well as by pharmacological agents such as isobutylmethylxanthine (IBMX) and thiazolidinediones (TZD). This process involves the activation of transcription factors such as PPARγ2 and C/EBPα or by the repression of other factors such as Runx2/Cbfa1(Fig. 5 and 6)(47-49). Lineage-specific gene activation in mature adipocytes induces the production of several marker proteins that are used as indicators of adipocyte differentiation such as lipoprotein lipase, glycerol-3-phosphate dehydrogenase and the fatty-acid acid-binding protein aP2 (49).

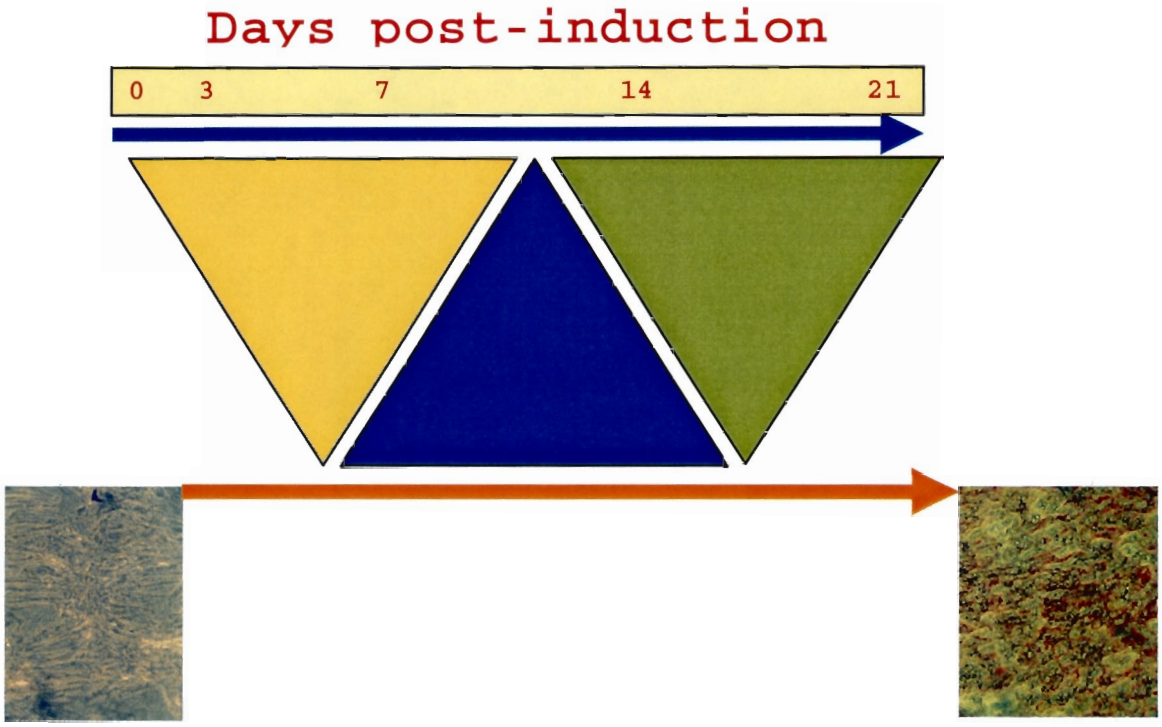

Figure 7. Schematic representation of the MSC differentiation into osteoblasts *in vitro*. Cultured MSC exposed to OIM will be committed to differentiate into osteoblasts. This process takes ±21 days divided to three periods: proliferation, matrix formation and mineralization represented by the yellow, blue and green triangles, respectively. After 21 days, fully differentiated osteoblasts are able to produce bone bone-matrix mineralization. The figure shows MSC in culture before exposure to OIM (left panel) and after exposure to OIM for 21 days (right panel). In the right panel, calcium deposits are stained with Alizarin red.

PPARγ belongs to the PPAR family of nuclear receptors that were initially described as orphan receptors (49). PPARγ is mainly found in brown and white adipose tissues and to a lesser extent in the large intestine, the retina and some tissues of the immune system. This receptor possesses a canonical domain structure in common with other nuclear receptors. This structure includes an amino-terminal A/B domain that is poorly conserved between the three PPAR isotypes, and contains a ligand-dependent transactivation function known as AF-1, whose phosphorylation contributes to the modulation of PPARγ activity (48).

After an appropriate agonist activates PPARγ2 in MSC, osteoblasts, fibroblast or even myocytes, there is consequent activation of fat-forming specific genes. Furthermore, fat-selective enhancers such as those in the aP2 and phosphoenolpyruvate carboxykinase (PEPCK) are activated, as are the genes for lipoprotein lipase (LPL), fatty-acid-transport protein, and the fatty-acid translocase (48). As mentioned previously, a key interaction in the adipogenic differentiation pathway is that between PPARγ and the CEB/Ps that augment the cellular response to adipogenic stimuli.

PPARγ2 is not only expressed early in AD but has also the potential to induce trans-differentiation of osteoblastic and fibroblastic cells into adipocytes. It has also shown a potential for blocking OB *in vitro* (46). This effect has been demonstrated in the murine-derived mesenchymal progenitor cell line U33/γ2, where an inhibitory effect of PPARγ2 was found to be due to the suppression of Runx2/Cbfa1 (46).

In summary, activation of the PPARγ2 transcription factor is a required step for the differentiation of pluripotent mesenchymal cells into adipocytes. Furthermore, PPARγ2 has the capacity to inhibit OB and to induce trans-differentiation of mature osteoblasts.

1.3.2 The regulation of adipogenic signaling

The ligands that activate PPARγ are physiologic and pharmacologic. Endogenous ligands include fatty acids and their derivates such as linoleic acid, 15-deoxy-12, 14-prostaglandin J2 and leukotriene B4. Pharmacological agents include hypolipidemic drugs (fibrates), anti-inflammatory agents such as indomethacin and fenoprofen, and insulin-sensitizing drugs such as Rosiglitazone (48). However, the prostaglandin G2 metabolite PGJ2 is the most potent natural ligand described so far (47,48).

Mice homozygous for targeted disruption of the gene encoding PPARγ2 are early embryonic lethal whereas conditional disruption results in defects in white and brown adipose tissue (48). A number of studies have shown that repression of PPARγ2 activity in cultured cells can inhibit the differentiation of precursors from the adipocyte lineage. IL-9, 9-cis retinoic acid and vitamin K2 all inhibited ligand-induced adipocytic differentiation of marrow stromal cell cultures by PPARγ and/or C/EBP-mediated pathways (47-49). When pre-adipocytes previously treated with thiazolidenione are exposed to either retinoic acid or $1,25(OH)_2D_3$, a potent inhibition of the thiazolidenione-induced AD was seen (49-51). The mechanisms by which these factors inhibit PPARγ2 might include occupancy of 60% the free space in the ligand-binding domain or, by competitive inhibition of binding to RXR, to form transcriptionally active heterodimers (48). Alternatively, since PPARγ2 and C/EBPα complement each other, the inhibition of their particular interaction may play a role in the inhibition of AD without affecting OB. In summary, exposure of mesenchymal precursors to PPARγ2 ligands invariably induces AD but has a variable effect on OB. In contrast, inhibition of PPARγ2 with steroid hormones potently inhibits AD.

1.4 Apoptosis and bone

1.4.1 Apoptotic pathways

Cell death by apoptosis is an important component of growth during embryogenesis, organogenesis and tissue morphogenesis (57). The concept of apoptosis, or programmed cell death, has changed in recent years after a number of different death mechanisms were described (58). In general, apoptosis is known as the process of cell death associated with caspase activation or caspase-mediated cell death (59). Caspases constitute a group of cysteine proteases with two aspartate cleavage sites, one of which excises the prodomain while the other cleaves the large domain from the small domain (57). There are two types of caspases: initiators (e.g. caspase-2, -8, or caspase-10) cleave a variety of key proteins to irreversibly alter cell function and activate cleavage of the prodomain of the second group, the executioner caspases (caspase-3,-6 or -7). Further more, executioner caspases activate non-caspase effectors (endonucleases) which initiate the process of nuclear fragmentation previous to phagocytosis by neighboring cells (57) (Fig. 8).

There are many mechanisms to activate apoptosis *in vitro* including radiation, serum starvation, antibodies against death receptors, etc. By contrast, the mechanisms that activate apoptosis *in vivo* are more complex and involve the confluence of multiple factors (60). Finally, one important phenomenon directly related to activation of apoptosis in multiple organs and tissues is aging (58,59).

Figure 8. Proposed mechanisms for osteoblast apoptosis. After known (hormone-deprivation, oxidative stress) apoptotic stimuli, TNF and Fas are activated in the bone microenvironment. TNF acts on the TNF receptor in osteoblasts that subsequently stimulates the TNDR-1-associated domain (TRAD). Furthermore, the activation of Fas will induce the activation of Fas-associated death domain (FADD) with the further activation of caspase-8. The result is an increase in the proapoptotic Bax and a decrease in the anti-apoptotic Bcl-2, thereby inducing apoptosis. The question marks indicate a potential but still undefined role on osteoblast apoptosis. From: Chan, G.K. and G. Duque. 2002. *Gerontology*. **48**: 62-71. (Adapted with author's permission).

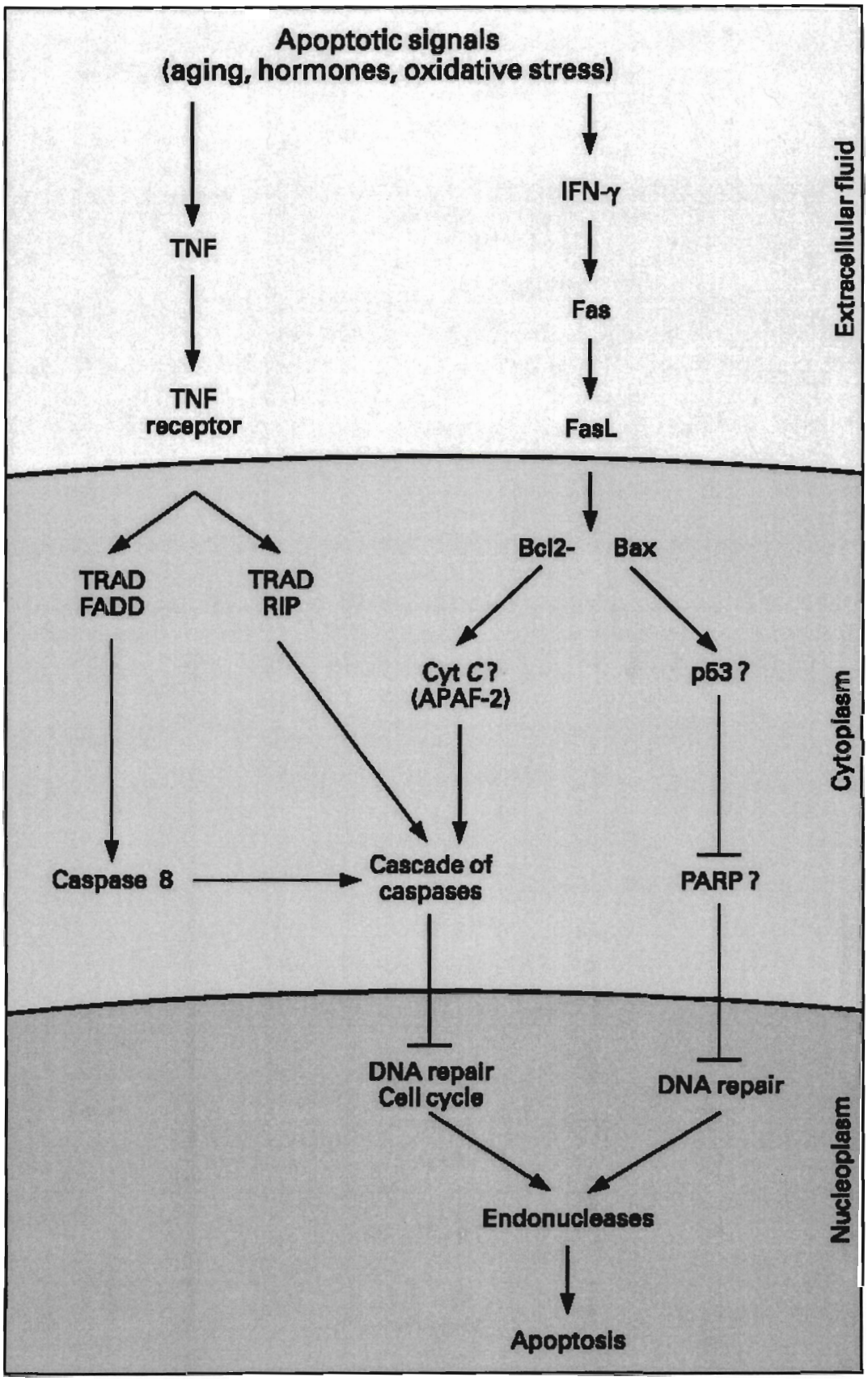
Apoptotic signals
(aging, hormones, oxidative stress)
TNF
TNF
receptor
IFN-γ
Fas
FasL
Extracellular fluid
TRAD
FADD
TRAD
RIP
Bcl2-
Bax
Cyt C?
(APAF-2)
p53 ?
Cytoplasm
Caspase 8
Cascade of
caspases
PARP ?
DNA repair
Cell cycle
DNA repair
Endonucleases
Apoptosis
Nucleoplasm

There are two well known apoptotic pathways that can be activated either by key proteins released into the cytosol by the mitochondria or as a consequence of activation of cell-surface death receptors (61). The mitochondria-activated pathway can be activated directly by apoptogens or indirectly by activation of caspase enzymes (8,11,61). Once pro-apoptotic members of the Bcl-2 family of proteins and certain Bax protein family members are inserted into the mitochondrial membrane, cytochrome c (cyto-c) is released into the cytosol (8,11,61). Once released, cyto-c interacts with apoptotic protease-activating factor 1 (Apaf-1) and pro-caspase-9 to form an apoptosome complex which activates caspase-9, which in turn finally activates the cascade of caspases (8,11,61). The second pathway or "death receptor activated" involves the activation of the TNF receptors (TNFR) superfamily (FADD,TRAF,TRADD,RIP etc.). These complexes will cleave and activate one or more initiator procaspases and as a result activate the cascade of caspases (Fig. 8)(11,61).

Apoptotic cells are recognized by specific morphologic features that distinguish them of from necrotic cells. These features include loss of cell junctions, collapse of the chromatin accompanied by fragmentation of DNA, membrane blebbing and finally phagocytosis by neighboring cells (8,11). A number of techniques are able to detect the apoptotic changes. The most commonly used techniques include Annexin V to detect changes in the cell membrane during the early phases of apoptosis, terminal deoxynucleotidyl transferase-mediated dUTP biotin nick end labeling (TUNEL) assay to document cell fragmentation, detection of DNA fragments by agarose gel electrophoresis and electronic microscopy(57,62).

1.4.2 Apoptosis in the bone microenvironment

The role of apoptosis in embryonic limb development, skeletal maturation, adult bone turnover and fracture healing is well known (11,61). Apoptosis regulates the loss of soft tissue between the embryonic digits during limb development (61), in addition, during fracture healing, osteoblasts and chondrocytes coordinate their levels of apoptosis (61). However, the most recent discoveries concerning the role of apoptosis in bone are oriented to elucidate its mechanisms during the process of bone turnover.

1.4.2.1 Osteoblast apoptosis

As previously mentioned, one of the three fates of mature osteoblasts is death by apoptosis (61,63-65). Although the activated pathways during the apoptotic process in osteoblasts remain unclear, some evidence has demonstrated that the activation of the death receptor Fas is the main mechanism involved in osteoblast apoptosis (62). Additionally, TNF-related apoptosis inducing ligand (TRAIL) activation by TNFα has also been described (Fig. 8)(64).

There are some factors that regulate apoptosis in osteoblasts acting as inhibitors (FGF-2, IGF-I and II, PDGF) or stimulators (TNF-α) (8,64). In addition, RANK-L and OPG have been implicated as regulators of cell survival (8,11). RANK-L has been shown to promote the survival of T cells, dendritic cells and osteoclasts (8); however its role in osteoblast apoptosis has not been elucidated. Furthermore, OPG can bind TRAIL, which induces apoptosis through cell-death receptors, and subsequently inhibits apoptosis in Jurkat cells. Although, an effect of OPG on osteoblast apoptosis has not been documented, the fact of TRAIL inhibition opens a door to future research.

1.4.2.2 Osteocyte apoptosis

Osteocyte apoptosis is probably responsible for many empty lacunae are seen in old bone (66). There is evidence that osteocytes die with increasing age of the individual, in some disease states, and after estrogen loss (67).

Although the mechanism to explain this process still remains unclear, a higher apoptotic index has been seen in cortical bone relative to trabecular bone and may be a consequence of the level of bone turnover at these sites. The replacement of apoptotic osteocytes in cortical bone may not occur to the same extent as in trabecular bone due to its lower rate of turnover (68). Some studies have demonstrated that bcl-2 levels are higher in low-turnover bone and this may also explain the higher frequency of apoptosis in osteocytes of cortical bone (68).

1.4.2.3 Osteoclast apoptosis

Apoptosis in the osteoclast has been widely described as the mechanism that regulates the number and activity of osteoclasts in the BMU (69). After osteoclasts finally stop resorbing bone, they die by apoptosis and are quickly removed by phagocytes during the early portion of the reversal phase (69,70).

Osteoclast apoptosis may happen with greater frequency in abnormal bone remodeling. For example, after E2 deprivation during the menopause (69-71) or in Paget's disease the number of apoptotic osteoclasts decreases (68). In both situations, the higher number of active osteoclasts will increase the level of bone resorption with the subsequent appearance of osteoporosis (70,72).

1.5 Age-related bone loss

1.5.1 Aging and bone

Aging is the consequence of an array of phenotypic variations that appear to involve intrinsic or constitutional properties in all cells and systems including qualitative and quantitative alterations in development, maturational structure and function. The concept of senescence of cells in culture is different since it refers to the limited number of population doublings that most diploid cells express when maintained in culture. By contrast, senescence of cells *in vivo* can be defined as the consequence of multiple internal and environmental factors that will trigger the mechanisms of aging and finally will affect the function of cells and their capacity to respond to stressful events.

As an individual ages, distinct changes take place in trabecular bone, cortical bone and bone marrow. Reductions in trabecular volume, number, and width have been well documented in specimens of older bone (8,15,73-75).These alterations are due to a variety of factors, including changes in gonadal status, nutrition, physical activity, and probably by the pure aging process (8,15,76).

Estrogen-deprived bone will favor the development of a milieu that is detrimental to bone maintenance by increasing factors such as ILs, TNFs, and CSFs thereby favoring osteoclast formation and inhibition of osteoclast apoptosis (1,8,77). This increase in active osteoclast numbers with an increase in osteoblast life expectancy results in uncoupling of bone turnover.

After the third decade of life, other important events take place in bone including increasing levels of bone marrow AD and osteoblast apoptosis (Fig. 9)(8). The mechanisms to explain these osteoblast differentiation and life-span-related phenomenon have not been elucidated.

Besides a reduction in trabecular bone volume in the elderly, there also exists a reduction in cortical bone (74). This reduction is attributed to bone resorption on the osteal surface that occurs at a greater rate than periosteal apposition growth (74-76). The result is a reduction in cortical width as aging progresses (74). In addition, there is an increasing number of apoptotic osteocytes and empty lacunae in cortical bone during aging (61). As the cortical bone shrinks, the bone at the interface adjacent to cancellous bone becomes porous, and its architecture no longer resembles cortical bone, but cancellous bone (75). Because lamellar bone deposition can only occur on preexisting bone, the change in the architecture of the endosteal surface as a result of increased porosity leads to a loss in ability to deposit new bone on the endosteal surface, and as a result, the cortical bone loss is most likely irreversible (75).

With aging, there is a significant change in osteoblasts function including their level of expression of most receptors to hormones, cytokines and GF (8,15). It is known that the number of E_2 and androgen receptors decreases with aging in normal osteoblasts (8,15). Similar changes in number and quality have been described in IGF, TGF and bone morphogenic proteins (BMPs) (8,15). However, the significance of these changes is poorly understood.

1.5.2 The deficit in OB

The maintenance of bone integrity would require the commitment and differentiation of pluripotent mesenchymal cells towards the osteoblastic lineage. One of the possible related mechanisms that may explain the reduction in bone formation during aging is most probably the decrease in the recruitment of osteoblasts with a lower differentiation of MSC into the osteogenic line (Fig. 9).

MSC are committed to differentiate into osteoblasts by many factors in the bone microenvironment (77). Among these, the family of BMPs plays an important role in the regulation of this process. BMPs are members the TGF-β family of signaling molecules and have been shown to be potent inducers of both osteoblast commitment and differentiation (78-83). There is a close interaction between the presence of specific BMPs (BMP-2,-4 and -7) (83-88)and the activation of the osteogenic pathway described in section 1.2.2. Once cells are committed towards the osteoblastic lineage, they are aptly named osteoprogenitors.

Osteoprogenitor-cell proliferation is enhanced by multiple factors including FGF, TGF-β, PTH and PTHrP, PGs and IGF (88-92). Most of these have been shown to be able to regulate Runx2/Cbfa1 expression (92-99). Although the process of differentiation of pluripotent MSC toward a mature osteoblastic phenotype is well known, changes in the level of its regulating factors in the bone microenvironment during aging have not been fully evaluated and could present a new area for research.

1.5.3 The increasing levels of adipogenesis(AD)

Any decrease in total bone volume results in an increase in bone marrow AD (8). This replacement of bone marrow with fat cells has been well documented in cases of age-related osteopenia (8,15) (Fig. 10).

Multiple mechanisms have been proposed to explain this increase in AD in aging bone. Marrow adipocytes may play a passive role by occupying space that is no longer required for hematopoiesis or they may be involved in general lipid metabolism involving the clearing and storing of circulating tryglycerides (8,15,45). Adipocytes are a source of

leptin that has been shown to be an angiogenic factor and may be associated with vascularization within the bone marrow (100).

Furthermore, bone marrow adipocytes may be a consequence of the inappropriate differentiation of the pluripotent MSC from other lineages (8,48,101-106). This theory can be explained by the evidence showing that the determining factors for the osteogenic differentiation of MSC are affected by aging (8). In addition, increasing levels of PPARγ and its ligand, PGJ2, which is seen in old bone, can induce adipogenic differentiation of MSC and osteoblasts (48) (Fig. 6).

BMPs (-2 and -4) have also been implicated in the differentiation and commitment of MSC towards the adipogenic lineage in a concentration dependent manner; high concentrations of BMP have been shown to enhance osteogenesis, whereas a low concentration of BMP enhances AD (107,108). Another mechanism that may explain the predominance of AD in bone marrow is the suppression of mitogen activated protein kinase (MAPK). Although there is evidence that any reduction in MAPK will lead to AD (109), studies assessing the relationship between MAPK and aging have shown a contradictory effect since aging induces high levels of MAPK expression in most of the systems investigated (8,109).

1.5.4 The higher number of apoptotic osteoblasts

It is well known that the process of cell dying throughout aging plays a pivotal role in the production of immunocompetent cells, the loss of neurons, and the generation of tumors and also in tissues that show functional deficit with age including bone (59). Aging *per se* will activate a mechanism that would induce intracellular and extracellular generation of

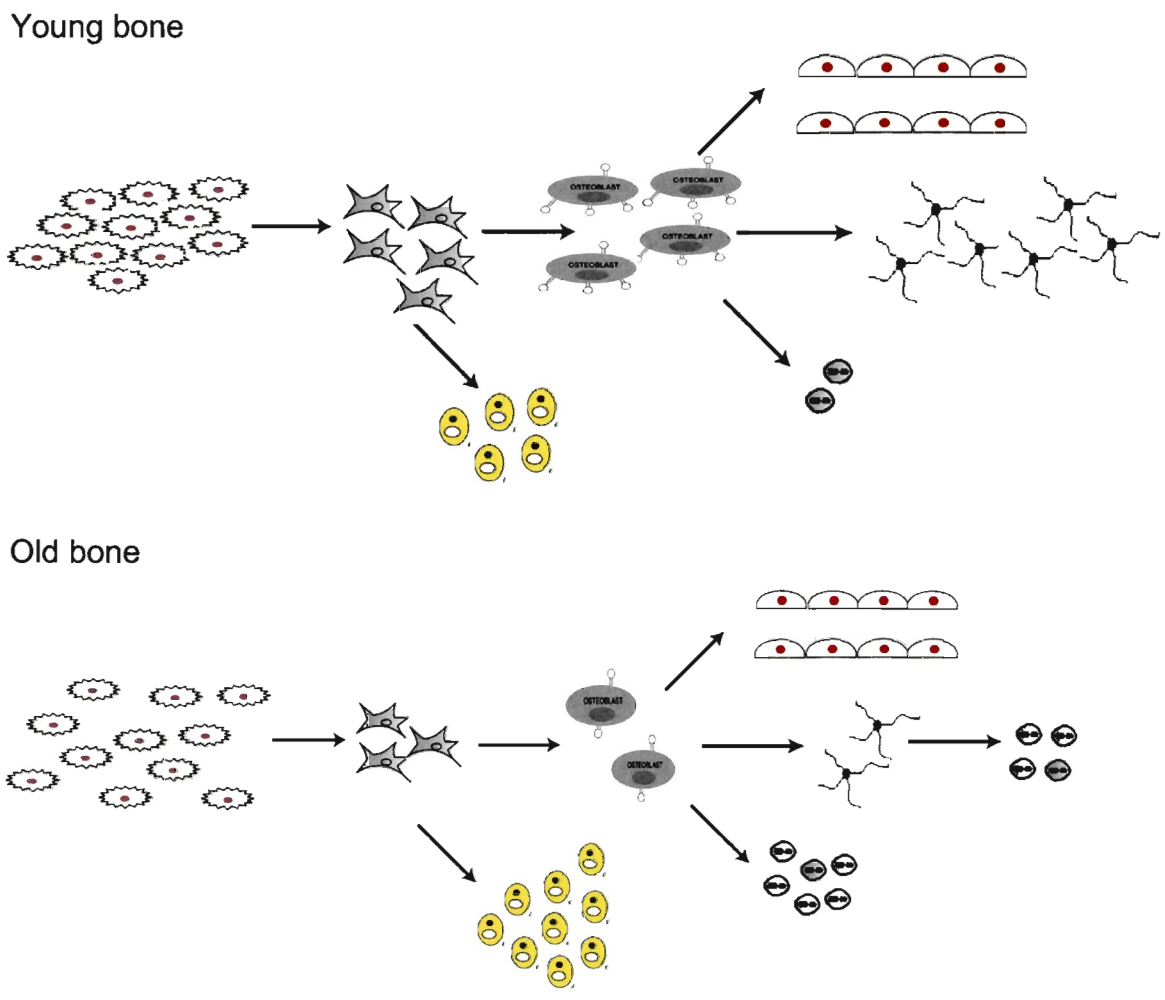

Figure 9. Cellular changes during age-related bone loss. The process of bone formation by osteoblasts depends on the number of confluent MSC into the bone marrow, the level of adipogenesis vs. osteoblastogenesis and the number of osteoblasts that become either osteocytes or lining cells versus those that die by apoptosis. With aging (Old bone) there is a lower confluence and recruitment of MSC and therefore there is a marked reduction in differentiate osteoblasts with increasing adipogenesis and osteoblast/osteocyte apoptosis. MSC Pre-osteoblast Adipocytes apoptotic OB lining cell osteocytes mature OB

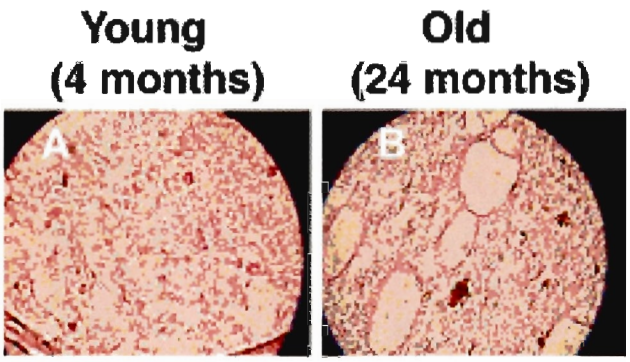

Figure 10. Increasing bone marrow AD in aging mice. Bone marrow cells are replaced by adipose tissue in aging bone, as shown by H+E staining of bone sections from young (A) and old (B) mice (magnification X40).

apoptotic signals that will encourage the self-destruction (59). These mechanisms are a subject of intense research.

In aging bone little is known about the effects of aging on apoptosis of osteoblasts, but a loss of viable osteocytes with increasing age has been described. Some experiments have shown the pathways involved in osteoblast apoptosis *in vitro* (62-66), however, these pathways have not been fully assessed in aging osteoblasts *in vivo* probably due to the technical difficult identifying and quantifying the exact number of apoptotic osteoblasts in bone sections (64).

1.5.4 Senile osteoporosis as a continuum

Senile osteoporosis, which develops in both sexes after the sixth decade of life, is the consequence not only of reduced trabecular width or "atrophy" but of both decreased trabecular width and increased trabecular spacing that contribute to bone loss with aging (8). However, these changes start much earlier in life, at around the third decade, when the peak bone mass is reached.

For an as-yet unknown reason (probably 50% genetics) (1,8), after the peak of bone mass is reached, there is a progressive and irreversible decline in bone mass that is aggravated in women during the menopausal years due to estrogen deprivation and its consequences on bone cells. Finally, after the sixth decade, another factor, aging, will explain the continuing decline in bone mass and thus the generation of weak bone with a higher risk of fracture.

1.6 Thesis objectives

The treatment of osteoporosis is based on the function of the target cell. For instance, anti-resorptive agents regulate the action of osteoclasts either by inhibiting their action or inducing osteoclast apoptosis (8). By contrast, anabolic treatment of senile osteoporosis should include the enhancement of osteoblastic activity either by stimulating OB and osteoblast recruitment, inhibiting AD to produce more mature osteoblasts, or finally by inhibiting osteoblast apoptosis (110).

As discussed above, with aging the number and the quality of osteoblasts decreases replaced by adipocytes or die more frequently by apoptosis than in young bone. Several issues pertaining to these processes have not been elucidated.

The working hypothesis of this thesis is that the aging process in the osteoblast not only affects the internal pathways that regulate its differentiation but also its interaction with external factors in the bone microenvironment such as hormones, GF and cytokines, and, in addition predispose them to die earlier by apoptosis.

The specific objectives devised to test this hypothesis aim to elucidate the following issues:

First, the changes in gene expression during osteoblast differentiation of MSC and the possible determination of new molecules involved in this process. The work described in Chapter Two establishes not only the gene changes that happen during osteogenic differentiation of human MSC (hMSC) *in vitro* but also describes a new and not previously reported pathway involved in osteoblast differentiation: the interferon-inducible genes (IFNIG). The same chapter describes how interferon gamma receptor knock-out mice ($IFGR^{-/-}$) are osteoporotic due to a deficit in osteoblast recruitment.

Second, the possible induction of OB by inhibiting AD and by regulating gene expression in bone marrow cells is described in Chapter Three in a well known mice model of senile osteoporosis, the SAM-P/6 mice. By using $1,25(OH)_2D_3$, a key molecule whose effect declines with aging, the experiments show not only that there is a gain in bone mass due to more osteoblastic activity but also that there is a significant inhibition of AD. We provide also an insight into the mechanisms involved by analyzing the changes in gene expression induced by $1,25(OH)_2D_3$ in trabecular cells.

Third, in Chapter Four, there is a reduction in vitamin-D receptors in mature osteoblasts from aged mice which was found to be reversible by E_2 where our experiments showed a recovery of the numbers and bio-response of VDR. In addition, in Chapter Four there is evidence of the anti-apoptotic effect of $1,25(OH)_2D_3$ on osteoblast apoptosis and the potentiation of that effect by E_2.

Fourth, in Chapter Five, the mechanism of osteoblast apoptosis inhibition by $1,25(OH)_2D_3$ is elucidated after the induction of apoptosis by both serum deprivation and Fas antibody (Ab). The work described in this chapter demonstrates that osteoblast apoptosis can be inhibited by the regulation of the Fas pathway and caspase-8 activity through the activation and inhibition of specific elements in these apoptotic pathways.

INTRODUCTION TO CHAPTER TWO

The process of MSC differentiation into either osteoblasts or adipocytes within the bone marrow is the consequence of the up and down regulation of multiple genes. This process might be affected by aging with a marked reduction in osteoblastogenesis with further reduction in the number of mature osteoblasts and thus in bone formation.

The elucidation of these changes in gene expression and its possible regulation will provide a new approach to the stimulation of bone marrow osteoblastogenesis and the maintenance of an appropriate bone mineral structure in late years.

In this chapter we used a human model of MSC differentiation to identify the gene changes during the two main phases of this process. We found that IFNγ is secreted by MSC into the bone marrow in an autocrine manner; subsequently, IFNγ acts as a stimulator of osteoblast differentiation through the stimulation of Runx2/Cbfa1. When the absence of IFNγ was assessed *in vivo*, a deficit in bone formation was found concomitant with features of low turnover osteoporosis.

In summary, we demonstrate that the production of IFNγ by confluent MSC is required for osteoblastogenesis and could play a role in the pathogenesis of senile osteoporosis.

CHAPTER 2

Interferon γ receptor Knock-Out induces bone loss through a decrease in bone formation

Gustavo Duque [1,2], Michael Macoritto[1], Natalie Dion[3], Louis George Ste. Marie[3], Richard Kremer[1].

[1] Calcium Research Laboratory, Department of Medicine, McGill University Health Centre, Montreal, Quebec, Canada

[2] Division of Geriatric Medicine, McGill University, Montreal, Quebec, Canada

[3] Centre Hospitalier de l'Université de Montreal, Research Center, Hôpital St. Luc, Montreal, Quebec, Canada.

The contents of this Chapter were submitted to the *Journal of Experimental Medicine*: Duque G, Macoritto M, Dion N, Ste. Marie LG, Kremer R. 2003. "Interferon γ receptor Knock-Out induces bone loss through a decrease in bone formation".

2.1 Summary

Mesenchymal stem cells (MSC) have the ability to differentiate into osteoblasts, adipocytes, chondrocytes or myocytes. In this study we first determine the genes involved in hMSC differentiation into osteoblasts by cDNA microarray analysis. We examined 12,000 human genes on the array Human Genome U95A (Affymetrix). In addition to the previously described pathways of osteoblast differentiation we found that a new set of genes known as "interferon-inducible genes" were rapidly and transiently up-regulated between 2.9 to 16.9 fold during this process. Furthermore we found that addition of interferon γ to hMSC stimulates the expression of Runx2/Cbfa1, a key regulator of osteoblast differentiation. We next assessed the role of interferon γ on bone turnover in mice expressing the interferon gamma receptor knock-out phenotype ($IFGR^{-/-}$). $IFGR^{-/-}$ mice had over 40% reduction in bone mass at both hip and spine as compared to $IFGR^{+/+}$ mice. We also noted a significant decrease in structural parameters of trabecular mass by 3D micro-CT surface/volume (BS/BV) and trabecular thickness (Tb.Th) and a significant increase in trabecular separation (Tb.Sp), $P < 0.01$. Histomorphometric analysis confirmed the decrease in BS/BV and Tb.Th and also demonstrated a significant decrease in cortical thickness (Ct.Wi) in $IFGR^{-/-}$ mice, $P < 0.01$. Histological analysis of bone sections indicated a marked reduction of osteoblast staining (alkaline phosphatase and osteopontin) as well as a reduction in Runx2/Cbfa1 and TRACP staining ($P < 0.01$) in $IFGR^{-/-}$ mice. Circulating levels of N-telopeptide and osteocalcin were also reduced by over 40% ($P < 0.01$) in $IFGR^{-/-}$ mice. Finally bone marrow cells obtained from $IFGR^{-/-}$ mice and induced to differentiate into osteoblasts showed over 70% reduction in the number of mineralized nodules as compared to bone marrow cells obtained from $IFGR^{+/+}$

mice ($P < 0.01$). Our data therefore demonstrate that interferon γ signaling regulates bone formation and that its deficiency results in low bone turnover osteoporosis.

2.2 Introduction

Senile osteoporosis is characterized by two major pathophysiological events that take place within the bone marrow: a decrease in osteoblast formation and a concomitant increase in adipocyte synthesis (8). Consequently, strategies aimed at treating senile osteoporosis should ideally regulate the balance between bone marrow AD and OB (8,37).

A particularly attractive approach would be to specifically target the process of differentiation of MSC into osteoblast. MSC are pluripotential cells that will differentiate into osteoblasts, adipocytes, chondrocytes or myocytes (37). MSC exposed to ascorbic acid *in vitro* produce a collagenous extracellular matrix and express specific genes associated with the osteoblastic phenotype such as ALP, OPN and OSN (37,76). The process of MSC differentiation into osteoblasts and the subsequent matrix production and mineralization lasts 2-3 weeks and requires not only the presence of ascorbic acid but also a source of organic phosphate (β-glycerol phosphate)(76). The dynamic changes in gene expression as cells differentiate to the osteoblast phenotype were recently described in a murine cell line with an osteoblast-like phenotype (32). A dynamic model was proposed based on the temporal changes post-induction of MSC that includes a proliferative phase (week 1), a collagen matrix deposition phase (week 2) and finally a mineralization phase (week 3)(32,111). Microchip gene array technology has been used to chart changes in gene expression during these three periods (31,32,39,111-114).

In this study, we used hMSC that display a stable phenotype, remained monolayer *in vitro* and can be induced to differentiate into adipocytes, chondrocytes, or osteoblasts (37). Our data indicate that *in vitro* IFNγ and IFNγ related genes are expressed transiently during the proliferative period and are necessary for the mineralization phase to proceed. In addition, we found that IFNγ induces early expression of Runx2/Cbfa1, an important transcription factor necessary for osteoblast differentiation (39,40). Furthermore, mice expressing the IFNγ receptor knock-out phenotype exhibit the characteristics of low turnover osteoporosis indicating that the IFNγ transduction pathway is a key regulator of bone turnover. This study therefore establishes that IFNγ is an important regulator of OB and its deficiency results in osteoporosis.

2.3 Materials and Methods

2.3.1 Osteogenic differentiation of mesenchymal stem cells in vitro

The induction of osteogenic differentiation of hMSC was described previously(76). Briefly, hMSC (BioWhittaker, Walkersville, Maryland) were plated at a density of 5 x 10^5 cells per well in 150 cm^2 dishes containing MSCGM (BioWhittaker, Walkersville, Maryland) with 10 % fetal calf serum (FCS) and incubated at 37°C for 24 hours. After the cells reached 60% confluence, media was replaced with either MSCGM or OIM (prepared with MSCGM, 10% FCS, dexamethasone, β glycerol phosphate and ascorbic acid) for 21 days. Media was changed every three days.

2.3.2 cDNA microarray analysis

Total RNA was extracted from hMSC treated with either MSCGM or OIM after the first and third week of differentiation using an Easy-Kit mini prep (Qiagen,Valencia, California). Generation of cDNA, fluorescent labeling, hybridization to the gene chip and data analysis were performed by the Genomics Laboratory at McGill University as previously described (115). We examined 12,000 human genes and ESTs (expressed sequences tags) on the array Human Genome U95A (Affymetrix, Inc. Santa Clara, CA, USA) and analyzed the results using the MicroDB™ Software (Affymetrix, Inc. Santa Clara, California). Expression values were compared between the differentiated and non-differentiated MSC using Student's t test. Genes with significant changes were then grouped depending on their known function. Gene functions were obtained by correlating them in the main scientific databases (MEDLINE, PUB-Med).This experiment was repeated twice by using the technique of biological duplicates as previously described (116,117).

2.3.3 Semi-quantitative RT-PCR

Total RNA (1 μg) was reverse transcribed with either random hexamers or oligo-dT using Qiagen One Step RT-PCR Enzyme Mix (Qiagen, Valencia, California). The resulting cDNA was amplified by 35 polymerase chain reaction cycles with an annealing temperature of 58 °C. Amplification of GAPDH was used as control. Primers were randomly selected from the list of genes with significant change after the first and third week of differentiation. Selected primers for the first week included IFI 35(5′–CTCTGCTCTGATCACCTTTGATCAC–3′upstream and 5′–GCTTCTGGAAGTGGATCTCCAGGA–3′downstream); IL10r(5′–

GAACCTGACTTTCACAGCTCAGTAC–3′upstream and 5′–TCAGGTGCTGTGGAAGAGAATTC–3′downstream);GRO 1(5′–GAACATCCAAAGTGTGAACGTGAAG–3′upstream and 5′–ATTTGCTTGGATCCGCCAGCCTCTA–3′downstream); and importin ((5′–GAGAATTGCAGAATTGGCCTGACCT–3′upstream and 5′–CTATGTCTGAGTACTTCATGCCA–3′downstream). For the third week, selected primers included: TGFBR2 (5′–TACATCGAAGGAGAGCCATTCGC–3′upstream and 5′–TGCAGCACACTCGATATGGACCAG–3′downstream); LRP5 (5′–GTCGTAGTCGATGGCAATGGCGT–3′upstream and 5′–ACGGACTCAGAGACCAACCGCATC–3′downstream); osteopontin (5′–ACTCTGGTCATCCAGCTGACTCGT–3′upstream and 5′–CTCCTAGGCATCACCTGTGCCATA–3′downstream); Osteocalcin (5′–TGGCCGCACTTTGCATCGCTGG–3′upstream and 5′–CGATAGGCCTCCTGAAAGCCGATG–3′downstream); and Osf2/Cbfa1(5′–TGGCCGCACTTTGCATCGCTGG–3′upstream and 5′–CGATAGGCCTCCTGAAAGCCGATG–3′downstream). The expected sizes of the nested amplification products were between 400 and 800 bp. Amplified products were analyzed by 2% agarose gel electrophoresis. The signals were quantified by densitometry and normalized according to Glyceraldehyde-3-Phosphate Dehydrogenase (GAPDH) density.

2.3.4 Interferon γ production in cell culture

hMSC were plated and osteogenic differentiation was induced as described above. The levels of IFNγ in the supernatant were measured from both MSCGM and OIM treated cells after the first, second and third week of differentiation by using the Human IFNγ Immunoassay (R & D systems, Minneapolis, Minnesota).

2.3.5 Treatment of differentiating MSC with IFNγ

hMSC were plated in 4 cm^2 dishes in a density of 4 x 10^4 cells per dish. At 60 % confluence, media was replaced with OIM containing either IFNγ (Sigma-Aldrich, St. Louis, Missouri) at different concentrations (1,10 and 100 ng/ml) or vehicle. After one week of treatment, media was aspirated and cells were stained for both ALP by using TT-blue+ (Sigma-Aldrich, St. Louis, Missouri) and mineralization by using Alizarin red (Sigma-Aldrich, St. Louis, Missouri). The number of ALP positive cells/field as well as the number of mineralized nodules were quantified in 10 different fields per well.

2.3.6 Detection of Runx2/Cbfa1 by Western blot analysis

hMSC were plated in 4 cm^2 dishes in a density of 4 x 10^4 cells per dish containing MSCGM with and without IFNγ (100 ng/ml). After different time intervals (1,2 and 3 weeks) cells were lysed separated by gel electrophoresis and then transferred to nitrocellulose membrane. After blocking, membranes were incubated overnight at 4°C using an Ab directed against either Runx2/Cbfa1 (Santacruz Antibodies, Santa Cruz, California), or tubulin (Sigma, St. Louis, Missouri), and the bound antibodies were detected with the corresponding secondary antibodies conjugated with horse radish

peroxidase. Blots were developed by enhanced chemiluminescence using Lumi-GLO reagents (Kirkegoard & Perry, Gaithensburg, Maryland).

2.3.7 Animals

We purchased IFGR$^{-/-}$ mice (strain name 129-Ifngr^{tm1}) from Jackson Laboratory (Bar Harbor, Maine). As a control strain we also purchased the strain name 129S1/SvImJ from the same source. Male and female were housed in cages in a limited access room. Animal husbandry adhered to Canadian Council on Animal Care Standards, and all protocols were approved by the McGill University Health Center Animal Care Utilization Committee.

2.3.8 Ex-vivo cultures of bone marrow cells

One side tibiae from four and eight week-old IFGR$^{-/-}$ and IFGR$^{+/+}$ (n= 12 per group per time point) were flushed using MSCGM, plated in 150 cm^3 dishes and incubated at 37°C for 24 hours. The floating cells containing mesenchymal stem cells were isolated and counted. 2 x 10^6 cells were seeded and then grown in 4 cm^2 dishes containing OIM. Media was changed every three days. At 21 days, media was removed and cultures were fixed in 10% v/v formol/saline solution for 5 minutes. Mineralized bone nodules were detected by Alizarin Red (pH 7.4) staining. The total number of bone nodules per dish was counted macroscopically. There were 24 dishes per group.

2.3.9 Bone mass measurements by dual energy X-ray absortiometry

DEXA analysis was performed four weeks in both groups. Hip and spine bone mineral density was measured using a PIXIMUS bone densitometer (PIXIMUS ^{TM}, GE medical

systems, Schenectady). A quality control phantom was used to calibrate the densitometer prior to each experiment.

2.3.10 Micro-CT of bone samples

Tibiae and spine were fixed in 10% formalin and scanned by micro-CT at ×40 magnification with a SkyScan 1072 and analyzed with a bone analysis software (ver2.2f, Aartselarr, Belgium). In tibiae, analyses of the trabecular bone were carried out in a 2.3-mm-thick region distal to the growth plate. For spine, we used L2 from both groups; the complete vertebra was analyzed. Parameters were acquired with a rotation of 0.9 degree between each picture with 2 frames averaging per angle and the x-ray source was set at 100 kV and 98 μA. The segmentation of the image was made by a global threshold and the voxel size is 21.90x21.90x21.90 μm; the same threshold setting was used for all the samples. Three-dimensional (3D) parameters and bone architectural measurements were made as previously described (118).

2.3.11 Histological and histomorphometrical analysis of bone

The details of these methods were described previously (119). One side femur from each animal in each group was dehydrated and embedded in methylmethacrylate (J-T Baker, Phillipsburg, New Jersey). Sections (5μm) were stained with Goldner's trichrome method. For the purpose of dynamic bone formation parameters, mice were injected with demeclocycline (SIGMA-Aldrich, St. Louis, Missouri) 20 mg/Kg of body weight seven and two days before killing. Thirty two to 40 fields were analyzed from each bone metaphysis. Histomorphometry was done with a semi automatic image analyzing system

combining a microscope equipped with a camera lucida and digitizing tablet linked to a computer using the OsteoMeasure Software (Osteometrics Inc., Decatur, Georgia). For immunohistochemistry sections were prepared and stained as previously described (120). Briefly, non-specific binding was blocked by addition of goat serum for 1 hour. Sections were then incubated with Ab to Runx2/Cbfa1, OSN, or OPN (Santa Cruz Biotechnology, Santa Cruz, CA, USA) for either 4h at room temperature or 8-24 h at 4°C. After washing with PBS, goat Ab to rabbit IgG were added to the sections at room temperature for 30 minutes, followed by 30 minutes incubation with 0.6% hydrogen peroxide + chromogen and then counterstained with hematoxylin. Control slides were incubated with rabbit IgG, according to manufacturer instructions, and triplicate tests and control slides were included in immunodetection.

2.3.12 Markers of bone turnover

Four and eight week-old $IFGR^{-/-}$ and $IFGR^{+/+}$ mice were sacrificed and blood was removed by cardiac puncture. OSN was measured in 20μl of serum using the mouse OSN immunoradiometric assay kit (Immutopics, San Clemente, California). N-telopeptide was measured in 20 µl of serum to assess osteoclastic activity using the RATtelopeptide kit (Osteometer Biotech, Hovedgade, Denmark).

2.3.13 Statistical analysis

Results of the static and dynamic histomorphometry and cell culture experiments were expressed as the mean ±SEM. Cell culture experiments were performed in triplicate and repeated three times. Differences between treated and non treated groups were determined by statistical analysis using Bartlett's test for homogeneity of variable and Turkey-

Kramer multiple comparisons test for histomorphometry measurements, all other variables were compared by using One-way Analysis of Variance (ANOVA). The animal experiment was repeated twice. A value of $P< 0.05$ was considered significant.

2.4 Results

2.4.1 IFNIG play a role in OB *in vitro*

hMSC were exposed to either MSCGM or an OIM for a total of three weeks. A human cDNA expression array containing a total of 12,000 genes was used to assess gene expression during the proliferative (week 1) and mineralization (week 3) phases of osteoblastic differentiation. The scatter plots of gene expression levels are shown for each time point, week 1(Fig. 11,A) and week 3 (Fig. 11,B) with mean mRNA expression levels averaged from MSCGM and OIM exposed cells plotted in a double-logarithmic scale. Genes identified as differentially expressed between MSCGM and OIM treated cells had a minimum of 2.5 fold increase or decrease in gene expression and appear above or under the red lines. We identified a significant change in a set of 103 genes at week 1 and another set of 104 genes at week 3. To confirm the results, we used semi quantitative reverse transcription-polymerase chain reaction (RT-PCR) on selected genes at each time point (Fig. 11, C and D). Densitometric quantification of the signals was performed normalized according with GAPDH showed a positive correlation with those found in the microarray analysis.

Subsequently, genes were grouped based on their known function in specific biological systems (Fig. 12). Genes that changed significantly at both week 1 and week 3 are indicated in bold. Genes previously identified as key elements in the osteoblastic

Figure 11. Gene expression changes after one and three weeks in hMSC under osteogenic differentiation.

For each gene, mean RNA expression levels averaged from MSCGM and OIM treated cells were plotted in a double-logarithmic scale. Genes identified as having a significantly different expression (± 2.5 fold up or down-regulation) after one (A) and three (B) weeks are above or under the red lines ($p<0.01$). Ordinate and abscissa are arbitrary fluorescent units. (C) and (D), randomly selected genes were tested by semi-quantitative RT-PCR and their level of expression was quantified by densitometry and normalized according to GAPDH density. The figure shows the levels of expression in the micro chip DNA array analysis (Affy) versus semi-quantitative RT-PCR (RT-PCR).

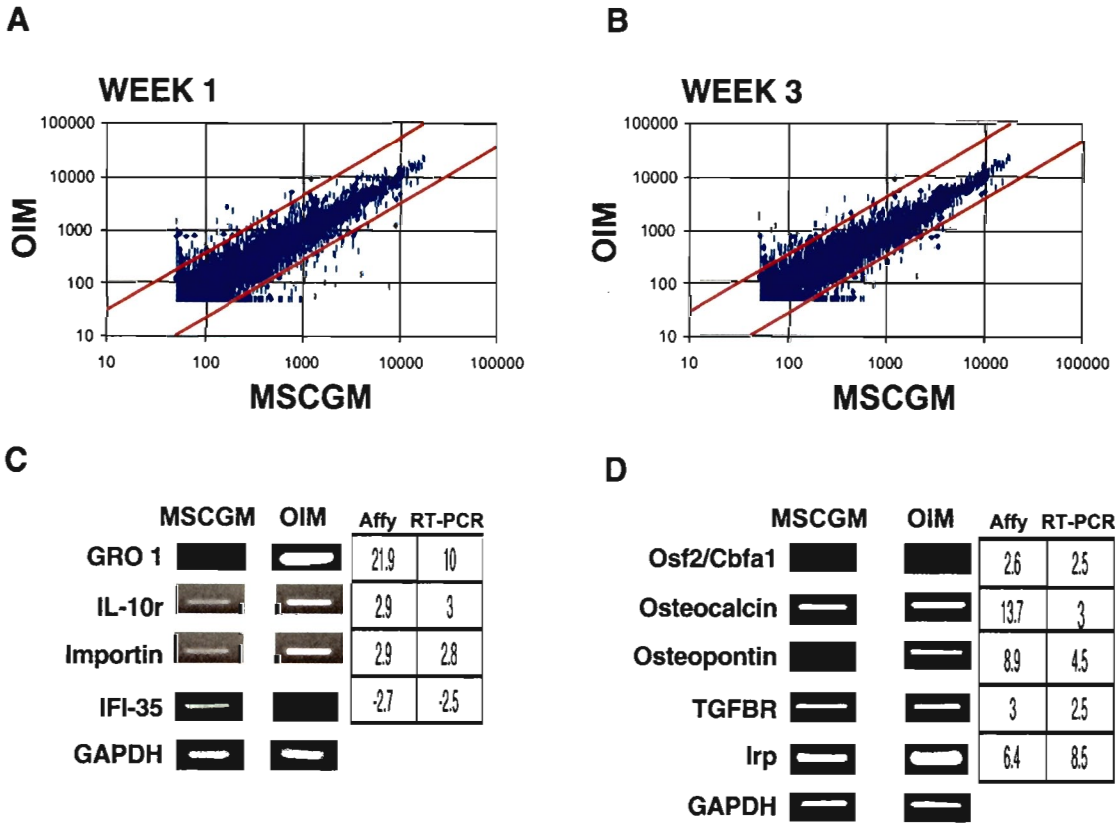
A
WEEK 1
OIM
MSCGM
100000
10000
1000
100
10
10
100
1000
10000
100000
B
WEEK 3
OIM
MSCGM
100000
10000
1000
100
10
10
100
1000
10000
100000
C
MSCGM
OIM
Affy
RT-PCR
GRO 1
21.9
10
IL-10r
2.9
3
Importin
2.9
2.8
IFI-35
-2.7
-2.5
GAPDH
D
MSCGM
OIM
Affy
RT-PCR
Osf2/Cbfa1
2.6
2.5
Osteocalcin
13.7
3
Osteopontin
8.9
4.5
TGFBR
3
2.5
Irp
6.4
8.5
GAPDH

differentiation pathway (11,28,31,32, 52,53,112,114) are indicated in blue and italic. In addition a new set of genes known as IFNIG (121-123) (in bold-red) displayed striking and transient changes in gene expression at week 1 returning to normal at week 3. Furthermore, at week 3 genes known as important regulators of the mineralization process and as markers of mature osteoblastic activity were up-regulated (124-126).

2.4.2 IFNγ induces OB *in vitro*

We first assessed the capacity of hMSC to secrete IFNγ prior to and following exposure to OIM. The conditioned medium of hMSC had near undetectable levels of IFNγ at week 1 and 2 but its levels increased significantly in the third week confirming previous reports of IFNγ production by confluent MSC (127,128). In contrast, hMSC exposed to OIM showed a dramatic and transient increase of IFNγ production in the conditioned medium at week 1 returning to baseline at week 2 (Fig. 13A). We then examined the capacity of IFNγ to alter the differentiation of hMSC. Addition of IFNγ to hMSC in the presence of OIM resulted in a significant and early induction of ALP expression, a marker of osteoblastic differentiation, as compared to non-treated cells (10% ± 2 vs. 76% ± 4, P <0.001) (Fig. 13B and C). Similar results were obtained by using alizarin red staining, a measure of mineralization (data no shown).

2.4.3 IFNγ induces Runx2/Cbfa1 expression *in vitro*

We assessed the effect of IFNγ on the expression of Runx2/Cbfa1. We found that adding IFNγ (100 ng/ml) to hMSC treated with OIM strongly increased Runx2/Cbfa1 expression at early time points as compared to non treated cells (Fig. 13,D)

Figure 12. Differentially expressed genes between hMSC exposed to either MSCGM or OIM after the first and third week of differentiation.

Bars represent the fold change of transcript levels of a particular gene between OIM and MSCGM treated cells (mean of 2 experiments using biological duplication)($p < 0.01$). Positive values (■) indicate that the transcript was more abundant in the OIM treated cells compared with the MSCGM treated cells; negative values (■)indicate the opposite. Abbreviations for gene names are given along with Genbank accession numbers. Genes in bold are those that changed at both time intervals. Genes in blue cursive are reported to be involved in the proliferative phase of osteoblast differentiation. Genes in bold-red are known as IFNIG.

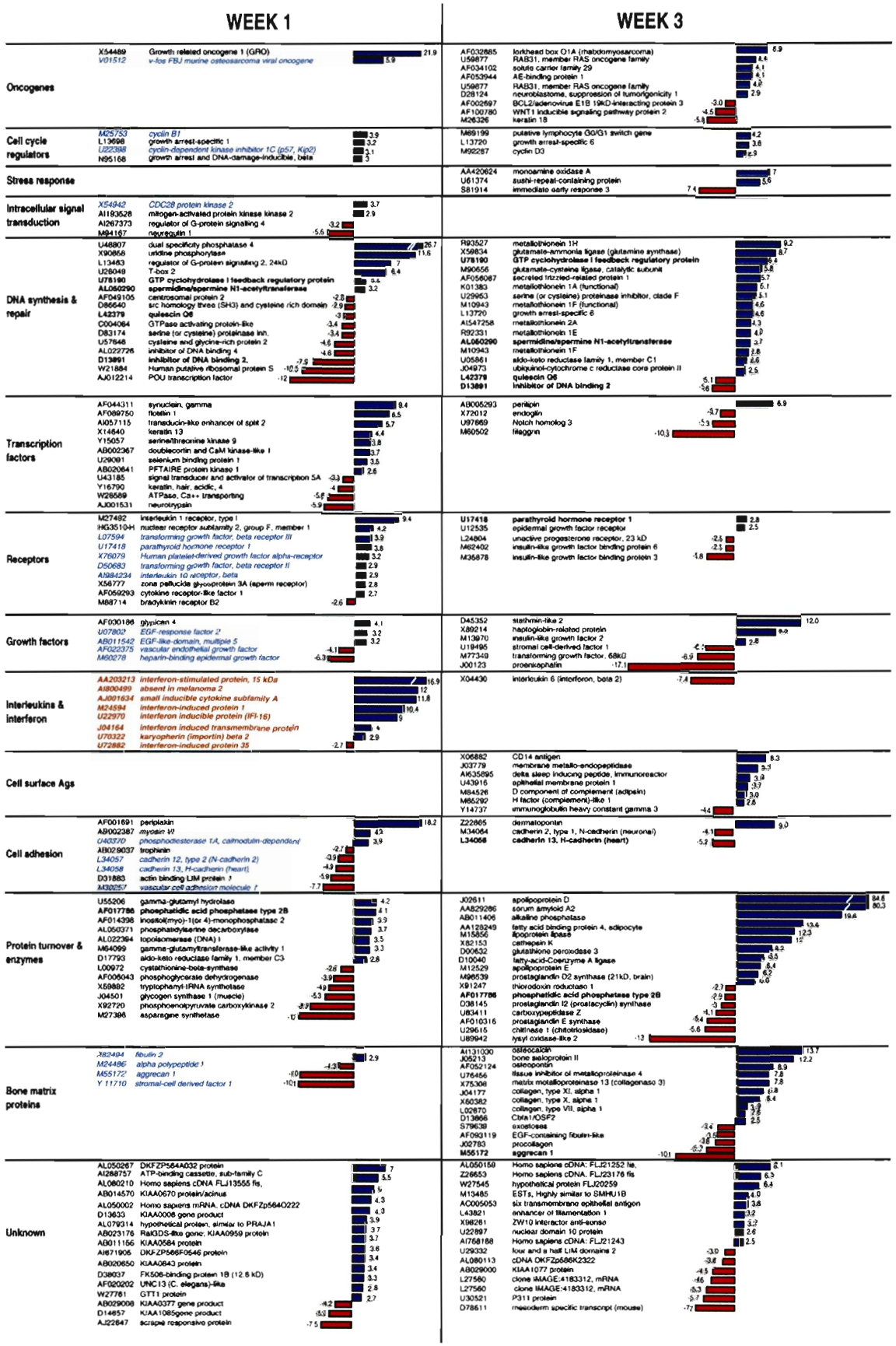
WEEK 1
WEEK 3
Oncogenes
Cell cycle regulators
Stress response
Intracellular signal transduction
DNA synthesis & repair
Transcription factors
Receptors
Growth factors
Interleukins & interferon
Cell surface Ags
Cell adhesion
Protein turnover & enzymes
Bone matrix proteins
Unknown

2.4.4 IFNγ regulates osteoblast differentiation *in vivo*

We then determined the effect of IFNγ on osteoblast differentiation *in vivo* in a mouse model in which the IFNγ receptor had been disrupted by homologous recombination, the IFN γ receptor knock-out model ($IFNGR^{-/-}$). These animals are normal at birth, are fertile, have a normal growth rate and body weight and cannot be differentiated from their $IFNGR^{+/+}$ counterpart, which we used as controls, except for subtle changes in the immune system (129,130). Initially, we cultured bone marrow cells derived from 4 and 8 week-old $IFNGR^{+/+}$ and $IFNGR^{-/-}$ mice in OIM. After three weeks of treatment, the number of mineralized nodules derived from $IFNGR^{-/-}$ was significantly reduced as compared to the ones derived from $IFNGR^{+/+}$ mice at 4 (21 ± 3 vs. 6 ± 4, $P < 0.001$) and 8 weeks of age (46 ± 2 vs. 12 ± 3, $P < 0.001$)(Fig. 14A and B).

2.4.5 Consequences of IFGR disruption on bone mass and bone turnover *in vivo*

We examined bone mineral density (BMD), micro architectural and morphometric changes in $IFNGR^{-/-}$ mice and in their normal counterpart $IFNGR^{+/+}$. BMD measured at the spine and femora (Fig. 14C) indicated that $IFNGR^{-/-}$ mice had a significantly lower bone mass as compared to $IFNGR^{+/+}$ mice ($0.06\ g/cm^2 \pm 0.005$ vs. 0.038 ± 0.004, $P < 0.001$ in spine and $0.046\ g/cm^2 \pm 0.002$ vs 0.03 ± 0.005, $P < 0.01$ in femur) at early time points but the two groups reached the same bone mass at around 24 weeks of age. Furthermore, measurement of structural parameters of trabecular mass by 3D-μCT analysis demonstrated a significant decrease in structural parameters in $IFNGR^{-/-}$ as compared to $IFNGR^{+/+}$ mice ($P < 0.01$)(Fig. 15A and B). We then performed histomorphometric analysis to determine the changes in bone architecture *in vivo*. We

found a significant reduction in structural parameters confirming the results obtained by 3D-μCT (Fig. 16A and B). Furthermore, histomorphometric analysis of the primary spongiosa showed that in IFNGR$^{-/-}$ mice there is a significant reduction in endochondral ossification demonstrated by a significant difference in the architecture of the septa (Fig. 16C).

In addition, we assessed both osteoblastic differentiation (Runx2/Cbfa1) and osteoblastic activity (ALP and OPN) in both IFNGR$^{+/+}$ and IFNGR$^{-/-}$ mice by enzymohistochemistry (ALP) (Fig. 16D) and immunohistochemistry (OPN and Cbf1) (Fig. 16E and F). We found a significant decrease in the level of ALP (13±1 % vs. 6±2, P <0.001) (Fig. 16D and G) and a marked reduction in OPN expressing osteoblasts as well as a marked reduction in Runx2/Cbfa1 expression (Fig. 16E and 1F) in mice lacking IFNGR. Moreover, a marked reduction in eroded surface osteoclast number and activity (ES/BS) was shown by histomorphometric analysis (Fig. 16B). Finally, the lower levels of osteoblastic activity and resorptive site osteoclastic activity in IFNGR$^{-/-}$ mice were documented by a very significant reduction in circulating levels of both OSN and N-telopeptide respectively as compared to their normal counterpart (Fig. 16H and I).

Finally, the lower levels of osteoblastic activity and resorptive site osteoclastic activity in IFNGR$^{-/-}$ mice were documented by a very significant reduction in circulating levels of both OSN and N-telopeptide respectively as compared to their normal counterpart (Fig. 16H and I).

Figure 13. The effect of IFNγ on the osteogenic differentiation of MSC.

(A) MSC treated with OIM secrete IFNγ in the supernatant after the first week of differentiation. By contrast, MSC treated with MSCGM produce IFNγ only after reaching confluence after the third week (* $P< 0.001$). (B) IFNγ in OIM treated cells accelerates the osteogenic differentiation of MSC after one week of treatment in a dose-dependent manner. (C) Staining of OIM with ALP demonstrate higher number of ALP expressing cells in the IFNγ treated cells as compared to control (upper panels for $4cm^2$ plates and lower panels for X100 magnification)(* $P<0.001$). (D) IFNγ (100 ng/ml) added to OIM induces early expression of Runx2/Cbfa1.The figure shows the levels of Runx2/Cbfa1 expression after 1, 2 and 3 weeks of osteoblast differentiation in MSCGM containing osteoblast differentiation factors versus hMSC grown in MSCGM alone. No change in Runx2/Cbfa1 expression was found after addition of IFNγ to MSCGM in the absence of OIM (upper panel).

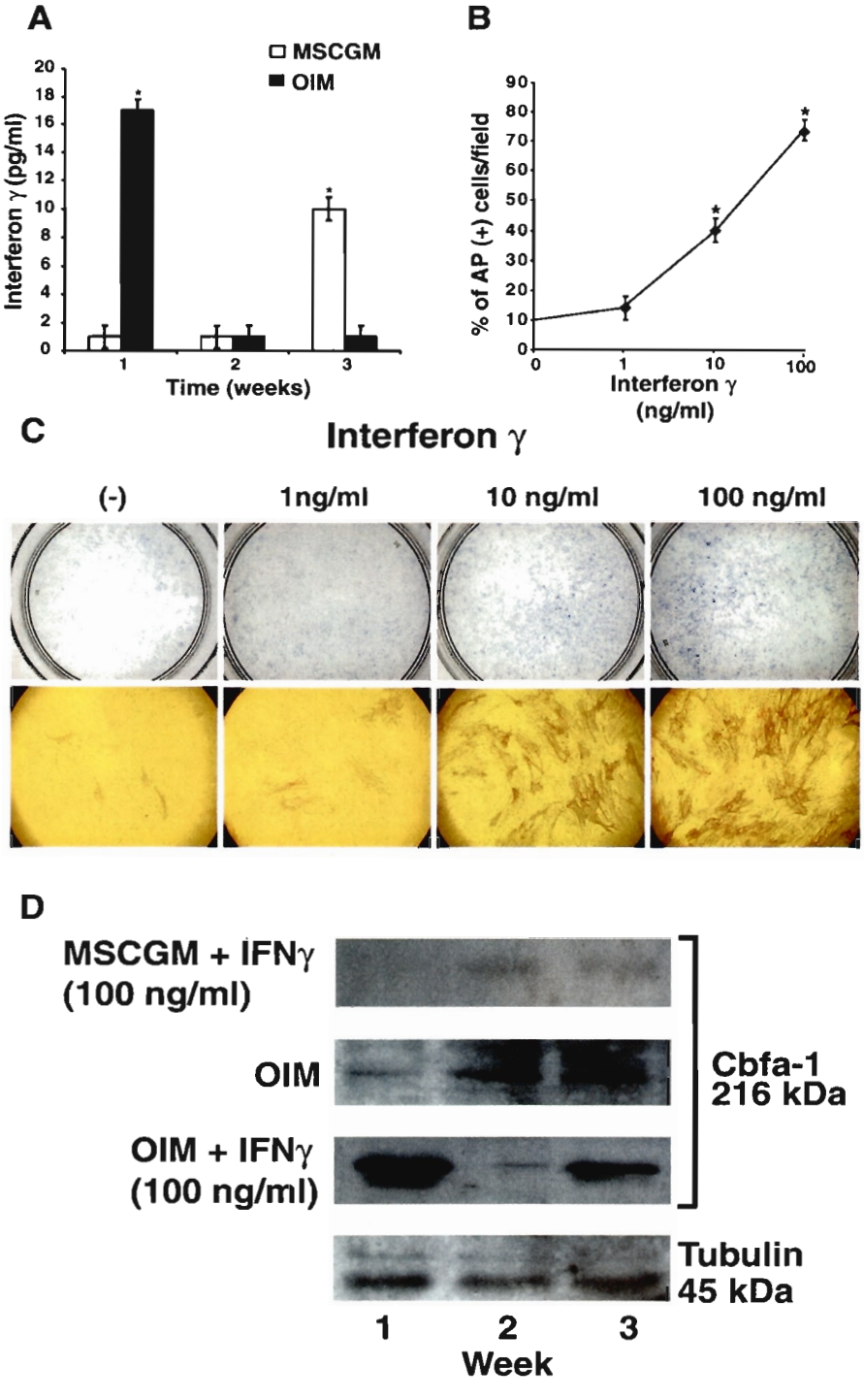
A
MSCGM
OIM
Interferon γ (pg/ml)
Time (weeks)
B
% of AP (+) cells/field
Interferon γ
(ng/ml)
C
Interferon γ
(-)
1ng/ml
10 ng/ml
100 ng/ml
D
MSCGM + IFNγ
(100 ng/ml)
OIM
OIM + IFNγ
(100 ng/ml)
Cbfa-1
216 kDa
Tubulin
45 kDa
Week

2.5 Discussion

In this study, we first attempted to understand the mechanism(s) that regulate the differentiation of hMSC into osteoblasts by determining the changes in gene expression that take place during this process (Fig. 11). We then classified those genes based on their known function in14 different groups (Fig. 12). The proliferative phase (week 1) was characterized by the expression of known genes belonging to the osteoblast differentiation pathway (11, 28,32,31,52,53,112-114).

Interestingly, we found a significant change in a transduction pathway previously not reported in osteoblast differentiation: IFNIG. Two of these genes belonged to the recently described IFNγ-induced nuclear factors (IFI-16 and absent in melanoma 2) (122,123,131) which are also known as Ifi200 and activate the transcription of IFNIG by their interaction with the IFN stimulated response elements (ISRE) playing an important role in cell differentiation and embryonic development (121-123,131).

Recently, it has been reported that the Ifi200 genes interact with casein-kinase 2 (CK-2)(132) a protein involved in osteogenic differentiation of hMSC(123). In addition, another IFNIG found to be up-regulated at the end of the proliferative phase is karyopherin also known as importin beta 2. This protein is activated by IFNγ and acts as a carrier of the activated STAT heterodimer from the cytoplasm to the nucleus (133).

The role of IFNs α,β and γ in bone is a subject of intense research. IFNα suppresses proliferation of osteoprogenitor cells (134) while IFNβ was recently shown to play a role in bone turnover since mice lacking IFN β exhibit severe osteopenia mostly due to enhanced OC (134).

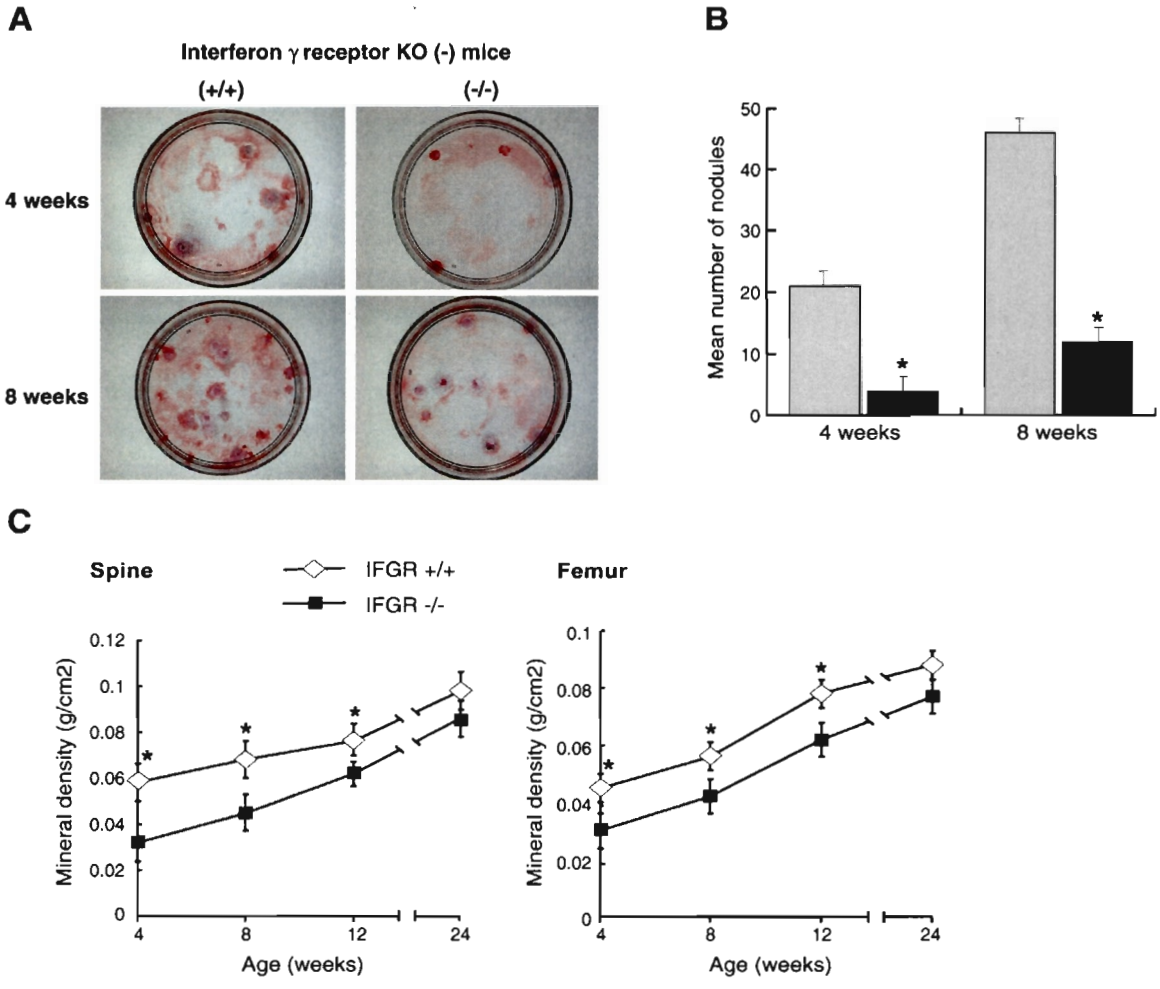

Figure 14. OB and BMD in mice deficient in IFNγ signaling at 4 and 8 weeks of age as compared to control mice.

(A) Induction of OB in ex-vivo cultures of bone marrow from $IFGR^{-/-}$ (right panels) and $IFGR^{+/+}$ mice (left panels). Note the increased number of bone forming nodules in the $IFGR^{+/+}$ mice as compared to the $IFGR^{-/-}$ mice.(B) $IFGR^{-/-}$ mice (■) show a decreased number of bone nodules per plate as compared to their $IFGR^{+/+}$ control (▣) (*p< 0.001).(C) Bone densitometry shows lower bone mass in the $IFGR^{-/-}$ mice as compared to $IFGR^{+/+}$ mice in both spine and femur at early ages (4-12 weeks) (*p<0.01) reaching the same level of BMD after 24 weeks of age.

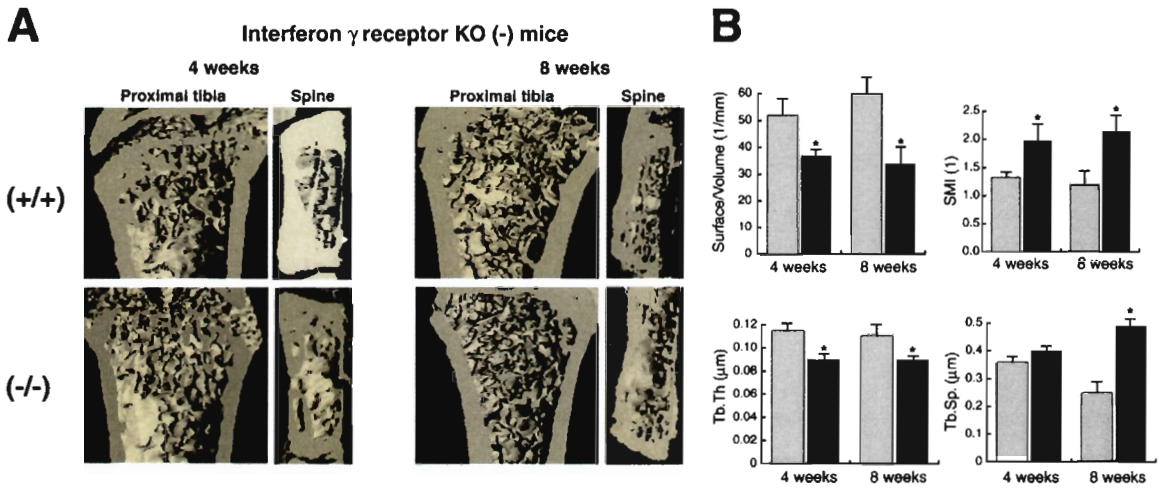

Figure 15. Microarchitectural changes in IFGR$^{-/-}$ mice compared to IFGR$^{+/+}$ mice. (A) After 3D μCT reconstruction of IFGR$^{-/-}$ and WT mice at two time points (4 and 8 weeks) IFGR$^{-/-}$ mice showed a decrease in cortical and trabecular thickness as compared to IFGR$^{+/+}$ mice. Morphometric analysis of both spine (L2) and tibiae showed decreased 3D trabecular bone volume fraction and thickness as well as more widely spaced and less connected trabeculae. (B) Quantification of 3D trabecular structural parameters in proximal tibiae included surface/volume (BS/BV), structural model index (SMI), trabecular thickness (TrTh) and trabecular separation (TrSp) measured from μCT images with isotropic resolution of 21 μm. Wilcoxon test of measurements showed a significant difference in all parameters between IFGR$^{+/+}$ (□) and IFGR$^{-/-}$ (■) mice (*P< 0.01).

Previous studies assessing the effect of IFNγ in bone have shown an inhibitory effect on osteoclastic activity and differentiation *in vitro* (136). In addition, overexpression of IFNγ in transgenic mice results in chondro-osseous lesions resembling osteochondrodysplasia (137). The role of IFNγ on bone formation has not yet been reported although nitric oxide (NO), a well known end-product of the activation of IFNγ pathway, seems to play a role in OB and bone formation (138-141). Recently, it was reported that IFNα and γ induce the expression of *Best5* a gene expressed during bone formation in rats (142).

Another significant finding in our study was the transient nature of IFNIG expression. Indeed IFNIG expressed at one week during the proliferative phase returned to baseline during the mineralization phase (Fig.12). IFNγ production by hMSC undergoing differentiation was also found to be expressed transiently and concomitantly with IFNIG (Fig. 13,A). The key role of IFNγ on osteoblast differentiation was further confirmed by adding IFNγ to hMSC exposed to a differentiation medium which enhanced their differentiation into osteoblasts in a dose-dependent fashion (Fig. 13, B and C).

An important finding was the observation that Runx2/Cbfa1, a key transcriptional activator of osteoblast differentiation that responds to multiple signal transduction pathways (143), was up-regulated after the transient and autocrine expression of IFNγ. Furthermore, IFNγ addition to hMSC together with an OIM but not in the absence of OIM strongly induced early Runx2/Cbfa1 expression (Fig. 13,D).

Figure 16. Histological, histomorphometrical and biochemical determination of parameters of bone turnover in the absence of IFNγ signaling.

(A) Histological analyses of distal femora from 8 week-old $IFNGR^{-/-}$ and $IFNGR^{+/+}$ mice; X31.25 (left panels) and X250 (right panels) magnifications of Goldner's trichrome staining. There is an evident reduction in the trabecular and cortical thickness in the longitudinal sections (green staining) of the femur from $IFNGR^{-/-}$ as compared to $IFNGR^{+/+}$.(B) Histomorphometrical analysis of $IFNGR^{-/-}$ mice (n=4 per group, data shown as mean ± s.e.*$P < 0.05$) shows a significant reduction in trabecular bone volume(BV/TV) and thickness (Tb.Th) in the $IFNGR^{-/-}$ mice (■)as compared to $IFNGR^{+/+}$(□) control . There is also a significant lower cortical thickness (Ct.Wi) in the $IFNGR^{-/-}$ mice. In addition, $IFNGR^{-/-}$ mice show a significant reduction of eroded surface (ES/BS) compared to $IFNGR^{+/+}$. (C) Histomorphometrical analysis of primary spongiosa of $IFNGR^{-/-}$ mice (■) shows a significant reduction in the volume (BV/TV, BS/TV) and thickness (Tb.Th) of septa as compared to $IFNGR^{+/+}$ (□) control. (D) histochemistry of ALP (blue staining) and TRACP (red staining) activities in the $IFNGR^{-/-}$ mice and the $IFNGR^{+/+}$ mice; X312.5 magnification. There is an evident reduction of ALP staining in the $IFNGR^{-/-}$ compared to the control. (E and F) Immunodetection of OPN and Runx2/Cbfa1 (dark brown staining, arrows); X340 magnification. There is a marked reduction in both OPN (E) and Runx2/Cbfa1 (F) expression in the $IFNGR^{-/-}$ mice as compared to $IFNGR^{+/+}$ mice. (G) Percentage of trabecular bone surface covered with ALP staining (ALP/BS). Compared to $IFNGR^{+/+}$ mice (□), $IFNGR^{-/-}$ mice (■) show a significant reduction of ALP/BS (* $P < 0.05$). (H) and (I), biochemical markers of bone turnover quantified in serum of 4 and 8 week-old $IFNGR^{+/+}$ (□)and $IFNGR^{-/-}$(■).

IFNGR$^{+/+}$ mice show a significant reduction in OSN (H) (osteoblastic activity) and N-telopeptide (I) (osteoclastic activity) concentrations in IFNGR$^{-/-}$ mice as compared to their normal IFNGR$^{+/+}$ control (*P < 0.001).

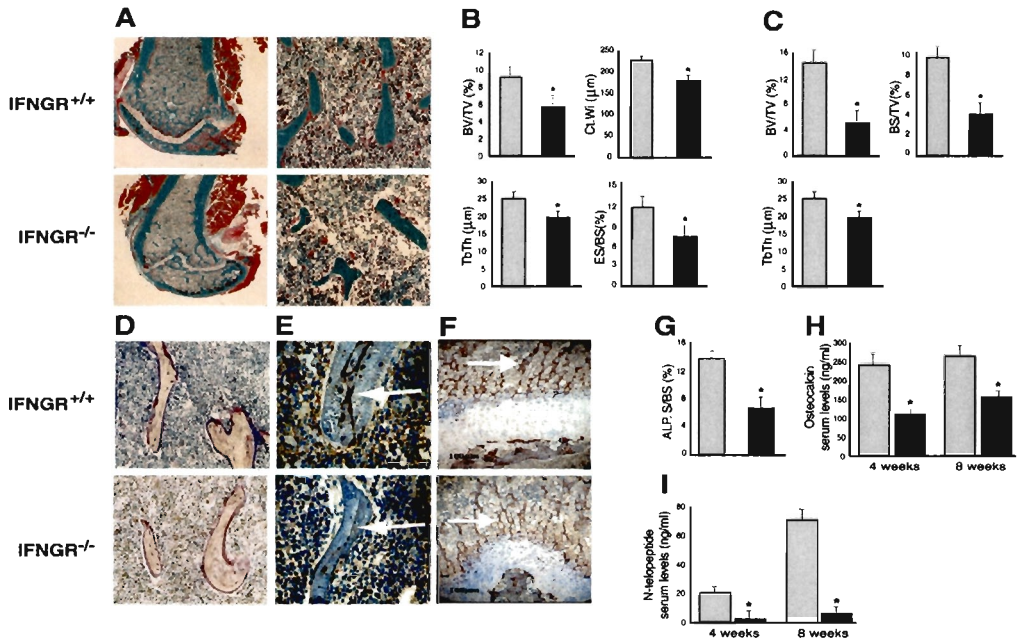

These results suggest that IFNγ not only precedes Runx2/Cbfa1 expression during the differentiation process of hMSC into osteoblast but also can regulate Runx2/Cbfa1 expression when added to hMSC committed to differentiate into osteoblasts.

We next examined the potential role of IFNγ *in vivo* in the $IFGR^{-/-}$ mouse model (129,130). First, we examined the capacity of bone marrow cells derived from $IFGR^{-/-}$ and $IFGR^{+/+}$ mice to differentiate into osteoblasts *in vitro* by culturing them in OIM. After three weeks, cells obtained from $IFGR^{-/-}$ bone marrow showed a marked delay to form bone nodules as compared to cells obtained from $IFGR^{+/+}$ mice (Fig. 14,A and B). These findings clearly indicate that IFNγ is an important regulator of osteoblast differentiation *in vivo* and its deficiency result in delayed bone formation.

We also found that IFGR knock out results in a lower bone mass at early time points in mice harboring this phenotype as compared to their normal counterpart. Interestingly, after 24 weeks of age both $IFGR^{-/-}$ and $IFGR^{+/+}$ mice reached the same bone mass (Fig. 14,C) suggesting a transient role of IFNγ in peak bone mass acquisition.

These changes were further assessed by looking at the bone architecture with micro-CT analysis in tibiae and spine of $IFGR^{-/-}$ and $IFGR^{+/+}$ mice. Indeed, $IFGR^{-/-}$ were found to have a very significant deficit in both trabecular and cortical architecture thereby confirming the generalized nature of the osteoporotic process (Fig. 15, A and B). These findings were further documented by histology (Fig. 16, A) and histomorphometry (Fig. 16, B) which demonstrated a decrease in trabecular and cortical thickness as well as a decrease of bone turnover in $IFGR^{-/-}$ mice as compared to their normal counterpart.

The mechanism underlying this reduced bone mass in $IFNGR^{-/-}$ mice can be explained by a reduction in the number of active osteoblasts observed in bone marrow cells obtained

from IFNGR$^{-/-}$ as compared to IFNGR$^{+/+}$ (Fig. 14B). Furthermore, this deficit in osteoblastic activity was also corroborated by lower ALP and OPN staining in histologic analysis of IFNGR$^{-/-}$ mice (Fig. 16D, E and G) and a decrease in the circulating levels of OSN (Fig. 16H) as compared to IFNGR$^{+/+}$ mice. In addition to the deficit in osteoblastic activity, the reduction in the number of mature osteoblasts in trabecular bone of IFNGR$^{-/-}$ mice could also be explained by the marked reduction in the number and quality of the septa in the primary spongiosa in IFNGR$^{-/-}$ mice (Fig. 16C) probably due to a reduction in osteoblast differentiation from the osteochondral junction, documented by lower levels of Runx2/Cbfa1 expression in IFNGR$^{-/-}$ mice (Fig. 16F), with a subsequent decrease in the formation of trabeculae. Furthermore, a reduction in osteoclastic activity (Fig. 16B and I) was also observed in IFNGR$^{-/-}$ mice probably due to a deficit in the recruitment and differentiation of new osteoclasts as a consequence of the lower number of osteoblast precursors.

In summary, these data clearly indicate that IFNγ plays a pivotal role in osteoblast differentiation *in vitro* and *in vivo*. IFNIG are significantly up-regulated during the proliferative period of osteoblastic differentiation of MSC and the lack of IFNγ receptor *in vivo* results in a reduction of osteoblastic differentiation of bone marrow cells with subsequent reduction in osteoclast differentiation and activation characteristic of low bone turnover osteoporosis.

In conclusion, using a genomic approach to better understand the mechanism of bone formation, we have identified IFNγ as a key player in this process and determined that its deficiency results in osteoporosis.

2.5 Acknowledgements

Dr. Duque holds a bursary from the Fonds de la Recherche en Santé du Québec.

INTRODUCTION TO CHAPTER THREE

A decisive advance in the elucidation of the molecular changes that occur during age-related bone loss would be the assessment of MSC plasticity and its regulation. In chapter 2 we have studied the mechanisms that regulate osteoblastogenesis and the importance of its stimulation in anabolic therapeutic strategies for osteoporosis. In this chapter, we not only demonstrate that the induction of osteoblastogenesis by 1,25 $(OH)_2D_3$ results in the formation of new bone but also that adipogenesis can be reversed in a model of senile osteoporosis, the SAM-P/6 mouse. Furthermore, by using $1,25(OH)_2D_3$ we not only evaluate a new role of this hormone on bone formation but also identify the changes in gene expression that might explain this effect.

This chapter describes a new role to $1,25(OH)_2D_3$ as a bone forming agent and identifies the potential genes that are required to stimulate osteoblastogenesis and inhibit adipogenesis as an approach to control MSC plasticity and, as a consequence, to induce bone formation.

CHAPTER 3

$1,25(OH)_2D_3$ acts as a bone forming agent in the hormone independent Senescence Accelerated Mouse (SAM-P/6) model of Osteoporosis.

Gustavo Duque [1,2], Michael Macoritto[1], Natalie Dion[3], Louis George Ste. Marie[3], Richard Kremer[1].

[1] Calcium Research Laboratory, Department of Medicine, McGill University Health Centre, Montreal, Quebec, Canada

[2] Division of Geriatric Medicine, McGill University, Montreal, Quebec, Canada

[3] Centre Hospitalier de l'Université de Montreal, Research Center, Hôpital St. Luc, Montreal, Quebec, Canada.

The contents of this Chapter were submitted to the *Journal of Clinical Investigation*: Duque G, Macoritto M, Dion N, Ste. Marie LG, Kremer R. 2003. $1,25(OH)_2D_3$ acts as a bone forming agent in the hormone independent Senescence Accelerated Mouse (SAM-P/6) model of Osteoporosis.

3.1 Summary

SAM-P/6 is a mouse model of senile osteoporosis with decreased bone formation rate and concomitant increased bone marrow AD. In this study, our aim was to examine the overall effect of $1,25(OH)_2D_3$ on bone cells in this model. Both sex 4-month old SAM-P/6 were infused continuously with $1,25(OH)_2D_3$(18pmol/24h) or vehicle for a period of 6 weeks. In $1,25(OH)_2D_3$ treated animals, histomorphometric analysis showed an increase in bone formation as well as a decrease in osteoclastic activity as compared to the non-treated group. These results were confirmed by MicroCT analysis of tibiae, Dual Energy X-ray (DEXA) and serum bone markers. In addition, oil red O staining of bone sections showed also an inhibitory effect of $1,25(OH)_2D_3$ on AD. *Ex-vivo* cultures of bone marrow cells taken from both groups and induced to differentiate in culture in the absence of $1,25(OH)_2D_3$ showed a more rapid and higher level of osteoblast differentiation in bone marrow cells derived from $1,25(OH)_2D_3$ treated mice. Finally, RNA obtained from trabecular cells of $1,25(OH)_2D_3$ treated and non-treated animals and analyzed by micro array showed that in addition to inducing known vitamin D target genes, $1,25(OH)_2D_3$ up regulated the expression of a wide array of genes previously unknown to be involved in the regulation of OB and AD. In summary, our results demonstrate that $1,25(OH)_2D_3$ increases bone mass by stimulating bone formation and inhibiting both OC and AD in a mouse model of defective OB, and suggest its potential usefulness as a therapeutic agent in senile osteoporosis.

3.2 Introduction

The process of age-related bone loss starts after the third decade of life superimposes the accelerated hormonally dependent process of post-menopausal osteoporosis and continues thereafter to constitute what is called senile osteoporosis (8).

From the pathophysiological standpoint post-menopausal osteoporosis is characterized by a lack of estrogen and subsequent increase in osteoclastic activity leading to bone resorption (2), whereas senile osteoporosis involves a decrease in OB with a concomitant increase in AD and osteoblast apoptosis (8). Furthermore, with age serum levels of vitamin D decrease (15,144,145) whereas the levels of PTH tend to increase (145) in response to a decrease in intestinal calcium absorption (15,143-146).

In addition to promoting calcium absorption in the gut, the active form of vitamin D, $1,25(OH)_2D_3$, has additional and sometimes divergent cellular effects on bone cells (146-148). *In vitro* $1,25(OH)_2D_3$ stimulates osteoclastic activity indirectly through activation of the RANK ligand at the surface of the osteoblast (2,145,146) while *in vivo* it promotes mineralized matrix formation in OVX animal models (149). In contrast to its *in vitro* effect, a recent report *in vivo* indicates that $1,25(OH)_2D_3$ inhibits OC by decreasing the pool of osteoclast precursors in the bone marrow (150). Furthermore, administration of vitamin D3 in elderly patients in double blind randomized clinical trials significantly increases BMD and reduces in the incidence of osteoporotic fractures by as yet unknown mechanism (s) (145,146).

In the present study, we used a hormonally independent model of osteoporosis the SAM-P/ 6 mouse. This strain of mice is characterized by a decrease in OB and an increase in AD within the bone marrow leading to bone loss and fractures mimicking the human

form of senile osteoporosis (73,151-156). SAM-P/6 start losing bone at 4 months of age and have a mean life span of 7.9 months as compared to a bone loss starting at 12.4 months and a life span of 24 months in their normal counterpart SAM-R/1TA (152). At 7 months spontaneous fractures occur in SAM-P/6 as a consequence of severe osteoporosis (151,155). Furthermore, in this hormonally independent model, ovariectomy does not lead to an increase in osteoclastic activity or a further decrease in bone mass (151).
In this study we demonstrate that $1,25(OH)_2D_3$ stimulates bone formation and inhibits AD by modulating the expression of genes within the bone microenvironment.

3.3 Materials and methods

3.3.1 Animals

SAM-/P6 and SAM-R/1TA mice were kindly provided by Dr. Toshio Takeda (Kyoto University, Kyoto, Japan). Male and female were housed in cages in a limited access room restricted to aging mice (light: dark 12h:12h). Bedding, food and water were given as previously described (120). Animal husbandry adhered to Canadian Council on Animal Care Standards, and all protocols were approved by the McGill University Health Center Animal Care Utilization Committee. The colony was free of any parasitic, bacterial, or viral pathogens as determined by a sentinel program.
At 4 months of age, mice (n=12 per group) in a 50:50 ratio of males and females were implanted with Alzet osmotic minipumps (Alzet, Cupertino, CA,USA) containing $1,25(OH)_2D_3$ (LEO Pharmaceuticals, Ballerup, Denmark) prepared as previously described (120) and delivering a constant infusion of either 18 pmol/24h of $1,25(OH)_2D_3$ or vehicle alone. Osmotic mini-pumps were replaced after 3 weeks for a total of 6 weeks

of treatment. Blood calcium levels were monitored at timed intervals by microchemistry (Kodak Ektachrome, Mississauga, ON, Canada) and corrected for albumin concentrations according to the formula: Plasma total calcium + [40-plasma albumin)]X 0.02. After 6 weeks of treatment, animals were sacrificed and femora isolated. One femur was used for histomorphometric analysis; the other femur was cut longitudinally and trabecular cells scraped, separated from red blood cells and suspended in 1 ml of conservation buffer Easy-Kit mini prep (Qiagen,Valencia, CA, USA) for further RNA extraction. In addition, both tibiae were flushed for *ex-vivo* cultures as described below.

3.3.2 Histological and histomorphometrical analysis of bone

The details of these methods were described previously (119). One side femur from each animal in each treatment group was removed at the time of killing, fixed, dehydrated in 70% ethanol, and embedded in methylmethacrylate (J-T Baker, Phillipsburg, NJ). Bone specimens were cut completely through. Sections of 5 μm were obtained using a polycut-E microtome (Reichert-Jung, Leica, Heerbrugg, Switzerland), placed on gelatin-coated glass slides, stained with Goldner's trichrome method and used for the structural and static parameters of bone remodeling. For the purpose of dynamic bone formation parameters, mice were injected with 20 mg/Kg demeclocycline (SIGMA-Aldrich, St. Louis, MI) seven and two days before sacrifice. Sections of 8-μm were left unstained for observation under UV light. Bone parameters were quantified in cancellous bone tissue at distances greater 0.4 mm from the growth plate methaphyseal junction to exclude the primary spongiosa. Thirty two to forty fields were analyzed from each distal femur metaphysis. Evaluation of bone turnover during remodeling included static evaluation using serial sections for various parameters and dynamic evaluation using fluorochrome

labeling of bone in situ. Histomorphometry was done with a semi automatic image analyzing system combining a microscope equipped with a camera lucida and digitizing tablet linked to a computer using the OsteoMeasure Software (Osteometrics Inc., Decatur, GA, USA).

3.3.3 Histochemistry

Detection of alkaline phosphatase (ALP) and tartrate-resistant acid phosphatase (TRACP) activity was carried out on 5 μm thick sections. Naphtol-AS-TR was used as substrate for both enzymes, and Fast Blue BB salt (SIGMA-Aldrich, St. Louis, MI, USA) and pararosaniline were used as couplers for ALP and TRACP respectively.

3.3.4 Micro-CT of bone samples

Tibiae were fixed in 10% formalin, scanned by micro-CT at ×40 magnification with a SkyScan 1072 and analyzed with a bone analysis software (ver2.2f, Aartselarr, Belgium). During scanning, the samples were enclosed in a tightly fitting rigid plastic tube to prevent movements. Analyses of the trabecular bone were carried out in a 2.3-mm-thick region of the tibia, distal to the growth plate of the knee joint. The software was used to separate regions of trabecular bone from cortical bone in the sections. Thresholding was then applied to the images to segment the bone from the background, and the same threshold setting was used for all the samples. The following three-dimensional (3D) parameters were measured: volume, surface, and surface-to-volume ratio. To calculate these, the software builds a 3D cuboidal voxel model of the bone. The following bone architectural measurements were then made: trabecular thickness and separation; details of these measurements have been published elsewhere (118).

3.3.5 Oil Red O staining of adipose tissue in bone marrow

To identify bone marrow AD, bone sections from all mice were stained using oil red O (SIGMA-Aldrich, St. Louis, MI). In brief, sections were washed with 70% ethanol and then stained with 60 % oil red in isopropanol. After 20 minutes, sections were washed, counterstained with hematoxylin and then analyzed under light microscopy, with adipose tissue staining strong red with blue nuclei. The proportion of adipocytes was calculated by the number of cells positive for oil red O staining in groups of 100 cells inside the bone marrow in 5 different fields.

3.3.6 Dual Energy X-ray Absorptiometry (DEXA) analysis

DEXA analysis was performed at time 0 (4 months) and at 3 and 6 weeks post osmotic pumps implantation. Hip and spine BMD was measured using a PIXIMUS bone densitometer (PIXIMUS ™, GE medical systems, USA). A phantom (PIXIMUS ™, GE medical systems, USA) was used to calibrate the densitometer prior to each experiment.

3.3.7 Ex-vivo cultures of bone marrow cells

At sacrifice both tibiae were flushed using Dubelcco's alpha modified medium (DMEM) (GIBCO, Grand Island, NY, USA) containing 5% heat-inactivated fetal calf serum (FCS), 100 U/ml of penicillin, and 100 U/ml of streptomycin placed in 150 cm^2 dishes and incubated at 37°C for 24 hours. After 24 hours, the floating cells containing mesenchymal stem cells were isolated and counted. 2 x 10^6 cells were seeded and then grown in 15 cm^2 grid dishes containing an Osteoblastogenesis Induction Medium (OIM) prepared with Mesenchymal Stem Cells Growth Media (MSCGM) (BioWhittaker, Walkersville, MD,

USA), 10% FCS, dexamethasone (1μmol/L), β glycerol phosphate (5 mmol/L) and ascorbic acid (100 μmol/L) for 21 days. Media was changed every three days. At 21 days, media was removed and cultures were fixed in 10% v/v formol/saline solution for 5 minutes. After fixation, bone mineralized nodules were stained for 20 minutes with Alizarin red S solution (40mM, pH4.2) (SIGMA-Aldrich, St. Louis, MI). The total number of bone nodules per dish was counted macroscopically. There were 24 dishes per group.

3.3.8 Biochemical assays

After 6 weeks of treatment, mice were sacrificed by cervical dislocation and blood removed by cardiac puncture. Serum was stored at –80°C for further analysis. Osteocalcin was measured in 200μl of serum using the mouse Osteocalcin-IRMA kit to assess bone formation (Immutopics, San Clemente, CA, USA). N-telopeptide was measured in 20 μl of serum using the RATtelopeptide kit to assess osteoclastic activity (Osteometer Biotech, Herlev, Hovedgade, Denmark). PTH was measured in 200 μl of serum and analyzed by using the mouse intact PTH immunoradiometric assay kit (Immutopics, San Clemente, CA, USA). Levels of 25-hydroxyvitamin D (25-OHD) were measured by radioimmunoassay in 50 μl of serum (IRS, Boldon, England). For those measures normal range was determined by measuring their serum levels in SAMR-1/TA mice (n=12) at the same age.

3.3.9 Micro array complementary DNA labeling, hybridization and scanning

Total RNA was extracted from trabecular cells according to a protocol for single-step RNA isolation based on the Easy-Kit mini prep (Qiagen,Valencia, CA, USA). Aliquots of total RNA were separated in sterile tubes and quantified. Generation of cDNA, fluorescent labeling and hybridization to the gene chip were performed by the Genomics Laboratory (University of Kingston, ON, CA). Briefly, mRNA was isolated and reverse transcribed with 5' Cy3- or Cy5-labeled random 9-mer (Operon Technologies Inc. Alameda, CA, USA). The paired reactions were combined and purified with a TE-30 column (Clontech, Palo Alto, CA, USA). Fluorescently labeled probes were then applied to the array for hybridization at 60 ^{o}C for 6.5 h. After hybridization the glass slides were washed with decreasing ionic strength and scanned with 10-μm resolution to detect Cy3 and Cy5. We examined 15,000 mouse genes and ESTs (expressed sequences tags) on the array 15K mouse cDNA clone set micro array (NIA, Bethesda, MD, USA)(157) and analyzed the results with the software GEM tool 4.4. A gridding and region detection algorithm was used to determine each element. The area surrounding each element image was used to calculate a local background and was subtracted from the total element signal. Background subtracted element signals were used to calculate Cy3/Cy5 ratios. The average of the resulting total Cy3 and Cy5 signal gives a ratio that was used to balance or normalize the signals. This experiment was repeated twice using a pool of RNA isolated from 6 mice RNA per group.

3.3.10 Micro array Data Processing

A set of 5440 genes on NIA 15K Mouse cDNA Clone Set micro array were consistently expressed across a range of tissues with variable expression levels. These 5440 genes

were then used to normalize the data from different micro array experiments as previously described (116,117). Briefly, the expression levels of the preselected genes were scaled to a "standard experiment" and the geometric mean of the scaling factors was calculated. This value served as the normalization factor for all genes represented on the micro array. The fold change between the levels of expression of any two genes on two different micro arrays was calculated according to a protocol at McMaster University (Ontario, Canada). The processed fluorescence values were placed into a table containing m rows, which represented the m genes, and n columns that corresponded to the n replicate experiments. The n replica experiments were considered to be independent. Using this assumption, each of the n replicates was compared with the others in a pairwise manner. This process resulted in a large number of replicate pairs. The expression values for each pair were plotted against those of other pairs in a scatter plot in which the distribution of points was around the $x = y$ diagonal. The data from these scatter plots were combined for all genes and rotated by 4. This manipulation transformed the $x = y$ axis from the latter plot to the $\ln (I) = 0$, which represents the signal-to-noise distribution derived from comparison of all replicates. To determine a signal-to-noise profile, a sliding histogram algorithm along the y axis was applied (116,157). A threshold was set at 80% of the maximum noise value. Genes with intensities below this threshold value were considered within the experimental noise. A 2 fold up or down regulation was considered significant. Genes with significant changes were then grouped depending on their known function. Gene functions were obtained by correlating them in the main scientific databases (MEDLINE, PUB-Med) using seven key words: vitamin D, osteoblast, osteoblastogenesis, adipocyte, adipogenesis, osteoclast and OC.

3.3.11 Semi-quantitative RT-PCR

Total RNA isolated from trabecular cells (1 μg) was reverse transcribed with either random hexamers or oligo-dT using Qiagen One Step RT-PCR Enzyme Mix (Qiagen, Valencia, CA, USA). The resulting cDNA was amplified by 40 polymerase chain reaction cycles with an annealing temperature of 58 °C. Negative controls (samples without the transcriptase enzyme or with water in place of RNA) were included at every step of sample preparation. Amplification of GAPDH was used as control. To prevent 'carryover' of amplified cDNA sequences, separate rooms and strict biosafety conditions were used for sample preparation and PCR. Primers were randomly selected from the list of genes with significant change. Selected primers included OSN (5′–TGGCCGCACTTTGCATCGCTGG–3′upstream and 5′–CGATAGGCCTCCTGAAAGCCGATG–3′downstream); Lipoprotein lipase (5′–AGACACAGCTGAGGACACTTGTC–3′upstream and 5′–TCCTTGGAGTTGCTCCTGTATGC–3′downstream);and C-Fos (5′–AACGCCGACTACGAGGCGTCATC–3′upstream and 5′–GCAGTTGGCAGGCAGAGTGTGATT–3′downstream). The expected sizes of the nested amplification products were between 600 and 800 bp. Amplified products were electrophoresed on a 1.5% agarose gel. The signals were quantified by densitometry and expression ratios were normalized according to GAPDH density.

3.3.12 Statistical methods

Results of the static and dynamic histomorphometry and cell culture experiments were expressed as the mean ±SEM. Cell culture experiments were performed in triplicate and repeated three times. Differences between treated and non treated groups were determined

by statistical analysis using Bartlett's test for homogeneity of variable and Turkey-Kramer multiple comparisons test for histomorphometry measurements, all other variables were compared by using One-way Analysis of Variance (ANOVA). The animal experiment was repeated twice. A value of $P< 0.05$ was considered significant.

3.4 Results

3.4.1 Bone Histomorphometry

Figure 17 shows Goldner's trichrome staining in vehicle treated (panels A and C) and $1,25(OH)_2D_3$ treated mice (panels B and D). Panels E and F show fluorescence staining with demeclocycline in bone specimens from vehicle treated (E) and $1,25(OH)_2D_3$ treated (F) animals. Panels G and H show ALP and TRACP stainings in bone sections from vehicle treated (G) and $1,25(OH)_2D_3$ treated (H) mice. Table 1 shows the complete set of histomorphometric measurements in both static and dynamic parameters as well as its statistical differences. Static histomorphometric analysis shows a significant increase in bone volume (BV/TV, $P<0.001$), trabecular number (Tr.N. $P< 0.001$), and trabecular thickness (Tb.Th. $P<0.001$) as well as cortical width (Ct.Wi. $P <0.05$) in the $1,25(OH)_2D_3$ treated group as compared to the $1,25(OH)_2D_3$ treated group (Table 1). Furthermore, a significant decrease in bone resorption parameters (ES/BS, and N.Oc/B.Pm) was observed in the $1,25(OH)_2D_3$ treated group as compared to the vehicle treated group(Table 1).

Concerning the static and dynamic parameters of bone formation, no significant difference was found between the two groups (The AjAR being spuriously high in the $1,25(OH)_2D_3$ treated group due to the very low value of OS/BS in this group) However

the mean wall thickness was significantly increased in the trabecular bone and in the sub periosteal areas. Additionally, micro-architectural changes assessed using 3D micro CT (3D-μCT) demonstrated morphological changes similar to those seen by histomorphometry (data no shown).

3.4.2 Bone marrow AD in SAM-P/6 mice treated with 1,25 $(OH)_2D_3$

Analysis of longitudinal bone sections obtained from $1,25(OH)_2D_3$ treated animals indicated a marked reduction in bone marrow AD with a significant difference in the percentage of adipocytes detected by oil red O staining (Fig. 18, A and C). In vehicle treated animals 78% ±4 cells were stained positive with red oil O as compared to only 12± 3 % in 1,25 $(OH)_2D_3$ treated mice animals (B and D) ($p < 0.001$). In addition, marked adiposity was found in the interstitial space of bone marrow in vehicle treated group.

3.4.3 Changes in bone mass in SAM-P/6 treated with $1,25(OH)_2D_3$

Dual-Energy X-ray absorptiometry (DEXA) was performed on SAM-P/6 at 4 months of age (peak bone mass) and after treatment with $1,25(OH)_2D_3$ or vehicle. Significant changes were observed in both lumbar spine (Fig. 18,E) and hip (Fig. 18, F) with values of 0.1±0.005 and 0.085±0.007 g/cm^2 at 6 weeks in $1,25(OH)_2D_3$ treated mice compared to 0.052±0.007 and 0.068±0.003 g/cm^2 in vehicle treated animals ($p<0.01$). These absolute values correspond to an increase of 40 ± 5% and 20 ± 4% at the hip and spine of the $1,25(OH)_2D_3$ treated mice as compared to a decline of –8 ±2 % and –5 ± 1,5 % respectively in the non-treated group during the same period. This time course difference can be seen shown in Fig. 18 (E and F) treatment with $1,25(OH)_2D_3$ resulted in a time

Figure 17

- *Histological and histomorphometrical analysis of bone*

Goldner's trichrome staining of proximal tibiae is shown in vehicle-treated mice (panels A, X40, and C, X100) and 1,25$(OH)_2D_3$ treated mice (B and D), Panels E and F show non-treated (E) and treated (F) fluorescence for demeclocycline. We found a significant lower trabecular volume and lower trabecular and cortical thickness in the vehicle-treated group as compared to the 1,25$(OH)_2D_3$ group. The quantification of dynamic and static parameters is shown in table 1. Interestingly, we found also a very significant inhibitory effect of 1,25$(OH)_2D_3$ on bone resorption measured by osteoclastic activity (ES/BS). This can be seen by $TRACP^+$ staining (red cells) for 1,25 $(OH)_2D_3$ treated animals (G) as compared to non-treated animals (H).

- *Micro-CT analysis of bone from SAM-P/6 treated with 1,25$(OH)_2D_3$*

The figure shows the differences in coronal sections in 1,25 $(OH)_2D_3$ treated (I) vs. vehicle-treated mice(K) and in the 3D digitally extracted segments (panel J for vehicle-treated and panel L for 1,25 $(OH)_2D_3$ treated mice). There is a higher trabecular(Tb) thickness and number as well as higher cortical thickness (Ct) in the 1,25$(OH)_2D_3$ treated group vs. the vehicle-treated mice. The measurements correlate with those obtained by histomorphometry (data no shown).

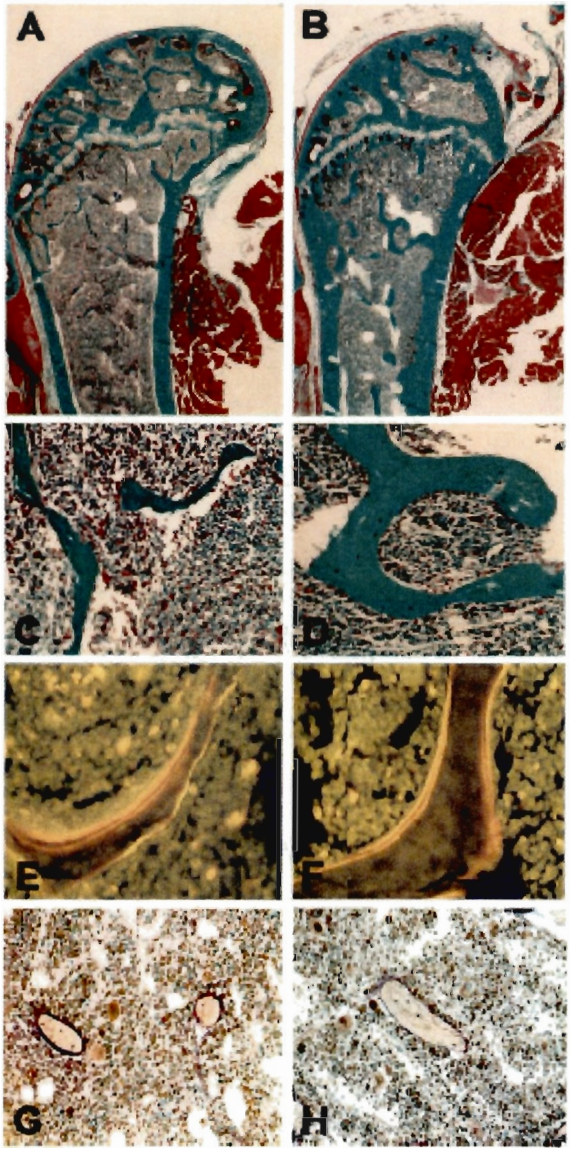
A
B
C
D
E
F
G
H

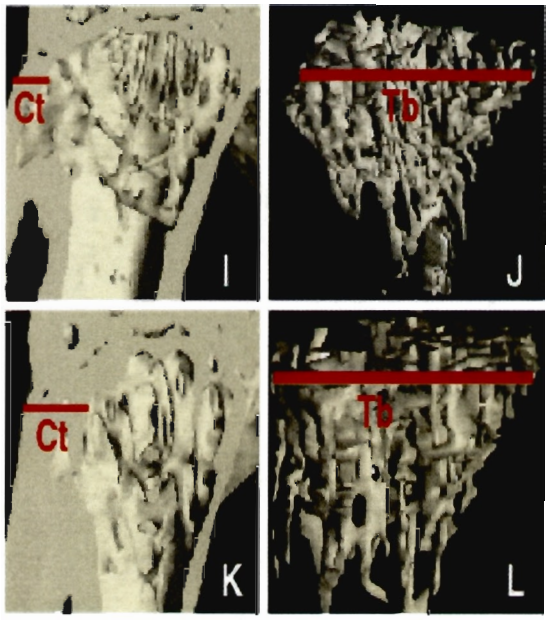
Ct
I
Tb
J
Ct
K
Tb
L

Table 1. Histomorphometrical analysis of bone in $1,25(OH)_2D_3$ treated vs. non-treated SAM-P/6 mice

	SAM-P/6 control	SAM-P/6 treated	p value
Static parameters			
BV/TV(%)	7.3 ± 1.6	15.7 ± 0.7	0.01
TbTh (μm)	26.4 ± 2.9	47.6 ± 2.4	0.01
TbSp (μm)	384 ± 53	256 ± 8.8	0.01
TbN (mm)	2.6 ± 0.3	3.3 ± 0.1	0.01
Ct.Wi (μm)	167 ± 6.7	202.1 ± 7.5	0.04
Corticale-I(μm)	148 ± 4.4	188.6 ± 8	NS
Corticale-II(μm)	186.1 ± 9.9	215.7 ± 7.3	0.01
OV/BV (%)	0.14 ± 0.08	0.012 ± 0.007	NS
OS/BS (%)	0.92 ± 0.43	0.12 ± 0.07	NS
ObS/BS (%)	0.2 ± 0.11	0.004 ± 0.003	0.01
Oth (μm)	1.5 ± 0.08	1.7 ± 0.2	NS
ES/BS (%)	8.3 ± 1.4	1.3 ± 0.3	0.001
NOc/Tar (/mm^2)	4.3 ± 0.4	2.3 ± 0.4	0.01
Noc/BPm (/mm)	3.1 ± 0.3	0.5 ± 0.08	0.01
Noc/Epm (/mm)	41.9 ± 5.7	40.8 ± 9.3	NS
Dynamic Parameters			
MS/BS (%)	17.2 ± 1.25	15.4 ± 6.8	NS
sLS/BS (%)	23 ± 1.8	20.7 ± 9.6	NS
dLS/BS (%)	5.75 ± 1	5.1 ± 3.1	NS
sLS/LS (%)	135 ± 9	139 ± 13.4	NS
dLS/LS(%)	32.5 ± 4.5	30.2 ± 6.7	NS
IrLTh (μm)	4.1 ± 0.28	4.2 ± 0.7	NS
MS/OS (%)	3277 ± 994	53780 ± 39674	0.01
MAR (μm/d)	0.82 ± 0.05	0.84 ± 0.14	NS
AjAR (μm/d)	25 ± 7	765.8 ± 655	0.001
BFR/BS	52.4 ± 6	61.7 ± 33	NS
BRF/BV	416 ± 59	245 ± 126	0.05
BFR/TV	28 ± 5	39 ± 20	NS

T.Ar: tissue area
B.Pm: bone perimeter
BV/TV: bone volume
Tb.Th: trabecular thickness
Tb.Sp: trabecular separation
Tb.N: trabecular number
Ct.Wi: cortical width
OV/BV: osteoid volume
OS/BS: osteoid surface
Ob.S/BS: osteoblast surface
O.Th: osteoid thickness
ES/BS: eroded surface
Oc.S/BS: osteoclast surface
M.Oc/T.Ar.: osteoclast number (per tissue area)
N.Oc/B.Pm:osteoclast number (per bone perimeter)
N.Oc/E.Pm: osteoclast number (per eroded centimeter)
MS/BS: Mineralizing surface
sLS/BS: single labelled surface per bone surface
dLS/BS: double labelled surface per bone surface
sLS/LS: single labelled surface per labelled surface
dLS/LS: double labelled surface per labelled surface
IrLTh: interlable thickness
MS/OS: mineralized surface
MAR: mineral apposition rate
Aj.Ar: adjusted apposition rate
BFR/BS: bone formation rate (per bone surface)
BFR/BV: bone formation rate (per bone volume)
BFR/TV: bone formation rate (per tissue area)

dependent increase in bone mass whereas vehicle treated animals lost bone during the same period.

3.4.4 Ex-vivo cultures of bone marrow cells

MSC obtained from $1,25(OH)_2D_3$ treated animals induced to differentiate had significantly more mineralized bone nodules (72±4) as compared to MSC obtained from vehicle treated animals (41± 3;$P< 0.05$)(Fig. 18, G and H).

3.4.5 Biochemical markers of bone formation and resorption

Both, $1,25(OH)_2D_3$ and vehicle-treated animals groups remained normocalcemic for the duration of the experiment (Table 2). Serum osteocalcin concentrations increased significantly ($P<0.05$) whereas serum N-telopeptide concentrations decreased significantly ($P<0.001$) in $1,25(OH)_2D_3$ treated animals as compared to vehicle-treated animals(Table 2). In addition, serum concentrations of PTH decreased significantly in $1,25(OH)_2D_3$-treated as compared to vehicle treated mice (Table 2) ($p<0.001$).No significant difference in serum 25-OHD levels were observed between both groups.

Figure 18

- *Effect of 1,25(OH)$_2$D$_3$ on bone marrow AD*

Longitudinal sections of proximal tibiae from 1,25(OH)$_2$D$_3$ were stained with oil red O for adipose tissue. Hematoxylin was used as counterstaining. Adipose tissue (AD) stained strong red with blue nuclei while all other bone marrow cells were stained light blue by hetatoxylin. A marked increase in adipocyte staining can be seen in vehicle-treated (A and C) as compared to 1,25(OH)$_2$D$_3$ treated mice (B and D). Note that most of the bone marrow space (BM) is occupied by adipose tissue in non-treated animals. Two different magnifications were used (40X for panels A and B and 100X for panels C and D)

- *DEXA analysis of SAM-P/6 mice treated with 1,25(OH)$_2$D$_3$.*

DEXA analysis was performed on male and female SAM-P/6 at 4 months (time 0) and following continuous administration by osmotic mini-pumps of 1,25(OH)$_2$D$_3$ or vehicle (see methods). Analysis was done at 3 weeks and 6 weeks in both SAM-P/6 treated (1,25(OH)$_2$D$_3$, n=12) and non- treated (vehicle, n=12) groups. BMD measured at the hip and lumbar spine showed a significant increase at both sites (E, spine; F, hip) in the 1,25(OH)$_2$D$_3$ treated group as compared to the vehicle-treated group. Each point represents the mean measurements ± SD of 12 different animals per group.*$p < 0.001$. This experiment was repeated twice.

- *Osteoblast differentiation in ex-vivo cultures of bone marrow cells derived from SAM-P/6 mice treated with 1,25(OH)$_2$D$_3$.*

Bone marrow cells were obtained after flushing both tibiae with Dubelcco's alpha modified medium(DMEM), grown in OIM for 21 days in 15cm^2 dishes and analyzed for the presence of mineralized bone nodules as described in methods. Mineralized bone

nodules were detected by Alizarin Red (pH 4.2) staining (G). The total number of bone nodules per dish was counted macroscopically. Panel H indicates that a significant and higher number of bone nodules was observed in bone marrow flushings of $1,25(OH)_2D_3$ treated SAM-P/6 as compared to the vehicle treated group. *$p < 0.05$ indicates a significant difference from control. Flushed bone marrow cells were obtained from 6 animals per group. Values represent mean ± SD of 12 determinations.

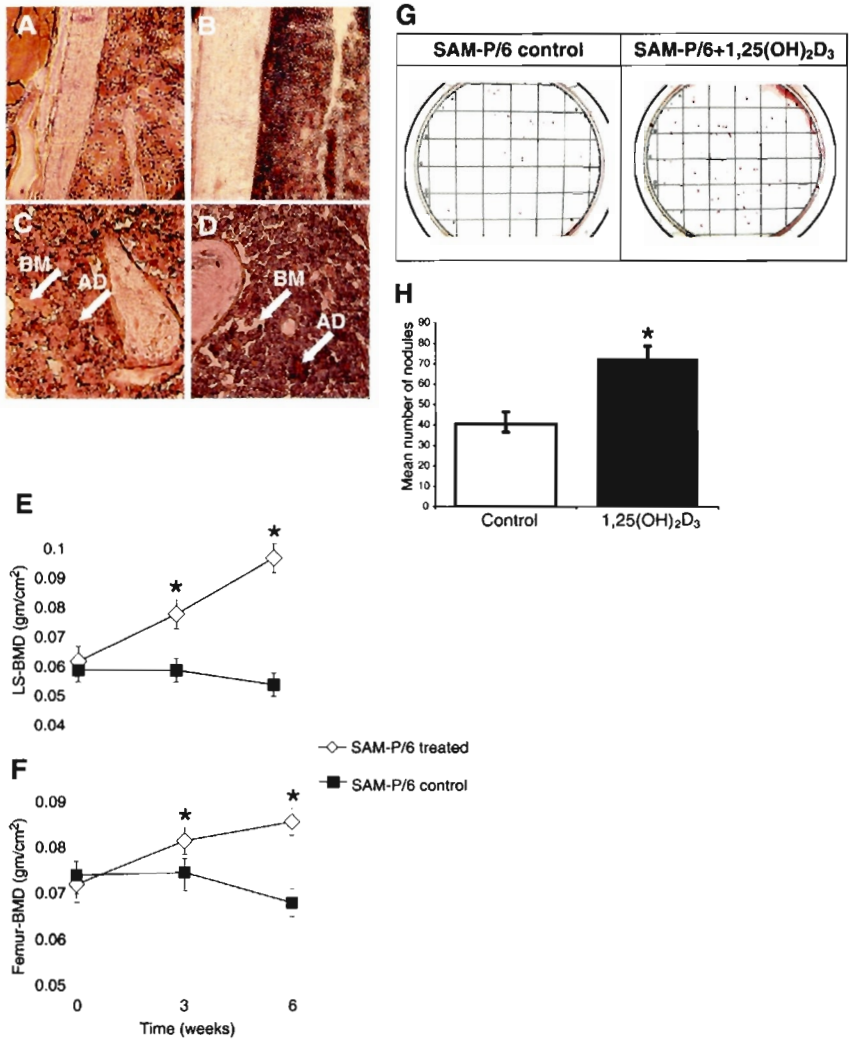

Table 2. Biochemical markers of osteoblastic and osteoclastic activity in SAM-P/6 mice treated with $1,25(OH)_2D_3$. Comparison with non-treated group.

Assay	*SAM-P/6-Control*	*SAM-P/6-1,25(OH)$_2$D$_3$*	*p value*
Ca++ [1.8-2.3]	1.9 ± 0.11	2.3 ± 0.043	NS
Osteocalcin [70-110 ng/mL]	58 ± 18	136 ± 14	0.05
N-Telopeptide [12-45 ng/mL]	18 ± 1	9.7 ± 1.1	0.001
PTH [16-28 pg/mL]	37 ± 14	9 ± 4	0.001
25(OH)vitamin D [50-70 ng/mL]	28 ± 10	25 ± 7	NS

3.4.6 Analysis of the changes in gene expression by microarray analysis

The plot graph showing the initial gene expression is shown in Fig. 19. A significant change was found in a total of 440 genes which are located above and under the lines (Fig. 19, A). The complete list of these genes can be seen in Table 3. Changes in gene expression were confirmed in three genes (calmodulin, C-Fos and lipoprotein lipase) by semi-quantitative RT-PCR. Figure 19 (B) shows the differences in expression of these genes in treated and non-treated animals. The quantification of expression changes was compared to a control GADPH and is shown in panel B.

In table 4 genes were grouped according to either their known regulation by $1,25(OH)_2D_3$ or to their function as stimulators/inhibitors of OB and/or AD. The table shows a total of 48 up-regulated genes known as regulators of osteoblastogenesis, adipogenesis or both. All of the genes are known to encode proteins that stimulate osteoblastogenesis. In addition, there is a higher number and expression of genes inhibiting adipogenesis (right column).

Figure 19. Gene expression in RNA extracted from trabecular cells of SAM-P/6 treated with $1,25(OH)_2D_3$

Panel A shows a scatter plot of gene expression levels for each gene, mean mRNA expression levels averaged from $1,25(OH)_2D_3$ treated and vehicle-treated groups were plotted on a double logarithmic scale. The red lines indicate a significant change in gene expression (± 2 fold) between treated and non-treated groups. Ordinate and abscissa are arbitrary fluorescent units. This experiment was repeated twice after pooling RNA obtained from 5 randomly selected mice per group. To deal with noise in the microarray datasets we used biological duplication technique as previously described (116,117). Panel B represents semi quantitative RT-PCR of selected genes. Expression levels for selected genes (calmodulin, C-Fos and Lipoprotein Lipase) were confirmed by semi-quantitative RT-PCR and normalized to GADPH expression. The figure shows the level of expression of the three genes in the $1,25(OH)_2D_3$ treated vs. the vehicle-treated group. The table in panel B compares the fold change in the 15K NIA array as compared to the changes in gene expression detected by RT-PCR. There is a significant correspondence between the two numbers for the three genes analyzed.

A

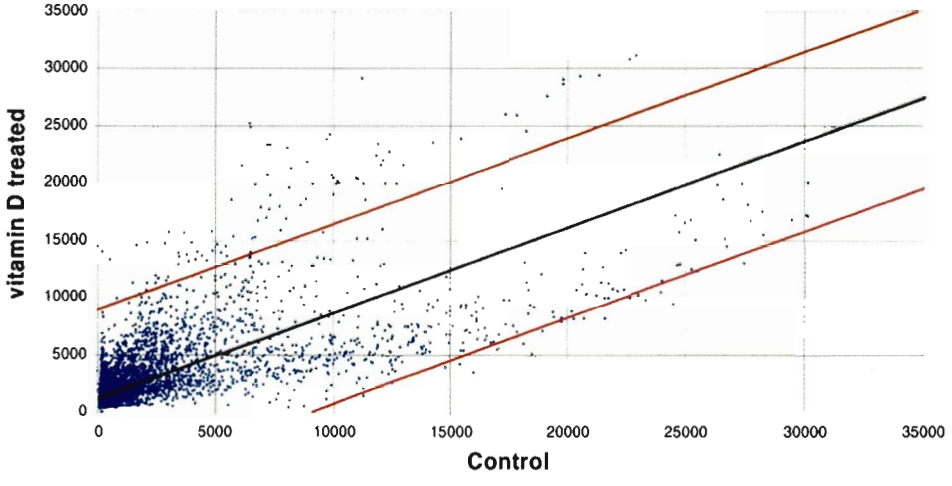

B

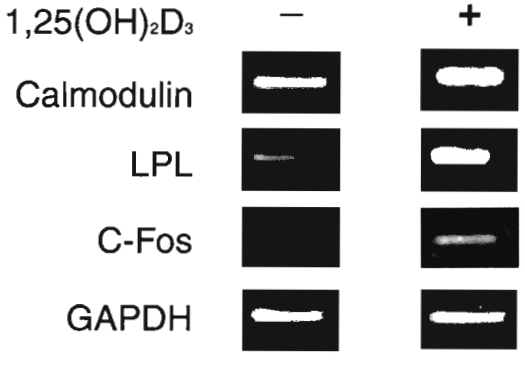

	Array	RT-PCR
Calmodulin	5.6	4
LPL	2.8	3.5
C-Fos	4	3.8

Table 3. Differentially expressed genes between $1,25(OH)_2D_3$ treated vs. non-treated SAM-P/6 mice

Up-regulated	Fold change
Growth Factors	average
H3152E02:neuronal differentiation related protein	7.1
H3115C04: epididymal secretory protein	6.5
H3147D11:Ranbp7 gene, Staf gene and Wee1	5.6
H3143B05:splicing factor (CC1.3)	5.0
H3125G06:ERO1-like (S. cerevisiae) (Ero1l-pending)	5.0
H3142F05:STAT6 (Stat6) gene, partial cds and NAB2 (Nab2)	4.5
H3107C11:EGF-containing fibulin-like extracellular matrix protein 2 (Efemp2)	3.2
H3109G10:hepatocyte growth factor activator inhibitor type 2 splice variant 2 (Hai2)	2.2
Proteins	
H3153A10:Homo sapiens DR1-associated protein 1 (DRAP1)	6.4
H3002D02:melanoma X-actin (Actx)	6.4
H3157B10:heat shock protein, DNAJ-like 2 (Hsj2)	6.1
H3140D11:Rattus norvegicus nucleolar phosphoprotein of 140kD	6.0
H3014E04:regulatory factor X-associated ankyrin-containing protein (Rfxank)	5.9
H3131F08:Ly6/neurotoxin 1 (Lynx1)	5.7
H3115F03:stimulated by retinoic acid gene 6 (Stra6)	5.7
H3058B12:ganglioside-induced differentiation-associated-protein 1 (Gdap1)	5.6
H3015H04:ribosomal protein L8 (Rpl8)	5.6
H3018E03:Rattus norvegicus transactivating protein BRIDGE	5.4
H3084H04:cerebellin 1 precursor protein (Cbln1)	5.4
H3123D01:synaptotagmin 4 (Syt4)	5.4
H3102E10:HS1 binding protein 3 (Hs1bp3-pending)	5.3
H3008B01:Homo sapiens TAR DNA binding protein (TARDBP)	5.3
H3119A03:synapsin I (Syn1)	5.3
H3151B06:Ranbp7 gene, Staf gene	5.2
H3125F04:hypothetical protein MDS015 (MDS015)	5.2
H3115F04:tuftelin-interacting protein 33 (TIP39)	5.1
H3145E05:RuvB-like protein 2 (Ruvbl2)	5.1
H3109B05:lactotransferrin (Ltf)	5.1
H3121A12:BM022 protein (BM022)	5.0
H3133E12:Homo sapiens p65 protein (HSAJ2425)	4.9
H3113C01:beta-globin	4.9
H3149G04:Rattus norvegicus mRNA for neurodegeneration associated protein 1	4.9
H3138F12:ryudocan core protein	4.9
H3137G02:gis5 mRNA for glucocorticoid-inducible protein	4.9
H3036D07:catenin src (Catns)	4.8
H3020C02:metallothionein-I (MT-I)	4.8
H3126A11:mRNA for a stretch regulated skeletal muscle protein	4.8
H3114H12:COL3A1 gene for collagen alpha	4.8
H3129B08:H19 and muscle-specific Nctc1	4.8
H3013C10:breast heat shock 73 protein (hsc73)	4.6
H3098D07:carboxyl terminal LIM domain protein 1 (Clim1)	4.6
H3109B11:fatty acid transport protein 4	4.6
H3119A05:smoothelin gene, alternatively spliced	4.6
H3123A02:alpha globin gene and flanking regions	4.6
H3138G01:vacuolar protein sorting 45 (yeast) (Vps45)	4.6
H3126A10:alpha globin gene and flanking regions	4.6
H3125H11:alpha globin gene and flanking regions:Mm.1568:g	4.6
H3117H08:Homo sapiens actin related protein 2/3 complex, subunit 4 (20 kD) (ARPC4)	4.5
H3119E11:ribosomal protein L23 (Rpl23) mRNA	4.5
H3118E11:beta-globin major gene	4.5
H3122H10:DNA for alpha globin gene and flanking regions	4.5
H3020G05:nebulin-related anchoring protein (Nrap)	4.5
H3100G02:meprin beta subunit isoform (Mep-1beta)	4.5
H3140H08:Kip1 C-terminus interacting protein-2 (Kic2)	4.5
H3113D09:myristoylated alanine rich protein kinase C substrate (Macs)	4.5
H3014D03:breast cancer metastasis-suppressor 1 (BRMS1)	4.5
H3122H11:DNA for alpha globin gene	4.5
H3008C09:HSP90=heat shock protein	4.5
H3006H04:syndecan 1 (Sdc1)	4.4

H3123F10:alpha globin	5.0
H3005E10:mRNA for sodium/potassium ATPase beta subunit	5.0
H3081H03:Fus-associated protein with serine-arginine repeats	5.0
H3140B05:presenilin 2	5.0
H3005B04:Homo sapiens hypothetical protein FLJ10488 (FLJ10488)	4.3
H3015G09:kidney predominant protein NCU-G1 (NCU-G1)	4.3
H3109G06:uterine lactotransferrin	4.3
H3054D01:Homo sapiens vacuolar protein sorting protein 11 (VPS11)	4.3
H3011B04:actin, gamma, cytoplasmic (Actg)	4.3
H3118G01:beta-1-globin:Mm.2329:g	4.3
H3110C09:plectin:Mm.21072:g	4.2
H3158G12:metallothionein-like 5, testis-specific (tesmin) (Mtl5)	4.1
H3130B09:zinc finger protein 59 (Zfp59)	4.1
H3157F05:Snf2-related CBP activator protein (SRCAP)	4.0
H3020D03:uncharacterized bone marrow protein BM036 (BM036)	4.0
H3139F10:Rattus norvegicus ERG2 protein	3.9
H3120F02:Human polyadenylate binding protein (TIA-1)	3.9
H3018B01:adaptor protein complex AP-2, alpha 1 subunit (Ap2a1)	3.9
H3020B08:ferritin light chain 1 (Ftl1)	3.9
H3020G04:basigin	3.8
H3141D04:Homo sapiens ribosomal protein S21 (RPS21	3.8
H3043A10:apolipoprotein A-I (Apoa1)	3.8
H3022A08:Homo sapiens CGI-96 protein	3.8
H3153A07:Homo sapiens zinedin (ZIN)	3.7
H3011G12:Mouse proliferin	3.7
H3130C02:calcineurin inhibitor	3.7
H3143A09:Homo sapiens BTB and CNC homology 1	3.7
H3010H04:cartilage associated protein (Crtap)	3.7
H3028G02:mRNA for nuclear protein ZAP	3.6
H3023G02:proteolipid protein 2 (Plp2)	3.6
H3017C09:Homo sapiens TATA box binding protein (TBP)	3.6
H3113B11:chondroitin sulfate proteoglycan 6	3.6
H3022B06:putative nuclear protein (HRIHFB2122)	4.4
H3122H09:DNA for alpha globin gene	4.4
H3129G01:SH3-domain GRB2-like B1 (endophilin) (Sh3glb1)	4.4
H3147A12:Homo sapiens HBV pX associated protein-8 (LOC51773)	4.4
H3097G02:Homo sapiens mRNA for KIAA1157	4.3
H3143E07:Homo sapiens hypothetical protein FLJ11071 (FLJ11071)	4.3
H3019F09:Homo sapiens hypothetical protein FLJ10330 (FLJ10330)	3.4
H3127G11:Homo sapiens myosin IC (MYO1C)	3.4
H3148E05:ribosomal protein L32-3A (3A)	3.4
H3140G05:diaphanous homolog 1 (Drosophila) (Diap1)	3.4
H3018E05:cytokeratin endo A	3.3
H3154G12:proteasome beta type subunit 5 (Psmb5)	3.3
H3046F12:heterogeneous nuclear ribonucleoprotein C (Hnrnpc)	3.3
H3008E11:core promoter binding protein mRNA	3.3
H3116F07:nuclear phosphoprotein similar to S. cerevisiae PWP1 (PWP1)	3.3
H3135A06:capping protein alpha 2 (Cappa2)	3.3
H3057B12:tubulin beta-3	3.2
H3150D06DJ-1 protein (DJ-1)	3.2
H3137A06:zona pellucida glycoprotein 2 (Zp2)	3.2
H3115F07:Homo sapiens phosphatidylinositol glycan, class C (PIGC)	3.2
H3032D07:Gallus gallus RRM-type RNA-binding protein hermes	3.2
H3029D06:Rattus norvegicus mRNA for class I beta-tubulin	3.2
H3140B08: mRNA for type 1 procollagen C-proteinase enhancer protein	3.2
H3082F06:tumor-associated calcium signal transducer 1 (Tacsd1)	3.2
H3155G05:Human sterol carrier protein-X/sterol carrier protein-2 (SCP-X/SCP-2)	3.2
H3126H09:Homo sapiens transmembrane protein (63kD), endoplasmic reticulum/Golgi intermediate compartment (P63)	3.2
H3119B11:mRNA for cytotoxic T-cell membrane glycoprotein Ly-3 3'flank:M	3.1
H3029G08:TLS-associated protein TASR-2	3.1
H3016F06:nuclear myosin I beta mRNA	3.1
H3085G06:Homo sapiens putative zinc finger protein NY-REN-34 antigen (LOC51131)	3.1
H3017E04:cathepsin Z precursor (Ctsz)	3.1
H3059D12:strain MilP mitocondrion	3.1

(Cspg6)	
H3008A04:excision repair 1 (Ercc1)	3.6
H3009H10:H+ ATP synthase subunit c	3.6
H3027D11:adaptor protein complex AP-1, mu 2 subunit (Ap1m2)	3.5
H3083B05:Fus-associated protein with serine-arginine repeats	3.5
H3019C04:Homo sapiens VPS28 protein (LOC51160)	3.4
H3032B04:Rattus norvegicus mRNA for phocein protein	2.7
H3129C10:Rattus norvegicus steroid sensitive gene-1 protein (SSG-1)	2.7
H3131H12:ribosomal protein L37a (Rpl37a)	2.7
H3135C12:Rattus norvegicus lamina associated polypeptide 1C (LAP1C)	2.7
H3153H01:poly(rC)-binding protein 4 (Pcbp4)	2.7
H3156E04:perlecan (heparan sulfate proteoglycan 2) (Hspg2)	2.7
H3156G10:villin 2 (Vil2)	2.6
H3158D11:matrix metalloproteinase 2 (Mmp2)	2.6
H3123C04:GNB3 gene for GTP-binding protein beta3 subunit	2.6
H3154D09:Homo sapiens retinoblastoma-binding protein 2 (RBBP2)	2.5
H3144D12:f-box and WD-40 domain protein 5 (Fbxw5)	2.5
H3143A02:prothymosin beta 4 (Ptmb4)	2.5
H3003H03:Rattus norvegicus formin binding protein 21	2.5
H3127D04:histidine rich calcium binding protein (Hrc)	2.5
H3010H07:pellino 1 (Peli1)	2.4
H3116A04:secreted acidic cysteine rich glycoprotein (Sparc)	2.3
H3033H05:Serf1 protein (Serf1), survival of motor neuron protein (Smn)	2.2
H3021A11:Mus musculus small zinc finger-like protein (Tim13)	2.2
H3118E02:choroidermia (Chm)	2.1
H3036E09:clone 1 fanconi anemia complementation group A (Fanca)	2.1
H3004B12:hepsin (Hpn)	2.0
Receptors	
H3148H04:Rattus norvegicus 5HT3 receptor	6.3
H3124F10:strain 129/Sv 22 kDa peroxisomal membrane protein PMP22 (Pxmp2)	6.0
H3153E06:B-cell receptor-associated protein 29 (Bcap29)	5.7
H3088B05:zinc finger protein 103 (Zfp103)	5.6

genome	
H3104A12:Homo sapiens cullin 3 (CUL3)	3.1
H3124H07:Mus musculus ovalbumin upstream promoter transcription factor II COUP-TFII	3.0
H3005F06:Mus musculus pelle-like protein kinase mRNA	3.0
H3001F01:Homo sapiens ephrin-A1 (EFNA1)	3.0
H3029A04:scip POU-domain protein	3.0
H3139C02:adducin 1 (alpha) (Add1)	3.0
H3010A12:Homo sapiens nuclear cap binding protein subunit 2	2.9
H3003B06:adaptor-related protein complex AP-3, delta subunit (Ap3d)	2.9
H3116F05:myotubularin homologous protein 3	2.9
H3082G02:cullin 1 (Cul1)	2.9
H3052D02:neighbor of Cox4 (Noc4)	2.8
H3121G10:Homo sapiens putative integral membrane transporter (LC27)	4.3
H3032C06:cDNA FLJ11688 fis,	4.2
H3093H10:Tcra enhancer-binding factor interacting protein 1	3.9
H3106D03:MHC class I cell surface glycoprotein	3.9
H3009H08:telomerase binding protein p23	3.9
H3105F01:prenylated RAB acceptor 1 (Pra1)	3.4
H3082B01:natural killer tumor recognition sequence (Nktr)	3.4
H3025B11:Fas-binding protein, BING1	3.3
H3022C02:interleukin-1 receptor 8 (TIR8)	3.3
H3065F05:calcium channel, voltage dependent, alpha2/delta subunit 3 (Cacna2d3)	3.2
H3054H04:potassium intermediate/small conductance calcium-activated channel	3.1
H3104A04:colony stimulating factor 3 receptor (granulocyte) (Csf3r)	2.9
H3087A06:Homo sapiens fetal Alzheimer antigen (FALZ)	2.7
H3020H05:Homo sapiens KDEL (Lys-Asp-Glu-Leu) endoplasmic reticulum protein retention receptor 2	2.5
H3124D01:Homo sapiens G protein-coupled receptor 22 (GPR22)	2.1
Cell cycle-Cell adhesion	
H3123G02:Homo sapiens CGI-99 protein (LOC51637)	7.3
H3055D06:strain MilP mitocondrion genome	6.7
H3123E02:cellular nucleic acid binding protein (Cnbp)	6.7
H3103B09:Rattus norvegicus mRNA for long type PB-cadherin	6.6

H3098H05:hepatitis virus receptor	5.5	H3084H05:tropomodulin 3 (Tmod3)	6.2
H3131B11:Rattus norvegicus selectin, endothelial cell, ligand (Glg1)	5.3	H3017F07:hypoxanthine guanine phosphoribosyl transferase (Hprt)	6.2
H3125G05:ERO1-like (S. cerevisiae) (Ero1l-pending)	4.8	H3131E08:cadherin 2 (Cdh2)	6.2
H3010H10:receptor (calcitonin)	4.7	H3058C12:gene for LKB1 serine/threonin kinase	6.0
H3146E08:Homo sapiens transmembrane protein 11 (11)	4.6	H3021G06:mas proto-oncogene and Igf2r gene for insulin-like growth factor type 2 and L41	6.0
H3133G04:Rattus norvegicus low affinity Na-dependent glucose transporter (SGLT2)	4.5	H3013G08:Homo sapiens actin related protein 2/3 complex, subunit 5	6.0
H3141H11:Homo sapiens anti-Mullerian hormone receptor, type II (AMHR2)	4.5	H3129B10:Homo sapiens loss of heterozygosity, 11, chromosomal region 2, gene A (LOH11CR2A)	5.9
H3015A01:major histocompatibility locus class III region-butyrophilin-like protein	4.4	H3157F03:Homo sapiens ribosomal protein L39 (RPL39)	5.9
H3109A02:Fc receptor, IgE, high affinity I, gamma polypeptide (Fcer1g)	4.4	H3021E08:calmodulin (Calm)	5.6
H3126G09:E2F-like transcriptional repressor protein	4.3	H3149H12:delta/YY1/NF-E1/UCRBP transcription factor exon 5	5.3
H3019D09:protein kinase C inhibitor (mPKCI)	4.3	H3109C11:TATA box binding protein (Tbp)-associated factor, RNA polymerase I, A (Taf1a)	5.2
H3152H01:ubiquitin specific protease 25 (Usp25)	4.2	H3146F01:Homo sapiens RHOA proto-oncogene multi-drug-resistance	5.2
H3025G07:cell division cycle 2 homolog (S. pombe)-like 2 (Cdc2l2)	4.2	H3020C01:nuclear RNA export factor 1 homolog (S. cerevisiae) (Nxf1)	4.7
H3123G08:RNA polymerase II 4 (14 kDa subunit) (Rpo2-4)	4.2	H3115G07:cyclin-dependent kinase inhibitor 3 (CDK2-associated dual specificity phosphatase) (CDKN3)	4.4
H3092G01:p38delta MAP kinase mRNA, complete cds	4.2	H3105B10:Cycb1=cyclin B1	4.4
H3081F12:Shcp52 (Shc) mRNA,	4.1	H3119F08mRNA for cyclin G	4.4
H3084G03:c-fos gene; cellular homolog to viral oncogene M	4.0	H3136G12:histone H1(0) gene	4.4
H3013E04:Homo sapiens adenylyl cyclase-associated protein (CAP)	4.0	H3129B09:Swi/SNF related matrix associated, actin dependent regulator of chromatin, subfamily a-like 1 (Smarcal1)	2.9
H3118D01:block of proliferation 1 (Bop1)	4.0	H3103H06:neighbor of A-kinase anchoring protein 95 (Nakap95-pending)	2.8
H3152G03:Human RNA polymerase II subunit hsRPB4	3.9	H3113H07:ubiquitin-activating enzyme E1C (Ube1c)	2.8
H3149F04:ERG-associated protein (ESET)	3.9	H3064C09:myeloblastosis oncogene-like 1 (Mybl1)	2.8
H3147A06:APEX nuclease	3.9	H3016H08:Homo sapiens cofactor required for Sp1 transcriptional activation, subunit 9 (33kD) (CRSP9)	2.8
H3129H07:TERF1-interacting nuclear protein 2 (Tin2)	3.9	H3068G02:ubiquitin conjugating enzyme 2e (Ubc2e)	2.8
H3122B01:gamma-1 adducin (Add1)	3.7	H3124D06:DNA fragmentation factor, 40 kD, beta subunit (Dffb)	2.8
H3151E11:Homo sapiens SHC (Src homology 2 domain-containing) transforming protein 1 (SHC1)	3.7	H3155H03:ribosomal protein L3 (Rpl3)	2.8
H3141H05:cadherin 2 (Cdh2)	3.7	H3012A01:mRNA of enhancer-trap-locus 1	2.6
H3137H05:Finkel-Biskis-Reilly murine sarcoma virus (FBR-MuSV) ubiquitously expressed (fox derived) (Fau)	3.6	H3092B10:ADP-ribosylation factor-like protein 3 (Arl3)	2.6
H3034C10:Homo sapiens transducin (beta)-like 3 (TBL3)	3.5	H3078B02:Finkel-Biskis-Reilly murine sarcoma virus (FBR-MuSV) ubiquitously expressed (fox derived) (Fau)	2.6
H3152C07:Homo sapiens ADP-ribosylation factor 3 (ARF3)	3.5	H3010D11:Homo sapiens hypothetical protein FLJ20154 (FLJ20154)	2.6

H3142D02:upstream transcription factor 1 (Usf1)	3.5
H3091G06:Homo sapiens protein phosphatase 4 regulatory subunit 2 (PPP4R2)	3.5
H3140A08:mitogen activated protein kinase 14 (Mapk14)	3.4
H3157F04:transcriptional activator alpha-NAC (Naca) gene	3.4
H3144E08:Homo sapiens FOXJ2 forkhead factor (LOC55810)	3.3
H3006B07:RAN binding protein 1 (Ranbp1)	3.3
H3151G11:potassium channel, subfamily K, member 1 (Kcnk1)	3.2
H3083F09:putative homeodomain transcription factor (Phtf)	3.2
H3107F10:Homo sapiens signal sequence receptor, alpha (translocon-associated protein alpha) (SSR1)	3.2
H3128C02:Tcra enhancer-binding factor interacting protein 1 (Tebfip-pending)	3.1
H3102C01:Homo sapiens sorting nexin 5 (SNX5)	3.1
H3116E09:Homo sapiens core histone macroH2A2.2 (MACROH2A2)	3.1
H3014C02:Homo sapiens eukaryotic translation elongation factor 1 gamma (EEF1G)	3.1
H3022E03:ubiquitin-activating enzyme E1, Chr X (Ube1x)	3.0
H3098H10:calbindin-28K (Calb1)	3.0
H3019E12:Homo sapiens F1F0-type ATP synthase subunit d	5.8
H3009C03:transglutaminase 1, K polypeptide (Tgm1)	5.6
H3149D12:Homo sapiens apyrase, lysosomal (LAP70)	5.3
H3029F11:hexokinase	5.3
H3140D05:Homo sapiens ectonucleotide pyrophosphatase/phosphodiesterase 5 (putative function) (ENPP5)	5.2
H3010D06:caseinolytic protease, ATP-dependent, (E. coli) proteolytic subunit homolog (Clpp)	5.2
H3158G10:glucosidase I	5.2
H3123G10:mannoside acetylglucosaminyltransferase 1 (Mgat1)	4.9
H3082C10:flap structure specific endonuclease 1 (Fen1)	4.8
H3126C04:eukaryotic translation initiation factor 2 alpha kinase 1 (Eif2ak1)	4.8
H3144D09:casein kinase II, beta subunit (Csnk2b)	4.7
H3008E02:caseinolytic protease, ATP-dependent, (E. coli) proteolytic subunit homolog (Clpp)	4.5
H3030A06:lysosomal alpha-mannosidase (Man2b)	4.5
H3022D03:galactokinase	4.5
H3062E02:isocitrate dehydrogenase	4.4
H3157D01:aspartate aminotransferase	4.3
H3117A12:mRNA for kinesin-related mitotic motor protein	2.4
H3078B09:Homo sapiens Kruppel-like factor 5 (KLF5)	2.3
Apoptosis	
H3140C03:major histocompatibility locus class II region; Fas-binding protein Daxx (DAXX)	4.8
H3149B05:Human TFIID subunits TAF20 and TAF15	4.7
H3029F01:p53 apoptosis-associated target (Perp)	4.6
H3147B08:RAB11B, member RAS oncogene family (Rab11b)	4.3
H3051F08:programmed cell death 8 (apoptosis inducing factor) (Pdcd8)	3.6
H3107B03:major histocompatibility locus class II region; Fas-binding protein Daxx (DAXX)	5.4
H3025D01:Mus musculus Bex1 protein (Bex1)	3.0
Cytokines	
H3119D11:interferon-inducible protein 16	5.3
H3106H07:Homo sapiens solute carrier family 21	3.9
H3159D07:cytokine inducible SH2-containing protein (Cish)	3.6
H3009D01:Homo sapiens interleukin enhancer binding factor 1 (ILF1)	3.6
H3153H12:Scya6, Scya9, Scya16-ps, Scya5 genes for small inducible cytokine A6	2.1
Enzymes	
H3155C02:Homo sapiens ubiquinol-cytochrome c reductase	6.8
H3125D06:Flavin containing monooxygenase	6.8
H3114F08:Beta galactosidase	6.6
H3159E08:hexokinase	6.3
H3149H01:Homo sapiens protein phosphatase 1	6.0
H3144C01:Homo sapiens glyoxalase I (GLO1)	5.9
H3146H03:Na K-ATPase beta-3	5.9
H3114F02:histone deacetylase 1 (Hdac1)	5.8
H3021E09:vacuolar adenosine triphosphatase subunit A	2.7
H3062E08:epoxide hydrolase 2, cytoplasmic (Ephx2)	2.7
H3090E05:P450 (cytochrome) oxidoreductase (Por)	2.6
H3134B07:protease (prosome, macropain) 26S subunit, ATPase 1 (Psmc1)	2.6
H3018A02:beta-1,4-galactosyltransferase III (B4galt3)	2.6
H3044F06:clone mouse1-1 putative	2.6

H3029F12:hexokinase	4.3
H3154C12:clone mouse1-1 putative protein phosphatase type 2C	4.3
H3097F06:Homo sapiens FACL5 for fatty acid coenzyme A ligase 5 (LOC51703)	4.2
H3128A11:heterogeneous nuclear ribonucleoprotein C (Hnrnpc)	3.9
H3101E12:small GTPase (Rab11a)	3.9
H3081F04:Homo sapiens phosphorylase kinase, beta (PHKB)	3.9
H3083C09:12-lipoxygenase=platelet-type [mice, NMRI, papillomas	3.9
H3150B06:phospholipase A2 group VII (platelet-activating factor acetylhydrolase, plasma) (Pla2g7)	3.7
H3115A05:phospholipase C, delta (Plcd)	3.5
H3142H07:N-acetylglucosamine galactosyltransferase (beta1-4GT) (EC 2.4.1.90)	3.5
H3152A02:Rat beta-galactoside-alpha 2,6-sialyltransferase	3.5
H3099B11:glutathione peroxidase (Gpx2)	3.2
H3131G04:DEAD (aspartate-glutamate-alanine-aspartate) box polypeptide 5 (Ddx5)	3.2
H3028B10:polymerase beta gene, exons 1 and 2	3.1
H3088A07:glutathione S-transferase, mu 2 (Gstm2)	3.1
H3155B07:Homo sapiens NADH dehydrogenase (ubiquinone) Fe-S protein 3 (30kD) (NADH-coenzyme Q reductase) (NDUFS3)	3.0
H3010G07:adenylate kinase 4 (Ak4)	3.0
H3134F03:glutathione transferase mu (GSTM1)	3.0
H3002B07:sepiapterin reductase gene, exons 1 and 2	3.0
H3138D08:paraoxonase 3 (Pon3)	2.8
H3007F06:lipoprotein lipase (Lpl)	2.8
H3084H07:Human clone A9A2BRB5 (CAC)n/(GTG)	5.4
H3050H04:18S rRNA gene, clones 5a,6,7	5.4
H3139E06:Homo sapiens mRNA; cDNA DKFZp761E0711	5.3
H3011F09:monoclonal non-specific suppressor factor beta	5.3
H3143B11:Homo sapiens full length insert cDNA clone ZD51E04	5.3
H3157C02:Homo sapiens cDNA FLJ12598 fis, clone NT2RM4001384	5.3
H3150B08:Homo sapiens dynamitin (dynactin complex 50 kD subunit) (DCTN-50)	5.3
H3119B01:strain MilP mitocondrion genome, complete sequence:Mm.155059:w	5.2
H3147F07:Homo sapiens mRNA; cDNA	5.1

protein phosphatase type 2C	
H3022C05:O.cuniculus mRNA for serine hydroxymethyltransferase	2.4
H3146E02:Human gene for dihydrolipoamide succinyltransferase, complete cds (exon 1-15)	2.2
H3046G06:Rattus norvegicus UDP-Gal-glucosylceramide beta-1,4-galactosyltransferase	2.1
Unknown	
H3144H01:Homo sapiens mitofilin	6.7
H3158E08:Homo sapiens cDNA-FLJ22557 fis	6.6
H3152A09:paxillin-like protein (Hic5)	6.5
H3149D09:split hand/foot deleted gene 1 (Shfdg1)	6.5
H3150B07:Homo sapiens clones 23667 and 23775 zinc finger protein (LOC57862)	6.3
H3146H08:Homo sapiens GL003 (GL003)	6.1
H3144F08:hemochromatosis (HFE) gene	6.0
H3056F09:strain MilP mitocondrion genome, complete sequence:Mm.133825:w	5.8
H3148D12:mRNA for elongation factor 1-alpha (EF 1-alpha)	5.8
H3159C01:Homo sapiens hypothetical protein STRAIT11499 (STRAIT11499)	5.8
H3113H06:Homo sapiens KIAA0396	5.8
H3012E07:Homo sapiens protein (peptidyl-prolyl cis/trans isomerase) NIMA-interacting, 4 (parvulin) (PIN4)	5.8
H3154C06:Homo sapiens hypothetical protein FLJ10702 (FLJ10702)	5.8
H3152A12:Homo sapiens mRNA; cDNA DKFZp564G2463 (from clone DKFZp564G2463)	5.7
H3147H04:Miwi like (MILI)	5.7
H3005C04:Homo sapiens cDNA FLJ14159 fis	5.7
H3042E12:Homo sapiens KIAA1046 protein (KIAA1046)	5.7
H3113H10:dynein, cytoplasmic, light chain 1 (Dnclc1)	5.7
H3126H07:Homo sapiens HSPC333	5.7
H3098H06:TAFII30 gene for mTAFII30 protein	5.6
H3146H12:Homo sapiens hypothetical protein (LOC51250)	5.6
H3124B06:mRNA for putative mc7 protein (mc7 gene)	5.5
H3133G09:MDS017 (MDS017)	5.5
H3122H05:strain MilP	5.5
H3155A03:Homo sapiens hypothetical protein (HSPC164)	5.5
H3109H09:bystin-like (Bysl)	5.5

DKFZp566E034 (from clone DKFZp566E034)	
H3094A08:Homo sapiens HT001 protein (HT001)	5.1
H3147E12:zinc finger protein 207 (Zfp207)	5.1
H3146E09:Homo sapiens mRNA for KIAA1254	5.1
H3146D06:Homo sapiens mRNA; cDNA DKFZp434L1850 (from clone DKFZp434L1850)	5.1
H3131E11:Homo sapiens clone RP11-173C1	5.0
H3121H06:Homo sapiens HSPC16	5.0
H3122A07:Homo sapiens mRNA for KIAA1301	4.9
H3133C06:Human Tcr-C-delta gene, exons 1-4; Tcr-V-delta gene, exons 1-2; T-cell receptor alpha (Tcr-alpha)	4.9
H3126A03:mRNA for mcdc21 protein	4.9
H3157C08:Homo sapiens cDNA- FLJ23055 fis	4.9
H3144H03:clone SMT3B-g1/mSMT3 SMT3B	4.8
H3151G06:xeroderma pigmentosum, complementation group C (Xpc)	4.8
H3126G12:Homo sapiens mRNA for KIAA0824	4.8
H3158D08:Homo sapiens cDNA FLJ11163 fis, clone PLACE1007178	4.7
H3158H02:Homo sapiens cDNA FLJ13041 fis, clone NT2RP3001297	4.7
H3001D09:Fus1 gene (Fus1)	4.7
H3152C06:mRNA for KIFC2	4.7
H3149E09:Homo sapiens cDNA- FLJ21082	4.6
H3159B11:Homo sapiens mRNA; cDNA DKFZp586B0918 (from clone DKFZp586B0918)	4.6
H3152D09:Homo sapiens cDNA FLJ20541	4.6
H3154H01:Human mRNA for KIAA0365	4.5
H3141H10:partial mRNA for hypothetical protein (ORF37 DNA)	4.5
H3113D11:Homo sapiens KIAA0161 gene product (KIAA0161)	4.5
H3067C04:Homo sapiens small nuclear ribonucleoprotein polypeptide B" (SNRPB2)	4.4
H3079C09:45S pre rRNA	4.4
H3061H04:Homo sapiens clone HH409	4.4
H3092A07:Homo sapiens hypothetical protein (HSPC232)	4.4
H3132H01:Homo sapiens eIF-2-associated p67	4.3
H3017D11:Homo sapiens cDNA- FLJ21762 fis	3.7
H3140B12:Homo sapiens mRNA; cDNA DKFZp586J2118	3.7
H3139H12:Homo sapiens cDNA- FLJ22720 fis, clone HSI14320	3.7
H3010G09:Homo sapiens cDNA FLJ13700 fis,	3.7

H3056D06:45S	5.5
H3006E03:Human cytochrome c-1	4.3
H3061F03:Homo sapiens jagged 1 (Alagille syndrome) (JAG1)	4.3
H3142B10:H19 and muscle-specific Nctc1 genes	4.3
H3111G01:Homo sapiens cDNA-FLJ22222	4.3
H3148A07:Homo sapiens MLN51 protein (MLN51)	4.2
H3135A09:Homo sapiens cDNA FLJ13043	4.2
H3155E11:Homo sapiens KIAA0941 protein (KIAA0941)	4.2
H3014D12:Homo sapiens hypothetical protein FLJ10377 (FLJ10377)	4.2
H3102F11:brain cDNA, clone MNCb-3154	4.2
H3027G02:Homo sapiens ANG2 (ANG2)	4.2
H3157A10:ret finger protein (Rfp)	4.1
H3137E11:IL-11Ralpha gene	4.1
H3010B06:Rat PMSG-induced ovarian	4.1
H3152H09:Homo sapiens KIAA0211 gene product	4.1
H3001H05:CPN10-like protein (Cpn10-rs1)	4.1
H3023E10:Homo sapiens splicing factor (45kD)	4.1
H3145B04:mdgl-1	4.0
H3013C11:gene for t-complex polypeptide 1	4.0
H3047D04:brain cDNA, clone MNCb-4327:Mm.24770:g	4.0
H3127D09:Homo sapiens cDNA-FLJ23275 fis	4.0
H3147C02:Rattus norvegicus GRIP-associated protein 1 short form	4.0
H3091A08:Homo sapiens ADP-ribosylation factor-like 1 (ARL1)	4.0
H3142D11:Homo sapiens mRNA in the region near the btk gene involved in a-gamma-globulineminemia	4.0
H3005H11:Homo sapiens cDNA FLJ20738	3.9
H3018C11:Homo sapiens U3 snoRNP-associated 55-kDa	3.9
H3021B09:Homo sapiens KIAA0750 gene product (KIAA0750)	3.9
H3144H02:b326h7, complete sequence	3.8
H3154A05:Homo sapiens cDNA FLJ12085 fis, clone HEMBB1002510, weakly similar to GYP7 PROTEIN	3.8
H3143G12:Homo sapiens hypothetical protein (CL25022)	3.8
H3151E02:strain MilP mitocondrion genome	3.8
H3081H04:brain cDNA, clone MNCb-1275, similar to Mus musculus F-box protein containing leucine repeats 6	3.8

H3087C12:Homo sapiens cDNA FLJ13936 fis, clone Y79AA1000802	3.6
H3086C11:Homo sapiens hypothetical protein FLJ11274 (FLJ11274)	3.6
H3073E08:Rattus norvegicus RM1	3.6
H3134F07:mRNA for nuclear protein ZAP	3.6
H3009H12:Homo sapiens cDNA FLJ20664 fis	3.5
H3115B07:S100A9 gene for S100A9	3.5
H3080G05:Homo sapiens mRNA for KIAA1311	3.5
H3017D05:Homo sapiens cDNA FLJ20536 fis, clone KAT11223, highly similar to AL050225 Homo sapiens	3.4
H3024B10:Homo sapiens cDNA FLJ11663 fis	3.4
H3065F10:mRNA for hypothetical protein expressed in thymocytes (clone MFT.M05.13/MTA.B10.066)	3.4
H3058F01:Homo sapiens HT021 (HT021)	3.4
H3063C10:Macaca fascicularis brain cDNA, clone-QnpA-21065	3.3
H3022G10:Rattus norvegicus ABC50	3.3
H3096E12:clone TSIP1 p53-induced apoptosis	3.3
H3131B09:Homo sapiens mRNA for KIAA1	3.3
H3091D09:queuine tRNA-ribosyltransferase (LOC60507)	3.3
H3004D09:Rattus norvegicus INS-1 winged helix	3.2
H3026F04:Human clone A9A2BRB5 (CAC)n/(GTG)n	3.2
H3012E05:Homo sapiens cDNA- FLJ21313 fis, clone COL02176	3.2
H3120H10:strain MilP mitocondrion genome, complete sequence	3.2
H3150C03:Homo sapiens hypothetical protein FLJ10276 (FLJ10276)	3.2
H3018B11:Homo sapiens mRNA; cDNA DKFZp434A139 (from clone DKFZp434A139)	3.2
H3129E01:Homo sapiens mRNA for KIAA0643	3.2
H3138A05:guanine nucleotide releasing factor 1 gene, exon 10	3.2
H3008D08:Homo sapiens mRNA; cDNA DKFZp564H0764	3.1
H3002A05:Homo sapiens cDNA- FLJ23442	3.1
H3158H05:Homo sapiens clone 23860	3.1
H3150C01:Homo sapiens mRNA for KIAA0660	3.1
H3132H09:Homo sapiens 14q32 Jagged2	3.1
H3140G12:H19 and muscle-specific Nctc1	3.1

(Fbl6)	
H3103C07:icos ligand (Icosl)	3.8
H3123G06:Homo sapiens hypothetical protein DKFZp761K1423 (DKFZp761K1423)	3.8
H3156B10:Homo sapiens cDNA-FLJ22025 fis	3.7
H3010H01:Human mRNA for KIAA0062 gene	3.7
H3085B11:Homo sapiens cDNA-FLJ23602 fis, clone LNG15735	3.7
H3025A02:Homo sapiens cDNA FLJ20845 fis	3.7
H3138B12:Homo sapiens hypothetical protein FLJ10583 (FLJ10583)	3.0
H3111E02:Homo sapiens hypothetical protein FLJ13220 (FLJ13220)	3.0
H3029H05:tdgf1 gene (exons 1-5)	3.0
H3091C10:hnRNP K homologue	3.0
H3114A08:eIF-1A (eIF-1A)	3.0
H3018B05:Homo sapiens hypothetical protein FLJ20399 (FLJ20399)	2.9
H3082E06:Homo sapiens enigma (LIM domain protein) (ENIGMA)	2.9
H3085F03:Homo sapiens hypothetical protein (LOC51247)	2.9
H3124G08:diaphanous homolog 3 (Drosophila) (Diap3-pending)	2.9
H3045F07:hypothetical brain protein similar to X96994 BR-1 protein (Helix pomatia) (LOC56412)	2.9
H3116C05:Homo sapiens mRNA; cDNA DKFZp434P106 (from clone DKFZp434P106)	2.9
H3154H02:Homo sapiens mRNA; cDNA DKFZp586E0820 (from clone DKFZp586E0820)	2.9
H3150F10:hypothetical protein from clone MNCb-1932, similar to Homo sapiens FLJ20644 (LOC59032)	2.9
H3075G06:molybdenum cofactor synthesis-step 1 proteins A and B splice type I (Mocs1)	2.9
H3150H02:Homo sapiens (subclone 2_b8 from P1 H56)	2.8
H3116D10:Homo sapiens hypothetical protein FLJ20850 (FLJ20850)	2.8
H3005H05:Homo sapiens cDNA-FLJ23445	2.8
H3136F08:LU mRNA for Lutheran antigen	2.8
H3095G06:RAB27A (Rab27a)	2.8
H3029G11:traube (LOC56321)	2.8
H3129D09:Homo sapiens mRNA; cDNA DKFZp761C169 (from clone DKFZp761C169)	2.8
H3082H11:mRNA for PC3B	2.8
H3134B06:protease (prosome, macropain) 26S subunit, ATPase 1 (Psmc1)	2.8
H3114E02:proteasome (prosome,	2.7

H3018H06:Homo sapiens clone CTB-10G5	3.1
H3139H05:Homo sapiens ribosomal protein S23 (RPS23)	3.0
H3004G12:P40-8, functional (P40-8)	3.0
H3147B09:Human mRNA for KIAA0308 gene	2.5
H3125D08:Homo sapiens hypothetical protein FLJ10579 (FLJ10579)	2.5
H3153F06:Homo sapiens CGI-147 protein (LOC51651)	2.5
H3150F06:farnesyltransferase, CAAX box, alpha (Fnta)	2.5
H3012H08:brain cDNA, clone MNCb-2442	2.4
H3015C04:Homo sapiens hypothetical protein FLJ20487 (FLJ20487)	2.4
H3124G06:Homo sapiens ribosomal protein S21 (RPS21)	2.4
H3080C09:Homo sapiens cDNA- FLJ22195 fis	2.4
H3127D01:small nuclear ribonucleoprotein B (Snrpb)	2.3
H3040H04:Homo sapiens cDNA- FLJ21919	2.3
H3006B10:H.sapiens clathrin light chain b	2.3
H3121G11:tetratricopeptide repeat domain (Ttc3)	2.3
H3081H07:Homo sapiens cDNA FLJ12439 fis	2.3
H3143F08:Homo sapiens cDNA- FLJ21370 fis	2.2
H3141H09:Homo sapiens HSPC227	2.2
H3061F04:Homo sapiens HYA22 protein (HYA22)	2.2

macropain) 26S subunit, non-ATPase, 7 (Psmd7)	
H3146H06:Homo sapiens CTL2	2.7
H3117D11:lumican (Ldc)	2.7
H3153B10:unr gene, 3' end, and N-ras proto-oncogene	2.7
H3091E12:Homo sapiens cDNA FLJ20547 fis	2.7
H3146B07:ribosomal protein S19 (Rps19)	2.6
H3150B01:ribosomal protein S15 (Rps15)	2.6
H3008B08:H.sapiens mRNA for pur alpha extended 3'untranslated region	2.6
H3139E03:CD82 antigen (Cd82)	2.6
H3056F03:Homo sapiens cDNA-FLJ22334 fis	2.6
H3144D06:Sec61 alpha isoform 2 (Sec61a2)	2.6
H3048H11:gene rich cluster, C8 gene (Grcc8)	2.6
H3132A04:Homo sapiens clone RP11-132A1	2.6
H3110G02:mRNA for SCID complementing gene 2	2.6
Down-regulated	
Growth factors	
H3057G12:transforming growth factor beta 1 induced transcript 4 (Tgfb1i4)	-1.9
Proteins	
H3042C07:Homo sapiens HBV pX associated protein-8 (LOC51773)	-2.0
Cell cycle-Cell adhesion	
H3075C08:Kruppel-like factor 4 (gut) (Klf4)	-1.8
H3041G03:solute carrier family 15 (H+/peptide transporter)	-1.9
Apoptosis	
H3131G08:nuclear RNA helicase Bat1 (LOC56472)	-2.1
Cytokines	
H3096A05:Rattus norvegicus rap7a	-2.2

3.5 Discussion

In the process of aging bone distinct changes take place with trabecular bone, cortical bone and bone marrow. In bone marrow an increase in AD and a decrease in OB are observed (8,15,153). Besides a reduction in trabecular bone volume, there is also a reduction in cortical bone (8) attributed to bone resorption on the endosteal surface that occurs at a greater rate than appositional growth (8). Changes in hormone levels potentiate the development of osteopenia and age related bone loss. After estrogen deprivation there is an increase in osteoclastic activity due to increasing levels of local factors such as interleukins, tumor necrosis factors and colony stimulating factors (2).

In addition to the cellular changes, with aging there is a reduction in serum levels of vitamin D due to lower intake and sun exposure (15,145,146,158), as a consequence there is a reduction in the absorption of calcium in the gut (146,158). This reduction in calcium absorption will induce an increase in the production of PTH with a subsequent increase in osteoclastic activity in bone and thus in bone resorption (15,146,158).

Vitamin D3 has proved to be beneficial in combination with Ca^{++} in reducing osteoporotic fractures in the elderly (146,147,158,159). Although the active form of vitamin D, $1,25(OH)_2D_3$, can correct secondary hyperparathyroidism that occurs in renal osteodystrophy (160) its benefits in the treatment of post-menopausal osteoporosis is inconclusive (145,147,161,162).

A new concept has emerged recently to explain the mechanism of action of vitamin D in bone: the "super-coupling or bone effect" (145). According to this concept $1,25(OH)_2D_3$ would have direct effects on bone cells in addition to its well known effects on intestinal Ca absorption and its suppressive effect on PTH secretion (145,158)

Table 4. Functional classification of differentially expressed genes between $1,25(OH)_2D_3$ treated vs. non-treated SAM-P/6 mice.

Gene expression patterns in $1,25(OH)_2D_3$ treated vs. non-treated SAM-P/6 mice were generated from 5 mice per group in two experiments. A ± 2 fold change in average gene expression was considered significant. Genes are listed with their Gene Bank ID and their fold change. The table shows a total of 48 up-regulated genes known as regulators of osteoblastogenesis, adipogenesis or both.

Those genes previously reported as regulated by vitamin D are shaded. A functional approach was used by identifying the specific gene function by its role in osteoblastogenesis and/or adipogenesis. All of the genes are known to encode proteins that stimulate osteoblastogenesis. Among them, genes known to stimulate adipogenesis are grouped in the left column while those known to inhibit adipogenesis are grouped in the right column. There is a higher number and expression of genes inhibiting adipogenesis (right column).

Osteoblastogenesis (+)

H3005C08: Laminin alpha 5	4.6
H3136G12: Histone H1	4.4
H3157D01: AST	4.3
H3011B04: Actin gamma	4.3
H3084G03: c-fos	4.0
H3022C02: IL-1 receptor	3.3
H3007F06: Lipoprotein lipase	2.8
H3158D11: Matrix metallop. 2	2.6
H3116A04: Sparc	2.3
H3029F11: Hexokinase	5.3
H3020C02: Metallothionein1	4.8
H3142F05: STAT6	4.5
H3018B01: AP-2 alpha subunit	3.9
H3156E04: Perlecan	2.7
H3150F06: Farnesyltransferase	2.5

Adipogenesis (+)

H3131E08: Cadherin 2	6.2
H3113C01: Beta Globin	4.9
H3144D09: Csnk2b	4.7
H3008C09: hsp 90	4.5
H3019D09: PKC inhibitor	4.3
H3123G08: Rpo-2	4.2
H3113B11: Cspg 6	3.6
H3027D11: AP-1	3.5
H3140A08: MAPK14	3.4
H3154G12: Proteasome beta	3.3
H3099B11:Glutation peroxidase	3.2
H3134F03: Glutation transferase	3.0
H3098H10: Calbindin 1	3.0
H3104A04:CSF receptor	2.9
H3021E09: Vascular ATPase A	2.7
H3109G10: HGF activator	2.2
H3157B10: HspJ2	6.1
H3123A01: Alpha globin	5.7
H3021E08: Calmodulin	5.6
H3115F04: Tuftelin	5.1
H3140B05: Presenilin 2	5.0
H3010H10: Calcitonin receptor	4.7
H3114H12: Collagen alpha	4.7
H3141H11: anti-mullerian rec. II	4.5
H3006H04: Syndecan 1	4.4
H3062E02: Isocitrate deOHase	4.4
H3137E11: IL-11	4.1
H3101E12: GTPase(Rab11a)	3.9
H3057B12: Tubulin beta 3	3.2
H3107C11: EGF-fibulin matrix	3.2
H3124H07: ovalbumin	3.0
H3138D08: Paraoxonase 3	2.8
H3117D11: Lumican	2.7

Adipogenesis (-)

In vitro. $1,25(OH)_2D_3$ stimulates OB and decreases AD in culture of bone marrow cells (163) and also inhibits osteoblast apoptosis (120). In addition, induces the expression of RANK-L at the surface of the osteoblasts precursors in bone marrow (2) which then binds to RANK at the surface of the osteoclasts to stimulate osteoclastic bone resorption. Our data using ex-vivo cultures of bone marrow cells derived from mice treated with $1,25(OH)_2D_3$ as well as histology and morphometry data show similar effects on OB and AD (Fig. 16, and 17).

Recent studies on the effect of $1,25(OH)_2D_3$ in bone *in vivo* have demonstrated an anabolic effect independently of PTH levels or calcium absorption by stimulating osteoblast activity in oophorectomized rat models (162). Thus, $1,25(OH)_2D_3$ stimulates bone matrix formation in vitamin D-replete animals (161,162). More recently, $1,25(OH)_2D_3$ was reported to have an inhibitory effect on osteoclast differentiation *in vivo* (150)

In this study we used the Senescence Accelerated Mouse SAM-6/P developed by Takeda et al (151,152) a widely accepted model for senile osteoporosis (153,154,164-167) due to their particular characteristics that correlate with those seen in senile osteoporosis in humans (8). The peak of the bone mass of SAM-P/6 is lower than of SAM-R/1TA, their normal controls (151). These mice are characterized from the cellular point of view by a severe decline in bone mass due not only to a premature decrease in the ability of mesenchymal progenitors of bone marrow to differentiate toward the osteoblastic lineage(154) but also to increased bone marrow AD(153,165). Furthermore, bone loss in this model is hormone-independent as shown by a lack of acceleration of bone loss after oophorectomy or orchiectomy (151,152). Biochemically, SAM-P/6 are characterized by an increase in urinary excretion rates of calcium, cAMP, and hydroxyproline while blood

calcium concentrations tend to decrease as compared to their control SAM-R/1TA (151,152,37). In addition high levels of urinary cAMP and urinary hydroxyproline correlate with increasing levels of PTH in serum of SAM-P/6 mice suggesting secondary hyperparathyroidism owing to decreased calcium absorption (151,152,166,167). Additionally, accelerated bone resorption due to increased osteoclastic activity has been reported in this strain most probably due to high levels of PTH (164).

Several treatments have been assessed in SAM-P/6 with variable results. It has been reported that SAM-P/6 can regain bone mass following treatment with PTH and calcium supplements but are not responsive to hormonal therapy (166,167). Furthermore, other treatments have been successful on increasing bone mass in SAM-P/6 including geranylgeranoic acid (168) and more recently by intrabone marrow injection of allogenic bone marrow cells (169)

Our initial objective was to assess the overall effect *in vivo* of $1,25(OH)_2D_3$ in this model of senile osteoporosis and at the same time assess the changes in gene expression in their trabecular cells. Animals tolerated well $1,25(OH)_2D_3$ administration as indicated by the absence of changes in weight or general well being and minor increase in calcium concentration during the course of the experiment.

Histomorphometric analysis of proximal tibiae (Fig. 17) showed a significant increase in indices of bone formation (BV/TV and Ct.Wi.) and there is a marked reduction in indices of bone resorption (ES/BS, NOc/Tar and NOc/BPm) following $1,25(OH)_2D_3$ administration (Table 1). In addition, the dynamic parameters (BRF/BV,AjAR,MS/OS) measured by fluorescent markers (Fig. 17, E and F) are higher in the $1,25(OH)_2D_3$ treated animals as compared to vehicle treated mice(Table 1). Furthermore, the number of ALP positive cells (osteoblasts) is higher in the $1,25(OH)_2D_3$ treated as compared to vehicle

treated mice whereas vehicle treated mice showed a higher number of $TRACP^+$ cells (osteoclasts) (Fig. 17, G, and H). Overall, both static and dynamic histomorphometric indices indicate that $1,25(OH)_2D_3$ stimulates matrix formation and inhibits bone resorption (Table 1). Subsequently, micro architectural data of tibiae using 3D micro CT (Fig. 17, I-L) correlated well histomorphometric data (table 1) for both cortical and trabecular parameters.

As indicated earlier SAM-P/6 are characterized by an increase in bone marrow AD and we could demonstrate here that $1,25(OH)_2D_3$ was a potent inhibitor of bone marrow AD *in vivo* (Fig. 18, A and B)extending recent *in vitro* data of $1,25(OH)_2D_3$ effect of bone marrow cells AD (163,37).

Overall, the architectural changes observed by microCT and morphometry translated in significant changes on bone mass in treated animals measured at timed intervals during $1,25(OH)_2D_3$ treatment. Indeed the positive effects of on bone mass occurred in both, femur and spine confirming that $1,25(OH)_2D_3$ acts on both cortical and trabecular bone.(Fig. 18, E and F).

The mechanism of $1,25(OH)_2D_3$ on bone turnover was further explored using *ex-vivo* cultures of MSC obtained from tibiae in both $1,25(OH)_2D_3$ and vehicle-treated groups. Interestingly, $1,25(OH)_2D_3$ treated mice had a higher number of bone forming nodules identified by Alizarin red staining as compared to control mice indicating that $1,25(OH)_2D_3$ likely affects the commitment of MSC into osteoblasts (Fig. 18, G and H).

From the mechanistic stand point it was important to analyze circulating concentrations of calcium regulating hormones (PTH and 25-OHD) and biochemical markers of bone turnover. Previous reports indicating that serum calcium circulations are low in SAM-P/6 were confirmed here. $1,25(OH)_2D_3$ tended to normalize calcium concentrations which

remained in the normal range throughout the experiment (Table 2). To assess if these calcium changes *per se* may have resulted directly or indirectly in the observed $1,25(OH)_2D_3$ effects we measured serum concentrations of PTH and 25-OHD in both groups. Concordant with previous reports PTH levels in vehicle treated SAM-P/6 mice were higher than the normal range (Table 2); in contrast, $1,25(OH)_2D_3$ treated mice showed a significant reduction in their serum concentrations of PTH after 6 weeks of treatment (Table 2). The reduction in serum levels of PTH might explain in part the reduction in osteoclastic activity seen in the $1,25(OH)_2D_3$ treated group (Fig. 17 and Table 1) since PTH is a well know stimulator of osteoclast differentiation and activity. Additionally to the normalization of PTH levels, the reduction in osteoclast activity seen in $1,25(OH)_2D_3$ treated mice can be explained by a direct effect of $1,25(OH)_2D_3$ on osteoclast formation as mentioned previously (149). Interestingly, in both groups the levels of 25-OHD were below the normal range. This finding correlates with the changes in serum levels of 25-OHD seen in moderate to severe vitamin D deficient elderly human subjects before and after treatment with $1,25(OH)_2D_3$ (6). Furthermore, serum markers of bone formation (OSN) and resorption (N-telopeptide) indicate that $1,25(OH)_2D_3$ has a marked effect on both markers similar to observations done by morphometry(Table 2). These changes in the bone microenvironment are also reflected by changes in gene expression. Earlier reports indicate that exposure to $1,25(OH)_2D_3$ of osteoblasts and trabecular cells result in a wide array of gene changes including: Biglycan, OPN, osteonectin, collagen alpha 1, DAP-like kinase, Calmodulin, lysophospholipase, smad2 etc(121,126,170).

We analyzed these gene changes in trabecular cells isolated from $1,25(OH)_2D_3$ or vehicle treated animals. Changes in gene expression in the 15K gene array which includes 32000

genes and ESTs (indicated a significant change (± 2 fold up or down regulation) in 440 genes (Fig 18, A and Table 3). Our functional classification (Table 4) indicated that genes previously shown to be regulated by vitamin D were among them including cadherin, calmodulin, c-fos, calbindin and AP-1. Subsequently, each of the 440 genes was classified according to its known function as regulator of either OB or AD or both. A total of 48 up-regulated genes were found (Table 4). The totality of the up-regulated genes were found to be involved in OB including Cadherin, calbindin, beta-globin, andactin gamma etc. 15/48 up-regulated genes were found to be stimulators of adipogenesis while a vast majority were inhibitors of proteins involved in adipogenesis. Overall, our functional analysis seems to indicate that $1,25(OH)_2D_3$ predominantly upregulates OB and inhibits AD.

Summary of our data indicate that $1,25(OH)_2D_3$ has a complex effect on cell and differentiation in the major components of the bone microenvironment *in vivo*. A gain in bone mass as a consequence of higher OB as well as lower AD and OC is observed indicating that $1,25(OH)_2D_3$ is a potent agent to correct senile osteoporosis in this model and warrants further investigation in human models.

4.6 Acknowledgements

Dr. Duque holds a bursary from the Fonds de la Recherche en Santé du Québec.

INTRODUCTION TO CHAPTER FOUR

Two important changes happen with aging in mature osteoblasts: a significant reduction in the number of receptors to hormones and GF, and, a shorter life span due to increased levels of apoptosis. Given that E_2 is known to inhibit osteoblast apoptosis and that the numbers of its receptors decrease with age, in this chapter we assessed if the reduction in VDR expression seen in aging osteoblasts was regulated by E_2 *in vitro* and *in vivo*. We found a significant interaction between E_2 and VDR and further determined the significance of this interaction on osteoblast activity and survival.

We found that some of the molecular changes in aging osteoblasts are indeed reversible and that E2 and vitamin D have a synergetic effect to further increase the life span of active osteoblasts in the BMU.

CHAPTER 4

Estrogens (E_2) regulate expression and response of 1,25-Dihydroxivitamin D_3 Receptors in bone cells: Changes with aging and hormone deprivation.

Gustavo Duque [1,2], Khadija El Abdaimi [1], Michael Macoritto [1],Marilyn M. Miller [3]
Richard Kremer [1]

[1]Calcium Research Laboratory, Department of Medicine, McGill University, Montreal, Quebec, Canada

[2]Division of Geriatric Medicine, McGill University, Montreal, Quebec, Canada

[3]Department of Gynecology and Obstetrics, McGill University, Montreal, Quebec, Canada

The contents of this Chapter were published in *Biochemical and Biophysical Research Communications*: Duque G., El Abdaimi K, Macoritto M, Miller MM, Kremer R. BBRC 299:446-454. 2002.

4.1 Summary

Studies on the effect of E_2 on the expression of vitamin D receptor (VDR) and its bioresponse in bone have demonstrated that E_2 modulate activity and increase the number of VDR *in vitro;* however, no *in vivo* studies have been pursued to assess this interaction. Our study identifies the changes in the number of VDR-expressing cells in bone of C57BL/6J young and old oophorectomized mice (4 months and 24 months) with and without 17 β Estradiol (E_2) replacement. A total of 36 mice were sacrificed; both tibiae and femora were isolated and VDR expression was quantified by northern blot, immunohistochemistry, immunofluorescence and flow cytometry. Among the intact mice there was a significant difference in the number of VDR-expressing osteoblasts between young (68%) and old (56%) ($p<0.04$). In young oophorectomized mice the number of VDR-expressing osteoblasts decreased from 68% to 46% after OVX and recovered to 72% after E_2 administration ($p<0.02$), while in the group of old mice, the number of VDR-expressing osteoblasts decreased from 56% to 48% after OVX ($p< 0.01$) and recovered to 85% after E_2 administration ($p<0.001$). Our results show that VDR expression in bone decreases with aging and estrogen deprivation but recovers after E_2 supplementation in both young and old mice with a more significant level of response in older bone. To evaluate the level of VDR bioresponse to E_2 we assessed the effect of E_2 supplementation to human osteoblasts (N-976) *in vitro*. Northern blot showed a significant up-regulation of VDR expression in E_2 treated cells as compared to non-treated cells ($p <0.05$). We also assessed the previously known anti-apoptotic effect of vitamin D in osteoblasts *in vitro* after serum deprivation by using either E_2, E_2+ $1,25(OH)_2D_3$ or $1,25(OH)_2D_3$ alone. We found a lower number of apoptotic cells and longer cell survival after 48 hours of treatment with $1,25(OH)_2D_3 + E_2$ as compared to

$1,25(OH)_2D_3$ or E_2 alone($p<0.002$). In summary, our results demonstrate that E_2 increases VDR expression in bone *in vivo* and potentiate the bioresponse of VDR in osteoblasts in *vitro*.

4.2 Introduction

Vitamin D is a secosteroid hormone that exerts its effects through its active form $1,25(OH)_2D_3$ in several target tissues, including bone, kidney, intestine and parathyroid (145,146). The major effects of vitamin D include bone development and metabolism, calcium homeostasis and regulation of cell growth and differentiation(172-174). Vitamin D exerts its effects via genomic and non-genomic mechanisms(172). The genomic mechanism involves the activity of VDR; these are *trans*-acting transcriptional factors which belong to the nuclear receptor superfamily. The binding of the hormone to the receptor dissociates co-repressors and facilitates the interaction between the VDR and co-activator proteins such as p160, steroid receptor coactivators (SRCs), and the protein complex called VDR-interacting protein (DRIP). These interactions modulate the chromatin structure and the contact with basal transcriptional factors (175).

The trans-activational complex regulates the gene transcription via the binding motifs in the promoter regions of target genes designated vitamin D response elements (VDREs). VDREs have been localized in genes such as calbindin, OSN, OPN, vitamin D 24-hydroxylase, cyclin dependent kinase inhibitor and TGF-β2. The non-genomic response involves the activation of nontranscriptional responses, including voltage dependent Ca+ influx, and G-protein dependent stimulation (172,176).

In osteoblasts, $1,25(OH)_2D_3$ regulates cell proliferation and differentiation through the VDR (177). Recent evidence has showed the effect of $1,25(OH)_2D_3$ in osteoblast-like cells survival through the inhibition of apoptosis *in vitro* (120,178).

Age has been shown to have a profound effect on several physiological events related to calcium and vitamin D metabolism. For example, variations of intestinal calcium absorption related to age have been demonstrated in both animal and human studies (179-181). Target cell responsiveness to $1,25(OH)_2D_3$ is impaired when receptor numbers are reduced or lacking (177). Therefore, changes in calcium metabolism with age may reflect alterations in the quantity and functionality of VDR in target tissue. It has been shown that the number of VDR decreases with age, and this could be responsible for functional changes in target tissue response to $1,25(OH)_2D_3$ associated with advanced age (182-184).

Estrogens also belong to the group of steroid hormones; they have their own nuclear receptors alpha and beta and modulate some of the mechanisms of bone turnover, including osteoclast survival and osteoblast-osteoclast interaction (67,68). Direct effects of estrogen in osteoblast cell lines and in ovariectomized rats have been shown such as inhibition of bone resorption and stimulation of bone formation (68). As with vitamin D, the level of estrogens decreases with age at the time of menopause. During estrogen deprivation the bone loses its balance between resorption and formation with a marked decline in matrix formation and bone mineralization (185). It has been also demonstrated that calcium malabsorption in osteoporosis can be corrected by estrogen therapy, suggesting a direct interaction between E_2 and vitamin D action (186,187).

The responsiveness of target cells to $1,25(OH)_2D_3$ can depend on the amount of VDR. Many factors can modulate VDR levels including glucocorticoids, prolactin, estrogens,

retinoids, and GF (172). Estrogens increase $1,25(OH)_2D_3$ expression and bioresponse in rat uterus (188), duodenal and colon mucosae (186,188), and liver (190); by contrast E_2 decrease VDR expression in the kidneys (190). The bioresponse of osteoblasts to VDR activation includes increasing cell differentiation (191) and lower apoptosis (178). *In vitro* studies have assessed the interaction between estrogen and VDR in bone cells showing that E_2 modulate VDR activity in osteoblast-like cells by increasing their expression and OSN secretion (192). Despite the available evidence, no *in vivo* studies have assessed the E_2 – VDR interaction in bone and its significance in the bioresponse to VDR activation. In this study we assess the changes in VDR expression in aging bone by comparing young vs. old C57BL/6J mice, an accepted model to study both estrogen deprivation (193), and age-related bone loss (194). We also compare VDR expression in a population of estrogen-exposed vs estrogen-deprived young and old animals. Finally, in order to assess the changes in the bioresponse of VDR to estrogens stimulation we compare the effect of $1,25(OH)_2D_3$ with and without E_2 on apoptotic osteoblasts *in vitro*. Thus, this study assesses not only the changes in the expression levels of VDR with age but also the interaction between steroid hormones in bone and their importance in bone physiology and metabolism.

4.3 Materials and methods

4.3.1 Animal tissue preparation

Five week-old virgin female C57BL/6J mice (Jackson Laboratory, Bar Harbour, ME) were housed triply in cages in a limited access room restricted to aging mice (light: dark 12h:12h). Bedding, food and water were as previously described (195). Animal

husbandry adhered to Canadian Council on Animal Care Standards, and all protocols were approved by the McGill University and Royal Victoria Hospital Animal Care Utilization Committee. The colony was free of any parasitic, bacterial, or viral pathogens as determined by a sentinel program. Only mice exhibiting a minimum of three regular estrus cycles as assessed by daily vaginal smears were included in the study.

Six treatment groups were evaluated. a) Normally cycling (young – 4 months, n=6; old – 24 months. n=6) (intact): b) OVX (young – 4 months, n=6; old – 24 months, n=6): c) OVX treated with 17 β Estradiol (young – 4 months, n=6; old – 24 months, n=6). The animals were OVX after 6 weeks of age and implanted with capsule containing 17β Estradiol (E_2). For OVX and insertion of the E_2 capsule, animals were anaesthetized with 2.2.2-tribromoethanol. E_2 capsules were prepared as previously described (196) and contained Estradiol 17-β (16mm) in polyethylene (P.E.) tubing (o.d. 2.80 mm: i.d. 1.77 mm). This size of P.E. capsule has demonstrated to produce physiologic levels of E_2 (9-12 pg/ml) in our colony(195). Animals were sacrificed by decapitation, bone marrow cells were obtained from the left femora and tibia by flushing with Dubelcco's alpha modified medium (DMEM). Red blood cells in marrow cells were hemolyzed in 0.017 M tris-HCl, pH 7.5, buffer containing 0.8% ammonium chloride. Hemolyzed bone marrow suspensions were rinsed twice with phosphate buffered saline (PBS) and either fixed with paraformaldehyde 4% or placed at –70 °C for further RNA extraction. Right-side limbs were placed in 10% formaldehyde for further histology analysis.

4.3.2 RNA isolation

Total RNA was extracted from bone marrow cells, according to a protocol for single-step RNA isolation based on acid guanidinium-thyocyanate-phenol-chloroform extraction using Tri-reagent solution (Triazol, Invitrogen Canada Inc, Hamilton, ON). Aliquots of total RNA were separated in sterile tubes and quantified.

4.3.4 Northern blot procedures

After denaturation, 25μg total RNA samples were electrophoresed in 1% agarose, 2.2 m formaldehyde gel, transferred to nylon membranes (Hybond N, Amersham) and hybridized with ^{32}P-labeled VDR probes. The probes were labeled with α ^{32}P-CTP by a random-primed DNA labeling procedure with Klenow polymerase.

4.3.5 Probe preparation by PCR

Complementary DNA sequences for the detection of mRNA transcripts of VDR genes by Northern blot procedures were obtained by RT-PCR using appropriate primers and reverse transcriptase enzyme. The PCR buffer consisted of 10 mM tris (pH 8.3), 50 mM KCl, 2 mM MgCl2, 0.01% gelatin, 0.2 mM deoxynucleotide triphosphates, and 1.25 U/50 μl *Taq* polymerase. The VDR-gene PCR primers consisted of bases in the sense direction (5'-CTCCTCCTTCCGCTTCAGGATCATCTC) and bases in the antisense direction (5'ATGGCGGCCAGCACTTCCCTGCCTGAC). The calculated PCR product length was 330 bp. The PCR program involved 3 cycles: 40 sec at 94°C, 60 sec at 50°C, and 90 sec at 72 °C.

4.3.6 Decalcification of tissues

EDTA-glycerol (EDTA-G) solution was prepared as previous described (197). 14.5 g EDTA, 1.25 g NaOH, and 15 ml glycerol were dissolved in distilled water and the pH was adjusted to 7.3. The solution was then made up to 100 ml and stored at 5°C.

After fixation, specimens were serially washed for 12 hours at 5°C in each of the following solutions: 0.01M PBS containing 5% glycerol, 0.01 M PBS containing 10% glycerol, and 0.01 M PBS containing 15% glycerol. The specimens were then decalcified in EDTA-G solution for 10-14 days at 5°C. This EDTA-G solution was replaced every 5 days. Progression of decalcification was checked by X-ray. To remove EDTA and glycerol from the decalcified tissues, they were washed at 5C for 12h successively in 15% sucrose and 15% glycerol in PBS; 20% sucrose and 10% glycerol in PBS; 20% sucrose and 5% glycerol in PBS; 20% sucrose in PBS; 10% sucrose in PBS; 5% sucrose in PBS and 100% PBS as previously described (196).

4.3.7 Detection of VDR by Immunohistochemistry

After decalcification, bone samples were embedded in low-melting-point paraffin in a Shandon Citadel 2000 automatic tissue processor (Shandon Scientific Limited, Runcorn, UK). Coronary and transverse sections (4μ) were made for the epiphyseal parts and the shaft, respectively. Sections were mounted on silane-coated glass slides (Fischer Scientific, Springfield, NJ, USA) and paraffin was removed with three washes of xylene and rehydrated with ethanol washes (80-50-30%) and PBS. Non-specific binding was blocked by addition of goat serum for 1 hour. Sections were then incubated with rabbit polyclonal IgG VDR Ab (Santa Cruz Biotechnology, Santa Cruz, CA, USA) for either 4h

at room temperature or 8-24 h at 4°C. After washing with PBS, goat antibodies to rabbit IgG were added to the sections at room temperature for 30 minutes, followed by a 30 minute incubation with 0.6% hydrogen peroxide + chromogen and then counterstained with hematoxylin. Control slides were incubated with rabbit IgG, according to manufacturer instructions, and triplicate tests and control slides were included in immunodetection.

4.3.8 Detection of VDR in bone by immunofluorescence

Bone sections were treated as described above, omitting the final step involving treatment of cells with hydrogen peroxide. After fixation in 4% paraformaldehyde, sections were washed with PBS and then incubated in 10% normal blocking serum in PBS for 20 minutes to suppress non-specific binding of IgG. Sections were incubated with rabbit polyclonal IgG VDR Ab (Santa Cruz Biotechnology, Santa Cruz, CA, USA) with 1.5% normal blocking serum overnight at 4°C and then incubated for 45 minutes with fluorescent conjugated secondary Ab (FITC-Santa Cruz, Santa Cruz, CA, USA) diluted to 2 μg/ml in PBS with 1.5% normal blocking. Control slides were incubated with rabbit IgG, according to manufacturer instructions, and triplicate tests and control slides were included in immunodetection.

4.3.9 Quantification of osteoblasts expressing VDR

Each longitudinal section was analyzed in six zones of 0.8 mm starting from the 1°-2° spongiosa interface and moving in the direction of the diaphysis as described by Tomkinson et al. (68). Osteoblasts were identified as cuboidal cells lining the osteoid-

covered trabecular perimeter. The sections were scored for the total number of osteoblasts and the number of osteoblasts expressing VDR. In all cases at least 100 osteoblasts were assessed per section.

In the immunoperoxidase stained sections, cells positive for VDR displayed a nucleus with punctillate brown staining from the peroxidase-labeled Ab as well as the blue from the hematoxylin. Under fluorescence, positive cells for VDR were found using the same technique; positive cells showed intense nuclear green fluorescence, negative controls showed light cytoplasmic and nuclear fluorescence.

4.3.10 Controls

In all immunofluorescence and immunochemistry detection methods for VDR, non-immune mouse serum and mouse IgG, in place of the primary Ab, were included as controls. Three tests and three control slides were included for each variable, and runs were performed on at least three different blocks from the same bone on separate occasions.

4.3.11 Cell sorting and flow cytometry

One femur of each mouse was flushed with 5 ml of phenol red-free Dulbecco's modified Eagle's Medium DMEM (GIBCO BRL, Gaithersburg, MD) containing 10% FBS to obtain marrow cells. After hemolysis as described above, cells were washed in PBS and then fixed in 4% paraformaldehyde, rinsed with PBS, and preserved with 75% ethanol at –20°C. Cell suspensions were incubated with rabbit polyclonal IgG VDR Ab (Santa Cruz Biotechnology, Santa Cruz, CA, USA) with 1.5% normal blocking serum for 1 hour at room temperature and then incubated for 45 minutes with FITC fluorescent conjugated

secondary Ab (Santa Cruz, CA, USA). Control samples, consisting of cells labeled with FITC Ab, but without VDR Ab, were used to align the cytometer and to set the fluorescent signal. Cells were analyzed by flow cytometry using a FACScan flow cytometer (Becton Dickinson, San Jose, CA, USA) at a peak fluorescence wavelength of 530 nm for fluorescein. The percentage of cells expressing VDR was determined after electronic subtraction of signal due to background fluorescence, which was determined using cells incubated with FITC-labeled dUTP without primary Ab. A minimum of 10^4 cells were analyzed. This experiment was repeated three times.

4.3.12 Culture of Human Osteoblasts

Newborn human calvaria osteoblast cell line N-976 was generated as described previously (197). These cells contain osteoblast precursors at various stages of differentiation, including cells already committed to the osteogenic pathway. These cells express specific osteoblast markers such as alkaline phosphatase, type I collagen, and osteonectin, as well as the vitamin D receptor. Cells were plated at a density of 2×10^4 cells/well in six well plates (Falcon, Becton-Dickinson, NJ, USA) in phenol red free DMEM (GIBCO, Grand Island, NY, USA) containing 5% heat-inactivated fetal calf serum (FCS), 100 U/ml of penicillin, and 100 U/ml of streptomycin. When cells reached 80% confluence, the medium was replaced with serum free medium containing 10^{-3}M thymidine (to block cell proliferation) and either $1,25(OH)_2D_3$ (10^{-8}M) (LEO pharmaceutical, Sweden) or Estradiol (10^{-7}M) (Sigma-Aldrich, St. Louis, MI, USA) or both. Cells were counted at time intervals of 24,48 and 72 hours in a coulter counter (Coulter Electronics, Beds, UK).

4.3.13 Effect of estrogen (E_2) on VDR expression in human osteoblasts in vitro

To determine VDR expression regulation by estrogens *in vitro*, N-976 cells were plated in phenol red free DMEM with 5% FCS as described above. After 24 hours, medium was replaced with phenol red free DMEM containing 5% FCS with or without Estradiol (10^{-7}M). After 48 hours treated and non-treated cells were trypsinized and RNA was extracted. Northern blot was performed as previously described. Due to the close match between human and mouse sequences for VDR (96%), complementary DNA sequences for the detection of mRNA transcripts of VDR genes by Northern blot procedures were obtained by RT-PCR using the same primers and reverse transcriptase enzyme as *in vivo* experiments.

4.3.14 MTS Formazan-Cell survival assay

N-976 cells were seeded at a density of $4x10^2$ cells/well in 96-well cluster plates (Falcon, Becton-Dickinson, NJ, USA) and grown to 30% confluence. After 24 h in phenol red free DMEM containing 5% FCS, the medium was replaced with serum free medium containing 10^{-3}M thymidine with either $1,25(OH)_2D_3$ (10^{-8}M)or estradiol (10^{-7}M) or both. MTS Formazan assesses mithocondrial function by the ability of viable cells to convert soluble 3-(4,5-dimethylthiazol-2-yl)-2,5-diphenyltetrazolium bromide (MTS) into an insoluble dark blue Formazan reaction product measured photometrically as previously described (198). A stock solution of MTS was dissolved in PBS at a concentration of 5mg/ml and was added in a 1:10 ratio (MTS/DMEM) to each well incubated at 37°C for 4h and the optical density determined at a wavelength of 570-630 nm on a microplate reader model 3550 (Biorad, Hercules, CA). In preliminary experiments the absorbance was found to be directly proportional to the number of cells over a wide range (2×10^2 to

50 x 10^3 cells/well). The percent survival was defined as [(experimental $_{absorbance}$ - blank $_{absorbance}$)/control $_{absorbance}$ - blank $_{absorbance}$)] x 100, where the control $_{absorbance}$ is the optical density obtained for 10 x 10^3 cells/well (number of cells plated at the start of the experiment), and blank $_{absorbance}$ is the optical density determined in wells containing medium and MTS alone.

4.3.15 Terminal deoxynucleotidyl transferase-mediated dUTP-biotin nick end labeling (TUNEL) assay

DNA cleavage was assessed by the terminal deoxynucleotidyl transferase-mediated dUTP biotin nick end labeling (TUNEL) reaction as described previously (200). Newborn human calvaria osteoblasts (N-976) were cultured in 2 well glass chamber slides (Angle Nun Int. Naperville, IL, USA) in serum free DMEM medium containing 10^{-3}M thymidine with or without 10^{-8}M 1,25$(OH)_2D_3$. At 48h cells were fixed in 4% paraformaldehyde for 10 minutes, washed in 10 mM tris-HCl, pH 8.0, and preincubated for 10 min at room temperature in the reaction buffer for terminal deoxynucleotidyl transferase (200-mM potassium cacodylate, 0.22 mg/ml BSA, and 25-mM tris HCl, pH 6.6). The preincubation buffer was then removed, and a reaction mixture containing 500 U/ml terminal deoxynucleotidyl transferase, 25 mM CoCl2, and 40 μM biotinylated dUTP was added for 60 min at 37°C. The reaction was terminated by the addition of 300 mM NaCl and 30mM sodium citrate for 25 min at room temperature and for 60 min at room temperature in the dark. After extensive washing in PBS cells were examined in a Leica fluorescence microscope. Propidium Iodine was used as counter staining. Those cells that stained individual apoptotic nuclei with green fluorescence were considered positive.

4.3.16 Statistical analysis

All results are expressed as mean ± SEM of 3 replicate determinations, and statistical comparisons are based on one-way analysis of variance (ANOVA) or Student's T-test. A probability value of $p<0.05$ was considered significant.

4.4 Results

Throughout this study, uterine weight served as an independent marker for estrogenic activity in the different mouse groups (data not shown). The markedly reduced uterine weight in OVX mice confirmed least exposure to estrogens in this group, compared with the intact and OVX+E_2 groups. Both of the OVX + E_2 groups had higher uterine weights which can be attributed to the supraphysiological dose of estradiol and to lack of the physiological cyclicity in estrogens production.

4.4.1 Effect of Estradiol on VDR transcription

Northern blot analysis showed a significantly higher level of VDR mRNA in the younger group than in the older group (Fig. 20)(*$p < 0.04$). Densitometric quantification of the signals produced by the hybridization in each treatment group, normalized according with GAPDH RNA expression indicated a decrease in VDR RNA content with aging, and an increase of approximately five fold in VDR RNA content in OVX estrogen-exposed mice vs estrogen-deprived mice, with more marked and significant response in older than in younger mice (**$p<0.002$).

Figure 20. VDR RNA expression in bone of young and old oophorectomized C57BL/6J mice with and without estrogen administration.

Total RNA was extracted from bone marrow cells with acid guanidinium-thyocyanate-phenol-chloroform using Tri-reagent solution (Triazol, Invitrogen Canada Corp. Hamilton, ON). After denaturation, 25μg of total RNA samples were electrophoresed in 1% agarose, 2.2% formaldehyde gel, transferred to nylon membranes and hybridized with a ^{32}P-labeled VDR probe. The signals were quantified by densitometry and normalized according with GADPH RNA expression. The bar graph shows the ratio between GADPH /VDR. A significant reduction in VDR expression from young to old mice was found (*$p<0.04$), while both groups experienced a similar reduction in the expression of VDR after OVX. Finally, after E_2 administration an increased expression in both groups was found, with a higher and significant increase in the old group (**$p<0.002$).

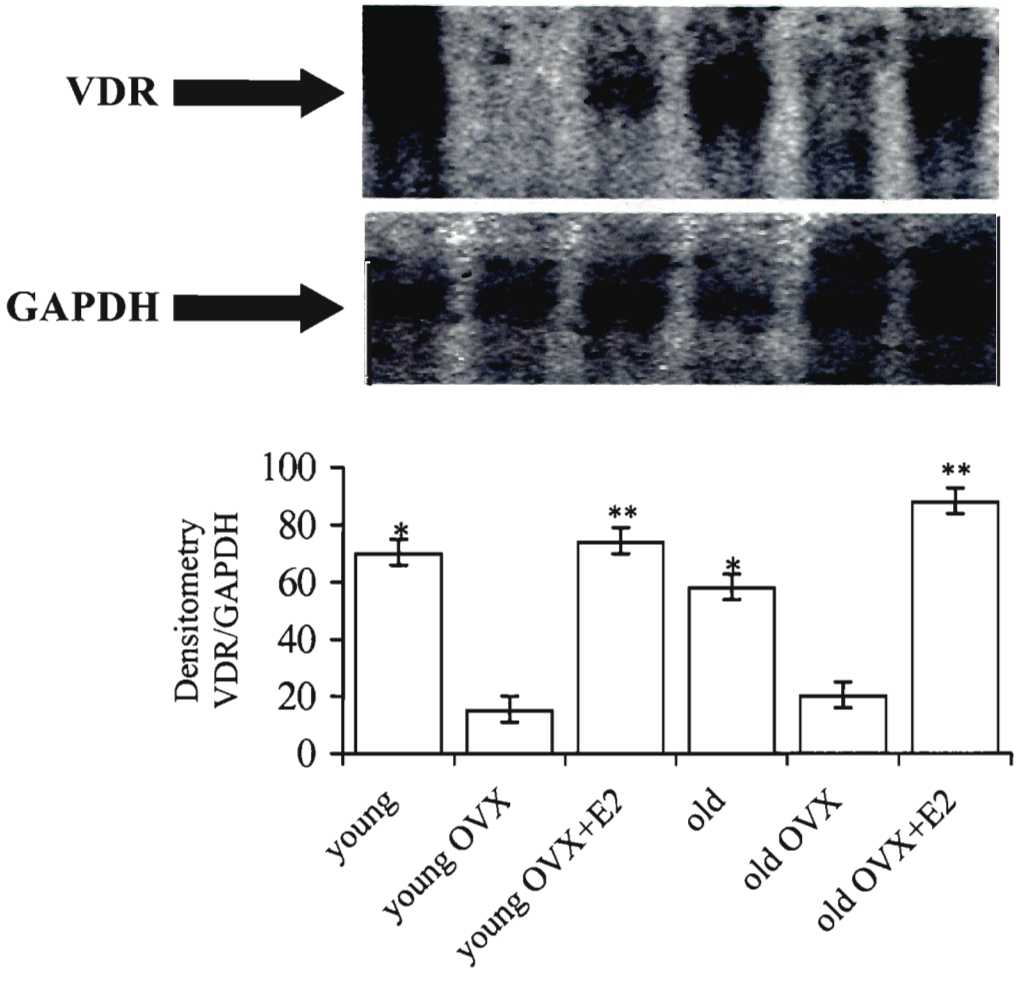
VDR
GAPDH
Densitometry
VDR/GAPDH
100
80
60
40
20
0
*
**
*
**
young
young OVX
young OVX+E2
old
old OVX
old OVX+E2

4.4.2 VDR in bone – immunohistochemistry and immunofluorescence

Quantification of VDR expressing osteoblasts by immunohistochemistry and immunofluorescence showed a significant reduction of VDR-expressing osteoblasts in old mice as compared to young mice, from 68% in young to 52% in old mice (Fig. 21 A and B) ($p<0.04$). In young oophorectomized mice the number of VDR decreased from 68% to 46% after OVX (Fig. 21, A and C) and recovered to 72% after E_2 administration ($p<0.02$) (Fig. 21,E), while in the group of old mice, the expression of VDR decreased from 56% to 48% after OVX ($p< 0.01$) (Fig. 21,B and D) and recovered to 85% after E_2 administration ($p<0.001$).(Fig. 21, F).

4.4.3 Flow cytometry

A higher level of VDR-expressing bone marrow cells was detected in both groups of old and young E_2 exposed mice vs. E_2 deprived mice (Fig. 22) with a higher and significant response in the older group vs the younger one (table)($p<0.001$).

4.4.4 Effect of estrogen (E_2) on VDR expression in human osteoblasts

The effect of E_2 on VDR expression in human osteoblasts is shown in Fig. 23 (upper panel). Densitometric quantification of VDR expression shows a significant VDR up-regulation in treated as compared to the normal VDR expression in non-treated cells (lower panel) ($p<0.05$).

Figure 21. Detection of VDR by immunohistochemistry and immunofluorescence.

After decalcification, bone samples were embedded in low-melting paraffin, coronary and transverse sections were made for the epiphyseal parts and the shaft respectively. Sections were treated as described in materials and methods for immunohistochemistry (top of each panel) and immunofluorescence (bottom of each panel). In both cases sections were incubated with rabbit polyclonal IgG VDR Ab (Santa Cruz Biotechnology, Santa Cruz, CA, USA). Each longitudinal section was analyzed as described by Tomkinson et al (68). The percentage of nuclear VDR-expressing osteoblasts was determined by counting groups of 100 osteoblasts per zone. The arrows in Fig. 20 show the positive nuclear expression of VDR in young (A) and old (B) non-OVX mice compared to young OVX (C) and old OVX (D). By contrast, the number of VDR-expressing osteoblasts increases in both young OVX (E) and old OVX (F) after estrogen supplementation.

The bars in the bottom show the percentage of VDR-expressing osteoblasts in each one of the groups. There is a significantly higher number of VDR-expressing osteoblasts in young vs. old (*$p<0.04$), and a higher number of VDR expressing osteoblasts in both groups after E_2 supplementation as compared to the OVX groups (**$p<0.001$).

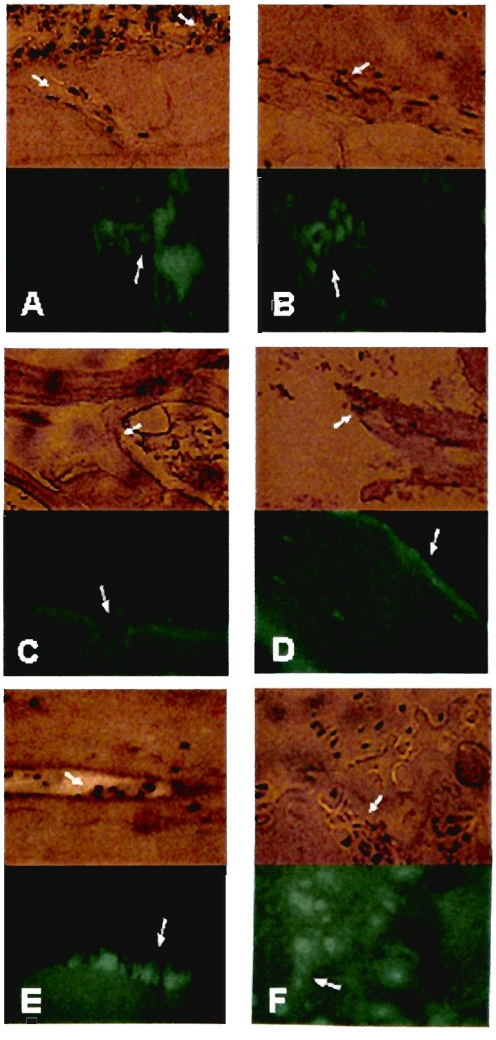
A
B
C
D
E
F

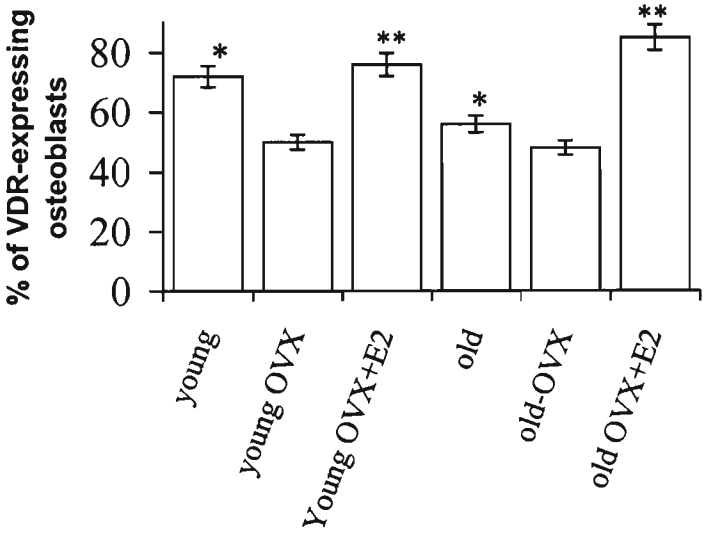
% of VDR-expressing osteoblasts
0
20
40
60
80
*
**
*
**
young
young OVX
Young OVX+E2
old
old-OVX
old OVX+E2

Figure 22. Flow cytometry quantification of VDR expression changes in bone after estrogen supplementation in old and young oophorectomized mice.

One femur from each mouse was flushed with 5 mil of phenol red-free DMEM (GIBCO BRL, Gaithersburg, MS,USA) containing 10% FBS to recover marrow cells. After hemolysis, cells were washed in PBS and then fixed in 4% paraformaldehyde. Cell suspensions were incubated with a rabbit polyclonal IgG VDR Ab (Santa Cruz Biotechnology, Santa Cruz, CA, USA) with 1,5% normal blocking serum for 1 hour at room temperature and then incubated for 45 minutes with a FITC fluorescent conjugated secondary Ab (Santa Cruz Biotechnology, Santa Cruz, CA, USA). Cells were analyzed by using a flow cytometer as described in methods. The percentage of cells expressing VDR was determined after electronic substraction of the signal due to background fluorescence. A minimum of 10^4 cells were analyzed. This experiment was repeated three times.

The figure shows the results of flow cytometry in young OVX (B) and old OVX (C). After estrogen supplementation the level of VDR expression increases in both groups with a more marked increase in the old (E) as compared to the young group (D). The percentages of VDR expressing cells are shown in table showing a significant increase in VDR-expressing cells in both groups with a more marked response in the older group.

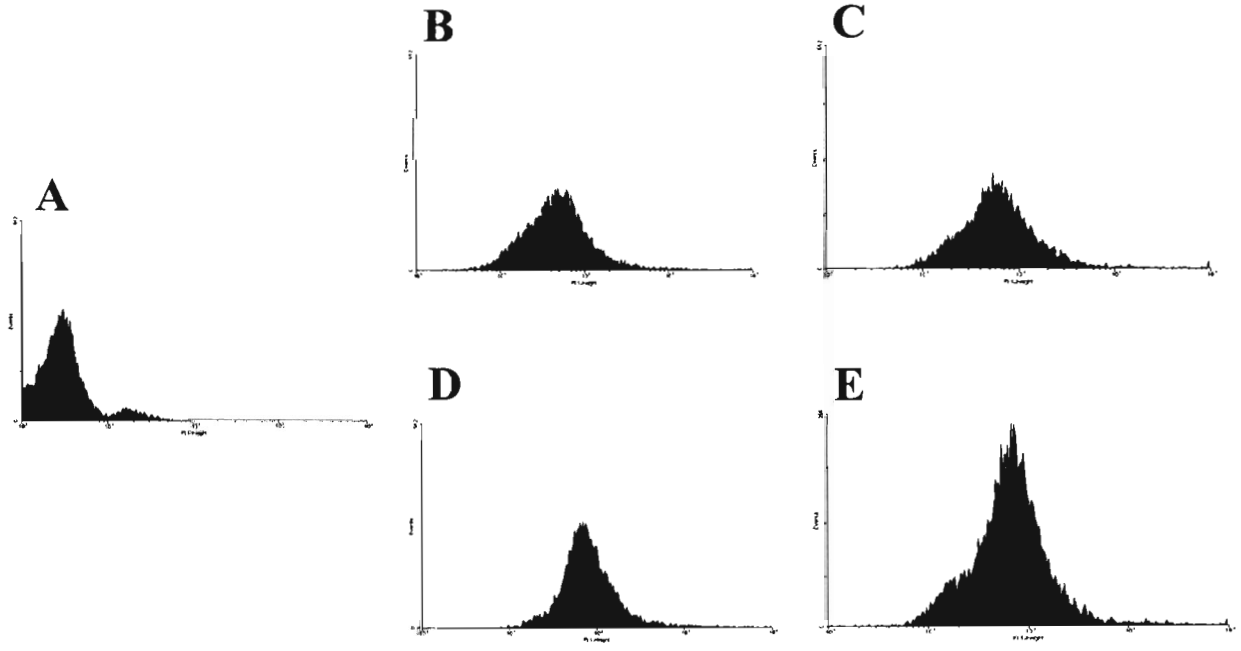
A
B
C
D
E

4.4.5 Effect of $1,25(OH)_2D_3$ and estrogens on proliferation and survival of human osteoblasts

We examined the effects of $1,25(OH)_2D_3$ alone or together with estradiol on proliferation of N-976 cells following induction of apoptosis by serum deprivation as described in the Methods. As can be seen in Fig. 24 (A), after different time intervals a significant increase in osteoblast number and survival was found in all three treated groups ($1,25(OH)_2D_3$, E_2 or $1,25(OH)_2D_3 + E_2$. However, we found that in the presence of $1,25(OH)_2D_3 + E_2$, the cells survived longer as compared with cells treated with either $1,25(OH)_2D_3$ or E_2 alone (*$p<0.01$).

4.4.6 TUNEL Assay

Green fluorescence was detected in apoptotic cells under fluorescent microscopy. Fig. 24 (B) shows a marked decrease of osteoblasts with chromatin condensation at the nuclear membrane, which indicates apoptosis, in the presence of $1,25(OH)_2D_3 + E_2$ at 48 hours as compared to cells treated with either $1,25(OH)_2D_3$ or E_2 alone . In addition, E_2 and $1,25(OH)_2D_3$ treated cells showed less apoptotic changes as compared with non-treated cells (lower right panel).

4.5 Discussion

In this study, we have assessed not only the effect of aging on steroid hormone interaction *in vivo* but also the significance of changing estrogens levels on the bioresponse of VDR *in vitro*. By using a OVX model, we have simulated postmenopausal osteoporosis and by

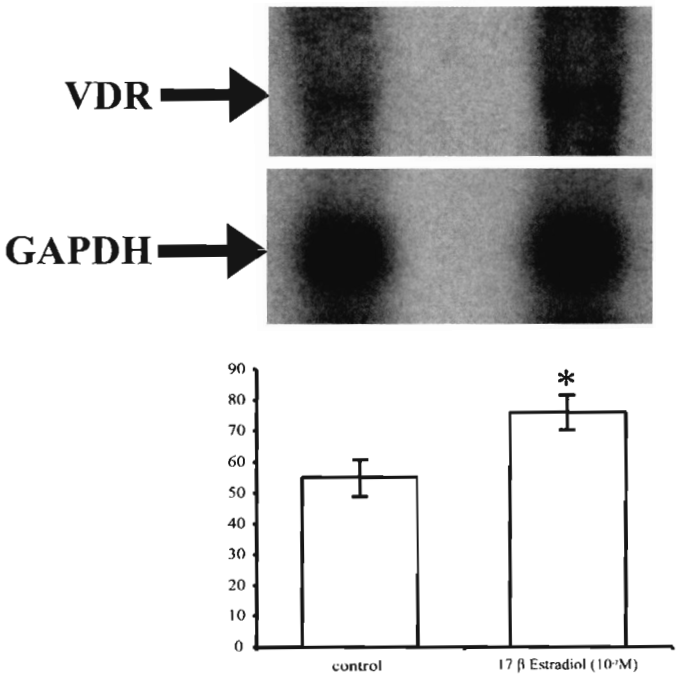

Figure 23. Expression changes of VDR RNA after estrogen (E_2) administration in human osteoblasts *in vitro*.

N-976 cells were plated in phenol red free DMEM with 5% FCS. After 24 hours, medium was replaced with phenol red free DMEM containing 5% FCS with or without Estradiol (10^{-7}M). After 48 hours RNA was extracted, denaturized, and then electrophoresed in 1% agarose, 2.2% formaldehyde gel, transferred to nylon membranes and hybridized with a ^{32}P-labeled VDR probe. The signals were quantified by densitometry and normalized according with GADPH RNA expression. The bar graph shows the ratio between GADPH /VDR. A significant up-regulation on VDR expression was found in the treated cells as compared to non-treated cells (*$p<0.05$).

Figure 24. Effect of $1,25(OH)_2D_3$ with and without E_2 on osteoblast apoptosis using cell survival and TUNEL assays.

Human osteoblasts (N-976) were plated in phenol red free DMEM containing 5% FCS for 24 hours. The medium was then replaced with serum free medium containing 10-3 M thymidine with either $1,25(OH)_2D_3$ (10^{-8}M) or E_2 (10^{-7}M) or both. After 24,48 and 72 hours cell activity was assessed by MTS Formazan as described in methods. A significant difference was observed at all time points between cells treated with either $1,25(OH)_2D_3$, E_2 or both as compared to non-treated cells (A) (*0.002). In addition, at 48 and 72 hours a significant difference in survival between cells receiving $1,25(OH)_2D_3$ or E2 alone vs. cells receiving both treatments was found (‡ 0.01).

Apoptotic cells were identified by using TUNEL assay. Cells were cultured in 2 well glass chamber slides in serum free medium as described in methods. After 48 hours cells were fixed and preincubated in the reaction buffer for terminal deoxynucleotidyl transferase. Biotinylated dUTP was added for 60 min at 37°C. Propidium iodine (PI) was used as counter staining and cells were examined in a Leica fluorescence microscope. The top of each panel in Fig. 23(B) shows a minimum of 10 cells per field stained with PI. In the bottom of each panel cells positive for DNA fragmentation show green fluorescence. The figure shows a higher proportion of apoptotic cells in the control cells (upper left panel) as compared with the treated groups. However, the number of cells showing DNA fragmentation is much lower in cells receiving both $1,25(OH)_2D_3$ + 17β Estradiol as can be seen in the lower right panel.

A

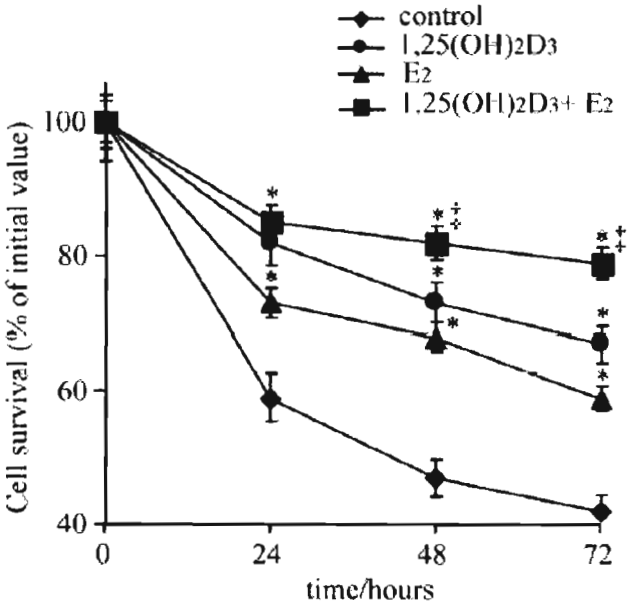
control
1,25(OH)2D3
E2
1,25(OH)2D3+ E2
Cell survival (% of initial value)
100
80
60
40
0
24
48
72
time/hours

B

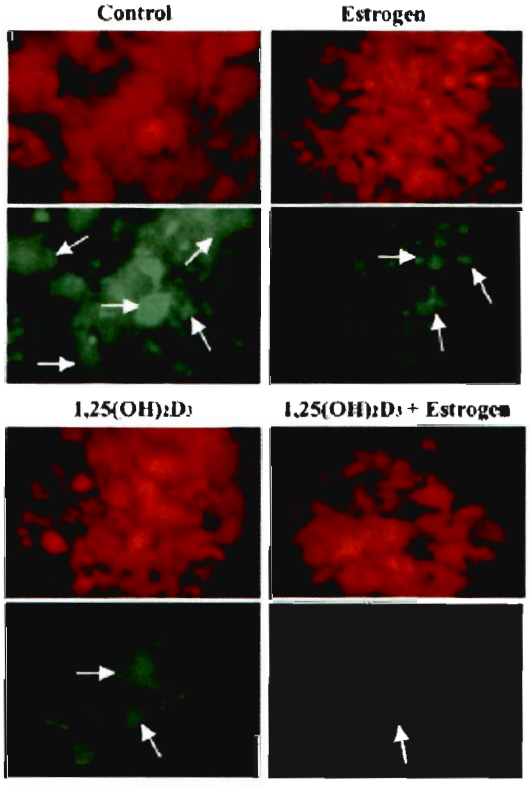
Control
Estrogen
1,25(OH)2D3
1,25(OH)2D3 + Estrogen

Table 5. Percentage of VDR-expressing bone marrow cells in young and old oophorectomized C57BL/6J mice with and without E_2 replacement.

	OVX	OVX+E_2
Young	15±4	26±4*
Old	10±2	58±6*

Bone marrow cells from femora were flushed and hemolized. After incubation with rabbit polyclonal IgG VDR Ab (Santa Cruz Biotechnology, Santa Cruz, CA USA) with 1,5% normal blocking serum for 1 hour at room temperature, cells were the incubated for 45 minutes with FITC fluorescent conjugated secondary Ab (Santa Cruz Biotechnology, Santa Cruz, CA, USA). A minimum of 1x 10^3 cells was analyzed by flow cytometry. The table shows the percentage of VDR expressing cells. (*) represents a significant difference. Data are representative of three different experiments.

using an aging model we have assessed the effect of age related bone loss in this interaction as well.

There is evidence that E_2 regulate the activity and expression of VDR in target organs like bowel (186,187,189) as shown by the increasing calcium absorption after E_2 supplementation in postmenopausal women (189). Other target organs with the same interaction but with unclear physiological significance are breast and uterus (188). In addition, an interaction between vitamin D and estrogens has been also documented in VDR knock out mice which present the typical findings of estrogen-deficient state demonstrating that the presence of VDR is essential in estrogen biosynthesis of both female and male gonads (199). The aging process in bone includes two different phenomenons: the first is determined by decreasing levels of circulating estrogens known as menopause, a process which involves increasing osteoclast activity, bone resorption and higher osteoblast apoptosis (185). The second phenomenon is known as age-related bone loss that includes decreased OB, increasing AD and increasing osteoblast apoptosis (8). The only previous evaluation of VDR expression changes with age was reported by Martinez et al. (200); they obtained primary cultures of human osteoblastic cells from two different donor age groups and they found a decreased VDR mRNA expression in cells of aged donors in mostly cortical bone.

In this study we assessed the changes of VDR expression by simulating both of the phenomena that happen to bone during aging, which are hormone deprivation and pure aging related bone loss. First, we assessed the effect of aging in VDR expression in bone by comparing two different C57BL/6J mice populations (4 and 24 months old). As shown in figure 20, we found a higher level of VDR mRNA expression in younger mice as

compared to an older mouse population. These results were confirmed by using immunohistochemistry and immunofluorescence to quantify the number of VDR-expressing osteoblasts in bone sections (Fig. 21). Our findings corroborate previous observations of reduction in the number of VDR in bone during aging (184).

We also assessed the effect of change in estrogens levels on VDR expression in bone by comparing estrogens deprived (after OVX) and estrogens exposed (OVX + E_2) mice. We found that after OVX, the level of VDR expressing osteoblasts decreased in both groups (Fig. 21, C and D) as well as their levels of mRNA expression decreased significantly as shown in Fig. 20. In contrast, when mice were exposed to E_2 there was a significant rise in the levels of VDR-expressing osteoblasts (Fig. 21) and mRNA expression (Fig. 20) in both groups with a greater increase in the older group. Interestingly, in OVX young and old mice exposed to E_2, the proportion of osteoblasts-expressing VDR was higher than in the intact mice. This may possibly be attributed to the supraphysiological dose of estradiol and to lack of the physiological "cyclicity" in estrogens production.

Several methods have been used to assess the bioresponse of VDR to E_2 *in vitro* including quantification of changes in cytosolic free calcium (202) or changes in OSN production (192). Initially, we assessed the effect of E_2 on VDR expression in a human osteoblasts (N-976) cell line. A significant up-regulation of VDR expression in E_2 treated osteoblasts was found (Fig. 22). These findings correlate with prior reports on the effect of E_2 on VDR expression in osteoblasts *in vitro* (201).

Previous studies have demonstrated the anti-apoptotic effect of both $1,25(OH)_2D_3$ (178) and E_2 (202) in human osteoblast-like cells. By using the anti-apoptotic effect of $1,25(OH)_2D_3$ as a marker of VDR bioresponse, we measured the effect of

E_2+1,25$(OH)_2D_3$, as compared either to E_2 or to 1,25$(OH)_2D_3$ alone on osteoblast apoptosis *in vitro*. Our results showed that E_2 potentiate the effect of vitamin D as an anti-apoptotic agent, suggesting that E_2 enhance the bioresponse of VDR in osteoblasts *in vitro* (Fig. 24, A and B).

The mechanism that could explain this interaction is still unclear. Osteoblasts express both estrogen and VDR and this expression is developmentally regulated (203). Estrogen could exert its effect on a genomic level directly by stimulating VDR gene transcription (204,205). There is evidence that 17βEstradiol enhance activity of an specific VDR promoter. In the study by Byrne et al (206), a hormonally responsive promoter region upstream of exon 1c in the VDR gene was found, demonstrating a regulation of cell sensitivity to 1,25$(OH)_2D_3$ via transcriptional regulation of the VDR promoter.

The present study in addition to previous observations concerning osteoblasts *in vitro* (8,200,206) indicates that E_2 increases total VDR mRNA content. There is also a higher response of the osteoblasts to the administration of E_2 and there is an important and significant difference in the expression of VDR between young and old bone under E_2 supplementation.

With aging, there is a decline in BMD associated not only to age-related bone loss but also to hormone deprivation. E_2 are a pivotal factor in the pathophysiology and treatment of menopausal osteoporosis and the mechanisms to explain their effect have been partially elucidated. In this study we demonstrate the interaction between E_2 and VDR *in vivo* and its significance *in vitro*. The intrinsic mechanisms to explain this interaction are still unknown, but the demonstration of this complementary effect of two steroid

hormones in bone may open an important field to search for new therapeutic interactions in the future.

4.6 Acknowledgments

Dr. Duque is supported by a fellowship from the Royal Victoria Hospital Research Institute and a bursary from the Fonds de la Recherche en Santé du Québec.

INTRODUCTION TO CHAPTER FIVE

The process of apoptosis of mature osteoblasts is the result of the activation of death domains by extrinsic (hormones and growth factors deprivation) and intrinsic factors (aging). The elucidation of the apoptotic pathways and the identification of their major regulatory points will offer a new approach to understand one of the fates of the aging osteoblast and the significance that inhibition of apoptosis could have on bone formation. In this chapter we describe the apoptotic pathways that are activated during osteoblast apoptosis. In addition, based on previous data described in chapter four, we identify the key steps to be regulated in order to inhibit osteoblast apoptosis and increase osteoblast survival and activity.

CHAPTER 5

Vitamin D exerts its anti-apoptotic effect in osteoblasts through a Fas related mechanism.

Gustavo Duque[1,2], Khadija El-Abdaimi[1], Janet E. Henderson[3], Abderrahim Lomri[4] and Richard Kremer[1].

[1]Calcium Research Laboratory, McGill University, Montreal, Quebec, H3A 1A1

[2]Division of Geriatric Medicine, McGill University, Montreal, Quebec, H3A 1A1

[3]Lady Davis Institute, McGill University, Montreal, Quebec,

[4]INSERM Unité 349, Lariboisière Hospital, Paris, France.

The contents of this Chapter were submitted to the *American Journal of Physiology*: *Endocrinology*: Duque G, El Abdaimi K, Henderson J, Lomri A, Kremer R. 2003. Vitamin D exerts its anti-apoptotic effect in osteoblasts through a Fas related mechanism.

5.1 Summary

Apoptosis plays an important role in the regulation of bone turnover. Previously, we showed that $1,25(OH)_2D_3$, the active form of vitamin D, may increase osteoblast survival by inhibiting apoptosis induced by serum deprivation. Human osteoblasts express the Fas receptor on their surface and its interaction with Fas ligand is necessary for human osteoblast apoptosis. To investigate the mechanism of $1,25(OH)_2D_3$ inhibition of apoptosis in osteoblasts isolated from human calvaria, cells were subjected to either serum deprivation or addition of Fas antibody. Visualization of apoptotic cells using annexin V revealed a significant decrease in apoptosis at 48 hours in the presence of $1,25(OH)_2D_3$ (16% ± 2%, $p<0.04$) compared with non-treated cells (45% ± 3%). Furthermore, flow cytometric analysis of TUNEL labelled osteoblast showed a significant decrease in apoptotic cells in $1,25(OH)_2D_3$ treated cultures (21% ± 2%) at 48 hours compared with non-treated cultures (44% ± 4%, $p<0.04$). To further explore the mechanism of $1,25(OH)_2D_3$ mediated inhibition of apoptosis we examined the changes in activation of death domain proteins, cleavage of caspases and mitochondrial regulators of apoptosis by western blot analysis. A significant inhibition of caspase-8 cleavage and activity in $1,25(OH)_2D_3$ treated cells was observed in conjunction with a decrease in the levels of the proapoptotic protein Bax and an increase in the expression of the antiapoptotic protein Bcl-2. Furthermore, the levels of $p21^{Cipi/WAF1}$, which inhibits the cleavage of caspase-8, was found to be highly induced in $1,25(OH)_2D_3$ –treated cells. In summary, these results demonstrate that the anti-apoptotic effect of $1,25(OH)_2D_3$ in human osteoblasts is mediated by the regulation of components of the mitochondrial and Fas-related pathway.

5.2 Introduction

The skeleton is a dynamic tissue in which there are continuous interactions between bone forming osteoblasts and bone resorbing osteoclasts. Together these cells form a basic multicellular unit (BMU) that continuously remodels the skeleton replacing old bone with new one (1). This remodeling process can be affected by multiple factors including hormone deprivation and aging during which apoptosis, or programmed cell death, may contribute to the imbalance between the number of osteoclasts and osteoblasts available in the BMU (207-209).

Apoptosis is an important determinant of the life span of cells in regenerating tissues (59) and represents a "physiological" mode of cell death (57). Cells undergoing apoptosis are recognized by condensation of chromatin, degradation of DNA into oligonucleosome-sized fragments, and formation of plasma and nuclear membrane blebs leading to the formation of apoptotic bodies (57,58). Both osteoclasts and osteoblasts can undergo apoptosis (61) Under physiological conditions osteoclasts undergo apoptosis and are quickly removed by local phagocytes once they have eroded bone to a specific distance from the central axis, in cortical bone, or to a particular depth from the surface in cancellous bone (61,64). Osteoclast apoptosis can be induced *in vitro* and *in vivo* by administration of estrogens (E_2) (64) or bisphosphonates (210), which leads to a decrease in bone resorption.

Mature osteoblasts can alter their phenotype to become either lining cells or osteocytes. However 65% of the osteoblasts present in a remodeling site cannot be accounted for in either of these ways and are thought to die by apoptosis (61). Recent evidence suggests that osteoblast apoptosis *in vitro* can be induced by serum deprivation (SD) (120,211) or

by the activation of CD95/Fas receptor by its ligand (63,212). The lack of growth factors, glucose and aminoacids during SD, activates an apoptotic pathway shared by TNFR, Fas/Apo1 and TRAIL-R/Apo2 pathway with subsequent ligand binding and the recruitment and activation of caspase-8 (213,214).

In addition, human osteoblasts express CD95/Fas, and both membrane-bound and soluble forms of the Fas-ligand (Fas-L) (63). Osteoblasts undergo apoptosis after being exposed to antibodies to the CD95/Fas receptor which activate two specific adaptor molecules such as Fas-associated death domain (FADD) and TNFα death domain (TRADD) with the subsequent activation of the caspases cascade (214). Furthermore, CD95/Fas is involved in the activation of the apoptotic pathway not only by directly inducing the cleavage of caspase-8 but also by increasing the ratio of Bax (pro-apoptotic factor) to Bcl-2 (antiapoptotic factor) which favors the formation of Bax homodimers (215) which activate the effector caspases. Additionally, tumor necrosis factor α (TNF-α) and interleukin 1α (IL-1α) are also known to activate the CD95/Fas pathway in human osteoblasts leading to recruitment and activation of caspase-8 (212,216).

The action of the active metabolite of vitamin D3, 1,25 dihydroxyvitamin D3 ($1,25(OH)_2D_3$), on bone is primarily indirect through the intestinal absorption of calcium (Ca^{++}) and phosphorus, which are necessary for mineralization of bone matrix and prevention of rickets and osteomalacia (217-219). In addition, $1,25(OH)_2D_3$ binds to vitamin D receptors (VDR) in osteoblasts and induces expression of receptor activator of NF-κB ligand (RANK-L) (220,221), which in turn mediates osteoclastogenesis and osteoclastic bone resorption (221). In previous work it was shown that $1,25(OH)_2D_3$ rescued serum-deprived osteoblasts from apoptosis (120). Since the mechanism to explain

this effect remains unknown, the assessment of the key elements of the CD95/Fas pathway that could be regulated by $1,25(OH)_2D_3$ might offer a new approach to the inhibition of osteoblast apoptosis and therefore to the promotion of osteoblastic activity and bone formation. The current work investigates the hypothesis that this anti-apoptotic effect could be mediated through down regulation of the CD95/Fas pathway and caspase-mediated cell death.

5.3 Materials and Methods

5.3.1 Culture of Human Osteoblasts

Two different newborn human calvaria osteoblast cell lines N-976 and N-704 were generated as described previously (197). These cells contain osteoblasts precursors at various stages of differentiation, including cells already committed to the osteogenic pathway. These cells express specific osteoblast markers like alkaline phosphatase, type I collagen, and osteonectin as well as the vitamin D receptor. Cells were plated at a density of 2×10^4 cells/cm^2 in six well plates (Falcon, Becton-Dickinson, NJ, U.S.A.) in Dubelcco's modified Eagle's Medium, DMEM (GIBCO, Grand Island, NY, U.S.A.) containing 5% heat-inactivated fetal calf serum (FCS), 100 U/ml of penicillin, and 100 U/ml of streptomycin. When cells reached 80% confluence, medium was replaced with either serum free medium or medium containing 1μg/ml of Fas Ab (Oncor, Gaithensburg,MD,USA)+ 5% FCS and either $1,25(OH)_2D_3$ (10^{-10} to 10^{-7}M) or vehicle alone.

5.3.2 Apoptosis measured by Annexin V staining

Newborn human calvaria osteoblasts (N-976 and N-704) were cultured in 2 well glass chamber slides (Nalge Nunc Int. Naperville, IL, USA) in serum free DMEM medium or in medium containing 1μg/ml of Fas Ab+ 5% FCS with or without 10^{-8}M $1,25(OH)_2D_3$. After 48 hours cells were resuspended in 100 μl Hepes buffer containing 140 mM $NaCl_2$, 2.5 mM $CaCl_2$, and stained with 5μl annexin V FITC (Roche, Nutley, NJ, USA) and Propidium Iodine (PI) (SIGMA, St. Louis, MI, USA) 5 μg/ml for 15 minutes at room temperature in the dark. Five thousand cells were measured on a FACScan flow cytometer and analyzed with WinMDI software. Results were expressed as the percentage (PI negative and annexin V positive) apoptotic cells.

5.3.3 Detection and quantification of apoptosis by Annexin V and TUNEL assay

DNA cleavage was assessed by the TUNEL reaction as described by Gavrieli et al (62). Newborn human calvaria osteoblasts (N-976 and N-704) were cultured in 2 well glass chamber slides (Nalge Nunc Int. Naperville, IL, USA); apoptosis was induced and cells were treated as previously described. After 48 hours cells were fixed in 4% paraformaldehyde for 10 minutes, washed in 10 mM tris-HCl, pH 8.0, and preincubated for 10 min at room temperature in the reaction buffer for terminal deoxynucleotidyl transferase reaction (200-mM potassium cacodylate, 0.22 mg/ml BSA, and 25-mM tris HCl, pH 6.6). The preincubation buffer was then removed, and a reaction mixture containing 500 U/ml terminal deoxynucleotidyl transferase, 25 mM CoCl2, and 40 μM biotinylated dUTP was added for 60 min at 37°C. The reaction was terminated by the addition of 300 mM NaCl and 30mM sodium citrate for 25 min at room temperature and

for 60 min at room temperature in the dark. Propidium Iodine (PI) (SIGMA, St. Louis, MI, USA) was added to cell suspensions at a concentration of 5 μg/ml. Cells were analyzed using a FACScan flow cytometer (Becton Dickinson, San Jose, CA, USA) at a peak fluorescence wavelength of 530 nm for fluorescein and over 620 nm using linear amplification for PI. The percentage of apoptotic cells was determined after electronic subtraction of signal due to background fluorescence, which was determined using cells incubated with FITC-labeled dUTP without terminal deoxynucleotidyl transferase. A minimum of 10^4 cells were analyzed. This experiment was repeated three times.

5.3.4 Western blot analysis

N976 and N704 cells (adherent and non-adherent) were treated as previously described and then lysed in 20 mM tris-HCl, pH 7,5, 200 mM DTT, 200 mM KCl, 0.5 ml glycerol and protease inhibitor tablets (Roche Diagnostics Canada, Laval, QC, Canada), freeze-thawed 3 times in a dry ice-ethanol bath and centrifuged at 11500 rpm for 15 minutes to remove insoluble material.

Apoptotic Jurkat cells (kind gift of Dr. Andrea LeBlanc, McGill University) were used as positive control cell. Lysates were dissolved in SDS electrophoresis buffer (Bio-Rad, Hercules, CA, USA) and proteins separated on SDS-polyacrylamide gels and subsequently electrotransfered to polyvinylidene difluoride membranes. After membrane blocking with PBS containing 0.1% Tween 20 and 5% non-fat dry milk, membranes were incubated overnight at 4°C using an Ab directed against either FADD,TRADD, caspase-8,-9,Bcl-2, Bax, $p21^{Cipi/WAF1}$ (Santacruz, Santacruz, CA, USA), Poly(ADP-Ribose) Polymerase (PARP) (Calbiochem, San Diego, CA, USA), or tubulin (Sigma, St. Louis, MO, USA). The bound antibodies were detected with the corresponding secondary

antibodies conjugated with horse radish peroxidase. Blots were developed by enhanced chemiluminescence using Lumi-GLO reagents (Kirkegoard & Perry, Gaithensburg, MA, USA).

5.3.5 Detection of Caspase-8 activity by colorimetry

N976 cells were cultured under serum deprivation or Fas Ab in the presence or absence of $1,25(OH)_2D_3$ (10^{-8}M). At 48 hours, cell lysates were obtained from both adherent and non-adherent cells. Lysates were then analyzed using ApoAlert Caspase Colorimetric assay (Clontech Laboratories, Palo Alto, CA, U.S.A.). This assay uses the spectophotometric detection of the chromophore p-nitroaniline (*p*NA) after its cleavage by active caspase-8 from the labeled caspase-specific substrate and therefore represents caspase activity. Optical density was determined at a wavelength of 405 nm on a microplate reader model 3550 (Biorad, Hercules, CA).

5.3.6 Statistical analysis

All results are expressed as mean ± SEM of 3 replicate determinations, and statistical comparisons are based on one-way ANOVA or Student's T-test. A probability value of $p<0.05$ was considered significant.

5.4 Results

5.4.1 Effect of $1,25(OH)_2D_3$ on apoptosis using *in vitro* labeling of osteoblasts

5.4.1.1 Annexin V

FACS analysis of cells stained with annexin V and propidium iodide is shown in Table 6. The percentage of apoptotic osteoblasts in non-treated cells was 45± 3 % and 52 ± 4% after SD and treatment with Fas Ab respectively. In contrast, the number of apoptotic cells was reduced to 16 ± 4 % in serum deprived cultures and those treated with Fas Ab in the presence of 10^{-8} M $1,25(OH)_2D_3$ ($p<0.01$).

5.4.1.2 TUNEL Assay

Fig 25 shows fluorescent images of serum deprived osteoblasts cultured for 48h in the absence (A,B) or presence (C,D) of 10^{-8}M $1,25(OH)_2D_3$ and stained with propidium iodide, to indicate cell numbers (A,C) and labelled with TUNEL, to identify fragmented DNA (B,D). The percentage of TUNEL positive cells was much greater in the un-treated cultures (B) compared with the $1,25(OH)_2D_3$ treated cultures (D)(Table 6)($p<0.01$).

5.4.2 Effect of $1,25(OH)_2D_3$ on the Fas and serum deprivation activated pathways

Initially, the activated pathway (s) after two different apoptotic stimuli was (were) assessed. There was not a significant different in the levels of TRADD in both, Fas Ab treated and serum deprived cells (Fig. 25). In contrast, although there was a more marked expression of FADD in Fas Ab treated cells, no differences after treatment with $1,25(OH)_2D_3$ was found. $1,25(OH)_2D_3$ showed a marked effect as inhibitor of caspase-8 cleavage after both apoptotic stimuli with a more important effect in the Fas Ab treated cells (Fig. 25). No cleavage of Caspase-9 was found in both groups.

Figure 25. *In situ* labeling of apoptotic osteoblasts.

N-976 human calvaria osteoblasts were cultured as described in Experimental Procedures in the absence (A and B) or presence (C and D) of $1,25(OH)_2D_3$ (10^{-8}M). After 48h, the cells were fixed, permeabilized and processed for TUNEL. For identifying purposes cells were counterstained with PI (panels A and C, 40X magnification). Panel B shows a typical example of osteoblasts with high DNA fragmentation after 48 hours of serum deprivation. Panel D shows cells cultured in presence of $1,25(OH)_2D_3$ (10^{-8}M) showing less DNA fragmentation. Only cells expressing apoptotic changes were visible following fluorescein staining. Data are representative of 3 different experiments.

The table shows the percentage of apoptotic cells after 48h in $1,25(OH)_2D_3$ (10^{-8}M) treated and non-treated cells by using two different labeling methods (Annexin V and TUNEL). In both methods, five thousand cells were measured on a FACScan flow cytometer and analyzed with WinMDI software as described in methods.

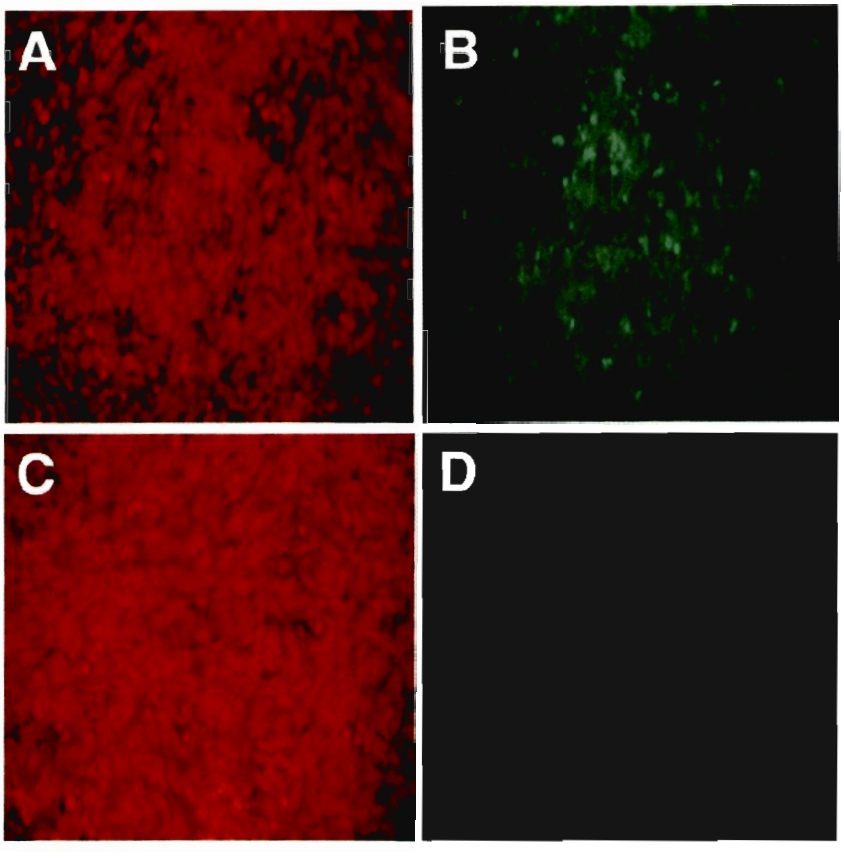
A
B
C
D

Table 6

	Serum Deprivation		Fas Ab	
	Annexin V	TUNEL	Annexin V	TUNEL
Control	45 ± 3	38 ± 4	52 ± 4	44 ± 3
$1,25(OH)_2D_3$	16 ± 2 *	18 ± 2 *	18 ± 4 *	21 ± 2 *

The table shows the percentage of apoptotic cells after 48h in $1,25(OH)_2D_3$ (10^{-8}M) treated and non-treated cells by using two different labeling methods (Annexin V and TUNEL). In both methods, five thousand cells were measured on a FACScan flow cytometer and analyzed with WinMDI software as described in methods. (*) represents a significant difference from control cells ($p<0.05$). Data are representative of three different experiments.

In both groups of apoptotic cells there is an increase in the synthesis of bcl family that is involved in the regulation of apoptosis. An important reduction in the level of the pro-apoptotic Bax was found in $1,25(OH)_2D_3$ treated cells while there was an increase in the level of the anti-apoptotic bcl-2 (Fig. 26). In addition, the cleavage of Poly (ADP-ribose)polymerase (PARP), a zinc-dependent DNA binding protein that recognizes DNA stand breaks and is regarded as a marker of caspase activation was assessed in cells exposed to both pro-apoptotic methods. As shown in figure 26, in cells treated with $1,25(OH)_2D_3$ the content of the 29kDa cleaved fragment was markedly reduced.

5.4.3 Changes in caspase-8 activity

Fig 27(A) shows a significant decrease in caspase-8 activity at 24 hours after induction of apoptosis in $1,25(OH)_2D_3$ treated cells compared with control, with a further decrease by 48 and 72 hours in both serum deprived and Fas Ab treated cultures ($p<0.01$).

5.4.4 Induction of $p21^{Cipi/WAF1}$ in $1,25(OH)_2D_3$ treated osteoblasts

Fig. 27(B and C) shows a significant higher expression of $p21^{Cipi/WAF1}$ in $1,25(OH)_2D_3$ treated osteoblasts as compared to non-treated cells. The levels of expression of $p21^{Cipi/WAF1}$ were determined by western blot (B), quantified by densitometry and normalized according with tubulin expression. The bar graph (panel C) shows the ratio between tubulin/$p21^{Cipi/WAF1}$. A significant up-regulation on $p21^{Cipi/WAF1}$ expression was found in the treated cells as compared to non-treated cells ($p<0.001$).

Figure 26. Changes in apoptosis related proteins in osteoblasts induced to undergo apoptosis in the presence of $1,25(OH)_2D_3$.

A. Apoptosis was induced in N976 and N704 cells by SD or Fas Ab in the presence or absence of $1,25(OH)_2D_3(10^{-8}M)$. Cells were lysed after 48h and whole cell lysates evaluated by Western blot using specific antibodies for FADD,TRADD, caspases-8,-9 (pro-caspase and cleaved fragments), Bax, Bcl-2 and PARP, using tubulin as a control. **B.** Scanning densitometric analysis is expressed as a ratio of tubulin to each of the specific proteins. * $p<0.01$, ** <0.001. Representative data from three different experiments is shown.

A

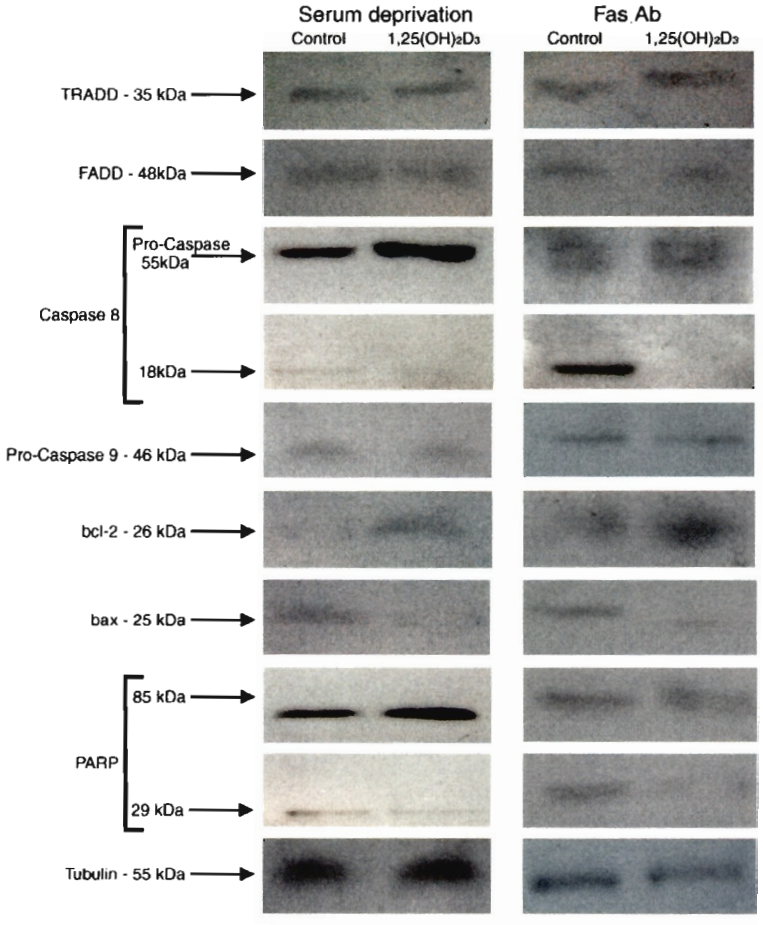
Serum deprivation
Fas Ab
Control
1,25(OH)2D3
Control
1,25(OH)2D3
TRADD - 35 kDa
FADD - 48kDa
Pro-Caspase 55kDa
Caspase 8
18kDa
Pro-Caspase 9 - 46 kDa
bcl-2 - 26 kDa
bax - 25 kDa
85 kDa
PARP
29 kDa
Tubulin - 55 kDa

B

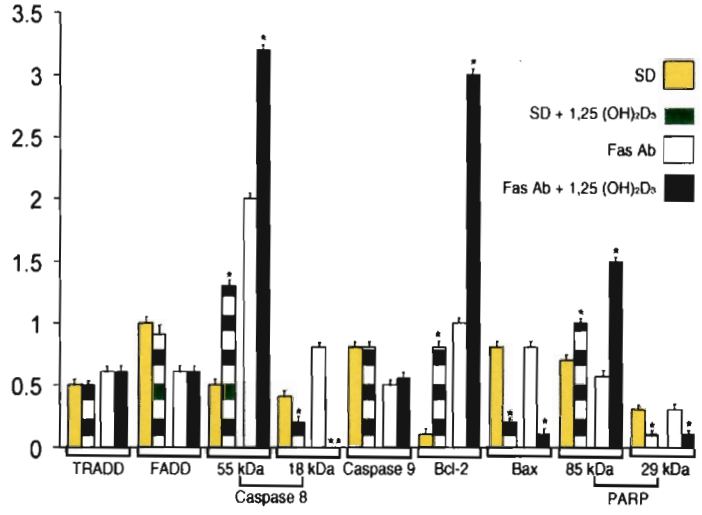
3.5
3
2.5
2
1.5
1
0.5
0
SD
SD + 1,25 (OH)2D3
Fas Ab
Fas Ab + 1,25 (OH)2D3
TRADD
FADD
55 kDa
18 kDa
Caspase 8
Caspase 9
Bcl-2
Bax
85 kDa
29 kDa
PARP

5.5 Discussion

Investigation of the role of apoptosis in mediating a balance between bone deposition and bone resorption has gained momentum in recent years as a consequence of understanding the mechanism of action of antiresorptive agents such as E_2 and bisphosphonates (222) and anabolic agents such as PTH (29). E_2 induces osteoclast apoptosis possibly through the induction or activation of TGF-ß (70). Similarly, bisphosphonates induce osteoclast apoptosis either by inhibiting post-translational phenylation of proteins (72) or by inhibiting specific enzymes of the mevalonate pathway and prenyl protein transferases (224,25). In the case of PTH, *in vivo* studies indicate that daily injections of PTH promote bone formation by increasing the lifespan of mature osteoblasts by inhibition of apoptosis (29).

Although osteoblast apoptosis is a physiological process that may play a role in determining the number of osteoblasts available in a BMU (4,8,9), the molecular pathways by which it is regulated remain to be identified. Previous work has identified $1,25(OH)_2D_3$ (120), E_2(10, 203), bisphosphonates (30,225) IL-6 (9), TGF-ß (64),vitamin K2 (226) and PTH (29) as anti-apoptotic agents in osteoblasts. These observations support the conjecture that inhibition of osteoblast apoptosis will increase the number of osteoblasts in a BMU, which will result in a gain in bone mass. In addition to its anti-apoptotic effect in osteoblasts, $1,25(OH)_2D_3$ has also shown to inhibit apoptosis in other cell lines including hair follicle keratinocytes of C57 BL/6 mice with chemotherapy induced alopecia (227), monocytes (228), and in human osteosarcoma cells (178).

In agreement with our previously published data on cell survival (120), the data shown in Figure 26 indicate that morphological indices of apoptosis were reduced in $1,25(OH)_2D_3$-

Figure 27

A. $1,25(OH)_2D_3$ inhibits caspase-8 activity in apoptotic osteoblasts.

N976 cells were serum deprived and cultured in the presence or absence of 10^{-8} M $1,25(OH)_2D_3$. Cell lysates prepared at the indicated times were processed as described and subjected to colorimetric analysis. The results are the mean ± SEM of 6 replicates and are representative of 3 different experiments. Significant differences in caspase-8 activity between $1,25(OH)_2D_3$-treated and un-treated control cells was seen starting at 24 hours after SD. * $p< 0.001$.

B and C. Changes in the expression of $p21^{Cipi/WAF1}$ induced by $1,25(OH)_2D_3$ in apoptotic osteoblasts. Cells were treated as previously described and then lysed after 48h of treatment with or without $1,25(OH)_2D_3$. Cell lysates were evaluated by Western blot with specific antibodies for $p21^{Cipi/WAF1}$ using tubulin as a control. Panel B shows a significant increase in $p21^{Cipi/WAF1}$ expression in $1,25(OH)_2D_3$ –treated as compared to non-treated cells. **C**. Scanning densitometric analysis is expressed as a ratio of tubulin. *$p<0.001$. Representative data from three different experiments is shown.

A

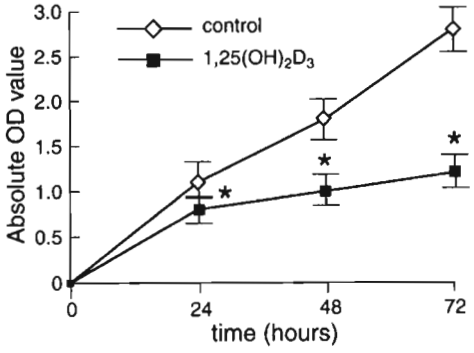
3.0
2.5
2.0
1.5
1.0
0.5
0
Absolute OD value
control
1,25(OH)2D3
*
*
*
0
24
48
72
time (hours)

B

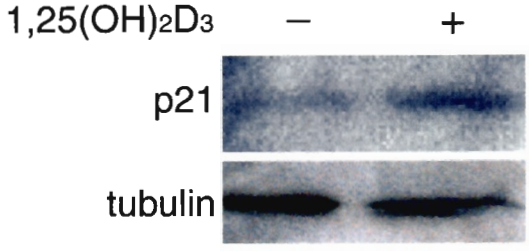
1,25(OH)2D3
–
+
p21
tubulin

C

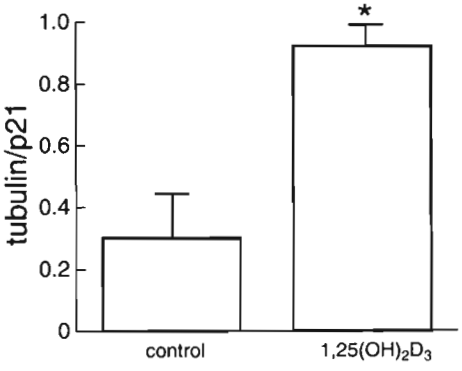
1.0
0.8
0.6
0.4
0.2
0
tubulin/p21
*
control
1,25(OH)2D3

treated cells under conditions of SD and Fas activation. Further analysis of the main elements of the CD95/Fas activated pathways (Fig. 27)demonstrated that while both FADD and TRADD were activated, $1,25(OH)_2D_3$ did not affect this level of the pathway. By contrast, at the caspase level no significant change in caspase-9 cleavage was found, which suggested that caspase-8 must be the prevailing initiator caspase in this pathway. In support of this conjecture was the significant down-regulation of caspase-8 cleavage (fig. 27) and activity (Fig. 28A) in the $1,25(OH)_2D_3$-treated cells compared with un-treated cultures of serum deprived or Fas Ab treated cells. Similarly, monocytes and human monoblastic U937 cells were shown to be Fas resistant after treatment with $1,25(OH)_2D_3$, through inhibition of caspase-8 cleavage(228).

In addition, at the mitochondrial level there was a concurrent reduction in the level of Bax and an increase in the level of Bcl-2 which is maybe induced either by a reduction in caspase-8 activity or a direct effect of $1,25(OH)_2D_3$ on the Bcl-2/Bax ratio. Furthermore, a subsequent reduction in PARP cleavage, which is a zinc-dependent DNA binding protein that recognizes strand breaks that is required for cleavage of the downstream effector caspases (229), was observed in $1,25(OH)_2D_3$ treated cells compared with control (Fig. 26). Overall, the effect of $1,25(OH)_2D_3$ on these specific regulatory points would contribute to the rescue of cells induced to undergo apoptosis.

The mechanism to explain the Fas resistance induced by vitamin D in other cell lines has been found to involve the induction of $p21^{Cipi/WAF1}$ which inhibits cell-cycle progression by binding G1 cyclin/CDK complexes and proliferating cell nuclear antigen (PCNA) through its N- and C terminal domains, respectively (230,231). The CDK-inhibitory domain of $p21^{Cipi/WAF1}$ is known to block the processing and cleavage of caspase-8 in mononuclear cells, additionally $p21^{Cipi/WAF1}$ interacts with caspase-3 to prevent Fas

mediated apoptosis and therefore PARP cleavage (232,233). Interestingly, $p21^{Cipi/WAF1}$ has demonstrated to be a mediator of the pro-differentiating and antiapoptotic effects of IL-6 type cytokines on human osteoblasts (233).

To determine if $p21^{Cipi/WAF1}$ has a role in the anti-apoptotic effect of $1,25(OH)_2D_3$ in osteoblasts, we assessed the change in $p21^{Cipi/WAF1}$ expression in $1,25(OH)_2D_3$ treated vs. non-treated cells. We found a significant increase in the expression of $p21^{Cipi/WAF1}$ in $1,25(OH)_2D_3$ treated cells (Fig. 27. B and C) which might therefore inhibit the cleavage of caspase-8 with the subsequent reduction in the levels of osteoblast apoptosis.

In summary, we have shown that $1,25(OH)_2D_3$ inhibits apoptosis *in vitro* in osteoblasts by suppressing the cleavage and activity of caspase-8. In addition, it was shown that the mitochondrial apoptotic pathway (Bax-Bcl-2) is also involved in osteoblast apoptosis and that $1,25(OH)_2D_3$ inhibits apoptosis by increasing the levels of Bcl-2 as a concomitant mechanism. A proposed model by which the inhibitory effect of $1,25(OH)_2D_3$ on osteoblast apoptosis is shown in Fig 28. The figure shows the main points of the apoptotic pathway, after the activation of CD95/Fas, that are regulated by $1,25(OH)_2D_3$ including an increase $p21^{Cipi/WAF1}$ which would subsequently reduce the recruitment and activation of caspase-8. In addition to the effect of $1,25(OH)_2D_3$ on caspase-8, the higher expression of Bcl-2 will potentiate the inhibition of apoptosis in a mithocondrial related mechanism.

In conclusion, in this study we described the mechanism to explain the anti-apoptotic effect of $1,25(OH)_2D_3$ in osteoblasts. Our findings elucidate the mechanisms involved in osteoblast apoptosis and its main regulatory points which could become important target when looking for the inhibition of osteoblast apoptosis with the subsequent gain in their function at the BMU as bone forming cells.

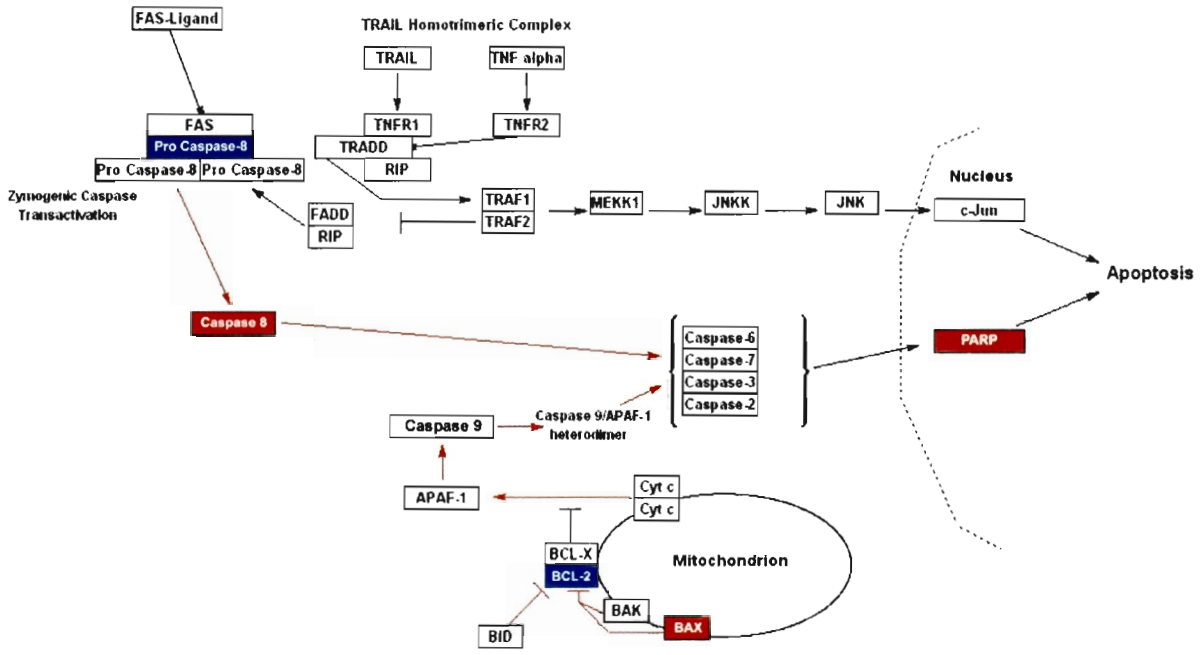

Figure. 28. A proposed mechanism of action of $1,25(OH)_2D_3$ on apoptotic osteoblasts. The elements that increase their expression after exposure to $1,25(OH)_2D_3$ are identified in blue (■) while those elements whose levels of expression are reduced are identified in red (■). The figure shows that the levels of expression of pro-caspase-8 increase while there is a reduction in the cleavage of this caspase. In addition the levels of the anti-apoptotic factor Bcl-2 are increased while Bax levels are decreased by $1,25(OH)_2D_3$. Finally, expression PARP a marker of effector caspase cleavage is decreased in the$1,25(OH)_2D_3$ treated cells. No differences in the expression of FADD or TRADD were found in the $1,25(OH)_2D_3$ treated vs. non-treated cells.

CHAPTER 6

Discussion

The primary objective of this thesis was to elucidate the mechanisms involved with the aging process in the osteoblast and their possible role in the genesis and regulation of age related-bone loss. We used a developmental approach by analyzing the three major steps in the osteoblast life span: its differentiation from MSC to pre-osteoblasts, the changes in the mature osteoblast including changes in receptors expression and bioresponses and finally the mechanisms of osteoblast apoptosis.

Initially, we used a genomic approach by using gene array analysis of MSC before and after their differentiation into osteoblasts. By using a human model of MSC differentiation into osteoblasts we found a variety of changes in gene expression that included genes encoding elements of the pathways involved in osteoblastic differentiation such as TGFβ (TGFβ-receptors II and III), EGF(EGF response factor 2) PTH-receptor, aggrecan 1 etc. Our results suggested a role for two pathways which have been either very recently reported (VEGF) or previously unknown (interferon inducible genes) as involved in the process of osteoblast differentiation. The group of genes known as IFNIG was up regulated in a transitory manner during the first week or proliferative phase of osteogenic differentiation of MSC. This finding is remarkable because although in previous gene array analysis some of these genes were already mentioned as up regulated (31,32) further studies were not pursued.

We decided to assess if IFN and IFNIG play a role in the process of osteogenic differentiation of MSC. Due to the fact that the role of IFN α and β on bone cells has been widely studied and that the majority of the IFNIG that we found as up-regulated were closely related to the IFNγ pathway, we decided to assess the role of this IFN in OB and osteoblast recruitment. As shown in Chapter Two, we not only found that IFNγ plays an important role during the early phases of osteoblastic differentiation of MSC but also that its absence induces osteoporosis in mice. In addition, we assessed the effect of IFN on the most important factor in osteoblast differentiation, the Runx2/Cbfa1. Interestingly, we found that IFNγ accelerates the differentiation of MSC into osteoblasts by inducing the expression of Runx/Cbfa1. Figures 9 and 10 illustrate the possible role of IFNγ as modulator of the osteoblastic differentiation of MSC. Based on the evidence described in chapter two, we can propose that confluent MSC secrete IFNγ in an autocrine manner. Subsequently, IFNγ pathway is activated with further up-regulation of IFNIG which therefore induce the expression of Runx2/Cbfa1 with the final induction of osteoblastic differentiation of MSC.

In addition, the complete lack of IFNγ could be replaced by other factors inside the bone microenvironment. This hypothesis might explain the transitory deficit in bone formation that is found in the IFGR knock out mice. Although these experiments were performed in young mice, further studies will be required to determine if the changes in IFNγ in the bone microenvironment with aging, their significance in the pathogenesis of the age-related bone loss and finally the elucidation of their precise role in the steps that happen upstream the activation of Runx/Cbfa1 during MSC differentiation.

In Chapter Three, we assessed the effect of $1,25(OH)_2D_3$ on bone in a non-hormone dependent model of senile osteoporosis, the SAM-P/6 mice. Our aim in this study was not only to see if $1,25(OH)_2D_3$, a hormone that reduces its action during aging, has an effect on the changes that happen in senile osteoporosis and aging osteoblast, but also to describe the gene changes that can explain this effect and, furthermore, to evaluate if there is a target genes or group of genes for future interventions to regulate the process of age-related bone loss.

Interestingly, we found that $1,25(OH)_2D_3$ was able to increase the activity of mature osteoblasts, the differentiation and commitment of MSC into osteoblasts and finally to markedly inhibit bone marrow AD. The complete evidence obtained from this study supports the concept of bone cells plasticity as a therapeutic approach for senile osteoporosis. Initially, $1,25(OH)_2D_3$ induced the recruitment and differentiation of MSC into mature osteoblasts as it could be seen in ex-vivo cultures of mesenchymal cells. In addition, $1,25(OH)_2D_3$ induced bone formation by two different ways: stimulating the activity of mature osteoblasts and inducing the trans-differentiation of adipocytes into active osteoblasts (Fig. 18). To understand the mechanisms that regulate this effect on cells plasticity, we analyze the gene changes in trabecular cells induced by $1,25(OH)_2D_3$. We found that there is a predominant up-regulating effect of $1,25(OH)_2D_3$ on genes known as inducers of osteoblastogenesis including some previously identified (Cadherin 2, beta globin, hsp90 etc) or unknown (HspJ2, alpha globin, calmodulin, presenilin 2, etc.) as regulated by $1,25(OH)_2D_3$. This evidence demonstrates that the effect of $1,25(OH)_2D_3$ is explained by the predominant up-regulation of strong inducers of osteoblastogenesis which simultaneously act as inhibitors of adipogenesis. Our results will help to understand the mechanisms of the regulation of osteoblast differentiation *in*

vivo and the significance of the regulation of cell plasticity as a therapeutic approach for senile osteoporosis.

In Chapter Four, we looked at the changes in the interaction between aging osteoblasts and two steroid hormones that play a pivotal role in their action and life span (8,145): vitamin D and E_2. Initially, we found that the expression of VDR in osteoblasts *in vivo* decrease with aging in an accepted model of hormonal and senile osteoporosis (C57CBL/6J mice). In addition, we found a significant reduction in VDR expressing osteoblasts after E_2 deprivation. This fact was significantly potentiated by aging. This evidence is important to delineate the interaction between these two steroid hormones and between steroid hormones and aging in the mature osteoblasts and may explain some of the changes that happen during the menopause in the function of osteoblasts and furthermore their effects on osteoblasts function during their wholesome aging process.

A striking finding in Chapter Four was the fact that not only vitamin D inhibits osteoblast apoptosis *in vitro* but also that using both E_2 and $1,25(OH)_2D_3$, their effect can be potentiated. This finding is important since it gives a significant role to the increase bioresponse of osteoblasts exposed simultaneously to E_2 and $1,25(OH)_2D_3$ and may offer a new approach to steroid receptors interaction and their role in the pathogenesis of senile osteoporosis.

Finally, the pathways involved in osteoblast apoptosis *in vitro* which have been previously described (8) were assessed in our model by using two different methods of induction of apoptosis. Our initial aim was to compare the pathways activated during either serum starvation or exposure to Fas Ab in normal human osteoblasts. We found that in both cases there is a predominance of the Fas activated pathway, which was

expected in the second case, and also that there is predominance of caspase-8 activation and subsequently of the cascade of caspases.

Additionally, we assessed the mechanism of action of vitamin D on osteoblast apoptosis. Based on the apoptotic pathways found in non-treated cells we found that vitamin D exerts its anti-apoptotic effect on normal human osteoblasts by regulating the activation of caspase-8 and by increasing the expression of bcl2 an anti-apoptotic factor for the mitochondrial apoptotic pathway (60). Accordingly, we proposed a model of inhibition of apoptosis in human osteoblasts that may become a target for the regulation of this process which plays an important role into the mechanisms of aging in osteoblasts.

6.1 Uncovering the gene regulation of OB: a new approach to build new bone.

The reduction is OB is due to a dysfunction of the transcription machinery that regulate the osteogenic differentiation of MSC (8) and an imbalance between the osteogenic and adipogenic factors with an increasing predominance of the former versus the later.

We found in our gene array analysis a good correlation between the genes that were previously known as up-regulators of MSC differentiation into osteoblasts (31,32). In week 1 we found that genes such as TGF-β, vascular endothelial growth factor (VEGF), Il-10 and calmodulin dependant genes were up-regulated. Furthermore, after week 3, we found a significant up-regulation of genes involved in the mineralization phase such as OSN, bone sialoprotein, OPN, and matrix metalloproteinase.

Additionally, there was a good correlation between the changes in gene expression and the cell phenotype. As shown in Fig. 6, after three weeks of exposure to osteogenic media

MSC acquire a fibroblast-like phenotype characteristic of mature osteoblasts and are also able to induce mineralization.

After the analysis of gene expression at the first and third week of differentiation we found that IFNIG were upregulated only after the first week in a transient manner. IFNs are important cytokines in the bone microenvironment. IFN I (α and β) are produced by leucocytes and fibroblasts and IFN II (γ) is released by activated T lymphocytes, natural killer and multipotential stem cells (122). IFN action is mediated through transcriptional control of a variety of target genes which include a novel family of inducible nuclear factors whose expression appears to be associated with myeloid differentiation (122) and more recently with odontoblastic differentiation of MSC through the activation of CK2 (132).

In Chapter Two, we assessed the production of IFN by MSC during their process of differentiation, interestingly, we found that IFNγ is secreted in a paracrine fashion by confluent MSC while in MSC exposed to OIM IFNγ is secreted earlier (week 1) and in a more significant quantity (Fig. 12,A and B). This evidence lead us to hypothesize that IFNγ is secreted into the bone microenvironment during the process of osteogenic differentiation of MSC and that IFNγ and IFNRG play an important role in this process (Fig. 28).

In addition, when OIM treated cells were exposed to IFNγ we found that they differentiate early into mature osteoblasts demonstrated by their change in phenotype and by both, their capacity of express ALP and by their potential to produce mineralized nodules (Fig. 12, C). To elucidate the mechanism that explains the osteogenic effect of

IFNγ we looked at its role in the differentiation pathway of MSC. We found that IFNγ is able to induce the earlier expression of Runx2/Cbfa1 (Fig. 12,D).

Based on previous research by other groups (45), and on the novel findings described on this work, we propose a new role of IFNγ and IFNIG upstream the expression of Runx2/Cbfa1 during the osteogenic differentiation of MSC (Fig. 28). Furthermore, new evidence supports the role either of IFNγ or its IFNIG on the process of osteoblast differentiation. When the IFNγ pathway is activated, one of the end products is NO recently described as an important factor in osteoblast differentiation (138-140). When BMD and OB was assessed in mice lacking NO synthase, a very significant and also temporal deficit in OB was found (138). This evidence may support our hypothesis that IFNγ and IFNRG play a transitory but important role in the regulation of osteoblast differentiation.

When the role of IFNγ in OB and osteoblast recruitment was assessed in the $IFNG^{-/-}$ mice, we found that they were osteoporotic with very particular features: a reduction in osteoblastic differentiation and activity, a deficit in endochondral ossification, and a marked deficit in osteoclastic activity (Fig.13-15). All this findings seem to be temporal since these mice recover their capacity of bone formation and after 24 weeks of age have the same BMD than their normal counterpart (Fig. 13).

A striking finding of our study was the temporary role of IFNγ and IFNIG on osteoblast differentiation, recruitment and activity. We postulate that although they play an important role in the regulation of the first phase of osteogenic differentiation of MSC and osteoblast recruitment they are overcome by new players involved in the same

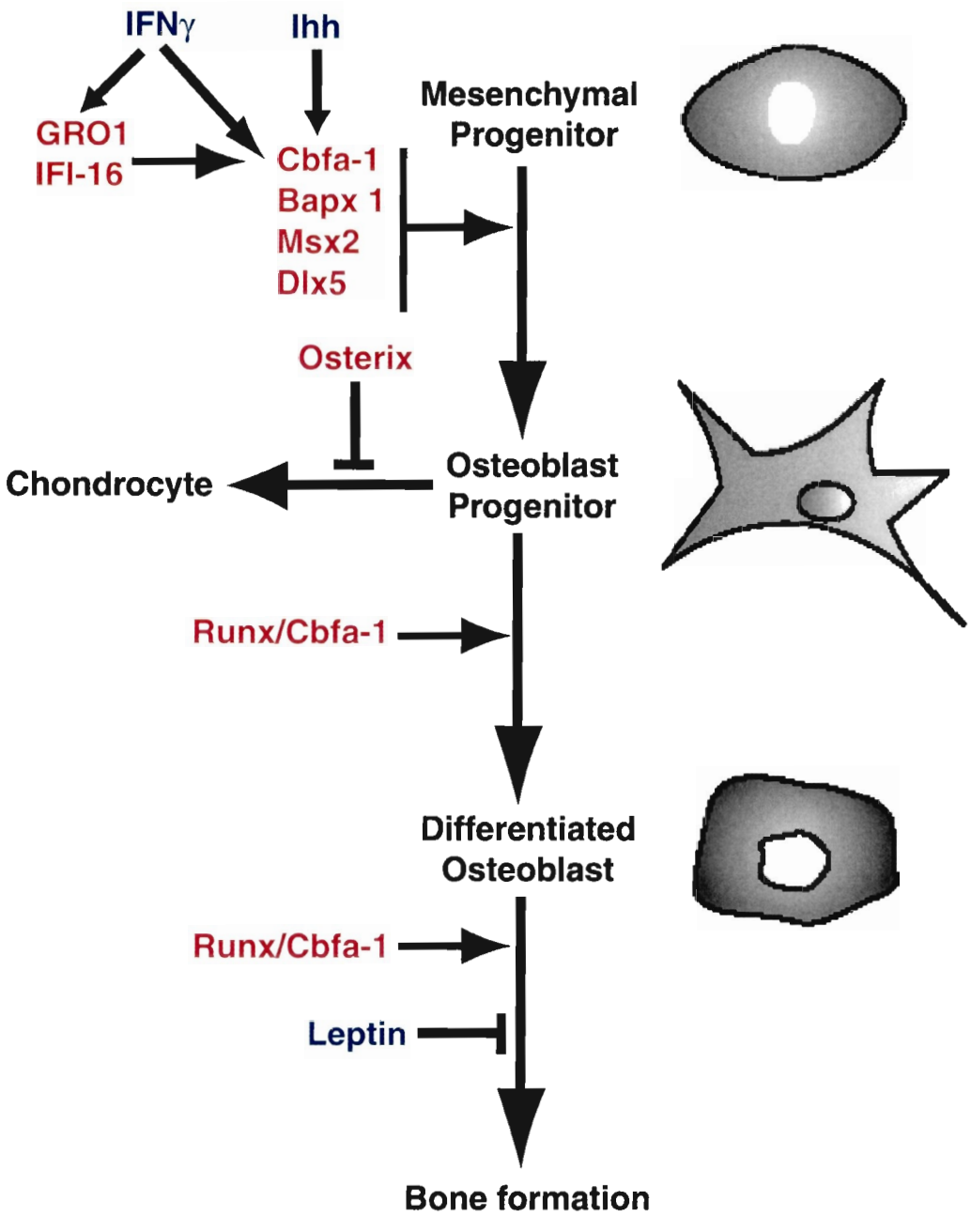

Figure 29. Proposed schematic diagram of the genetic control of osteoblast differentiation and function. Transcription factors are indicated in red, secreted molecules are in blue. Black arrows indicate the stimulatory (arrowhead) or inhibitory (line head) of these molecules.

process that may include other cytokines and GF. Afterwards, once the Runx2/Cbfa1 system is activated the process of differentiation is completed (Fig. 29).

6.2 The gain of bone mass by inhibiting bone marrow AD: the advantages of cell plasticity

Although much has been written about the increasing levels of AD in aging bone (8,153) the mechanism to explain and regulate this phenomenon remains unclear. It is known that there is a predominance of pro-adipogenic factors like PPARγ and CEBPα inside the bone marrow of old mice while the levels of osteogenic factors decrease (48).

In Chapter Three, we used an accepted model of senile osteoporosis which has shown the main features of this syndrome (152,153). Studies assessing the effect of different hormones and compounds (165-169) in this mice model have shown that it is possible to re-gain bone mass while increasing the levels of OB and bone formation. However, there are not studies showing the effect that replacing adipose tissue by osteogenic tissue has in the bone microarchitecture and BMD and, more interestingly, the genes that should be regulated to obtain these specific effects. Our study showed that, first, $1,25(OH)_2D_3$ was able to increase the BMD and improve all markers (architectural and serological) of bone formation(Fig.16,17,G and H, Table 1 and 2) ; second, adipose tissue was markedly replaced by osteogenic tissue into the bone marrow (Fig. 17, A-D); and third, when we assessed the changes on gene expression induced by vitamin D in trabecular cells we found a significant change in 440 genes, most of them previously unknown to be regulated by this hormone (Table 3).

Since our aim was to give a functional significance to our findings, we decided to group these genes in those involved in AD and OB (Table 4). Amongst the OB inducing genes we found some of the most commonly reported such as cadherin, IL-11, c-fos, Cspg6, AP-1, calbindin etc. (Table 4).

Concerning adipogenic genes, we found that an important group of genes that inhibit AD were up-regulated by vitamin D including calmodulin, tubulin beta3, glutathione peroxidase, and calmodulin (Table 4). Furthermore, a significant inhibition of osteoclastic activity was found in the vitamin D treated mice. Although this effect has been already described *in vivo* in other strain of mice (150), the mechanisms to explain this effect remain unclear. We went further by assessing the possible link between the hormone changes in the SAM-P/6 treated with $1,25(OH)_2D_3$ and the inhibition in osteoclasts number and activity. We found a very significant reduction in serum concentrations of PTH (Table 2), an important regulator of osteoclasts activity and differentiation, in the $1,25(OH)_2D_3$ as compared with the vehicle treated group which may explain the important reduction in osteoclastic activity seen in our model (Fig. 16, and Table 1).

The concept of cell plasticity in the bone environment involves the transformation of osteoblasts into adipocytes and vice versa. The genes involved in the regulation of this process were elucidated in our study by not only increasing OB, osteoblast recruitment and bone formation but also by replacing mature adipocytes with mature osteoblasts. We show in (Table 4) how some of the genes up-regulated by $1,25(OH)_2D_3$ play divergent roles by stimulating osteoblast differentiation and inhibiting AD with a predominance of "osteogenic" genes.

In table 4 we proposed a genomic approach to the process of osteoblast and adipocyte differentiation after the exposure of aging mice to vitamin D. Although this model applies

to the specific effect of this compound, we offer a novel list of unrecognized factors that can be assessed in the future.

6.3 Steroid hormones and the aging osteoblast: A potentially reversible decline in their interaction with the external world

The reduction in the number and bioresponse of VDR with aging *in vivo* has been demonstrated in several organs such as intestine and kidney (186-189). By contrast in bone, the reduction in VDR expression has been only documented *in vitro* (191). In Chapter Four we are the first to document a significant decline in the number of VDR in osteoblasts in C57Bl/6J mouse model, an accepted model for both senile and hormone dependent osteoporosis (194)(Fig. 19-21).

In addition, we assessed if the deprivation of E_2 has any effect on VDR expression. We found that in both young and old oophorectomized animals there is a significant reduction in VDR expression in the osteoblasts (Fig. 20-22). Our results elucidate a new interaction between these two steroid hormones since demonstrate that E_2 can regulate the expression of VDR and thus their bioresponse. By contrast, when oophorectomized mice were supplied with E_2, their proportion of VDR expressing osteoblasts came back to normal in the young group with a much higher and significant response in the old group (Fig. 22). These results demonstrate that although there is a reduction in the number of active osteoblast in old bone, they conserve their potential of recovering the expression of receptor to steroid hormones.

Finally, to assess if effectively there is a regulation of the bioresponse of VDR after exposure to E_2, we assessed the effect of either E_2 and/or vitamin D on osteoblast apoptosis *in vitro* (Fig. 23,24). Initially, we showed that the same effect of E_2 on VDR

expression found *in vivo* was also found in our cell model *in vitro*(Fig. 23). Subsequently, we found that when given simultaneously to apoptotic osteoblasts $1,25(OH)_2D_3$ and E_2 have an additive effect as inhibitors of apoptosis (Fig. 24).

To sum up, Chapter Four brings not only a new evidence on the changes in the number and bioresponse of VDR in aging osteoblasts but also opens a new field of research into the possible mechanisms involved in this interaction and the possible therapeutic utility of the regulation of the action of steroid hormones on bone cells.

6.4 The inhibition of apoptosis: the last piece of the puzzle

We analyzed the phenomenon of apoptosis in osteoblasts from two perspectives, first, we tried to elucidate its possible mechanisms, and second, we essayed to inhibit it in order to offer a longer life span to mature osteoblasts.

Even though osteocyte apoptosis has been well documented (67), the demonstration of osteoblast apoptosis *in vivo* has multiple difficulties due to the fact that its detection and quantification in bone sections has multiple difficulties(61). However, evidence demonstrates that there is a percentage of osteoblasts that do not become either lining cells or osteocytes which most probably die by apoptosis (8,61). The importance of studying osteoblast apoptosis underlies in the theory that if osteoblasts have a longer life span then their role on building bone mass is enhanced due a higher amount of mature osteoblasts in the BMU.

Based on this theory, in Chapter Five we have used two *in vitro* models of osteoblast apoptosis to test first, the pathway that is activated during these processes and, second, to elucidate the key target points to modulate these pathways.

Initially, the two used methods to induce apoptosis, SD and exposure to Fas Ab, demonstrated a significant activation of the Fas related pathway. These findings correlate with previous studies that reported an important role of the activation of the Fas-FasL related pathway on osteoblast apoptosis (63). Furthermore, we found that the activation of the Fas-FADD pathway in osteoblasts induces both, the cleavage of caspase-8 and the activation of the Bax-Bcl-2 mithocondrial pathway with increasing levels of the pro-apoptotic Bax expression (Fig. 25).

Previous studies have demonstrated the inhibitory effect on osteoblast apoptosis of several compounds including PTH, calcitonin, and IL-6. In our study, we decided to assess the effect of an important regulator of calcium and bone metabolism, $1,25(OH)_2D_3$, on osteoblast apoptosis. $1,25(OH)_2D_3$ inhibits apoptosis in mononuclear cells by inhibiting the cleavage of caspase-8 and by inducing resistance to Fas activation; the two main mechanisms involved in osteoblast apoptosis (228).

As in Chapter Three and Four, we found a new and important role of $1,25(OH)_2D_3$ on osteoblasts. In this case since we found that $1,25(OH)_2D_3$ inhibits apoptosis in human osteoblasts *in vitro* not only by a similar mechanism than the previously reported in mononuclear cells (inhibition of the cleavage of caspase-8 and induction of Fas-resistance) but also by increasing the expression of the anti-apoptotic Bcl-2 inside the mitochondrial pathway. These results will be fundamental for future research on the regulation of osteoblast apoptosis since the pathway was fully identified as well as the possible mechanisms to promote the survival of the human osteoblasts *in vitro*.

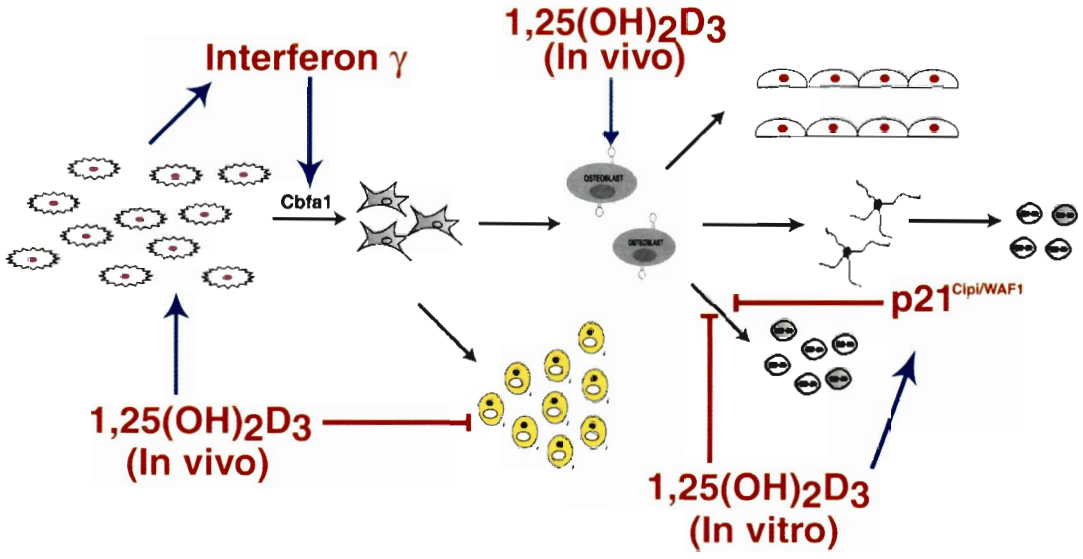

Figure 30. Summary of the molecular mechanisms regulating the genesis and the fate of osteoblast. IFNγ is secreted in an autocrine manner by confluent MSC. The secretion of IFNγ in the bone marrow microenvironment will induce the expression of Runx2/Cbfa1 and thus the osteoblastic differentiation of MSC. In vivo, the process of osteoblastogenesis and the replacement of adiposity by new bone could be regulated by $1,25(OH)_2D_3$ through a predominant up-regulation of genes encoding osteogenic proteins. In addition, the response of mature osteoblasts to $1,25(OH)_2D_3$ is increased by the administration of E2 *in vivo*. Finally, apoptosis in osteoblast is predominantly induced by Fas activation which could be inhibited by the stimulation of $p21^{Cipi/WAF1}$ with further inhibition of the cleavage and recruitment of caspase 8.

Blue arrows: stimulation; Red lines: inhibition.

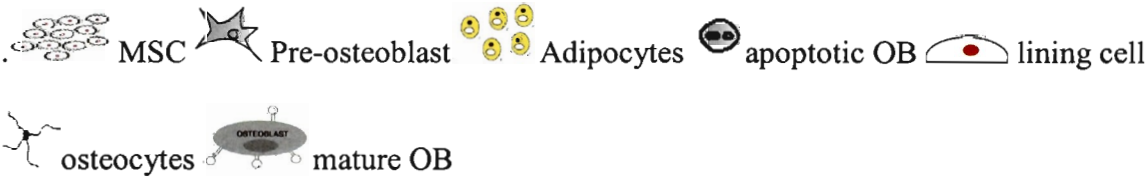

6.5 Conclusion

We hypothesized that to regulate the molecular changes that happen in aging osteoblasts we should identify and control the internal pathways involved in their differentiation, their interaction with external factors in the bone microenvironment and finally their death by apoptosis. During the analysis of the pathways involved in osteoblast differentiation we found a new and important player in this process: IFNγ. Additionally, we found that the role of IFNγ in osteoblast differentiation happens upstream of the most important regulator of this process, the Runx2/Cbfa1 factor. This finding will open a new and interesting area of research to elucidate the interaction and time-related significance between the two molecules.

We also found in an animal model of senile osteoporosis that it is possible to inhibit AD and stimulate OB with further gain in bone mass. Although in this case we used $1,25(OH)_2D_3$ as the regulator of this process our main interest was to look at the gene regulation of osteoblast differentiation *in vivo* and the possible interventions to prevent AD with aging. Moreover, we found significant changes in the number and bioresponse of VDR in aging osteoblasts *in vivo*. This change was reverted by E_2 in a previously unknown steroid hormone interaction. Finally, we not only confirmed the apoptotic pathways activated during the process of osteoblast apoptosis *in vitro*, but also demonstrated a new effect of $1,25(OH)_2D_3$ as inhibitor of this process. In addition we identified new target elements for the regulation of osteoblast apoptosis: the cleavage of caspase-8 and the induction of resistance to Fas. All these findings illuminate our understanding of the molecular changes in the aging osteoblasts and bring together very

important information about not only the changes that happen during aging but also the target pathways to regulate these changes.

REFERENCES

1. Lian, J.B., G.S. Stein, E. Canalis, P.G. Robey, and A. Bolskey. In M.J. Favus, *Primer on the Metabolic Bone Diseases and Disorders of Mineral Metabolism*. 1999. Fourth Edition. Lippincott Williams & Wilkins.

2. Goltzman, D. 2002. Discoveries, drugs and skeletal disorders. *Nat Rev Drug Discov.* **1**: 784-796.

3. Kalu D: Aging-bone; in Masoro E, Handbook of Physiology. A critical, comprehensive presentation of physiological knowledge and concepts. vol. 1 (New York, Oxford University Press 1995).

4. Manolagas, S.C., and R.L. Jilka. 1995. Bone marrow, cytokines, and bone remodeling. Emerging insights into the pathophysiology of osteoporosis. *New England Journal of Medicine.* **332**: 305-311.

5. Aubin, J.E. 1998. Advances in the osteoblast lineage. *Biochem. and Cell Biology.* **76***:* 899-910.

6. Ducy, P., T. Schinke, and G. Karsenty. 2000 The osteoblast: a sophisticated fibroblast under central surveillance. *Science.* 289:1501-1504.

7. Hughes, D.E., K.R. Wright, D.E. Hughes, K.R. Wright, L. Xing, and A. Dai. 1999. Recent advances in bone biology provide insight into the pathogenesis of bone diseases. *Laboratory Investigation.* **79***:* 83-94.

8. Chan, G.K. and G. Duque. 2002. Age-related bone loss: old bone, new facts. *Gerontology.* **48**: 62-71.

9. Manolagas, S.C., T. Bellido, and R.L. Jilka. 1995. New insights into the cellular, biochemical, and molecular basis of postmenopausal and senile osteoporosis: roles of IL-6 and gp130. *International Journal of Immunopharmacology* 17*:* 109-116.

10. Marie, P. 1997. Growth factors and bone formation in osteoporosis: roles for IGF-I and TGF-beta. *Revue Du Rheumatisme, English Edition.* **64**:44-53.

11. Manolagas, S.C. 2000. Birth and death of bone cells: basic regulatory mechanisms and implications for the pathogenesis and treatment of osteoporosis. *Endocrine Reviews.* **21**: 115-137

12. Manolagas, S.C. 1995. Role of cytokines in bone resorption. *Bone.* **17**: 63S-67S.

13. Manolagas, S.C., and R.S. Weinstein. 1999. New developments in the pathogenesis and treatment of steroid-induced osteoporosis. *J Bone Miner Res.***14**:1061-1066 .

14. Teitelbaum, S.L. 2000. Bone resorption by osteoclasts. *Science.* **289**: 1504-1508.

15. Clifford, J. Rosen, Julie Glowacki, and John P. Bilezikian. *The Aging Skeleton*, 1st. Edition. 1999 Academic Press. San Diego, CA. USA.

16. Parfitt, A.M. 1994. Osteonal and hemi-osteonal remodeling: the spatial and temporal framework for signal traffic in adult human bone. *Journal of Cellular Biochemistry.* **55**: 273-286.

17. Bergot, C, A.M. Laval-Jeantet, F. Preteux, and A. Meunier. 1988. Measurement of anisotropic vertebral trabecular bone loss during aging by quantitative image analysis. *Calcif Tissue Int.* **43**:143-149.

18. Parfitt, A.M., C.H. Mathews, A.R.Villanueva, M. Kleerekoper, B. Frame, , and D.S. Rao. 1983. Relationships between surface, volume, and thickness of iliac trabecular bone in aging and in osteoporosis. Implications for the microanatomic and cellular mechanisms of bone loss. *J Clin Invest.* **72**:1396-1409.

19. Girasole, G., R.L. Jilka, G. Passeri, S. Boswell, G. Boder, D.C. Williams, and S.C. Manolagas. 1992.17 beta-estradiol inhibits interleukin-6 production by bone marrow-

derived stromal cells and osteoblasts in vitro: a potential mechanism for the antiosteoporotic effect of estrogens. *J Clin Invest* **89**: 883-891.

20. Kimble, R.B., S. Srivastava, F.P. Ross, A. Matayoshi, and R. Pacifici, 1996. Estrogen deficiency increases the ability of stromal cells to support murine osteoclastogenesis via an interleukin-1and tumor necrosis factor-mediated stimulation of macrophage colony-stimulating factor production. *J Biol Chem.* **271**: 28890-28897.

21. Pacifici, R., C. Brown, E. Puscheck, E. Friedrich, E. Slatopolsky, D. Maggio, R. McCracken, , and L.V. Avioli. 1991. Effect of surgical menopause and estrogen replacement on cytokine release from human blood mononuclear cells. *Proc Natl Acad Sci U S A.* **88**: 5134-5138.

22. Ralston, S.H., R.G. Russell, and M. Gowen. 1990. Estrogen inhibits release of tumor necrosis factor from peripheral blood mononuclear cells in postmenopausal women. *J Bone Miner Res.* **5**: 983-988.

23. Duppe, H., P. Gardsell, O. Johnell, and B.E. Nilsson. 1992. Bone mineral content in women: trends of change. *Osteoporos Int.* **2**: 262-265.

24. Suponitzky, I., and M. Weinreb. 1998. Differential effects of systemic prostaglandin E2 on bone mass in rat long bones and calvariae. *J Endocrinol.* **156**:51-57

25. Hakeda, Y., Y. Nakatani, N. Kurihara, E. Ikeda, N. Maeda, and M. Kumegawa. 1985. Prostaglandin E2 stimulates collagen and non-collagen protein synthesis and prolyl hydroxylase activity in osteoblastic clone MC3T3-E1 cells. *Biochem Biophys Res Commun.* **126**: 340-345.

26. Linkhart, T.A., S. Mohan, and D.J. Baylink, 1996. Growth factors for bone growth and repair: IGF, TGF beta and BMP. *Bone.* **19**:1S-12S.

27. Baylink, D.J., R.D. Finkelman, and S. Mohan. 1993. Growth factors to stimulate bone formation. *J Bone Miner Res.* **8**: S565-72.

28. Reyes-Botella, C., M.F. Vallecillo-Capilla, and C. Ruiz, 2002. Effect of different growth factors on human cultured osteoblast-like cells. *Cell Physiol Biochem.* **12**: 353-358.

29. Jilka, R.L., R.S. Weinstein, T. Bellido, P. Roberson, A.M. Parfitt, and S.C. Manolagas. 1999. Increased bone formation by prevention of osteoblast apoptosis with parathyroid hormone. *J Clin Invest.* **104**: 439-446.

30. Plotkin, L.I., R.S. Weinstein, A.M. Parfitt, P.K. Roberson, S.C. Manolagas, and T. Bellido, 1999. Prevention of osteocyte and osteoblast apoptosis by bisphosphonates and calcitonin. *J Clin Invest.* **104**: 1363-1374

31. Seth, A., B.K. Lee, S. Qi, and C.P. Vary. 2000. Coordinate expression of novel genes during osteoblast differentiation. *J Bone Miner Res.* **15**: 1683-1696.

32. Beck, G.R.Jr., B. Zerler, and E. Moran, 2001. Gene array analysis of osteoblast differentiation.*Cell Growth Differ.* **12**:61-83.

33. Rozman, C., E. Feliu, L. Berga, J.C. Reverter, C. Climent, and M.J. Ferran. 1989. Age-related variations of fat tissue fraction in normal human bone marrow depend both on size and number of adipocytes: a stereological study. *Exp Hematol* **17**:34-37.

34. Gimble, J.M., C.E. Robinson, X.Wu, , and K.A. Kelly. 1996. The function of adipocytes in the bone marrow stroma: an update. *Bone.* **19**:421-428.

35. Diascro, D.D., R.L. Vogel, T.E. Johnson, K.M. Witherup, S.M. Pitzenberger, S.J. Rutledge, D.J. Prescott, G.A. Rodan, and A. Schmidt. 1998. High fatty acid content in rabbit serum is responsible for the differentiation of osteoblasts into adipocyte-like cells. *J Bone Miner Res* **13**: 96-106.

36. Park, S.R., R.O. Oreffo, and J.T. Triffitt. 1999. Interconversion potential of cloned human marrow adipocytes in vitro. *Bone.* **24**: 549-554.

37. Nuttall, M.E., A.J. Patton, D.L. Olivera, D.P. Nadeau, and M. Gowen. 1998. Human trabecular bone cells are able to express both osteoblastic and adipocytic phenotype: implications for osteopenic disorders. *J Bone Miner Res.* **13**: 371-382.

38. Nuttall, M.E. and J.M. Gimble. 2000. Is there a therapeutic opportunity to either prevent or treat osteopenic disorders by inhibiting marrow adipogenesis? *Bone.* **27**: 177-184.

39. Ducy, P., R. Zhang, A.L. Geoffroy Ridall, and G. Karsenty. 1997. Osf2/Cbfa1: a transcriptional activator of osteoblast differentiation. *Cell.* **89**: 747-754.

40. Ducy, P. 2000. Cbfa1: a molecular switch in osteoblast biology. *Dev Dyn.* **219**: 461-471.

41. Mundlos, S., F. Otto, C. Mundlos, J.B. Mulliken, A.S. Aylsworth, S. Albright, D. Lindhout, W.G. Cole, W. Henn, J.W. Knoll, M.J. Owen, R. Mertelsmann, B.U. Zabel, and B.R. Olsen. 1997. Mutations involving the transcription factor CBFA1 cause cleidocranial. *Cell 89:* 773-779

42. Otto, F., A.P. Thornell, T. Crompton, A. Denzel, K.C. Gilmour, I.R. Rosewell, G.W. Stamp, R.S. Beddington, S. Mundlos, B.R. Olsen, P.B. Selby, and M.J. Owen. 1997. Cbfa1, a candidate gene for cleidocranial dysplasia syndrome, is essential for osteoblast differentiation and bone development. *Cell.* **89**: 765-771.

43. Kobayashi, H., Y. Gao, C. Ueta, A. Yamaguchi, and T. Komori. 2000. Multilineage differentiation of Cbfa1-deficient calvarial cells in vitro. *Biochem Biophys Res Commun.* **273**: 630-636.

44. Xiao, G., D. Jiang, P. Thomas, M.D. Benson, K. Guan, G. Karsenty, and R.T. Franceschi, 2000. MAPK pathways activate and phosphorylate the osteoblast-specific transcription factor, Cbfa1. *J Biol Chem* **275**: 4453-4459.

45. Nakashima, K., X. Zhou, G. Kunkel, Z. Zhang, J.M. Deng, R.R. Behringer, and B. de Crombrugghe. 2002. The novel zinc finger-containing transcription factor osterix is required for osteoblast differentiation and bone formation. *Cell.* **108**:17-29.

46. Jackson, S.M., and L.L. Demer. 2000. Peroxisome proliferator-activated receptor activators modulate the osteoblastic maturation of MC3T3-E1 preosteoblasts. *FEBS Lett.* **471**: 119-124

47. Tontonoz, P., E. Hu, and B.M. Spiegelman. 1994. Stimulation of adipogenesis in fibroblasts by PPAR gamma 2, a lipid-activated transcription factor. *Cell.* **79**: 1147-1156.

48. Duque, G. 2003. Will reducing adipogenesis in bone increase bone mass? : PPAR gamma 2 as a key target in the treatment of age related bone loss. *Drug News & Perspectives*. (In press).

49. Tontonoz, P., E. Hu, R.A. Graves, A.I. Budavari, and B.M. Spiegelman. 1994. mPPAR gamma 2: tissue-specific regulator of an adipocyte enhancer. *Genes Dev.* **8**: 1224-1234 .

50. Hu, E., P. Tontonoz, and B.M. Spiegelman. 1995. Transdifferentiation of myoblasts by the adipogenic transcription factors PPAR gamma and C/EBP alpha. *Proc Natl Acad Sci U S A.* **92**: 9856-9860 .

51. Hu, E., J.B. Kim, P. Sarraf, and B.M. Spiegelman. 1996. Inhibition of adipogenesis through MAP kinase-mediated phosphorylation of PPARgamma. *Science* **274**: 2100-2103.

52. Deckers, M.M., M. Karperien, C. van der Bent, T. Yamashita, S.E. Papapoulos, and C.W. Lowik. 2000. Expression of vascular endothelial growth factors and their receptors during osteoblast differentiation. *Endocrinology.* **141**: 1667-1774.

53. Dallas, S.L., D.R. Keene, S.P. Bruder, J. Saharinen, L.Y. Sakai, G.R. Mundy, and L.F. Bonewald. 2000. Role of the latent transforming growth factor beta binding protein 1 in fibrillin-containing microfibrils in bone cells in vitro and in vivo. *J Bone Miner Res.* **15**: 68-81.

54. Lanske, B., A.C. Karaplis, K. Lee, A. Luz, A. Vortkamp, A. Pirro, M. Karperien, , L.H.K. Defize, C. Ho, R.C. Mulligan, A.B. Abou-Samra, H. Juppner, G.V. Segre, and H.M. Kronenberg. 1996. PTH/PTHrP receptor in early development and Indian hedgehog-regulated bone growth. *Science.* **273**: 663-666.

55. Vortkamp, A., K. Lee, B. Lanske, G.V. Segre, H.M. Kronenberg, , and C.J. Tabin. 1996. Regulation of rate of cartilage differentiation by Indian hedgehog and PTH-related protein. *Science.* **273**: 613-622 .

56. Chuang, P.T., and A.P. McMahon. 1999. Vertebrate Hedgehog signalling modulated by induction of a Hedgehog-binding protein. *Nature.* **397**: 617-621.

57. Wyllie, A.H., J.F. Kerr, and A.R. Currie. 1980. Cell death: the significance of apoptosis. *International Review of Cytology.* **68**: 251-306.

58. Ellis, R.E., J.Y. Yuan, and H.R. Horvitz. 1991. Mechanisms and functions of cell death. *Annual Review of Cell Biology.* **7**: 663-698.

59. Duque, G. 2000. Apoptosis in cardiovascular aging research: Future directions. *Am J of Geriatric Cardiology.* **270**: 263-264.

60. Mathiasen, I.S., U. Lademann, and M. Jaattela. 1999. Apoptosis induced by vitamin D compounds in breast cancer cells is inhibited by Bcl-2 but does not involve known caspases or p53. *Cancer Research.* **59**: 4848-4856

61. Weinstein, R.S., and S.C. Manolagas. 2000. Apoptosis and osteoporosis. *Am J Med.* **108**:153-164.

62. Gavrieli, Y., Y. Sherman, and S.A. Ben-Sasson. 1992. Identification of programmed cell death *in situ* via specific labeling of nuclear DNA fragmentation. *J. Cell. Biol.* **119**:493-501.

63. Kawakami, A., K. Eguchi, N. Matsuoka, M. Tsuboi, T. Koji, S. Urayama, K. Fujiyama, T. Kiriyama, T. Nakashima, P.K. Nakane, and S. Nagataki. 1997. Fas and Fas ligand interaction is necessary for human osteoblast apoptosis. *J Bone Miner Res.* **12**:1637-1646.

64. Jilka, R.L., R.S. Weinstein, T. Bellido, A.M. Parfitt, and S.C. Manolagas. 1998. Osteoblast programmed cell death (apoptosis): modulation by growth factors and cytokines. *J Bone Miner Res.* **13**: 793-802.

65. Werner, A.B., E. de Vries, S.W. Tait, I. Bontjer, and J. Borst, 2002. TRAIL receptor and CD95 signal to mitochondria via FADD, caspase-8/10, Bid, and Bax but differentially regulate events downstream from truncated Bid. *J Biol Chem.* **277**:40760-7.

66. Noble, B.S., H. Stevens, N. Loveridge, and J. Reeve. 1997. Identification of apoptotic changes in osteocytes in normal and pathological human bone. *Bone.* **20**: 273-282.

67. Tomkinson, A., E.F. Gevers, J.M. Wit, J. Reeve, and B.S. Noble. 1998. The role of estrogen in the control of rat osteocyte apoptosis. *J Bone Miner Res.* **13**: 1243-1250

68. Tomkinson, A., J. Reeve, R.W. Shaw, and B.S. Noble. 1997. The death of osteocytes via apoptosis accompanies estrogen withdrawal in human bone. *J of Clin. Endocrino. and Metab.* **82**: 3128-3135.

69. Lutton, J.D., B.S. Moonga, and D.W. Dempster. 1996. Osteoclast demise in the rat: physiological versus degenerative cell death. *Experimental Physiology.* **81**: 251-260

70. Hughes, D.E., A. Dai, J.C. Tiffee, H.H. Li, G.R. Mundy, and B.F. Boyce. 1996. Estrogen promotes apoptosis of murine osteoclasts mediated by TGF-beta. *Nature Medicine.* **2**: 1132-1136.

71. Jilka, RL, G. Hangoc, G. Girasole, G. Passeri, D.C. Williams, J.S. Abrams, B. Boyce, H. Broxmeyer, and S.C. Manolagas. 1992. Increased osteoclast development after estrogen loss: mediation by interleukin-6. *Science.* **257**: 88-91.

72. Luckman, S.P., F.P. Coxon, F.H. Ebetino, R.G. Russell, and M.J. Rogers. 1998. Heterocycle-containing bisphosphonates cause apoptosis and inhibit bone resorption by preventing protein prenylation: evidence from structure-activity relationships in J774 macrophages. *J Bone Miner Res.* **13**: 1668-1678.

73. Tsuboyama, T., K. Takahashi, M. Matsushita, H. Okumura, T. Yamamuro, M. Umezawa, and T. Takeda. 1989. Decreased endosteal formation during cortical bone modelling in SAM-P/6 mice with a low peak bone mass. *Bone Miner.* **7**:1-12.

74. Parfitt, A.M. 1984. Age-related structural changes in trabecular and cortical bone: cellular mechanisms and biomechanical consequences. *Calcif Tissue Int* **36**: S123-128.

75. Frost, H.M. Lamellar Bone can deposit only on pre-existing bone, regardless of whether that consists of fibrous (woven) or lamellar bone; in Thomas CC: *The Physiology of Cartilaginous, Fibrous and Bony Tissue,* chapter 5. 1972. Springfield, MA, USA...

76. Pittenger, M.F., A.M. Mackay, S.C. Beck, R.K. Jaiswal, R. Douglas, J.D. Mosca, M.A. Moorman, D.W. Simonetti, S. Craig, and D.R. Marshak. 1999. Multilineage potential of adult human mesenchymal stem cells. *Science.* **284**: 143-147

77. Gori, F., T. Thomas, K.C. Hicok, T.C. Spelsberg, and B.L. Riggs. 1999. Differentiation of human marrow stromal precursor cells: bone morphogenetic protein-2 increases OSF2/CBFA1, enhances osteoblast commitment, and inhibits late adipocyte maturation. *J Bone Miner Res.* **14**: 1522-1535 .

78. Thies, R.S., M. Bauduy, B.A. Ashton, L. Kurtzberg, J.M. Wozney, and V. Rosen. 1992. Recombinant human bone morphogenetic protein-2 induces osteoblastic differentiation in W-20-17 stromal cells. *Endocrinology.* **130**: 1318-1324 .

79. Wang, E.A., D.I. Israel, S. Kelly, and D.P. Luxenberg. 1993. Bone morphogenetic protein-2 causes commitment and differentiation in C3H10T1/2 and 3T3 cells. *Growth Factors* **9**:57-71

80. Yamamoto, N., S. Akiyama, T. Katagiri, M. Namiki, T. Kurokawa, T. and Suda. 1997. Smad1 and smad5 act downstream of intracellular signalings of BMP-2 that inhibits myogenic differentiation and induces osteoblast differentiation in C2C12 myoblasts. *Biochem Biophys Res Commun.* **238**: 574-580 .

81. Shafritz, A.B., E.M. Shore, F.H. Gannon, M.A. Zasloff, R. Taub, M. Muenke, and F.S. Kaplan. 1996. Overexpression of an osteogenic morphogen in fibrodysplasia ossificans progressiva. *N Engl J Med.* **335**: 555-561.

82. McCulloch, C.A., M. Strugurescu, F. Hughes, A.H. Melcher, and J.E. Aubin. 1991. Osteogenic progenitor cells in rat bone marrow stromal populations exhibit self-renewal in culture. *Blood.* **77**: 1906-1911

83. Owen, M.E. Bone growth at the cellular level: A perspective. in Dixon AD: *Factors and Mechanisms Influencing Bone Growth,* 1982. Alan R. Liss, New York, USA.

84. Rodan, S.B., G. Wesolowski, K. Thomas, and G.A. Rodan. 1987. Growth stimulation of rat calvaria osteoblastic cells by acidic fibroblast growth factor. *Endocrinology* **121**: 1917-1923 .

85. Martin, I., A. Muraglia, G. Campanile, R. Cancedda, and R. Quarto. 1997. Fibroblast growth factor-2 supports ex vivo expansion and maintenance of osteogenic precursors from human bone marrow. *Endocrinology*. **138**: 4456-4462.

86. Nakamura, T., K. Hanada, M. Tamura, T. Shibanushi, H. Nigi, M. Tagawa, S. Fukumoto, and T. Matsumoto. 1995. Stimulation of endosteal bone formation by systemic injections of recombinant basic fibroblast growth factor in rats. *Endocrinology*. **136:** 1276-1284 .

87. Hock, J.M., E. Canalis, and M. Centrella. 1990. Transforming growth factor-beta stimulates bone matrix apposition and bone cell replication in cultured fetal rat calvariae. E*ndocrinology* . **126**: 421-426.

88. Noda, M., and J.J. Camilliere. 1989. In vivo stimulation of bone formation by transforming growth factor-beta. *Endocrinology*. **124**: 2991-2994 .

89. Du, P., Y. Ye, P.K. Seitz, P.K. Seitz, L.G. Bi, H. Li, C. Wang, D.J. Simmons, , and C.W. Cooper. 2000. Endogenous parathyroid hormone-related peptide enhances proliferation and inhibits differentiation in the osteoblast-like cell line ROS 17/2.8. *Bone.* **26**: 429-436.

90. Cornish, J., K. Callon, A. King, S. Edgar, and I.R. Reid. 1993. The effect of leukemia inhibitory factor on bone in vivo. *Endocrinology*.**132***:*1359-66.

91. Cornish, J., K.E. Callon, S.G. Edgar, and I.R. Reid, 1997. Leukemia inhibitory factor is mitogenic to osteoblasts. *Bone.* **21**: 243-247.

92. Lecanda, F., L.V. Avioli, and S.L. Cheng, 1997. Regulation of bone matrix protein expression and induction of differentiation of human osteoblasts and human bone marrow stromal cells by bone morphogenetic protein-2. *J Cell Biochem.* **67**: 386-396.

93. Maliakal, J.C., I. Asahina, P.V. Hauschka, and T.K. Sampath. 1994. Osteogenic protein-1 (BMP-7) inhibits cell proliferation and stimulates the expression of markers characteristic of osteoblast phenotype in rat osteosarcoma (17/2.8) cells. *Growth Factors.* **11**: 227-234.

94. Jee, W.S., and Y.F. Ma. 1997. The in vivo anabolic actions of prostaglandins in bone. *Bone* **21**: 297-304.

95. Weinreb, M., I. Suponitzky, and S. Keila. 1997. Systemic administration of an anabolic dose of PGE2 in young rats increases the osteogenic capacity of bone marrow. *Bone.* **20**:521-6.

96. Hock, J.M., M. Centrella, and E. Canalis. 1988. Insulin-like growth factor I has independent effects on bone matrix formation and cell replication. *Endocrinology.* **122**: 254-260.

97. Canalis, E., and B. Gabbitas. 1994. Bone morphogenetic protein 2 increases insulin-like growth factor I and II transcripts and polypeptide levels in bone cell cultures. *J Bone Miner Res* **9**: 1999-2005.

98. Keila, S., A. Kelner, and M. Weinreb. 2001. Systemic prostaglandin E2 increases cancellous bone formation and mass in aging rats and stimulates their bone marrow osteogenic capacity in vivo and in vitro. *J Endocrinol.* **168**: 131-139.

99. Delany, A.M., J.M. Pash, and E. Canalis, 1994. Cellular and clinical perspectives on skeletal insulin-like growth factor I. *J Cell Biochem* **55**: 328-333.

100. Sierra-Honigmann, M.R., A.K. Nath, C. Murakami, G. Garcia-Cardena, A. Papapetropoulos, W.C. Sessa, L.A. Madge, J.S. Schechner, M.B. Schwabb, P.J. Polverini, and J.R. Flores-Riveros. 1998. Biological action of leptin as an angiogenic factor. *Science*. **281**: 1683-1686.

101. Jia, D., and J.N. Heersche. 2000. Insulin-like growth factor-1 and -2 stimulate osteoprogenitor proliferation and differentiation and adipocyte formation in cell populations derived from adult rat bone. *Bone*. **27**: 785-794.

102. Knutsen, R., Y. Honda, D.D. Strong, T.K. Sampath, D.J. Baylink, and S. Mohan. 1995. Regulation of insulin-like growth factor system components by osteogenic protein-1 in human bone cells. *Endocrinology*. **136**: 857-865

103. Meunier, P., J. Aaron, C. Edouard, and G. Vignon. 1971. Osteoporosis and the replacement of cell populations of the marrow by adipose tissue. A quantitative study of 84 iliac bone biopsies. *Clin Orthop*. **80**:147-154.

104. Minaire, P., P. Meunier, C. Edouard, J. Bernard, P. Courpron, and J. Bourret. 1974. Quantitative histological data on disuse osteoporosis: comparison with biological data. *Calcif Tissue Res*. **17**:57-73.

105. Wang, G.J., D.E. S.I. Sweet, Reger, and R.C. Thompson. 1977 Fat-cell changes as a mechanism of avascular necrosis of the femoral head in cortisone-treated rabbits. *J Bone Joint Surg Am*. **59**:729-735

106. Ahrens, M., T. Ankenbauer, D. Schroder, A. Hollnagel, H. Mayer, and G. Gross. 1993. Expression of human bone morphogenetic proteins-2 or -4 in murine mesenchymal

progenitor C3H10T1/2 cells induces differentiation into distinct mesenchymal cell lineages. *DNA Cell Biol* **12**: 871-880.

107. Asahina, I., T.K. Sampath, P.V. and Hauschka. 1996. Human osteogenic protein-1 induces chondroblastic, osteoblastic, and/or adipocytic differentiation of clonal murine target cells. *Exp Cell Res*. **222**: 38-47.

108. Ji, X., D. Chen, C. Xu, S.E. Harris, G.R. Mundy, and T. Yoneda. 2000. Patterns of gene expression associated with BMP-2-induced osteoblast and adipocyte differentiation of mesenchymal progenitor cell 3T3-F442A. *J Bone Miner Metab*. **18**: 132-139.

109. Jaiswal, R.K., N. Jaiswal, S.P. Bruder, G. Mbalaviele, D.R. Marshak, and M.F. Pittenger. 2000. Adult human mesenchymal stem cell differentiation to the osteogenic or adipogenic lineage is regulated by mitogen-activated protein kinase. *J Biol Chem:* **275**: 9645-9652.

110. Duque G. 2001. Anabolic agents to treat osteoporosis in older people: is there still place for fluoride? Fluoride for treating postmenopausal osteoporosis. *J Am Geriatr Soc.* 49:1387-1389.

111. Quarles, L.D., D.A. Yohay, L.W. Lever, R. Caton, and R.J. Wenstrup. 1992. Distinct proliferative and differentiated stages of murine MC3T3-E1 cells in culture: an in vitro model of osteoblast development. *J Bone Miner Res*.**7**: 683-692.

112. Furushima, K., K. Shimo-Onoda, S. Maeda, T. Nobukuni, K. Ikari, H. Koga, S. Komiya, T. Nakajima, S. Harata, and I. Inoue. 2002. Large-scale screening for candidate genes of ossification of the posterior longitudinal ligament of the spine. *J Bone Miner Res*. **17**: 128-137.

113. Raouf, A. and A. Seth. 2002. Discovery of osteoblast-associated genes using cDNA microarrays. *Bone*. **30:** 463-471.

114. Ducy, P. and G. Karsenty. 1998. Genetic control of cell differentiation in the skeleton. *Curr Opin Cell Biol.* **10**: 614-619.

115. Lin, R., Y. Nagai, R. Sladek, Y. Bastien, J. Ho, K. Petrecca, G. Sotiropoulou, E.P. Diamandis, T.J. Hudson, and J.H. White. 2002. Expression profiling in squamous carcinoma cells reveals pleiotropic effects of vitamin D3 analog EB1089 signaling on cell proliferation, differentiation, and immune system regulation. *Mol Endocrinol.* 16, 1243-1256.

116. Mills, J.C., K.A. Roth, R.L. Cagan, and J.I. Gordon, 2001. DNA microarrays and beyond: completing the journey from tissue to cell. *Nat Cell Biol.* **3:** E175-178

117. Barta, P., J. Monti, P.G. Maass, K. Gorzelniak, D.N. Muller, R. Dechend, F.C. Luft, N. Hubner, and A.M. Sharma. 2002. A gene expression analysis in rat kidney following high and low salt intake. *J Hypertens.* **20**, 1115-1120.

118. Borah, B., G.J. Gross, T.E. Dufresne, T.S. Smith, M.D. Cockman, P.A. Chmielewski, M.W. Lundy, J.R. Hartke, and E.W. Sod. 2001. Three-dimensional microimaging (MRmicroI and microCT), finite element modeling, and rapid prototyping provide unique insights into bone architecture in osteoporosis. *Anat Rec.* **265,** 101-110.

119. El Abdaimi, K., N. Dion, V. Papavasiliou, P.E. Cardinal, L. Binderup, D. Goltzman, L.G. Ste-Marie, and R. Kremer. 2000. The vitamin D analogue EB 1089 prevents skeletal metastasis and prolongs survival time in nude mice transplanted with human breast cancer cells. *Cancer Res.* **60**: 4412-4418.

120. Duque, G., K.E. El-Abdaimi, M. Macoritto, M.M. Miller, and R. Kremer. 2002. Estrogens (E2) regulate expression and response of 1,25-dihydroxyvitamin D3 receptors in bone cells: changes with aging and hormone deprivation. *Biochem Biophys Res Commun.* **299**: 446-454.

121. Patrone, L., M.A. Damore, M.B. Lee, C.S. Malone, and R. Wall. 2002. Genes expressed during the IFN gamma-induced maturation of pre-B cells. *Mol Immunol.* **38**: 597-606.

122. Schindler, C., and S. Brutsaert. 1999. Interferons as a paradigm for cytokine signal transduction. *Cell Mol Life Sci.* **55**: 1509-1522.

123. Landolfo, S., M. Gariglio, G. Gribaudo, and D. Lembo. 1998. The Ifi 200 genes: an emerging family of IFN-inducible genes. *Biochimie.* **80**: 721-728.

124. Wang, J., M.J. Glimcher, J. Mah, H.Y. Zhou, and E. Salih. 1998. Expression of bone microsomal casein kinase II, bone sialoprotein, and osteopontin during the repair of calvarial defects. *Bone.* **22**: 621-628.

125. Lian, J.B., G.S. Stein, J.L. Stein, and A.J. van Wijnen. 1998. Osteocalcin gene promoter: unlocking the secrets for regulation of osteoblast growth and differentiation. *J Cell Biochem.* **Suppl.30-31**: 62-72.

126. Beck, G.R. Jr., E.C. Sullivan, E. Moran and B. Zerler. 1998. Relationship between alkaline phosphatase levels, osteopontin expression, and mineralization in differentiating MC3T3-E1 osteoblasts. *J Cell Biochem.* **68**, 269-280.

127. Guo, Z., J. Yang, X. Liu, X. Li, C. Hou, P.H. Tang, and N. Mao. 2001. Biological features of mesenchymal stem cells from human bone marrow. *Chin Med J (Engl).* **114**: 950-953.

128. Dormady, S.P., O. Bashayan, R. Dougherty, X.M. Zhang, and R.S. Basch. 2001. Immortalized multipotential mesenchymal cells and the hematopoietic microenvironment. *J Hematother Stem Cell Res.* **10**: 125-140.

129. Huang, S., W. Hendriks, A. Althage, S. Hemmi, H. Bluethmann, R. Kamijo, J. Vilcek, R.M. Zinkernagel, and M. Aguet. 1993. Immune response in mice that lack the interferon-gamma receptor. *Science.* **259**: 1742-1745.

130. Van den Broek, M.F., U. Muller, S. Huang, R.M. Zinkernagel, and M. Aguet. 1995. Immune defence in mice lacking type I and/or type II interferon receptors. *Immunol Rev.* **148**: 5-18.

131. Dawson, M.J., N.J. Elwood, R.W. Johnstone, and J.A. Trapani 1998. The IFN-inducible nucleoprotein IFI 16 is expressed in cells of the monocyte lineage, but is rapidly and markedly down-regulated in other myeloid precursor populations. *J Leukoc Biol.* **64**: 546-554.

132. Briggs, L.J., R.W. Johnstone, R.M. Elliot, C.Y. Xiao, M. Dawson, J.A. Trapani, and D.A. Jans. 2001. Novel properties of the protein kinase CK2-site-regulated nuclear-localization sequence of the interferon-induced nuclear factor IFI 16. *Biochem J.* **353**, 69-77.

133. Kohler, M., C. Speck, M. Christiansen, F.R. Bischoff, S. Prehn, H. Haller, D. Gorlich, and E. Hartmann. 1999. Evidence for distinct substrate specificities of importin alpha family members in nuclear protein import. *Mol Cell Biol.* **19:** 7782-7791.

134. Oreffo, R.O., S. Romberg, A.S. Virdi, C.J. Joyner, S. Berven, and J.T. Triffitt. 1999. Effects of interferon alpha on human osteoprogenitor cell growth and differentiation in vitro. *J Cell Biochem.* **74**: 372-385.

135. Takayanagi, H. S. Kim, K. Matsuo, H. Suzuki, T. Suzuki, K. Sato, T. Yokochi, H. Oda, K. Nakamura, N. Ida, E.F. Wagner, and T. Taniguchi. 2002. RANKL maintains bone homeostasis through c-Fos-dependent induction of interferon-beta. *Nature.* **416**:744-749.

136. Fox, S.W. and T.J. Chambers. 2000. Interferon-gamma directly inhibits TRANCE-induced osteoclastogenesis. *Biochem Biophys Res Commun.* **276**: 868-872.

137. Nii, A., D.A. Reynolds, H.A. Young, and J.M. Ward. 1997. Osteochondrodysplasia occurring in transgenic mice expressing interferon-gamma. *Vet Pathol.* **34**: 431-441.

138. Armour, K.E., K.J. Armour, M.E. Gallagher, A. Godecke, M.H. Helfrich, D.M. Reid, and S.H. Ralston. 2001. Defective bone formation and anabolic response to exogenous estrogen in mice with targeted disruption of endothelial nitric oxide synthase. *Endocrinology.* **142**, 760-766.

139. Aguirre, J., L. Buttery, M. O'Shaughnessy, F. Afzal, I. Fernandez de Marticorena, M. Hukkanen, P. Huang, I. MacIntyre, and J. Polak. 2001. Endothelial nitric oxide synthase gene-deficient mice demonstrate marked retardation in postnatal bone formation, reduced bone volume, and defects in osteoblast maturation and activity. *Am J Pathol.* **158:** 247-257.

140. Van't Hof, R.J. and S.H. Ralston. 2001. Nitric oxide and bone.*Immunology.***103**: 255-261.

141. Togari, A., M. Arai, M. Mogi, A. Kondo, and T. Nagatsu. 1998. Coexpression of GTP cyclohydrolase I and inducible nitric oxide synthase mRNAs in mouse osteoblastic cells activated by proinflammatory cytokines. *FEBS Lett.* **428**: 212-216.

142. Grewal, T.S., P.G. Genever, A.C. Brabbs, M. Birch, and T.M. Skerry. 2000. Best5: a novel interferon-inducible gene expressed during bone formation. *FASEB J.* **14**: 523-531.

143. Franceschi, R.T. and G. Xiao. 2003. Regulation of the osteoblast-specific transcription factor, Runx2: Responsiveness to multiple signal transduction pathways. *J Cell Biochem.* **88:** 446-454

144. Nishii, Y. 2003. Rationale for active vitamin D and analogs in the treatment of osteoporosis. *J Cell Biochem.* **88**:381-386.

145. Suda, T., Y. Ueno, K. Fujii, and T. Shinki. 2003. Vitamin D and bone. *J Cell Biochem.***88**: 259-266.

146. Lips, P. 2001. Vitamin D deficiency and secondary hyperparathyroidism in the elderly: consequences for bone loss and fractures and therapeutic implications. *Endocr Rev.* **22**:477-501.

147. Nishii, Y. 2002. Active vitamin D and its analogs as drugs for the treatment of osteoporosis: advantages and problems. *J Bone Miner Metab.* **20**:57-65.

148. Van Leeuwen, J.P., M. van Driel, G.J. van den Bemd, and H.A. Pols. 2001Vitamin D control of osteoblast function and bone extracellular matrix mineralization. *Crit Rev Eukaryot Gene Expr.* **11**:199-226.

149. Erben, R.G., S. Bromm, and M. Stangassinger. 1998. Short-term prophylaxis against estrogen depletion-induced bone loss with calcitriol does not provide long-term beneficial effects on cancellous bone mass or structure in ovariectomized rats. *Osteoporos Int.* **8**: 82-91.

150. Shibata, T., A. Shira-Ishi, T. Sato, T. Masaki, A. Masuda, A. Hishiya, N. Ishikura, S. Higashi, Y. Uchida, M.O. Saito, M. Ito, E. Ogata, K. Watanabe, and K. Ikeda. 2002. Vitamin D hormone inhibits osteoclastogenesis *in vivo* by decreasing the pool of osteoclast precursors in bone marrow. *J Bone Miner Res.* **17**:622-629.

151. Matsushita, M., T. Tsuboyama, R. Kasai, H. Okumura, T. Yamamuro, K. Higuchi, K. Higuchi, A. Kohno, T. Yonezu, and A. Utani. 1986. Age-related changes in bone mass in the senescence-accelerated mouse (SAM). SAM-R/3 and SAM-P/6 as new murine models for senile osteoporosis. *Am J Pathol.* **125**:276-283.

152. Takeda, T., M. Hosokawa, and K. Higuchi. 1997. Senescence-accelerated mouse (SAM): a novel murine model of senescence. *Exp Gerontol.* **32**:105-109.

153. Kajkenova, O., B. Lecka-Czernik, I. Gubrij, S.P. Hauser, K. Takahashi, A.M. Parfitt, R.L. Jilka, S.C. Manolagas, and D.A. Lipschitz. 1997. Increased adipogenesis and myelopoiesis in the bone marrow of SAMP6, a murine model of defective osteoblastogenesis and low turnover osteopenia. *J Bone Miner Res.* **12**:1772-1779.

154. Jilka, R.L., R.S. Weinstein, K. Takahashi, A.M. Parfitt, and S.C. Manolagas. 1996. Linkage of decreased bone mass with impaired osteoblastogenesis in a murine model of accelerated senescence. *J Clin Invest.* **97**:1732-1740.

155. Silva, M.J., M.D. Brodt, and S.L. Ettner. 2002. Long bones from the senescence accelerated mouse SAMP6 have increased size but reduced whole-bone strength and resistance to fracture. *J Bone Miner Res.* **17**:1597-1603.

156. Lecka-Czernik, B., E.J. Moerman, R.J. Shmookler-Reis, and D.A. Lipschitz. 1997. Cellular and molecular biomarkers indicate precocious *in vitro* senescence in fibroblasts from SAMP6 mice. Evidence supporting a murine model of premature senescence and osteopenia. *J Gerontol A Biol Sci Med Sci.* **52**:B331-6.

157. Soriano, B., P. Bean, J. Gaydos, and B. Tabakoff. 2002. Streamlining microarray technology in a prototype core laboratory. *Am Clin Lab.* **21**:22-25.

158. Vieth, R., Y. Ladak, and P.G. Walfish. 2003. Age-related changes in the 25-hydroxyvitamin D versus parathyroid hormone relationship suggest a different reason why older adults require more vitamin D. *J Clin Endocrinol Metab.* **88**:185-191.

159. Hauselmann, H.J., and R. Rizzoli. 2003. A comprehensive review of treatments for postmenopausal osteoporosis. *Osteoporos Int.* **14**:2-12.

160. Ho, L.T., and S.M. Sprague. 2002. Renal osteodystrophy in chronic renal failure. *Semin Nephrol.* **22**:488-493.

161. Erben, R.G., L. Mosekilde, J.S. Thomsen, K. Weber, K. Stahr, A. Leyshon, S.Y. Smith, and R. Phipps. 2002. Prevention of bone loss in ovariectomized rats by combined treatment with risedronate and 1alpha,25-dihydroxyvitamin D3. *J Bone Miner Res.* **17**:1498-1511.

162. Erben, R.G., S. Bromm, and M. Stangassinger. 1998. Therapeutic efficacy of 1alpha,25-dihydroxyvitamin D3 and calcium in osteopenic ovariectomized rats: evidence for a direct anabolic effect of 1alpha,25-dihydroxyvitamin D3 on bone. *Endocrinology.* **139**:4319-2438.

163. Kelly, K.A., and J.M. Gimble. 1998. 1,25-Dihydroxy vitamin D3 inhibits adipocyte differentiation and gene expression in murine bone marrow stromal cell clones and primary cultures. *Endocrinology.* **139**:2622-2628.

164. Kawase, M., M. Tsuda, and T. Matsuo. 1989. Accelerated bone resorption in senescence-accelerated mouse (SAM-P/6). *J Bone Miner Res.* **4**: 359-364.

165. Kodama, Y., Y. Takeuchi, M. Suzawa, S. Fukumoto, H. Murayama, H. Yamato, T. Fujita, T. Kurokawa, and T. Matsumoto. 1998. Reduced expression of interleukin-11 in bone marrow stromal cells of senescence-accelerated mice (SAMP6): relationship to osteopenia with enhanced adipogenesis. *J Bone Miner Res.* **13**:1370-1377.

166. Takahashi, K., T. Tsuboyama, M. Matsushita, R. Kasai, H. Okumura, T. Yamamuro, Y. Okamoto, K. Kitagawa, and T. Takeda. 1994. Effective intervention of low peak bone mass and bone modeling in the spontaneous murine model of senile osteoporosis, SAM-P/6, by Ca supplement and hormone treatment. *Bone.* **15**:209-215.

167. Takeda, N., T. Tsuboyama, R. Kasai, K. Takahashi, M. Shimizu, T. Nakamura, K. Higuchi, and M. Hosokawa. 1999. Expression of the c-fos gene induced by parathyroid hormone in the bones of SAMP6 mice, a murine model for senile osteoporosis. *Mech Ageing Dev.* **108**:87-97.

168. Wang, X., J. Wu, Y. Shidoji, Y. Muto, N. Ohishi, K. Yagi, S. Ikegami, T. Shinki, N. Udagawa, T. Suda, and Y. Ishimi. 2002. Effects of geranylgeranoic acid in bone: induction of osteoblast differentiation and inhibition of osteoclast formation. *J Bone Miner Res.* **17**:91-100.

169. Ichioka, N., M. Inaba, T. Kushida, T. Esumi, K. Takahara, K. Inaba, R. Ogawa, H. Iida, and S. Ikehara. 2002. Prevention of senile osteoporosis in SAMP6 mice by intrabone marrow injection of allogeneic bone marrow cells. *Stem Cells.* **20**:542-551.

170. Farach-Carson, M.C., and Y. Xu. 2002. Microarray detection of gene expression changes induced by 1,25(OH)(2)D(3) and a Ca(2+) influx-activating analog in osteoblastic ROS 17/2.8 cells. *Steroids.* **67**:467-470.

171. Norman, A.W., W.H. Okamura, J.E. Bishop, and H.L. Henry. 2002. Update on biological actions of 1alpha,25(OH)(2)-vitamin D(3) (rapid effects) and 24R,25(OH)(2)-vitamin D(3). *Mol Cell Endocrinol.* **197**:1-13.

172. Bortman, P., M.A.A.K. Folgueira, M.L.H. Katayama, I.M.L. Snitcovsky, and M.M. Brentani. 2002. Antiproliferative effects of 1,25-dihidroxyvitamin D3 on breast cells-A mini review. *Braz J Med Biol Res.* **35**: 1-9.

173. Haussler, M.R., and A.W. Norman. 1969. Chromosomal receptor for a vitamin D metabolite. *Proc Natl Acad Sci USA.* **62**:155-162.

174. Bouillon, R., W.H. Okamura, and A.W. Norman. 1995. Structure-function relationships in the vitamin D endocrine system. *Endocr. Rev.* **16**.200-257.

175. Rachez, C., M. Gamble, C.P. Chang, G.B. Atkins, M.A. Lazar, and P.L. Freedman. 2000. The DRIP complex and SRC-1/p160 coactivators share similar nuclear receptor binding determinants but constitute functionally distinct complexes. *Mol. Cell. Biol.* **20:** 2718-2726.

176. Nemere, I., Y. Yoshimoto, and A.W. Norman. 1984. Studies on the mode of action of calciferol. LIV. Calcium transport in perfused duodena from normal chicks: Enhancement with 14 minutes of exposure to 1α25-dihydroxivitamin D_3. *Endocrinology.* **115**: 1476-1483.

177. Norman, A. 1998. Receptors for $1\alpha,25(OH)_2D_3$: past, present and future. *J Bone Miner Res.* **13**: 1360-1369.

178. Hansen, C.M., D. Hansen, P.K. Holm, and L. Binderup. 2001. Vitamin D compounds exert anti-apoptotic effects in human osteosarcoma cells in vitro. *J Steroid Biochem Mol Biol.* **77:** 1-11.

179. Kowarski, S., and D. Schachter. 1969. Effects of vitamin D on phosphate transport and incorporation into mucosal constituents of rat intestinal mucosa. *J. Biol. Chem.* **244**:211-217.

180. Ireland P., and J.S. Fordtran. 1973. Effect of dietary calcium and age on jejunal calcium absorption in humans studied by intestinal perfusion. *J. Clin. Invest.* **52**:2672-2681.

181. Bender A.D. 1968. Effect of age on intestinal absorption: implications for drug absorption in the elderly. *J Am Geriatr Soc.* **16**:1331-1339.

182. Armbrecht, H.J., T.V. Zenser, and B.B. Davis. 1980. Effect of age on the conversion of 25-hydroxyvitamin D3 to 1,25-dihydroxyvitamin D3 by kidney of rat. *J. Clin. Invest.* **66**:1118-1123.

183. Armbrecht, H.J., T.V. Zenser, and B.B. Davis. 1980. Effect of vitamin D metabolites on intestinal calcium absorption and calcium binding protein in young and adult rats. *Endocrinology* **106**: 469-475.

184. Horst R.L., J.P. Goff, and T.A. Reinhardt, 1990. Advancing age results in reduction of intestinal and bone 1,25-dihydroxyvitamin D receptor. *Endocrinology.* **126**:1053-1057.

185. Compston, J.E. 2001. Sex steroids and bone. *Physiol. Rev.* **81**: 420-437.

186. Schwartz, B., P. Smirnoff, S. Shany, and Y. Liel, 2000. Estrogen controls expression and bioresponse of 1,25-dihydroxyvitamin D receptors in the rat colon. *Mol and Cell Biochemistry* **203**: 87-93.

187. Gennari, C., D. Agnusdei, P. Nardi, and R. Civitelli, 1990. Estrogen preserves a normal intestine responsiveness to 1,25-dihydroxivitamin D in oophorectomized women. *J. Clin. Endocrinol. Metab.* **71**: 1288-1293.

188. Walters, M.R. 1981. An estrogen-stimulated 1,25-dihydroxyvitamin D3 receptor in rat uterus. *Biochem. Byophys. Res. Commun.* **103**:721-726.

189. Liel, Y., P. Shany, P. Smirnoff, and B. Schwartz. 1999. Estrogen increases 1,25-dihydroxyvitamin D receptors expression and bioresponse in the rat duodenal mucosa, *Endocrinology*. **140**: 280-285.

190. Duncan, W.E., A.R. Glass, and H.L. Wray. 1991. Estrogen regulation of the nuclear 1,25-dihydroxyvitamin D3 receptor in rat liver and kidney. *Endocrinology*. **129**: 2318-2324.

191. Chen T.L., C.M. Cone, and D. Feldman. 1983. Effects of 1 alpha,25-dihydroxyvitamin D3 and glucocorticoids on the growth of rat and mouse osteoblast-like bone cells. *Calcif Tissue Int.* **35:** 806-811.

192. Liel, Y., S. Kraus, J. Levy, and S. Shany. 1992. Evidence that estrogens modulate activity and increase the number of 1,25-dihydroxyvitamin D receptors in osteoblast-like cells (ROS 17/2.8). *Endocrinology.* **130**:2597-2601.

193. Jesionowska, H., K. Karelus, and J.F. Nelson. 1990. Effects of chronic exposure to estradiol on ovarian cyclicity in C57BL/6J mice: Potentiation at low doses and only partial suppression at high doses. *Biol. Reprod.* **43**:312-317.

194. Haloran B.P., V.L. Ferguson, S.J. Simske, A. Burghardt, L.L. Venton, and S. Majumdar, 2002. Changes in bone structure and mass with advancing age in the male C57BL/6J mouse. *J. Bone Miner. Res.* **17:** 1044-1050.

195. Joshi, D., R.B. Billiar, and M.M. Miller. 1993. Modulation of hypothalamic Mu-opioid receptor density by estrogen: A quantitative auto radiographic study of the female C57BL/6J mouse. *Brain Res Bull* **30**:629-634.

196. Mori, S., T. Sawai, T. Teshima, and M. Kyogoku. 1988. A new decalcifying technique for immunohistochemical studies of calcified tissue, especially applicable to cell surface marker demonstration, *J. Histochem. Ctytochem.***36**: 111-114.

197. Oyajobi, B.O., A. Lomri, M. Hott, and P.J. Marie. 1999. Isolation and Characterization of human clonogenic osteoblast progenitors immunoselected from fetal bone marrow stroma using STRO-1 monoclonal antibody. *J Bone Miner Res.* **14**:351-361.

198. Mosmann T. 1983. Rapid colorimetric assay for cellular growth and survival: application to proliferation and cytotoxicity assays. *J. Immunol. Methods.* **65**:55-63.

199. Kinuta, K., H. Tanaka, T. Moriwake, K. Aya, S. Kato, and Y. Seino. 2000. Vitamin D is an important factor in estrogen biosynthesis of both female and male gonads. *Endocrinology.* **141**:1317-1324.

200. Martinez P., I. Moreno, De F. Miguel, V. Vila, P. Esbrit, and M.E. Martinez. 2001. Changes in osteocalcin response to 1,25-Dihydroxyvitamin D3 stimulation and basal vitamin D receptor expression in human osteoblastic cells according to donor age and skeletal origin. *Bone.* **29**: 35-41.

201. Lieberherr, M. 1987. Effects of vitamin D3 metabolites on cytosolic free calcium in confluent mouse osteoblasts. *J. Biol. Chem.* **262**:13168-13173.

202. Bodine, P., R.A. Henderson, J. Green, M. Aronow, T. Owen, G. Stein, J. Lian, and B. Komn. 1998. Estrogen receptor alpha is developmentally regulated during osteoblast differentiation and contributes to selective responsiveness of gene expression. *Endocrinology.* **139.** 2048-2057.

203. Cooper, L.F., J.C. Tiffee, J.P. Griffin, H. Hamano, and Z.Guo. 2000. Estrogen-induced resistance to osteoblast apoptosis is associated with increased hsp27 expression. *J Cell Physiol.* **185**: 401-407.

204. Willson, T.M., J.D. Norris, B.L. Wagner, P.B. Asplin, H.R. Brown, S.A. Jones, H. Henke, S. Sauls, S. Wolfe, D.C. Morris, and D.P. Mcdonell. 1997. Dissection of the molecular mechanism of action of GW5638, a novel estrogen receptor ligand, provides insights into the role of estrogen receptor in bone. *Endocrinology.* **138:** 3901-3911.

205. Miyamoto, K., R.A. Kesterson, H. Yamamoto, Y. Taketani, E. Nishiwaki, S. Tatsumi, Y. Inoue, K. Morita, E. Takeda, and W. Pike. 1997. Structural organization of the human vitamin D receptor chromosomal gene and its promoter. *Mol. Endocrinol.* **11**:1165-1179.

206. Byrne, I.M., L. Flanagan, M.P.R. Tenniswood, and J. Welsh. 2000. Identification of a hormone-responsive promoter immediately upstream of exon 1c in the human vitamin D receptor gene. *Endocrinology.* 141:2829-2836.

207. Manolagas, S.C., and R.L. Jilka. 1995. Mechanisms of disease: Bone marrow, cytokines, and bone remodeling-emerging insights into the pathophysiology of osteoporosis. *N Engl J Med.* **332**: 305-311.

208. Polunovsky, V.A., B. Chen, C. Henke, D. Snover, C. Wendt, D.H. Ingbar, and P.B. Bitterman. 1993. Role of mesenchymal cell death in lung remodeling after injury. *J Clin Invest.* **92**: 388-397.

209. Kitajima, I., Y. Soejima, I. Takasaki, H. Beppu, T. Tokioka, and I. Maruyama. 1996. Ceramide-induced nuclear translocation of NF-kappa B is a potential mediator of the apoptotic response to TNF-alpha in murine clonal osteoblasts. *Bone.* **19**: 263-270 .

210. Hughes, D.E., K.R. Wright, H.L. Uy, A. Sasaki, T. Yoneda, G.D. Roodman, G.R. Mundy, and B.F. Boyce. 1995. Bisphosphonates promote apoptosis in murine osteoclasts in vitro and in vivo. *J Bone Miner Res* **10**: 1478-1487.

211. Hughes, D.E., and B.F. Boyce. 1997. Apoptosis in bone physiology and disease. *Mol Pathol.* **50**: 132-137.

212. Tsuboi, M., A. Kawakami, T. Nakashima, N. Matsuoka, S. Urayama, Y. Kawabe, K. Fujiyama, T. Kiriyama, T. Aoyagi, K. Maeda, and K. Eguchi. 1999. Tumor necrosis factor α and interleukin-1β increase the Fas-mediated apoptosis in human osteoblasts. *J Lab Clin Med* **134**: 222-231.

213. Hill, P.A., A. Tumber, and M.C. Meikle. 1997. Multiple extracellular signals promote osteoblast survival and apoptosis. *Endocrinology* .**138**: 3849-3858.

214. Chao, W., Shen, Y., Li, L., and Rosenzweig, A. (2002) *J Biol Chem.* **277**,31639-31645.

215. Kischkel, F.C., S. Hellbardt, I.. Behrmann, M. Germer, M. Pawlita, P.H. Krammer, and M.E. Peter. 1995. Cytotoxicity-dependent APO-1 (Fas/CD95)-associated proteins form a death-inducing signalling complex (DISC) with the receptor. *Embo J.* **14**: 5579-5588.

216. Bang, S., E.J. Jeong, I.K. Kim, Y.K. Jung, and K.S. Kim. 2000. Fas- and tumor necrosis factor-mediated apoptosis uses the same binding surface of FADD to trigger signal transduction. *J Biol Chem.* **275**: 36217-36222.

217. Norman, A.W., J.A. Putkey, and I. Nemere. 1982. Intestinal calcium transport: Pleiotropic effects mediated by vitamin D. *Fed Proc.* **41**: 78-83.

218. Ozono, K., T. Sone, and J.W. Pike. 1991. Perspectives: The genomic mechanism of action of 1,25-dihydroxyvitamin D_3. *J Bone Miner Res.* **6**: 1021-1027.

Urayama, S., Kawakami, A., Nakashima, T., Tsuboi, M., Yamasaki, S., Hida, A., Ichinose, Y., Nakamura, H., Ejima, E., Aoyagi, T., Nakamura, T., Migita, K., Kawabe, Y., and Eguchi, K. (2000) *J Lab Clin Med.* **136**, 181-193.

219. Clements, M.R., M. Davies, M.E. Hayes, C.D. Hickey, G.A. Lumb, E.B. Mawer, and P.H. Adams. 1992. The role of 1,25 dihydroxyvitamin D in the mechanism of acquired vitamin D deficiency. *Clin Endocrinol (Oxf)* **37**: 17-27

220. Burgess, T.L., Y. Qian, S. Kaufman, B.D. Ring, G. Van, C. Capparelli, M. Kelley, H. Hsu, W.J. Boyle, C.R. Dunstan, S. Hu, and D.L. Lacey. 1999. The ligand for osteoprotegerin (OPGL) directly activates mature osteoclasts. *J Cell Biol.* **145**: 527-538.

221. O'Brien, C.A., I. Gubrij, S.C. Lin, R.L. Saylors, and S.C. Manolagas. 1999. Identification of an OSF-2 binding site in the murine RANKL/OPGL gene promoter: A

potential link between osteoblastogenesis and osteoclastogenesis. *J Biol Chem.* **274**: 19301-19308.

222. Manolagas, S.C., and R.S. Weinstein. 1999. New developments in the pathogenesis and treatment of steroid-induced osteoporosis. *J Bone Miner Res.* **14**: 1061-1066.

223. de Pollak, C., E. Arnaud, D. Renier, and P.J. Marie. 1997. Age-related changes in bone formation, osteoblastic cell proliferation and differentiation during postnatal osteogenesis in human calvaria. *J Cell Biochem.* **64**: 128-139.

224. Goldstein, J.L., and M.S. Brown. 1990. Regulation of mevalonate pathway. *Nature.* **343**: 425-430.

225. Luckman, S.P., D.E. Hughes, F.P Coxon, R. Graham, G. Russell, and M.J. Rogers. 1998. Nitrogen-containing bisphosphonates inhibit the mevalonate pathway and prevent post-translational prenylation of GTP-binding proteins, including Ras. *J Bone Miner Res.* **13**: 581-589.

226. Urayama, S., Kawakami, A., Nakashima, T., Tsuboi, M., Yamasaki, S., Hida, A., Ichinose, Y., Nakamura, H., Ejima, E., Aoyagi, T., Nakamura, T., Migita, K., Kawabe, Y., and Eguchi, K. (2000) *J Lab Clin Med.* **136**, 181-193.

227. Schilli, M.B., R. Paus, and A. Menrad. 1998. Reduction of intrafollicular apoptosis in chemotherapy-induced alopecia by topical calcitriol-analogs. *J Invest Dermatol.* **111**: 598-604.

228. Niikura, Y., T. Nonaka, and S. Imajoh-Ohmi. 2002. Monitoring of caspase-8/FLICE processing and activation upon Fas stimulation with novel antibodies directed against a cleavage site for caspase-8 and its substrate, FLICE-like inhibitory protein (FLIP). *J Biochem (Tokyo).* **132**:53-62.

229. Smulson, M.E., Simbulan-Rosenthal, C.M., Boulares, A.H., Yakovlev, A., Stoica, B., Iyer, S., Luo, R., Haddad, B., Wang, Z.Q., Pang, T., Jung, M., Dritschilo, A., and Rosenthal, D.S. (2000) *Adv Enzyme Regul.* **40**, 183-215.

230. Xu, S.Q., and El-Deiry, W.S. (2000) *Biochem Biophys Res Commun.* **269**, 179-190.

231. Suzuki, A., Tsutomi, Y., Akahane, K., Araki, T., and Miura, M. (1998) *Oncogene.* **17**, 931-939.

232. Nuti, R., E. Bonucci, D. Brancaccio, J.C. Gallagher, C. Gennari, G. Mazzuoli, M. Passeri, and P. Sambrook. 2000. The role of calcitriol in the treatment of osteoporosis. *Calcif Tissue Int* **66**: 239-240.

233. Bellido, T., C.A. O'Brien, P.K. Roberson, and S.C. Manolagas. 1998. Transcriptional activation of the p21(WAF1,CIP1,SDI1) gene by interleukin-6 type cytokines. A prerequisite for their pro-differentiating and anti-apoptotic effects on human osteoblastic cells. *J Biol Chem.* **273**:21137-21144.

ORIGINAL CONTRIBUTIONS

The following findings reported in this thesis constitute original scientific contributions:

1- The finding of the gene changes that occur in a human model or osteogenic differentiation of mesenchymal stem cells *in vitro*.

2- The finding of a new role for the interferon γ and IFNGRG as regulators of early osteoblastogenesis.

3- The demonstration that mice lacking Interferon γ activity are osteoporotic.

4- The demonstration that Interferon γ regulates the expression of Cbfa1

5- The demonstration of Interferon γ as a new bone forming agent.

6- The finding that adipogenesis in bone marrow of SAM-P/6 mice can be reverted by $1,25(OH)_2D_3$.

7- The demonstration of $1,25(OH)_2D_3$ as a new bone forming agent.

8- The demonstration that VDR expression and bio-response decreases during aging in osteoblasts *in vivo*.

9- The finding that E_2 can revert the decreasing levels of VDR in aging osteoblasts *in vivo*.

10- The finding that Fas-FasL is the predominant apoptotic pathway in human osteoblasts *in vitro*.

11- The demonstration that $1,25(OH)_2D_3$ has an anti-apoptotic effect on human osteoblasts *in vitro*.

12- The demonstration that the cleavage of caspase-8 and induction of Fas resistance are the key mechanisms to inhibit apoptosis in osteoblasts.

APPENDIX 1: ANIMAL USE PROTOCOL AND REPORT FROM THE ANIMAL CARE COMMITTEE FOR THE USE OF SAM-P/6 MICE

McGill University
Animal Use Protocol

FOR OFFICE USE ONLY

Project #	4719
Investigator #	782
Approval End Date	Oct. 31, 2002
Facility Committee	RVH

☐ New Application

☒ Renewal of Project # 4219

1. Investigator Information

Principal Investigator: Dr. Richard Kremer — Telephone: (514) 843-1632

Department: Calcium Research Laboratory, Room H4.67 — Fax: (514) 843-1712

Address: RVH, 687 Pine Avenue West, Montreal, Quebec H3A 1A1

E-mail: gduque@rvhmed.lan.mcgill.ca

Animal Use: Research ☒ Teaching ☐ Specify Course number:

Project Title: Changes in bone mass and apoptotic markers in the senescense accelerated mouse (SAM) treated with modulators of bone turnover.

2. Funding Source

External ☒ Internal ☒ FRSQ

Source(s): Helen McCall Hutchinson Research Award, ~~RVH Research Institute and Leo Foundation (Denmark)~~

Peer Reviewed source: Yes ☒ No ☐ *If no, see instructions - section 2

Awarded ☒ Pending ☐

Funding Period: From: 1999 To: 2002

Proposed Start Date of Research: (Day/Month/Year) 01/01/01

Expected Date of Completion: (Day/Month/Year) 31/01/2002

ACTION	✓	DATE
P.I.	✓	Nov. 5 '01
FACC	✓	"
RGO	✓	"
VET	✓	"
DB	✓	"
Completed		

3. Emergency: Person(s) designated to handle emergencies (2 emergency telephone numbers must be indicated)

Name: Gustave Duque — Phone #: Work: (514) 843-1632 — Alternative #: (514) 720-7473

Name: Vasilios (Bill) Papavasiliou — Phone #: Work: (514) 843-1632 — Alternative #: (514) 699-1564

Certification:

The information in this application is exact and complete. I agree to follow the policies and procedures set forth by the Facility Animal Care Committees and McGill University, as well as those described in the "Guide to the Care and Use of Experimental Animals" prepared by the Canadian Council on Animal Care. I shall request the Animal Care Committee's approval prior to any deviations from the procedures described within.

Principal Investigator/Course Director		Date	January 29, 2001

Approval:

Chairperson, Facility Animal Care Committee		Date	May 18, 2001
University Animal Care Officer		Date	5/22/01
Approved period for animal use	Beginning: Nov. 1, 2001	Ending	Oct. 31, 2002

NOTE REVIEWER'S MODIFICATION(S) ON PAGE 2

Jun 14 01

MAY 25 2001

Revised 02/97

Expiration date: Jan. 31, 2001

4. Research Personnel and Qualifications (See Instructions - Section 4)

Give the names of all individuals who will work with animals in this study (including the Principal Investigator) and their employment classification (investigator, technician/research assistant, under graduate or graduate student, fellow or student supervisor). The Principal Investigator certifies that all personnel listed in this section will be provided with the specific training and/or experience which qualifies them to perform the procedures described in the protocol. Each person listed in this section must initial to indicate s/he have read this Application.

NAME	CLASSIFICATION	INITIAL
Richard Kremer	Investigator	
Gustavo Duque	Research Fellow	
Bill Papavasiliou	Technician	

5. Reviewer's Modification(s): The following modification(s) have been made to this Application during the review process. Please make these changes to your original documentation. You must comply with the recommended changes as a condition of approval for this Application.

6. Summary (See Instructions - Section 6)

BACKGROUND INFORMATION: (Include here the potential benefit to human or animal health or to the advancement of scientific knowledge) - LAY TERMINOLOGY

In this project we will determine the potential benefit of modulators of bone turnover (vitamin D and bisphosphonates) in the treatment of involutive osteopenia and osteoporosis.

GLOBAL AIM OF THE STUDY: (Include here the principal direction of the study) - LAY TERMINOLOGY

To determine if vitamin D and bisphosphonates improve the survival and the activity of osteoblasts, thus stimulating bone formation.

SPECIFIC OBJECTIVE(S) OF THE STUDY: (Distinct from procedures) - LAY TERMINOLOGY

1) To determine if vitamin D and bisphosphonates can prevent programmed cell death in osteoblasts.

2) To determine the mechanism of action of vitamin D and bisphosphonates on osteoblast survival.

3) To identify genes involved in the prevention of osteoblast cell death.

4) To analyse these genes using knockout or transgenic technology.

SUMMARY OF PROCEDURES REQUIRED FOR CCAC ANIMAL USE DATA FORM: (Please give a descriptive summary (40 words or less) that indicates inlay terms the procedures used) - LAY TERMINOLOGY

Senescense Accelerated Mice SAMP/6 will be grown under conventional conditions. Bone densitometry will be performed at ages 3 and 10 months. At 3 months the mice will be treated with vitamin D, alendronate or placebo. At 10 months the mice will be sacrificed by decapitation.

7.a) Animal Subject Description:

Animal Species	Strain	Age	Sex	Weight	# needed at one time	Total per year	#/cage
Senescense Accelerated Mice	SAMP/6	2-10 months	M & F	25-30g	45	180	2
Senescense Accelerated Mice	SAMP/1	2-10 months	M & F	25-30g	30	120	2

Animals used for genetic alterations:

Category	Total per year
Oocyte donors	
Pseudo-pregnent females	
Stud males	
Other (specify):	
Other (specify):	

Phenotype: After a period of normal development, these mice reveal a characteristic feature of aging, early onset and irreversible advance of senescense manifested by a loss of normal behavior, various skin lesions, hair loss and lordokyphosis. Their mean life span is 12.7 months.

Please justify the number of animals to be used: (See instructions - section 7)

1) SAMP/6 (Senescense accelerated in bone): 15 control animlas, 15 animals treated with vitamin D and 15 animals treated with alendronate per experiment to have sufficient power. 4 experiments are planned; thus 180 animals are required.

2) SAMP/1 (Senescense accelerated non-bone affected): Used as control group. 60 animals are required. 15 animals willbe required as a control for each experiment.

Please justify the need for live animals versus alternate methods, (e.g. tissue culture):

SAMP/6 is the closest model for human bone aging to be used. There is not any in vitro model of aging in bone.

Describe the characteristics of the animal species selected that justify its use in the proposed study, (consider such characteristics as body size, species, strain, breed, data from previous studies or unique anatomic or physiologic features).

SAMP/6 mice is the optimal model for involutive osteopenia or osteoporosis type II, where the rate of osteoblast cell death is increrased and therefore there is a deficit in bone formation. This type of mice age earlier than normal mice (10 months) and their bones show early osteoporotic changes affecting osteoblasts independently of the hormonal status of the animal.

Purpose of Animal Use (See Instructions - Section 7) 1 [X] 2 [ ] 3 [ ] 4 [ ] 5 [ ]

7.b) Animal Husbandry & Care

Special cages No [X] Yes [ ] Specify

Special diet No [ ] Yes [X] Specify CE-2, Nihon CLEA, containing calcium 1.01% and phosphorus 0.85%.

Special handling No [X] Yes [X] Specify

Is there any component to the proposed procedures which will result in immunosuppression or decreased immune function, (e.g. stress, radiation, steroids, chemotherapeutics)?

No [X] Yes [ ] Specify

Multiply Facility Housing? Yes [ ] No [X]

Indicate all facilities where animals will be housed: H3 Animal Room - RVH

State area(s) where procedures will be conducted on live animals: Building: Royal Victoria Hospital Room # H3 Animal Room

If animal housing location and animal use procedure location are in different buildings, briefly describe procedures for transporting animals:

Animals will be transported to bone densitometry by groups of 10 in their cages. Bone densitometry will be performed at the RVH, Department of Radiology.

8. Proposed Procedures with Animals: Provide description of surgical procedures, Immunizations, behavioural tests, immobilization, food/water deprivation, requirements for post operative care, sample collection, substance administration, etc.

A) SAMP6/SAMP1 Mice

(1) One male per 2 females will be placed in a cage for breeding until the expected population is reached. A total of 2 males and 4 females for breeding purposes.

(2) Maintained under conventional conditions.

(3) At 3 months, bone densitometry will be performed on a QDR-2000 plus densitometer (Hologic, Walthman). Before scanned, animals will be sedated (intramuscularly) with Ketamine (60-100mg/kg), Xylazine (4-8mg/kg) and Acepromazine-NaCl (15mg/kg) IM. Scans will be done with the animals positioned prone.

(4) Subcutaneous implantation of an Alzet osmotic minipump (model 2004, Alza Corporation, Palo Alto, CA) under anesthesia. The pump contains either $1,25(OH)_2D_3$ or Alendronate or vehicle alone delivered at a continuous dose for up to 4 weeks. In cases of difficult pump location or infection, an intra-peritoneal catheter will be used. The pump willbe removed at the end of the experiment under anaesthesia (xylazine & ketamine) and skin closed by stitches.

(5) Blood is taken from the saphenous vein. We take a total of 150μl of blood at monthly intervals.

B) Monitoring and sacrifice

(1) The animals will be monitored every 2 months. Weight, blood samples will be collected for measurement of serum calcium levles and biochemical markers of osteoblast activity (osteocalcin, procollagen).

(2) One group of animals will be sacrificed after 4 months and a second group of animals will be sacrificed after 10 months.

(3) At 10 months the mice in the study will be sacrificed by decapitation with anesthesia and blood samples and bones collected.

Name the drug(s) proposed for anaesthesia, analgesia or tranquilization, indicate the dosage in ml/kg body weight and route of administration:

Ketamine (60-100 mg/kg), Xylazine (4-8 mg/kg) and Acepromazine-NaCl (15 mg/kg)IM.

Specify person(s) who will be responsible for animal monitoring, including post operative care: Bill Papavasiliou Phone# 843-1632
Gustavo Duque 843-1632

9. Pain and Discomfort: Categorize pain and discomfort level in accordance with the CCAC guidelines which accompany this application.

B [ ] C [ ] D [X] E [ ]

10. Danger and Hazard to Staff and to Animal Population:

Attach a copy of Biohazard and/or Radiation Safety permits if appropriate.

Indicate which, if any, of the following will be used in the animals. N/A

Radioisotopes [ ] Carcinogens [ ] Infectious agents [ ] Transplantable tumors [X]

Amount involved per animal experiment: N/A

Route of administration Oral [ ] Injection [ ] Other [ ] (specify) _____

Frequency of administration _____

Number of animals involved _____

Survival time after administration _____

After administration, animals will be housed in: [ ] the animal care facility

[ ] the laboratory under supervision of laboratory personnel

The cages will be labeled with biohazard or radiation labels Yes ☐ No ☐

Describe measures that will be used to reduce risk to the environment and animal facility personnel:

11. Method of Euthanasia:

SPECIES (specify)						
	anaesthetic overdose, agent		route			
Mice	exsanguination with anaesthesia, agent					
	cervical dislocation					
	decapitation: with anaesthesia	X	specify	Ketamine / Xylazine	without anaesthesia	☐
	CO_2 chamber					
	other (specify)					
	not applicable (explain)					

BIOHAZARDS CONTAINMENT CERTIFICATION REPORT OF BIOHAZARDS COMMITTEE

Required for all Applications Proposing Research Involving Biohazards

Funds from the Medical Research Council of Canada may not be used for research involving recombinant DNA molecules or animal viruses and cells unless the proposed research has been found acceptable by a Biohazards Committee appointed and operating in accord with the Health and Welfare Canada and MRC Laboratory Biosafety Guidelines (1990), and the research involving biohazards will be carried out under the required level of containment facilities.

ATTESTATION DE CONFINEMENT DES RISQUES BIOLOGIQUES RAPPORT DU COMITÉ SUR LES BIORISQUES

Obligatoire pour toutes les demandes concernant des recherches comportant des risques biologiques

Les fonds que le Conseil de recherches médicales du Canada a accordés ne pourront servir à des recherches impliquant la manipulation de molécules d'ADN produites par recombinaison et des cellules et virus animaux à moins qu'un Comité sur les biorisques établi et dirigé conformément aux Lignes directrices (1990) de Santé et Bien-être social Canada et du CRM en matière de biosécurité en laboratoire n'ait convenu que la recherche proposée répond à ces normes et que la recherche comportant des risquesbiologiques respectera le niveau requis de confinement physiques.

STATEMENT FROM THE INSTITUTION* IN WHICH THE RESEARCH WILL BE PERFORMED

The Biohazards Committee established by

McGill University

has examined the application for research funds entitled:

Changes in bone mass and apoptotic markers in the senescense accelerated mouse (SAM) treated with modulators of bone turnover.

submitted by

Richard Kremer, MD, PhD

DÉCLARATION DE L'ÉTABLISSEMENT* OÙ SE DÉROULERA LA RECHERCHE

Le Comité sur les risques biologiques établi par

a étudié la demande de financement de la recherche intitulée.

Helen McCall Hutchison
RVH Research Institute

MRC Grant Number
No de subvention du CF

présentée par

and certifies that the proposed research will be carried out under containment conditions meeting level 2 in accord with the MRC's Guidelines.

et a convenu que la recherche proposée respectera le niveau de confinement conformément aux directives du CRM.

Date: January 31, 2001

Signatures:

Dana Baran

(Signature)

Dr. Dana Baran, Chairperson
RVH Biohazards Committee

(Print name of Institution's* representative for Research Involving Biohazards /
Nom en lettres moulées du délégué de l'établissement* en matière de recherche comportant des risques biologiques)

Applicant(s) / Candidat(s)

Date

*Institution includes universities, hospitals, research institutes of companies

*Par établissement, on entend les universités, les hôpitaux, les instituts de recherche ou les compagnies

APPENDIX 2: REPORT FROM THE ANIMAL CARE COMMITTEE FOR THE USE OF C57BL6/J MICE

c level

McGill University
Animal Use Protocol – Research

Guidelines for completing the form are available at www.mcgill.ca/fgsr/rgo/animal/

Protocol #: 4108
Investigator #: 160
Approval End Date: MARCH 31, 2003
Facility Committee: SCI

__ Pilot __ New Application X Renewal of Protocol # 4108

Title (must match the title of the funding source application): Effect of estrogen on the cholinergic system

1. Investigator Data:

Principal Investigator:	Dr. Keith Franklin	**Office #:**	398-6081
Department:	Psychology	**Fax#:**	398-4896
Address:	1205 Dr. Penfield Ave., Montreal, Quebec, H3A 1B1	**Email:**	keith@hebb.psych.mcgill.ca

2. Emergency Contacts: Two people must be designated to handle emergencies.

Name:	K. Franklin	Work #:	398-6081	Emergency #:	488-2734
Name:	P. Lauzon	Work #:	398-6091	Emergency #:	381-6230

3. Funding Source:

External US Alzheimer's Association__ Source (s):	Internal __ Source (s):
Peer Reviewed: X__ YES __NO**	Peer Reviewed: __ YES __ NO**
Status : X__ Awarded __ Pending	Status: __ Awarded __ Pending
Funding period: 1/1/00 to 31/8/02	**Funding period:**

ACTION	✓	DATE
CCS	✓	Mar 3'02
DS		
APPROVED		

** All projects that have not been peer reviewed for scientific merit by the funding source require 2 Peer Review Forms to be completed . e.g. Projects funded from industrial sources. Peer Review Forms are available at www.mcgill.ca/fgsr/rgo/animal/

Proposed Start Date of Animal Use (d/m/y): or ongoing X__

Expected Date of Completion of Animal Use (d/m/y): or ongoing _X_

Investigator's Statement: The information in this application is exact and complete. I assure that all care and use of animals in this proposal will be in accordance with the guidelines and policies of the Canadian Council on Animal Care and those of McGill University. I shall request the Animal Care Committee's approval prior to any deviations from this protocol as approved. I understand that this approval is valid for one year and must be approved on an annual basis.

Principal Investigator: Keith Franklin K. Franklin **Date:** 22 April 2002

Approval Signatures:

Chair, Facility Animal Care Committee:		**Date:**
University Veterinarian:	Rel Lett	**Date:** 5/02/02
Chair, Ethics Subcommittee(as per UACC policy):		**Date:**
Approved Period for Animal Use	**Beginning:** April 1, 2002	**Ending:** MARCH 31, 2003

APR 26 2002